AN ELECTROPHYSIOLOGICAL STUDY OF THE SOMATIC MUSCLE CELLS OF ASCARIS SUUM

Peter Thorn

Dissertation submitted to the University of Edinburgh for the degree of Doctor of Philosophy

September, 1986

Preface

The experimental work described in this thesis was performed under the supervision of Dr. R. J. Martin and Dr. K. Gration during the tenure of an SERC-CASE studentship with Pfizer Central Research. The work of Section II has been published in two papers:

(1) Martin, R.J. and Thorn, P. (1984). A high conductance anion channel in the somatic muscle cells of *Ascaris suum*. Journal of Physiology *354* 46P.

(2) Thorn, P. and Martin, R.J. (1987) A high conductance calcium-dependent chloride channel in *Ascaris suum* muscle. Quarterly Journal of Experimental Physiology *72* pp31-49.

Copies of both papers are included in the appendix.

I declare that the experimental work is my own and that this dissertation has not been previously submitted to any other University.

Peter Thorn

Acknowledgments

My thanks are due to Dr. R. Martin for obtaining the grant, allowing me the use of the laboratory and for his continued help throughout my three years. I am grateful to Dr. K. Gration and Dr. I. Harrow for their helpful discussions during my time at Pfizer Central Research. I would also like to thank the technical staff of the old Department of Veterinary Pharmacology for their help, and Ms. F. Manson who provided the photographic services.

The work was supported by a CASE-SERC Studentship with Pfizer Central Research.

CONTENTS

APPENDIX I

'Probear' computer programme in binomial analysis of data.

APPENDIX II

'Campion' computer programme used to calculate probability of channel opening.

APPENDIX III

Reprints
Martin, R.J. and Thorn, P. (1984). A High Conductance Anion Channel in Somatic Muscle Cells of *Ascaris suum*. Journal of Physiology 354 46P.

Thorn, P. and Martin, R.J. (1987). A High-Conductance Calcium-Dependent Chloride Channel in *Ascaris suum* Muscle. Quarterly Journal of Experimental Physiology 72 pp31-49.

List of Tables

List of Figures

Summary

The electrophysiological properties of muscle cells in the nematode Ascaris suum have been studied extensively (review DeBell 1965). However, details of the ionic mechanisms regulating the spontaneous activity of the somatic muscle cell membrane are still poorly understood. The study described in this thesis, used the patch-clamp technique to examine ion channels in the soma membrane of the muscle cells. In addition, two-electrode voltage-clamp was used to observe the membrane currents of the muscle cell somata.

The patch-clamp experiments demonstrated the presence of a high-conductance chloride channel (200pS) spontaneously active at the resting potential. This channel was voltage sensitive. When the patch was depolarized the mean open time of the channel and the probability of opening were both reduced. An additional feature of this voltage sensitivity was the appearance of sub-conductance levels when the patch was depolarized.

In patches that contained more than one channel the proportion of time spent with 1,2,3...N channels open was analysed in terms of the binomial distribution. The results indicated that the binomial distribution was not a good approximation to the data. From this analysis it was concluded that either the channels in the same patch did not have the same probability of opening, or that channel openings were not

independent of each other.

Experiments showed that the probability of chloride channel opening was dependent on the concentration of intracellular calcium. Increasing the concentration of calcium led to an increase in the probability of channel opening. The significance of the calcium sensitivity remains unknown. It was proposed that these channels were responsible for the high resting permeability to chloride.

The voltage-clamp experiments demonstrated the presence of two currents activated by membrane depolarization. When the muscle cells were bathed in Ringers containing calcium, depolarization activated an inward current, followed by a large outward current. The inward current increased in amplitude when the calcium concentration of the bathing solution was increased, and was blocked by lanthanum. The outward current was activated by steps to +55 mV from a holding potential of -35 mV. This current had a steep rise and slow decay and was found to be carried by potassium ions. Depolarizing steps of increased amplitude, increased the outward current amplitude and decreased the time to peak of the current. Experiments were carried out to determine the kinetics of the outward current.

Two blockers of potassium currents were tried in Ascaris, these were TEA and 4-AP. TEA [69 mM] was used in the study of the inward current and blocked most of the outward current. Bath

application of 4-AP [5 mM] blocked a fast-transient component of the outward current. The current remaining after 4-AP application had a slow rise time, and a slow decay approximated by a single exponential, with a time constant of 1.1 s. The 4-AP resistant current showed less steady-state inactivation than the gross outward current. Computer analysis was used to subtract the 4-AP resistant outward current from the gross outward current. The subtracted current represented the current blocked by 4-AP. The decay of the 4-AP blocked current was approximated by a single exponential, with a time constant of 10.4 ms. The function of both of these potassium conductances was thought to be to repolarize the cell after a spike.

Introduction to the Thesis

Ascaris suum is an intestinal nematode parasite of pigs and is closely related to Ascaris lumbricoides the parasite of man. Adult female worms produce eggs in the gut, the eggs are passed out and lie on the ground. Eggs picked up by eating contaminated food hatch in the gut and the young larvae burrow through the mucosal wall into the blood stream. The usual route followed by the larvae is to the lungs and from there they pass out of the blood stream and migrate up the trachea. They are subsequently swallowed and mature to adults in the gut.

I present here the results of electrophysiological experiments on the large somatic muscle cells of Ascaris suum. The study falls into two sections:

1) observations of single channel currents in the soma membrane using the patch-clamp;

2) measurements of the currents of the soma produced by membrane potential changes under voltage-clamp.

The patch clamp study demonstrated a large conductance chloride channel, dependent on voltage and intracellular calcium concentration. Measures of the mean open time and probability of opening were obtained from computer analysis of the single

channel currents. The experiments were designed to lead to an understanding of the function of the high conductance chloride channel. A knowledge of the behaviour of the membrane could lead to the development of novel anthelmintics.

The soma of the somatic muscle cells of Ascaris suum were voltage clamped. The voltage clamp project was designed to observe the currents produced in the soma. Experiments showed an outward potassium current activated by depolarizing voltage clamp steps. The current activation and inactivation were studied.

SECTION I

Prologue

Introduction

The anatomy and pharmacology of Ascaris suum musculature, have been the subject of many investigations (review DeBell 1965). Ascaris muscle cells send projections (arms) to synapse at the nerve cords, instead of the more usual manner of motor neurones projecting to form neuromuscular junctions at the muscle. Single electrode intracellular recording of the resting potential Ascaris suum somatic muscle cells was first carried out by Jarman (1959). The muscle cells have a complex resting membrane potential composed of spontaneous slow waves and spikes (Weisblat, Byerly and Russell 1976). Ascaris suum has also been used in assays of anthelmintic drugs (Toscano-Rico 1926). The muscle cells of Ascaris suum have been shown to have γ-amino butyric acid (GABA), (Del Castillo, De Mello and Morales 1964b) and acetylcholine (ACh), (Del Castillo, De Mello and Morales 1963) receptors. The following review outlines the previous work carried out on the somatic muscle cells of Ascaris suum.

Anatomy of Ascaris

Fig. 1 shows a transverse section of Ascaris 4 cm from the rostral end. The figure shows the important anatomical features of the worm. The central gut is surrounded by a region filled with perienteric fluid. This cavity is enclosed by the somatic muscle cells, with the muscle cell bodies arranged over

Fig. 1: Diagram of a cross-section through the anterior region of Ascaris suum. The dorsal and ventral nerve cords are held in extensions of the hypodermis, which form a cup like structures. The somatic muscle cells send arm like projections to make contact with the nerve cords, and also to interdigitate and make electrical contacts with other muscle cells. Underlying the cell bodies of the muscle cells, are the contractile muscle spindles which all lie longitudinally to the body wall. All the muscle cell bodies (bags) project into the body cavity which is filled with perienteric fluid. In the centre is the gut.

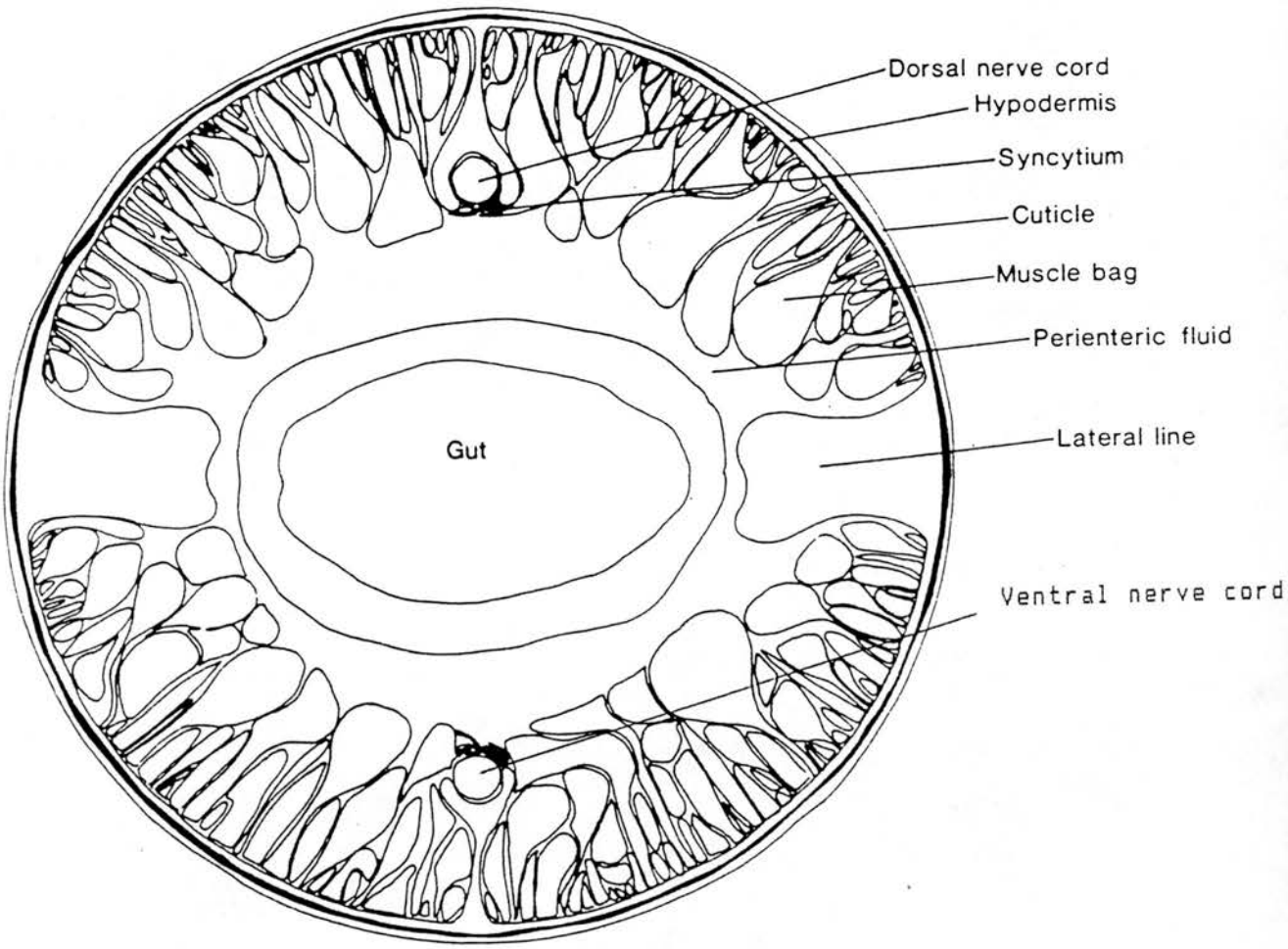
Dorsal nerve cord
Hypodermis
Syncytium
Cuticle
Muscle bag
Perienteric fluid
Gut
Lateral line
Ventral nerve cord

the contractile muscle spindles. A layer of connective tissue overlies the muscle cell bodies. The muscle spindles all lie longitudinally, there are no circular muscles. Forward movement of Ascaris is accomplished by a swimming motion of the body with muscle blocks from opposing sides of the body alternately contracting and relaxing. Underlying the muscle cells there is a cellular hypodermal region and a cuticle.

Each muscle sends a projection or arm to the syncytium and receives synaptic contact from motor neurones and is electrically coupled to the arms of adjacent muscle cells (Debell, Del Castillo and Sanchez 1963, Rosenbluth 1965). Two nerve cords run dorsally and ventrally down the length of the worms. The muscle layer is divided longitudinally by two broad hypodermal ridges called the lateral lines. In the female the gonad consists of a long uterine sac running in the peritoneal cavity and opening in the vulva. The anus is situated further rostrally.

An H shaped tubule runs along the length of the worm in the lateral line and has been proposed to act as a regulator of ion balance (Lee 1965). However, it is probable that muscle, gut and other cell layers subserve many of the requirements of ion regulation.

Many studies of the nematode anatomy were carried out by various authors in the 19th century. Rohde (1885) and Butchli (1874) observed that the nerves of the circumpharyngeal ring were directly connected to the longitudinal nerves that ran along the lateral lines. Cappe de Ballon (1911) introduced the terms spindle, belly, and arm, for the contractile region, the cell body and the projection to the nerve cord, respectively, of the somatic muscle cells (see Fig.2B).

Rosenbluth (1963, 1965) described the general structure of the somatic muscle cells under electron microscope. Rosenbluth (1963) observed glycogen granules and a cytoskeletal layer underlying the plasma membrane of the cell bodies of the somatic muscle cell. The arms were found to project from any portion of the bag and to become narrower in diameter as they approached the nerve cord. The arms were described as separating into finger-like projections and interdigitating with adjacent arms over the nerve cord . The points of contact between muscle cells were described as tight junctions with little or no extracellular space (Rosenbluth 1965). Rosenbluth (1965) tentatively suggested tight junctions formed the low resistance pathway between muscle cells described by DeBell et al (1963). However, the morphology of these junctions was diverse and was taken to indicate a diversity of function (Rosenbluth 1965). The synaptic contact between the nerve and muscle cells was in the form of an en-passage synapse with a 500 Å gap between the cells. The presynaptic area of the motor neurone at the synapse

possessed a number of specializations, including vesicles and mitochondria (Rosenbluth 1963).

Stretton (1976) used electron microscopy and light microscopy to study the morphology of the muscle cells. Stretton (1976) found that nearly all muscle cells had multiple arms (mean 2.7) and received innervation from both the major (dorsal and ventral) and minor nerve cords. Cells nearer the main nerve cords had only one arm projecting to this cord. An interesting observation was that not all muscle cells made contact with the nerve cord. Stretton, Fishpool, Southgate, Dommoyer, Walrond, Moses and Kass (1978) studied the motorneurones of Ascaris suum. Stretton et al (1978) observed five repeating segments down the length of the worm, each segment composed of 11 neurones. Seven types of neurone, inhibitory and excitatory made up the 11 neurones of a segment and each homologous type in each segment behaved identically to stimulation. All cell bodies were found in the ventral nerve cord. Four types of cells projected their axons via commissures to neuromuscular junctions in the dorsal nerve cord. Three types of neurones had ventral neuromuscular junctions. Two had dendrites within the ventral nerve cord and the other had dendrites in the dorsal nerve cord (Stretton et al 1978). Stimulation of the ventral nerve cord while recording from dorsal musculature, and cutting all but one commissure enabled the input to the musculature, to be isolated to only one motorneurone. Of the cells with projections to the dorsal nerve cord, three types gave a depolarizing response and one a

hyperpolarizing response to stimulation (Stretton et al 1978). These experiments illustrate relatively simple intercellular relationships found in the neuromuscular system of Ascaris suum.

Electrophysiology of the Somatic Muscle Cells of Ascaris suum.

The ionic constituents of Ascaris body fluids were first analysed by Hobson, Stephenson and Beadle (1951a). Experiments were carried out on worms ligated at both ends to exclude effects of the alimentary canal and excretory system (Hobson et al 1951a). These experiments showed the worm actively maintained a lower perienteric chloride concentration than that of the bathing solution. This ability to excrete chloride was shown to be a mechanism of the somatic muscle cells, the underlying hypodermis or the cuticle. Harpur and Popkin (1973) also showed that Ascaris was capable of actively maintaining a low concentration of chloride in the perienteric fluid. Hobson, Stephenson and Eden (1951b) analysed the ionic constituents of the pig gut contents, the natural environment of the worm, and those of Ascaris body fluids. This analysis forms the basis for the ionic composition of Artificial Perienteric Fluid (APF) used by Weisblat, Byerly and Russell (1976).

The ionic basis of the resting potential seen in the somatic muscle cells, was explored by Del Castillo, De Mello, and Morales (1964a). The resting membrane potential was observed to be little affected by changes in the potassium concentration of the bathing Ringer (Del Castillo et al 1964a). In contrast,

changes in chloride concentration produced large effects on the membrane potential as predicted by the Nernst equation. Large changes in resting potential were also observed (Del Castillo et al 1964a) in response to changes in the extracellular sodium concentration. Ion flux experiments performed by Caldwell and Ellory (1968) demonstrated a permeability ratio of 1:4:7 for potassium, sodium and chloride respectively.

Brading and Caldwell (1971) proposed that an electrogenic pump was responsible for maintaining the resting potential. Somatic muscle cells were bathed in a wide variety of Ringers by Brading and Caldwell (1971). An additional factor had to be introduced into the Goldman Constant Field equation to account for changes in the resting membrane potential. This factor was interpreted as the contribution of an active electrogenic pump to the maintenance of the membrane potential (Brading and Caldwell 1971). Caldwell (1974) in a theoretical treatment of the active transport mechanism of Ascaris, concluded that a sodium and or a chloride pump could be involved in maintaining the resting potential of the muscle cells.

Spontaneous spike potentials and slow waves in the muscle cells were first recorded with an intracellular micropipette by Jarman (1959). The ionic basis of this activity has been the subject of a number of studies. Jarman and Ellory (1969) suggested that the spike potentials were dependent upon the inward flux of calcium. In a later study on the spontaneous

activity of the somatic muscle cells Weisblat et al (1976) demonstrated that the maximum amplitude of the spike potentials increased 30 mV for every decade increase in the calcium concentration, as calculated by the Nernst equation for a calcium current. The slow waves persisted in low calcium and also in sodium free Ringer. Removal of sodium and calcium effectively abolished slow wave activity. However in these experiments (Weisblat et al 1976) no measure of input resistance was made and therefore interpretation of some of their results is difficult.

Debell et al (1963) measured the potentials of the somatic muscle cells with intracellular micropipettes. Resting potentials of around -30 mV were observed, (Debell et al 1963) with spontaneous depolarizing slow waves of 5 mV and depolarizing spikes of varying amplitude superimposed on the resting potential. The spikes were not a constant amplitude, and had a variable duration (around 50 ms). Often the rate of rise of the spike was slower than the rate of decay. Spikes were always associated with the depolarizing slow waves. The duration of the slow waves varied from 100 to 1000 ms.

Debell et al (1963) used a second micropipette to pass current into the cell bodies while recording the resting membrane potential with the other electrode. These experiments were carried out to determine the site of spike initiation. Depolarization of the muscle cell elicited an electrotonic

response in the same cell, similar in amplitude and duration to the spontaneous spikes. Brief stimulation of the nerve cord produced spikes recorded from the cell body (Debell et al 1963). The latency, and amplitude of the spikes were dependent on the position of the stimulating electrodes, the magnitude of the applied voltage and the frequency of stimulation.
Hyperpolarizing current was injected directly into muscle cell bodies, and the potential was recorded from the same cell body, a decline in spike amplitude accompanied by a hyperpolarization of the resting potential was observed. In other experiments current was passed into a cell body while recording the spontaneous activity of an adjacent cell body (Debell et al 1963). Hyperpolarizing current passed into one cell produced a decrease in spike amplitude in an adjacent cell, accompanied by a 3 mV hyperpolarization of the resting potential. Interactions of this kind were observed when hyperpolarizing current was injected into any of the surrounding cell bodies. These results were taken to indicate that the electrical activity was initiated at the neural ends of the arms. The arms form a syncytium over the nerve cord and this was thought to be the pathway for the effects of current passage on adjacent cells (Debell et al 1963).

Additional evidence on the site of initiation of spikes, came from passing of current directly into cells of the syncytium using a micropipette (Del Castillo, De Mello, Morales 1967). Outward current injected into the cell bodies produced a

single spike. In contrast outward current injected into the syncytium region produced a train of spikes. The frequency of the spikes was dependent on the magnitude of depolarization.

The pharmacology of Ascaris suum has been studied in an attempt to find anthelmintic agents. Toscano-Rico (1926) used a cylindrical section of the worm and using a kymograph recorded contraction in response to the application of various drugs including nicotine. Del Castillo, De Mello and Morales (1963, 1964b, 1964c) in a series of experiments, demonstrated a depolarizing effect of acetylcholine [10^{-6} M] applied at the syncytial region of the muscle cells, this depolarization was blocked by tubocurarine [10^{-3} M]. Bath applied piperazine [10^{-2} M] produced a chloride dependent hyperpolarization of the somatic muscle cells of Ascaris (De Castillo et al 1964c). Both piperazine [10^{-2} M] and γ-amino butyric acid (GABA) [10^{-6} M] iontophoretically applied at the syncytial region produced a hyperpolarizing response recorded in the cell bodies of Ascaris (Del Castillo et al 1964b). The results of the above experiments were taken to indicate the presence of acetylcholine receptors and GABA receptors on the postsynaptic membrane of the somatic muscle cells at the syncytium (De Castillo et al 1963,1964a,1964b).

The easy accessibility of the cell bodies of the somatic muscle has enabled the relatively new patch clamp technique to be used to study single-channel currents. Martin (1985) looked at the single-channel currents produced by GABA and piperazine. GABA [1 uM] produced channel openings with a conductance of 22 pS, and a mean open time of 32 ms. Piperazine [500 μM] produced channel openings with a conductance of 22 pS and a mean open time of 14 ms (Martin 1985). The difference in potency of piperazine and GABA may be described by the shorter mean open time produced by piperazine and the increased concentration of piperazine required to produce the same opening rate as GABA (Martin 1985).

SECTION II

A High Conductance Calcium-Dependent Chloride Channel in the Somatic Muscle Cells of Ascaris Suum

INDEX

Summary

The properties of a high-conductance calcium-dependent chloride channel in the body muscle membrane of the nematode parasite Ascaris suum, were examined with the patch-clamp technique.

These channels were seen in about 20% of all patches and occasionally up to 15 channels were seen in a single patch. Patches were made in the soma region of the muscle cells. A few patches made in the spindle region showed similar current records to the high-conductance channel. Out of 200 patches containing channels, 5 had channel currents indicating one channel present, the rest were multichannel patches.

In Ascaris Ringer (symmetrical 175 mM chloride) the I/V relationships of the chloride channel appeared linear during hyperpolarization with a slope conductance of 200 pS, depolarization reduced the slope conductance. These observations demonstrated an inward rectification of the chloride channel.

Cation and anion substitution experiments showed this channel to be permeable to chloride ions. In artificial perienteric fluid, APF, (symmetrical 78 mM chloride) the channel conductance was 114 pS.

Sub-conductance states were observed when the patch was

depolarized. The channel conductance showed saturation with increased chloride concentrations.

The channel was voltage-sensitive: the open probability and the mean open time of the channel decreased when the patch was depolarized. Mean channel open times between 2.4ms and 215ms were observed.

At a given potential open probabilities and mean open times were widely different in different patches. This was taken to indicate the influence of an unknown factor on channel opening. Mean open times of between 2.4 ms and 215 ms were observed in different patches at different potentials.

Frequency histograms of the distributions of open and closed times were fitted with 2 and 3 exponentials respectively. This suggested complex channel kinetics with multiple open and closed states.

The distributions of the probabilities of observing N channels open in multichannel patch records were not always well fitted by the binomial distribution. It is suggested that adjacent channels could have different probabilities of being open.

Calcium applied to the intracellular surface of the patch, increased in a dose-dependent manner the number and probability of the channels being open.

Aims and Introduction to the Patch-clamp Experiments

In this study the patch-clamp technique was applied. This method physically and electrically isolates a small patch of membrane and enables the currents passing through individual channels to be measured (Sakmann and Neher 1984, Hamill, Marty, Neher, Sakmann and Sigworth 1981). Patch clamping has a number of advantages over voltage-clamping in a study of this kind:

1. single channel currents are readily identified and can be studied in isolation from other currents,

2. unlike voltage-clamp a small isolated patch of membrane is studied and problems associated with voltage-clamp, such as space clamp, are circumvented,

3. solutions of extreme ionic composition can be placed in the pipette with minimal disturbance to the rest of the preparation.

Martin (1985) in his patch-clamp study of the GABA channel of the muscle cells of Ascaris, observed a large conductance channel, spontaneously active in cell-attached patches at the resting potential. The experiments described in this chapter and in two papers (Martin and Thorn 1984, Thorn and Martin 1987), were carried out to determine the characteristics of this large conductance channel and attempt to ascertain its function in the overall physiology of the somatic muscle cells of Ascaris.

Previous studies on the somatic muscle cells of Ascaris suum, have shown a high resting permeability to chloride (Del Castillo et al 1964a, Caldwell and Ellory 1968). Del Castillo et al (1964a) measured the changes in the resting potential of muscle cells bathed in solutions of different ionic composition. The results indicated a resting permeability to chloride. Caldwell and Ellory (1968) used radioactive tracer experiments to determine a permeability ratio of 1:3:7 for potassium, sodium and chloride respectively. Hobson et al (1952a) have shown that chloride was actively transported across the muscle cell and hypodermal layers. Weisblat et al (1976) went on to study the spontaneous electrical activity of Ascaris muscle cells, but their studies on the permeability of these currents were limited by the use of one intracellular electrode.

The work described in this chapter of the thesis indicated that the spontaneously active channel observed by Martin (1985) was largely permeable to chloride. The conductance in symmetrical solutions of 170 mM Cl was 200 pS. Recent single channel work in a variety of other cell types has shown large conductance anion channels, which are maximally open at 0 mV.

High conductance, voltage sensitive chloride channels have been described in the following epithelial cells: A6 cell line derived from Xenopus kidney epithelial tissue (Nelson, Tang and Palmer 1984), basolateral membrane of rabbit urinary bladder epithelium (Hanrahan, Alles and Lewis 1985), apical membrane of

renal derived epithelial cell line, Madin-Darby canine kidney, MDCK cells (Kolb, Brown and Murer 1985) and pulmonary alveolar cells (Schneider, Cook, Gage and Young 1985). Voltage-dependent chloride channels have also been described in rat skeletal muscle, (Blatz and Magleby 1983), Schwann cells (Gray, Bevan and Ritchie 1984) and mitochondria (Schein, Colombini and Finkelstein 1976). High conductance, voltage sensitive chloride channels have a conductance between 450 pS in the Schwann cell (Gray et al 1984) and 360 pS in the A6 cell line derived from Xenopus epithelium (Nelson et al 1984).

The permeability of some high conductance, voltage sensitive chloride channels channels has been studied, and the selectivity of the channel for different ions calculated. An index of the ionic selectivity, of a channel can be drawn from the permeability ratio of the channel, for an anion species over a cation species. Gray et al (1984) determined the permeability ratio of sodium to chloride in the Schwann cell by using a different concentration of NaCl on each side of a patch, and determining the reversal potential of the chloride channel. A derivation of the Goldman-Hodgkin-Katz equation was then used to calculate a permeability ratio of sodium to chloride (P_{Na}/P_{Cl}) of 0.2 (Gray et al 1984). Using KCl solutions across the membrane, a P_K/P_{Cl} ratio of 0.06 was calculated (Gray et al 1984). In similar experiments the P_K/P_{Cl} ratio of the anion channels of other tissues has been calculated. The P_K/P_{Cl} ratio of the chloride channel in urinary bladder

epithelial cells was 0.059 (Hanrahan et al 1985). In the chloride channel of pulmonary alveolar cells the ratio was 0.015 (Schneider et al 1985), and in the chloride channel of mitochondria the ratio was found to be 0.14 (Schein et al 1976). The range of permeability ratios in the different types of channels suggest that the molecular mechanisms for selectivity are different.

The permeability of the Ascaris chloride channel was investigated in experimants described in this thesis using similar techniques to those outlined above. The channel was bathed in assymetric KCl solutions and the permeability ratio of K to Cl was calculated from the reversal potential.

In this study, analysis of the channel records of Ascaris showed that in addition to a full conductance state the chloride channel had smaller conductance states. The variability in the conductance of the Ascaris channel shows similarities with sub-conductance states described in high conductance, voltage sensitive chloride channels. Channel openings to conductance levels below that of the full conductance level have been described for the chloride channels of Schwann cells (Gray et al 1984) and pulmonary alveolar cells (Krouse, Schneider and Gage 1986). In Schwann cells one sub-conductance level was described. Its' conductance was approximately half the full conductance state, and appeared when the patches were held for long periods at potentials between 0 and 30 mV (Gray et al 1984). The large

conductance, voltage sensitive chloride channel of pulmonary alveolar cells displayed any of 6 sub-conductance states, all of which were integer multiples of 60 pS (Krouse et al 1986). The possibility that the current records obtained from the pulmonary alveolar cells represented the activity of 6 independent channels, was rejected on the grounds that the frequency of appearance of the sub-conductance levels was consistent with the common gating mechanism of a single channel (Krouse et al 1986).

High conductance, voltage sensitive chloride channels inactivate at membrane potentials away from 0 mV. The time course and potential dependence of this inactivation varied in the different cell types. For example in the Schwann cells the channel inactivation followed an exponential decline with a time constant of under 1 s, and reactivated when returning the membrane potential to 0 mV with a time constant of 100 ms. (Gray et al 1984). The mean open time and the probability of opening of the chloride channels in A6 epithelial tissue were reduced when the membrane potential was stepped to a range outside +/- 20 mV (Nelson et al 1984). The time course of inactivation in the A6 epithelial cells was a few seconds, while that of activation was up to 30 s. (Nelson et al 1984).

The Ascaris chloride channel in this study, is shown to have a high conductance, similar to the high conductance, voltage sensitive chloride channels, and might be expected to show a similar voltage dependence. This was investigated by

experiments described in this thesis, by holding the patch at different potentials and measuring the open probability and the mean open time. Quantification of this effect proved to be difficult, in part because of large variabilities in the probability of channel opening and the mean open time, of channels in different patches. Unexplained changes in channel behaviour have been noted for the chloride channel of rat skeletal muscle (Blatz and Magleby 1983), and Schwann cells (Gray et al 1984).

Blatz and Magleby (1983) described a bursting behaviour of the chloride channel in rat skeletal muscle, and suggested that the channel activity was modulated by an unknown intracellular factor. Patch isolation in Schwann cells led to an increase in chloride channel opening. Gray et al (1984) proposed that this was due to the removal of an intracellular modulating factor that was inactivating the channel.

A number of reports have shown chloride conductances dependent on intracellular calcium concentration. These reports are of interest because of an observation in the experiments of this thesis, of an initial increase in the probability of chloride channel opening, when a patch was isolated from the cell. The majority of the work on calcium-dependent chloride conductances has been on the gross cellular currents. Patch-clamp experiments on the mollusc Lymnaea stagnalis show the calcium-dependent chloride channel to have a conductance of 200 pS (Geletyuk and Kazachenko 1985). In rat lacrimal gland

the measured conductance was 5 pS (Marty, Tan and Trautman 1984) and in mouse spinal cord neurones the single channel conductance was 22 pS (MacDonald, Owen and Barker 1985). The large differences between these figures is in contrast to the conductances of the high conductance, voltage sensitive chloride channels.

The calcium-dependent chloride channels show some voltage dependence. In the calcium-dependent chloride channels of Xenopus oocytes, depolarizing voltage-clamp steps have been shown to activate the chloride conductance, and produce a large outward current (Miledi 1982, Miledi and Parker 1984, Barish 1983). Calcium-dependent chloride conductances have been described in cultured mouse spinal neurones (Owen, Segal and Barker 1984) and cultured rat sensory neurones (Mayer 1985). Owen et al (1984) described the chloride current as activating when depolarizing voltage-clamp pulses were applied, and proposed that the current acts to repolarize the membrane after an action potential. The chloride channel of Lymnaea stagnalis showed an increase in the probability of opening when the patch was hyperpolarized (Geletyuk and Kazachenko 1985). However, the voltage dependence of the Lymnaea chloride channel was affected by the extracellular potassium concentration; with a low extracellular potassium concentration [less than 15 mM] the channel was activated by depolarizing membrane potential steps (Geletyuk and Kazachenko 1985).

Qualitative studies have demonstrated the dependence of these chloride channels on the intracellular calcium concentration. In the salivary glands of Calliphora an increase in the chloride permeability was produced by application of 5-HT (Berridge, Lindley and Prince 1975). It was proposed that 5-HT activated a calcium-dependent chloride permeability. More direct evidence for the calcium dependence of the chloride conductance of Xenopus oocytes, has been found by Miledi (1982), who described an increase in the amplitude of the outward chloride current when the extracellular calcium concentration was raised. The current was blocked when the cells were bathed in lanthanum (Miledi 1982). Bader, Bertrand and Schwartz (1982) voltage-clamped the solitary rod inner segments of the salamander retina. Using pharmacological agents and ion substitution experiments Bader et al (1982) described potassium, chloride and calcium currents. The amplitude of the chloride current in solitary rod inner segments was dependent on the length of a depolarizing prepulse and was abolished by intracellular injection of the calcium chelator, EGTA (Bader, et al 1982). Bader et al (1982) concluded that the chloride current was dependent on the concentration of intracellular calcium. In the lacrimal gland cells of rat Marty et al (1984) stimulated the chloride conductance either by bath applied carbamycholine or by using a high calcium concentration in the bathing Ringer with the calcium ionophore, A23187. The current was blocked by bath applied EGTA [5 mM], indicating that the chloride current was dependent on the calcium concentration (Marty et al 1984).

Gelytuk and Kazachenko (1985) changed the calcium concentration at the intracellular surface of an isolated inside-out patch and showed that the probability of opening of the chloride channel changes from 0.01 in a 'calcium-free Ringer' to 0.1 in a 1 mM calcium solution.

Experiments described in this thesis, were carried out on the Ascaris chloride channel to determine if the channel was dependent on intracellular calcium concentration. Subsequent experiments went some way towards quantification of the effect of calcium on the Ascaris chloride channel.

METHODS

The Preparation

Specimens of Ascaris suum were obtained from either the Gorgie Road slaughter house in Edinburgh, or the Carlisle slaughter house. Worms were removed from the guts of freshly killed pigs and placed in an insulated container filled with Lockes solution at 37°C. Male and female Ascaris of about 20 cm in length were used in these experiments. Worms were maintained in Locke solution for up to four days in a water bath (Grant) at 32°C. Worms that were not active when disturbed were not used in these experiments.

The Dissection and Experimental Chamber

A 2 cm cylindrical anterior section of the worm was taken and slit along one of the lateral lines. The section was then opened and pinned cuticle side down onto a layer of Sylgard that lined the experimental chamber, and the gut carefully teased away to reveal the cell bodies. The bath contained 1.5 ml of fluid and was maintained at a constant temperature of 30°C by a water jacket. An inlet and drain in the bath allowed perfusion of the preparation. A gravity feed perfusion system was used to eliminate any electrical interference that might be produced by an electric pump. Store bottles containing the

Fig. 2A: Diagram of the experimental chamber viewed from above. The opened section of the worm is shown, the gut has been removed and the cell bodies of the somatic muscle cells lie exposed. Two electrodes are shown on the diagram in the position used for voltage-clamp recording. The position of the electrode used in patch clamp recording is the same as for voltage-clamp. The perfusion inlet and outlet are shown. During most experiments the perfusion was turned off when recording in the isolated inside-out patch configuration. A water jacket is shown surrounding the experimental chamber. Water, maintained at a constant temperature, was circulated through the jacket to control the temperature of the preparation. The position of the agar bridge bath electrode is shown in the bottom right corner of the chamber.

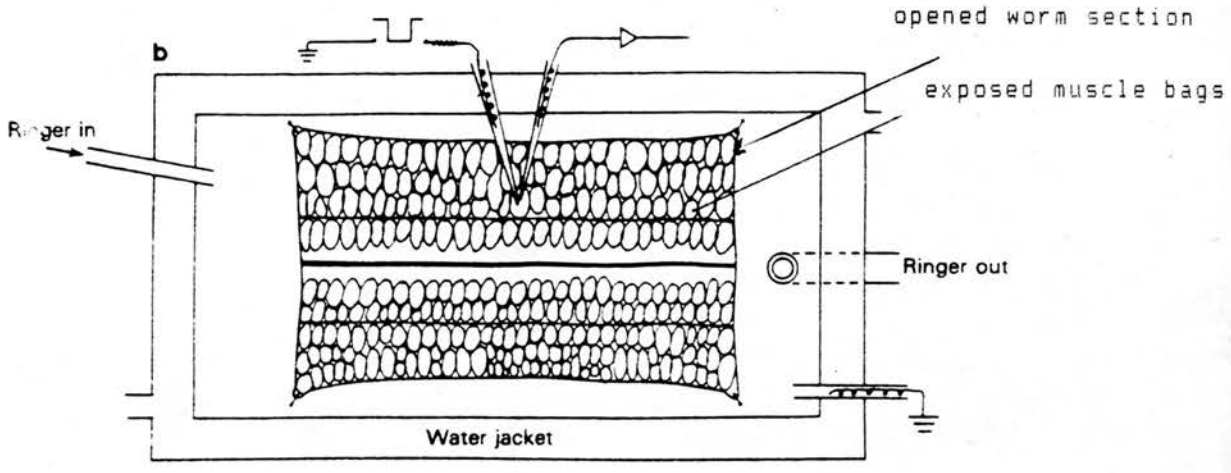
b
opened worm section
exposed muscle bags
Ringer in
Ringer out
Water jacket

TABLE 1: Solutions used in the patch clamp experiments. Complete substitution of chloride with acetate was used to make up Acetate Ringer. Ringers were adjusted to pH 7.6 with maleic acid or HCl with Tris buffer, and NaOH with HEPES buffer. Maleic acid was used in the Low-Cl and Acetate Ringers.

TABLE 1 SOLUTIONS : ELECTROLYTE CONCENTRATIONS mM

	NaCl	NaAc	KCl	$CaCl_2$	$MgCl_2$	Glucose	Tris	HEPES
Ascaris Ringer	135	-	3.0	3.0	15.7	3.0	5.0	-
Tris Ringer	-	-	-	3.0	15.2	3.0	140	-
1/5 Ascaris Ringer	27	-	0.6	0.5	3.14	0.6	1.0	-
Low-Cl Ascaris Ringer	50	85	3.0	3.0	15.7	3.0	5.0	-
A.P.F.	23	110	24	6.0	5.0	11	-	5.0
Low-Ca A.P.F.	23	110	24	-	11	11	-	5.0
NaCl Ringers	50->500	-	-	1	-	-	-	5.0

The Ringers containing 5 mM Tris were corrected to pH 7.6 with Maleic acid; Tris Ringer containing 140 mM Tris was corrected to pH 7.6 with HCl; the Ringers containing HEPES were corrected to pH 7.6 with NaOH. Low-Ca A.P.F. contained a total Ca of 3.7 µM as measured by flame photometry; this gave an estimated free-Ca of 1.5µM. A Zero-Ca A.P.F. Ringer was prepared by adding 0.5 mM EGTA to the Low-Ca A.P.F.

perfusing Ringers were held 50 cm above the preparation. Polythene tubes connected the store bottles to the bath, and were enclosed within larger diameter tubing, that contained the circulating water of the water jacket surrounding the experimental chamber. This preheated the perfusing Ringers to 30°C. A thermocouple device was used to check the accuracy of the temperature at which the preparation was maintained.

Fig. 2A illustrates the main aspects of the experimental chamber. The preparation was viewed from above using an Olympus Zoom microscope and illuminated from below using a 6 V DC lamp.

Ringer Solutions

Table 1 is a summary of the composition of the Ringers used in these patch-clamp experiments. Del Castillo et al (1964) used 1/3 seawater in their experiments and this forms the basis for Ascaris Ringer. The relatively high chloride and low potassium concentration was ideal for the study of chloride channels in the experiments described in this section. Artificial Perienteric Fluid (APF), (Weisblat et al 1976), was used in some experiments. The composition of APF was based on the analysis by Hobson et al (1952b) of the ionic composition of the fluid of the perienteric cavity of Ascaris suum. With isolated inside-out patches, calcium concentrations of 3 mM in Ascaris Ringer and 6 mM in APF in the bathing Ringer would activate the chloride channel (see Fig. 21). This made observation of the channel

easier. The other solutions in the table were used in the various experiments to study the permeability of the channel. The 1/5 Ascaris Ringer was corrected to the osmolarity of Ascaris Ringer by adding sucrose. Low-chloride Ascaris Ringer was produced by the partial replacement of chloride 1:1 with Acetate. Zero-chloride Ascaris Ringer was produced by total replacement of chloride with Acetate. NaCl Ringers were used in the study of channel saturation. The study of the putative cation channel used KCl Ringers. Tris Ringer solution was based on Ascaris Ringer with all the cations replaced by Tris. Calcium Ringers used free calcium concentrations of between 10^{-6} and 10^{-1} M. The free calcium concentration in each solution was calculated from the ionic strength of the solution and the activity coefficient. The ionic strength was calculated using the following equation:

$$\text{Ionic strength} = 0.5 \quad (c \times z^2) \quad M$$

where: c = concentration and z = valency of each ion species in the solution.

The activity coefficient of calcium in a solution of the calculated ionic strength may be found from tables (Robinson and Stokes 1972).

$$\text{Free Ion concentration} = c \times \alpha$$

where: c = calcium concentration and α = activity coefficient

The free calcium concentration of Ascaris Ringer with no added calcium was measured by flame photometry to be 3.75 μM.

In all solutions the Ringers were adjusted to pH 7.6 using either maleic acid or HCl with Tris buffer and NaOH or KOH with a HEPES buffer. All the patch electrode solutions were filtered through a 0.45 μm milliphore filter.

Fabrication of Electrodes

The bath electrode was made up of an Agar Ringer jelly, set into a polythene tube. A length of silver/silver chloride wire was inserted into this tubing. The wire was prepared either by fusing silver wire with molten silver chloride, or, by passing alternating current through a wire dipped in KCl (3M). Agar was made up with the Ringers being used in the experiments to minimize junction potentials.

Patch pipettes were made from glass microhaematocrit tubing (Hawksley Cat. No. 1604, external diameter 1.4 mm) pulled on a vertical microelectrode puller (SRI cat. no. 2001), using a two stage pull to produce a tip diameter of 0.5 μm. The electrode tips were then fire polished by holding them close to a heated wire under a microscope for a few seconds until a visible change in tip geometry was seen. This polishing rounded the jagged edges of the pipette tip. Filled electrodes had a resistance of 3 MΩ.

Enzyme Treatment

It was necessary to apply enzymes to the preparation in order to clean away any matrix that overlay the cell membranes. Collagenase (1mg/1ml in Ringer) was bath applied for a period of one half to one and a half hours depending on the appearance of the preparation. After collagenase treatment the preparation was washed liberally with clean Ringer to remove any debris.

Temperature/Collagenase Effects

Resting membrane potentials were measured from cell bodies under different conditions. At 33°C the mean resting potential was -29 mV. After application of collagenase for 2 hours the mean resting potential was -25 mV, a drop of 4mV. The temperature was then lowered to room temperature, 22°C, and the mean resting potential was -2 mV. A subsequent temperature increase to 33°C led to an increase in resting potential to -14 mV. These experiments showed that the resting potential was affected by collagenase treatment and had a temperature dependence.

Patch Potentials

The potential across the patch was changed by applying a voltage to the pipette. In the results the 'transpatch potential' refers to the potential across the patch membrane. The transpatch potential is stated as the voltage of the

solution on the cytoplasmic side of the patch, with respect to the voltage of the solution on the extracellular side of the patch. With cell-attached patches the transpatch potential is the sum of the potential applied to the pipette and the resting membrane potential of the cell. Resting potentials of the cells were not routinely measured and the quoted transpatch potentials for cell-attached patches were not corrected for the effect of the resting potentials.

Junction Potentials

Differential movement of ions across the pipette and bath electrode can set up junction potentials, so that applied potentials to the patch are offset. Junction potentials were routinely measured for each pipette and corrected for. All the experiments reported here, used an Agar bridge bath electrode to minimize the effect of junction potentials. An experiment was conducted to study the effects of changing the bathing Ringer to a 1/5 diluted Ringer on the measured standing potential. The mean difference between the standing potentials measured in the two Ringers was +2 mV indicating that only a small change in the standing potential was caused by the bath electrode.

Recording

Fig. 2B is a diagram of a somatic muscle cell and also shows the recording position of the patch electrodes. The pipette was first lowered into the the bath and a constant

voltage pulse of 100 mV applied across it. The current output of the amplifier showed a current deflection which was a measure of the pipette resistance. The pipette was then pressed against the cell membrane and changes in the measured resistance monitored. A large increase in resistance was often seen and this forms the first requirement in the formation of a seal. The pipette was left in this position and suction applied to the pipette. A sudden dramatic increase in the resistance indicated the formation of a gigaseal. These changes in resistance were due to the formation of a close junction between the pipette and the cell membrane. This type of patch is called a cell-attached patch.

Having produced a cell-attached patch an isolated inside-out patch may be formed by removing the pipette from the cell membrane. The gigaseal remains intact and the intracellular side of the membrane becomes exposed to the bathing Ringer. Occasionally in these experiments, some patches showed channel currents of small amplitude (20 pS) and slow rise times. The small amplitude channel currents were thought to be due to the formation of a vesicle at the pipette tip. In most cases the vesicle could be broken by withdrawing the pipette from the bath and exposing it to air (Hamill et al 1981). This ruptured the vesicle and channels of full amplitudes and with rectangular current waveforms were observed.

Fig. 2B: Diagram of a single muscle cell and recording technique. The cell is divided into three main regions: the cell body or bag region, the contractile muscle spindle and the arm. The muscle is electrically coupled to adjacent muscle cells and also receives synaptic contact with the nerve cords at the syncytium. The bag membrane was the main recording site in these experiments. Both cell-attached patches (1) and isolated inside-out patches (2) were used.

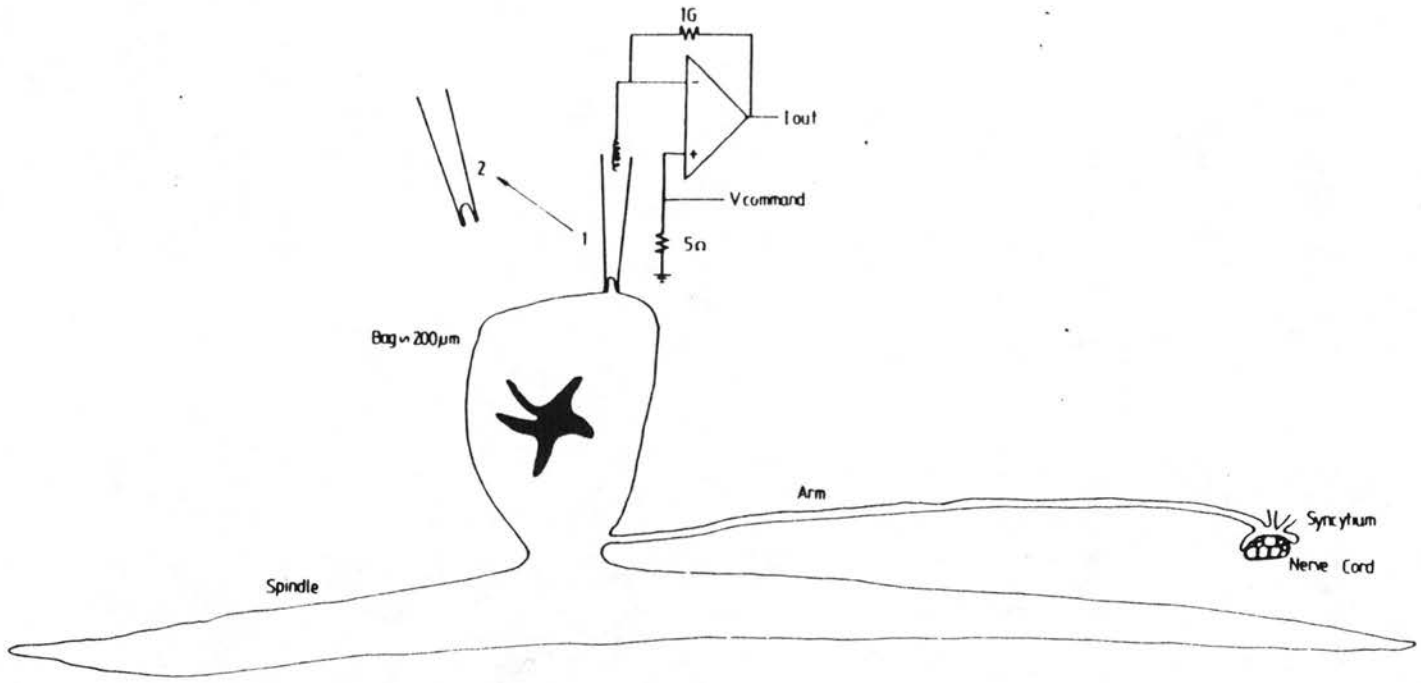
1G
I out
2
1
V command
5Ω
Bag ⌀ 200µm
Arm
Syncytium
Nerve Cord
Spindle

Currents were monitored using either a laboratory made amplifier based on a Teledyne Philbrick 1035 op-amp, or a List EPC7. The former had a 1 GΩ feedback resistor and a 3 dB cut off of 1 KHz. The output of the List was actively filtered using a Kemo VBF/4 at 1 KHz (3dB). Both types of amplifier were calibrated using RC circuits at the inputs.

Signals were recorded on a Racal Store Four F.M. tape recorder which had a slowest frequency response of 1250 Hz (1dB), and monitored on a Tektronix (5103N) oscilloscope and a calibrated Lectromed (Type MX216) chart recorder.

Data Analysis

Mean open times of the channel were obtained using a programme written in Fortran for the Cromemco computer by Dr.A.D.Short. This programme used a two cursor threshold level to detect channel openings and closings, these were set at 30% and 70% of the full channel amplitude. The channel current had to cross the 70% level before an opening was registered and then cross the 30% level before a closing was registered. The output of the computer gave the number of events and the mean open time. With single channel patches the mean open time could be read directly. For multichannel patches the cursors were set to each of the channel levels and the mean open time calculated from the sum of the total time open at each channel level divided by the total number of events.

The time spent with the channel or channels open calculated as a fraction of the total recording time, was expressed as the probability of channel opening (P_o). The probabilities of opening of the channel could not be calculated using the Cromemco computer, because of errors introduced by the programme not detecting long openings or closings at the beginning and end of the sample. Another attempt at measuring the probability of opening was made using a Reichart Young Videoplan. Chart recordings were placed onto the Reichart Young drawing board and an electronic pen was used to trace along each channel opening. The computer then added up lengths of all the openings, and along with a measure of the total sample length, calculated the percentage of time spent open.

Analysis of probability of opening was improved by the use of a BBC micro computer with a Unilab interface. Channel current records, stored on tape as voltages, were replayed from the tape recorder into an analog port of the Unilab interface. The computer programme was written in Basic by Dr. R.J.Martin and modified by myself for use in this application (see appendix I, Campion). The unilab interface was set up with an appropriate voltage range, for example +/- 1 V. The computer digitized this voltage range into 256 equally spaced points. The incoming current signal was sampled every 10 µs, and the programme stored the current amplitudes in the appropriate element of the 256 array. A frequency/amplitude histogram was plotted which showed

peaks at each of the channel current levels (see Fig. 15), including the zero current level when all the channels were closed. The area under each peak was a measure of the time spent at each of the different channel levels. The total area under the graph was used to calculate the proportion of time spent with 1,2,3...N channels open. The mean probability of channel opening was calculated from the proportion of time 1,2,3...N channels were open divided by the total number of channels observed in the patch.

The distributions of mean open time against transpatch potential, and probability of opening against transpatch potential, were fitted by polynomial functions using a BMDP programme (P5R). The programme fitted polynomials of up to 5 degrees, and was used to estimate the most appropriate function to describe the distributions. In this way the observed distributions were described as adequately fitted by a straight line ($y = ax + b$), a square function ($y = cx^2 + ax + b$), or a cube function ($y = dx^3 + cx^2 + ax + b$). An analysis of variance was performed to test the adequacy of the fit at each degree. If the addition of a further degree did not significantly improve the fit to the data, then the distribution was described by that number of degrees. In some experiments no difference was found in fitting the various degrees and the distribution was therefore left undescribed.

The slope and intersect of the I/V plots were calculated using a linear regression programme on a Texas calculator or on a BBC computer programme. Graphical presentation of the results was made either manually or using graphical programmes written for use with the 'Easygraph' package by Mr. N. Stroud of Edinburgh Regional Computing Centre (ERCC), Edinburgh.

RESULTS

The following results were from over 1000 successful gigaseal patches. Single channel currents due to the opening of the high-conductance chloride channel described in this section, were seen in over 200 of these patches. In these experiments, channels of a smaller conductance were very rarely observed and when seen were excluded from the analysis. The seal resistance of the patches was between 1 and 100 GΩ.

The observed occurrence of the high conductance channel was variable. At some periods during the course of this work almost every patch contained channels. At other times, periods of weeks passed in which either no seals were produced, or successful patches did not show any channel openings. Worms obtained in the same week usually showed similar characteristics of sealing and channel occurrence. The failure to obtain channel currents could have been due to uncontrolled factors that modulate channel activity such as protein phosphorylation (Blatz and Magleby 1983). When channels were seen in a patch, usually the opening of more than one channel (up to 15) was observed.

In bathing solutions containing calcium, the isolation of a patch from the cell often resulted in an increase in the maximum number of simultaneously open channels. This observation is

similar to that made with chloride channels of human trachea (Welsh 1986), MDCK cells (Kolb et al 1985) and Schwann cells (Gray et al 1984) and it has been postulated (Gray et al 1984) that it is due to the removal of an intracellular inhibitory factor. Evidence will be presented, that in the high conductance anion channel of Ascaris muscle, an increase in calcium at the intracellular surface of the patch, underlies the increase in the channel opening.

Some channel records in isolated inside-out patches showed small amplitude channel openings with slow rounded rise times. These records were thought to result from the resealing of the membrane surrounding the patch after it was ripped off the cell to form a vesicle. Removing the pipette from the bathing Ringer and exposing the vesicle to air (Hamil et al 1981) was usually found to produce channel openings of normal appearance and high conductance. Air exposure was carried out routinely for isolated inside-out patches where channel openings were small and of a rounded appearance.

In a few experiments, channel currents were observed when the bathing Ringers of isolated inside-out patches were changed. More usually, channel opening ceased within 20 s of isolating a patch and starting perfusion. This was thought to be due to a removal of an intracellular controlling factor.

Experiments were carried out to determine whether the loss

Fig. 3: Current records obtained from an isolated inside-out patch. The patch was held at a transpatch potential of -50 mV and the channel currents were inward (downwards). The triangles above the records indicate the application of a 1s air puff to the surface of the solution in the experimental chamber. After the first application of air the channel openings decreased in frequency. After the second application of air the channel openings decreased more and after 12 s no more openings were observed. The patch was held at -50 mV for 10 mins but no channel openings were observed.

Patch type: isolated inside-out patch.

Solutions: symmetrical *Ascaris* Ringer.

Temperature: 30°C.

Transpatch potential: -50 mV.

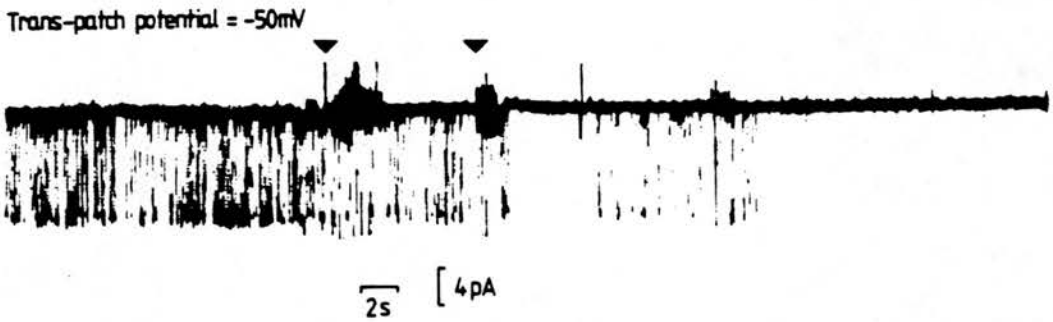
Trans-patch potential = -50mV
2s
4pA

of channel activity during perfusion was due to mechanical disturbance or other factors such as changes in ionic constitution. Fig. 3 shows the current records obtained from an isolated inside-out patch with Ascaris Ringer on both sides of the membrane. The triangles above the current records show the times when air was blown gently onto the bath surface to cause circulation of the bathing Ringer. It was apparent that the channel currents gradually and irreversibly disappeared. Irreversible loss of channel activity could indicate the loss of a component of the channel protein or the dilution of a factor present at the intracellular surface of the patch. Some isolated inside-out patches did not show a loss of activity when perfused. This was presumed to be due to the retention at the intracellular surface of the postulated modulating factors.

Fig. 4A illustrates current records typical of the high conductance channel. These records were obtained from an isolated inside-out patch with Ascaris Ringer both in the pipette and in the bathing solution. Fig. 4A shows the current records obtained at four different transpatch holding potentials (voltage of the cytoplasmic side of the patch with respect to the extracellular side of the patch). The currents at depolarizing potentials were outward, (upward) and those at hyperpolarizing potentials were inward, (downward). The currents were seen to reverse direction at approximately 0 mV. When the patch was depolarized, the mean open time decreased, as did the probability of opening.

Fig. 4A: Current records obtained at different transpatch potentials showing a high conductance channel. The records were obtained from an isolated inside-out patch held at +34 mV, +24 mV, -16 mV and -46 mV. The channel currents are inward (downward) at -16 mV and -46 mV, and outward (upward) at +34 mV and +24 V. Up to two channels are seen. The current levels with no channels open are indicated by 'C'. The current levels with one channel open are indicated by 'O_1' , and with two channels open by 'O_2'.

Patch type: isolated inside-out patch.

Solutions: Symmetrical solutions (Ascaris Ringer).

Temperature: 30°C.

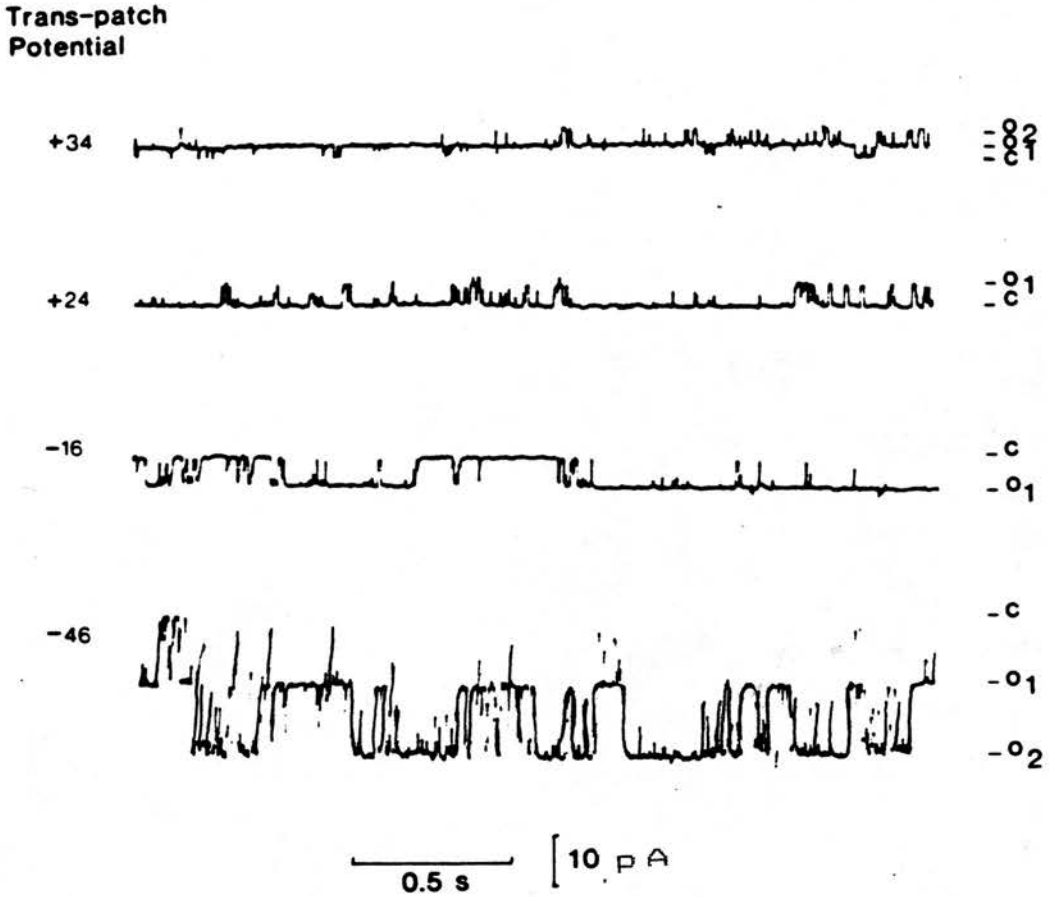
Trans-patch
Potential
+34
+24
−16
−46
o2
o1
c1
o1
c
c
o1
c
o1
o2
0.5 s
10 pA

Fig. 4B: Current-voltage graph of the single-channel current amplitude plotted against transpatch potential from the same experiment as the current records of Fig. 3A. The relationship is linear at hyperpolarized potentials, although there are deviations at depolarized potentials. This type of I/V relationship indicates inward rectification of the chloride channel.

The line drawn on the graph at hyperpolarized potentials was calculated by linear regression. The calculated conductance was 220 pS. The line drawn at depolarized potentials was drawn by eye.

Patch type: isolated inside-out patch.

Solutions: Symmetrical solutions of *Ascaris* Ringer.

Temperature: 30°C.

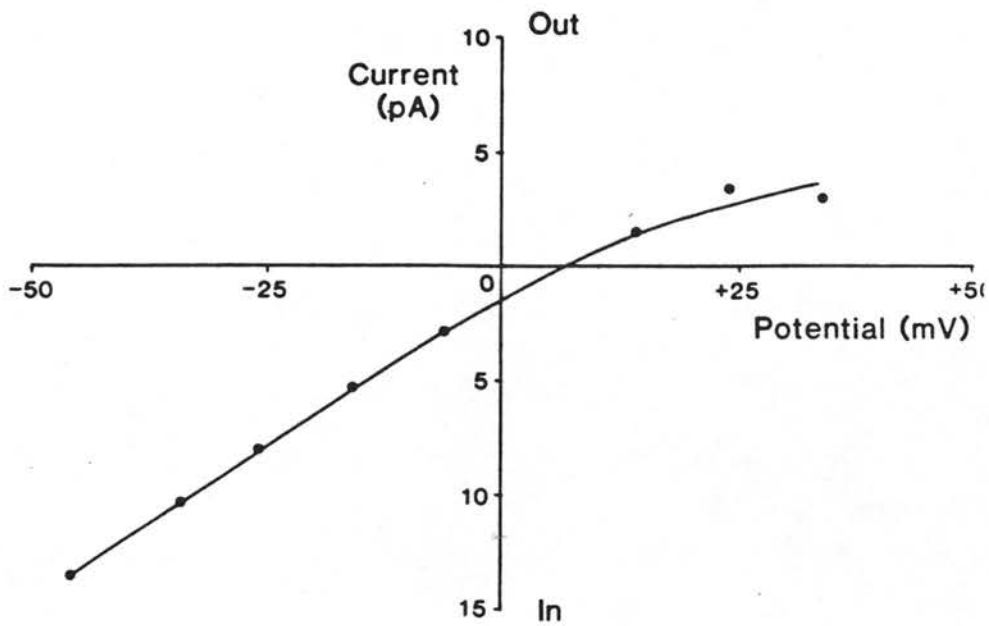
Out
10
Current
(pA)
5
−50
−25
0
+25
Potential (mV)
5
10
15
In

Fig. 4B shows the I/V plot of the high conductance channel obtained from the same experiment as the current records in Fig. 4A. The I/V plot was linear in the hyperpolarizing, range but the reduced current amplitudes in the depolarizing range indicate a reduction in the conductance. This graph is typical of the I/V plots and indicates that inward current could pass more easily through the channel than outward current. The single channel current records showed a reduced channel conductance when the patch was depolarized. The points obtained between transpatch potentials of 0 and -50 mV were linear. The line drawn in Fig. 4B for hyperpolarized values was obtained by linear regression. In the range of potentials from 0 to +50 mV the points obtained were non-linear and the line was drawn by eye. The mean conductance calculated from the linear portion of the I/V plot was 200 +/-7 pS (mean +/- SE) for 20 experiments in Ascaris Ringer.

Chloride Channel Permeability

The next series of experiments were carried out to determine the selectivity of the channel to different ion species. Initially the experiments were designed to look at the reversible effects of ion substitution in the bathing Ringer using isolated inside-out patches. The success of these experiments was limited by the irreversible loss of channel currents when perfusing an isolated inside-out patch. Yellen (1982) patch-clamped neuroblastoma cells and used a microperfusion method employing a multibarelled pipette delivery

system to perfuse the intracellular surface of isolated inside-out patches. Gray et al (1984) used a microperfusion system where the intracellular surface of an isolated inside-out patch was placed in a small bowl that contained Ringer flowing out at a slow rate. Both these methods were used, but in both cases loss of channel currents still occurred. Various other methods were used to enclose or shield the patch from the direct flow of the perfusing Ringer with no success. Later experiments were performed where the patch was isolated in bathing solutions of a different composition and no attempt was made to change the solution after patch isolation. In these experiments reversible changes in parameters such as conductance, reversal potential etc, could not be demonstrated, but the permeability and the selectivity of the channels could be studied.

Preliminary experiments (N=10) where the Ringer in the pipette was changed for a Ringer diluted by one fifth (the osmolarity was adjusted by the addition of sucrose), indicated that the high conductance channel was selectively permeable to anions. In these experiments the reversal potential of the currents was expected to shift by 40 mV in the depolarizing direction if the channel was selective to anions and 40 mV in the hyperpolarizing direction if the channel was selectively permeable to cations. The magnitude of the predicted shifts were calculated using the Nernst equation. All the experiments showed a shift in the depolarizing direction of up to 40 mV and this was taken to indicate that the channel was selectively

Fig. 5: A current voltage graph of single channel current amplitude against the transpatch potential of an isolated inside-out patch, with Tris Ringer in the pipette.
The circles represent the points obtained with Tris Ringer on the extracellular side of membrane patch and Ascaris Ringer on the intracellular side.
The squares represent the points obtained from the same experiment with Tris Ringer on both the intracellular side and the extra cellular side of the membrane patch.

Insert: In the top left hand corner is an example of the current records obtained at -15.3 mV with Tris Ringer on both sides of the patch. The channel opening is in the downward direction.

Patch type: isolated inside-out patch.
Solutions: a. (circles) Ascaris Ringer in bath, Tris Ringer in the pipette.
b. (squares) symmetrical Tris Ringer.
Temperature: 30°C.

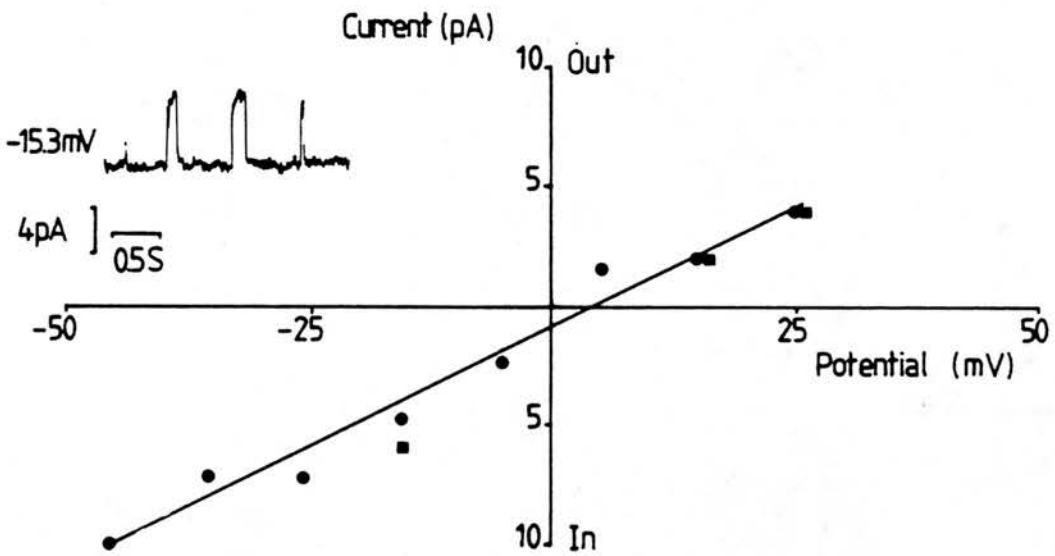
Current (pA)
10
Out
5
-15.3mV
4pA
0.5S
-50
-25
25
50
Potential (mV)
5
10
In

permeable to anions.

In 7 experiments where the cations were replaced with the large impermeant cation Tris, the channel conductance and the reversal potential of the channel currents showed no apparent change. Fig. 5 shows an I/V plot taken from an isolated inside-out patch experiment performed in this series. The pipette contained Tris Ringer and the bath contained Ascaris Ringer. Also shown are three points (squares) obtained from the same patch where the bathing solution was changed for Tris Ringer. The mean conductance from these experiments was 204 +/- 16 pS (mean +/- SE). These experiments were taken to indicate that the channel was not appreciably permeable to cations since the total removal of the permeant cations had no effect on the channel.

Fig. 6 illustrates the effect of a reduction of the chloride concentration on the intracellular side of an isolated inside-out patch. Fig. 6A shows the I/V relationship and Fig. 6B shows representative examples of the current records before and after reduction in the chloride concentration. The patch was isolated in Ascaris Ringer, and the I/V plot was drawn from the current records, obtained from the currents at different holding potentials. The slope of the line measured by linear regression gave a conductance of 200 pS. The patch was then perfused with a Ringer, where the chloride concentration was lowered to 90 mM by

Fig. 6A: A current-voltage relationship of the channel current amplitudes plotted against transpatch potential. The solution on the extracellular side of the patch was Tris Ringer throughout this experiment. The bathing solution at the intracellular surface of the patch was changed from Ascaris Ringer to a low-chloride Ascaris Ringer (90 mM chloride). The squares on the graph show the points obtained with Ascaris Ringer at the intracellular surface of the patch. The triangles represent the points obtained with low-chloride Ascaris Ringer at the intracellular surface of the patch. The circles represent the points obtained after returning to Ascaris Ringer. Lines were calculated by linear regression.
Continuous line: Ascaris Ringer intracellular (conductance =200 pS). Dotted line: Low chloride Ascaris Ringer (conductance = 100 pS)

Fig. 6B: Examples of current records obtained from the same experiment as that in Fig. 6A. The upper record shows channel records obtained with Ascaris Ringer at the intracellular surface of the patch, at a transpatch potential of -35 mV. The lower record shows channel records obtained with low-chloride Ascaris Ringer at the intracellular surface of the patch, at a transpatch potential of -35 mV.

Patch Type: isolated inside-out patch.

Temperature: 30°C.

A

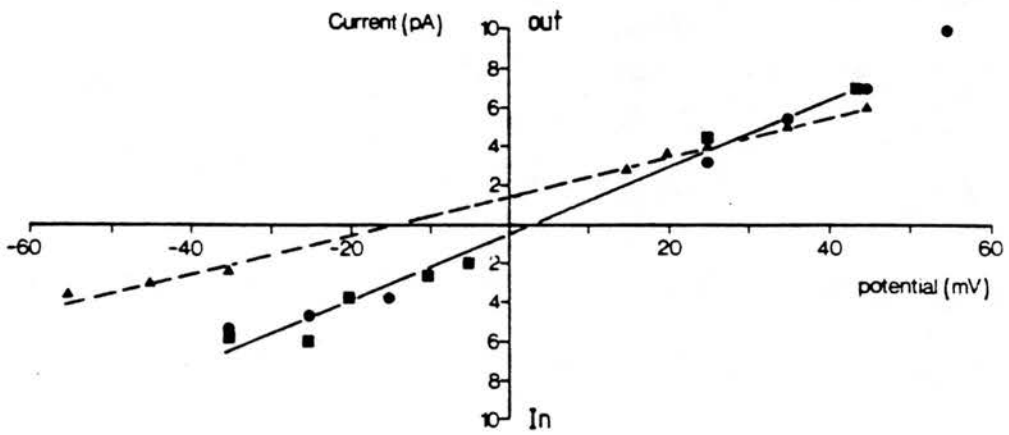
Current (pA)
out
In
potential (mV)
-60
-40
-20
20
40
60
10
8
6
4
2

B

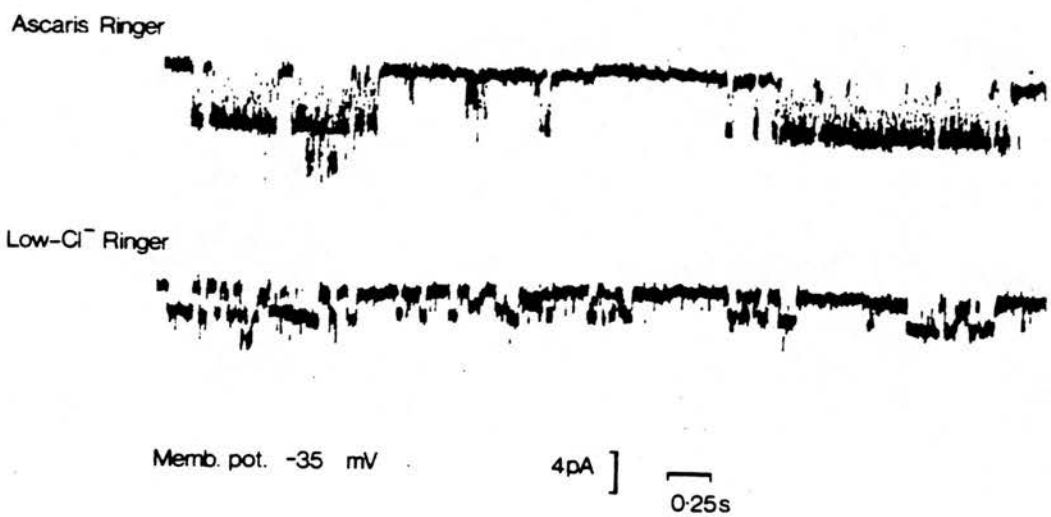
Ascaris Ringer
Low-Cl⁻ Ringer
Memb. pot. -35 mV
4pA
0·25s

substitution of chloride with acetate. The I/V plot was then drawn from the current records and gave a calculated conductance of 100 pS. Finally the patch was perfused with Ascaris Ringer. The effect of this change in the chloride concentration was to produce a reversible hyperpolarizing shift in the reversal potential, and a reduction in the conductance. The shift in reversal potential was 18 mV, exactly that predicted by the Nernst equation for a chloride selective channel. The conductance changed from 200 pS with Ascaris Ringer on both sides of the membrane, to 100 pS with the low chloride Ringer on the intracellular side of the patch. This reduction in conductance is predicted by the Goldman Constant Field Equation for a channel permeable to chloride.

The problems associated with the perfusion of isolated inside-out patches led to the use of cell-attached patches in which the bathing Ringer was replaced with a zero chloride Ringer, again by the replacement of the chloride with acetate. Fig. 7 shows an I/V plot from a cell-attached patch where the bathing Ringer was changed for a chloride free Ringer. In 10 experiments conducted in this way all showed a hyperpolarizing shift in the reversal potential. However interpretation of these results was difficult. Quantification of the shift in terms of the predicted Nernst equation was impossible, because the intracellular chloride concentration was unknown. After the reduction in the resting potential of the cells due to enzyme treatment (see methods), it was thought to be unlikely that the cells would be able to control the intracellular chloride

Fig. 7: The current-voltage graph plotted from an experiment on a cell-attached patch with Ascaris Ringer in the pipette. The bathing Ringer was replaced with a chloride-free Ascaris Ringer. The triangle represent the points obtained with Ascaris Ringer in the bath. The crosses represent the points obtained with chloride-free Ascaris Ringer in the bath.
Lines were calculated by linear regression.
The line through the triangles had a calculated conductance of 225 pS and a reversal potential of +3 mV.
The line through the crosses had a calculated conductance of 174 pS and a reversal potential of -12 mV.

Patch type: cell-attached patch.
Solutions: a: in the pipette, Ascaris Ringer; in the bath, Ascaris Ringer.
b: in the pipette Ascaris Ringer, in the bath chloride-free Ascaris Ringer.
Temperature: 30°C.

I/V Plot from Cell-attached Patch.
AR/AR and AR/Cl-Free Ringer

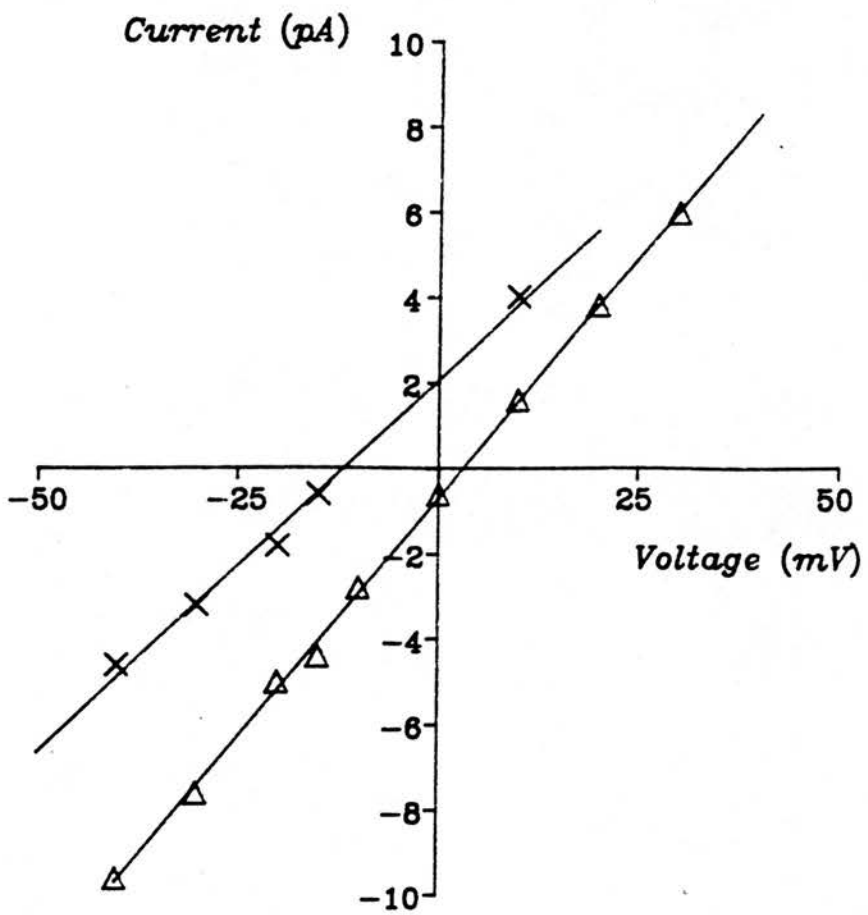

Fig. 8: The current-voltage graph plotted from an experiment on an isolated inside-out patch, with 250 mM KCl in the pipette and 200 mM KCl in the bath. The line was drawn by linear regression from the linear portion of the graph.
The calculated conductance was 247 pS, and the reversal potential was -6.7 mV.

Patch type: isolated inside-out patch.
Solutions: 250 mM KCl on the extracellular surface of the patch, 200 mM KCl on the intracellular surface of the patch.
Temperature: 30°C.

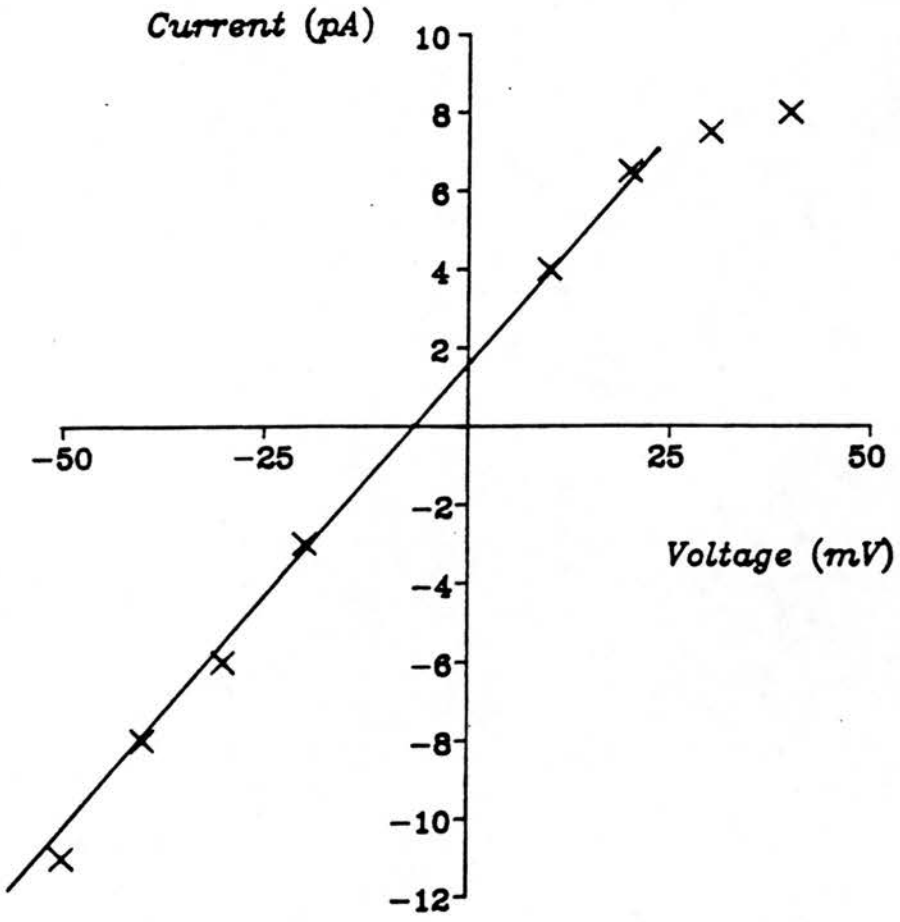
Current (pA)
10
8
6
4
2
-50
-25
25
50
-2
-4
-6
-8
-10
-12
Voltage (mV)

concentration. Martin (1985) measured the reversal potential of the GABA response in Ascaris somatic muscle cell bodies, before and after application of collagenase. The reversal potential was -65 mV before collagenase treatment and -7 mV after collagenase treatment (Martin 1985). This observation was taken to indicate an increased intracellular chloride concentration. The reduction in the chloride concentration of the bathing Ringer, would therefore be expected to lead to an efflux of chloride from the cells. The extent of this efflux and the effect on the resting potential of this change were unknown. If the effect on the resting membrane potential of the cells was according to a simple Donnan Equilibrium, then its direction would be the same as that observed for the reversal potential of the currents, and could explain these shifts whether the channel was cation or anion selective. The results from these experiments are difficult to interpret in the light of these facts.

Experiments were carried out where the patch was isolated into bathing Ringers of different composition to the solution in the pipette. The solutions used in these experiments contained KCl as the major salt, with a low concentration of calcium and HEPES buffer. The inclusion of calcium in the pipette was found to be necessary; without it seals were very difficult to form.

Fig. 8 shows the I/V plot obtained from an isolated inside-out patch with 250 mM KCl on the extracellular surface of

Fig. 9: The current-voltage graph plotted from an experiment on an isolated inside-out patch, with 50 mM KCl in the pipette and 200 mM KCl in the bath.
The line was drawn by linear regression.
The calculated conductance was 122 pS and the reversal potential was +39 mV.

Patch type: isolated inside-out patch.
Solutions: 50 mM KCl at the extracellular surface of the patch, 200 mM KCl at the intracellular surface of the patch.
Temperature: 30°C.

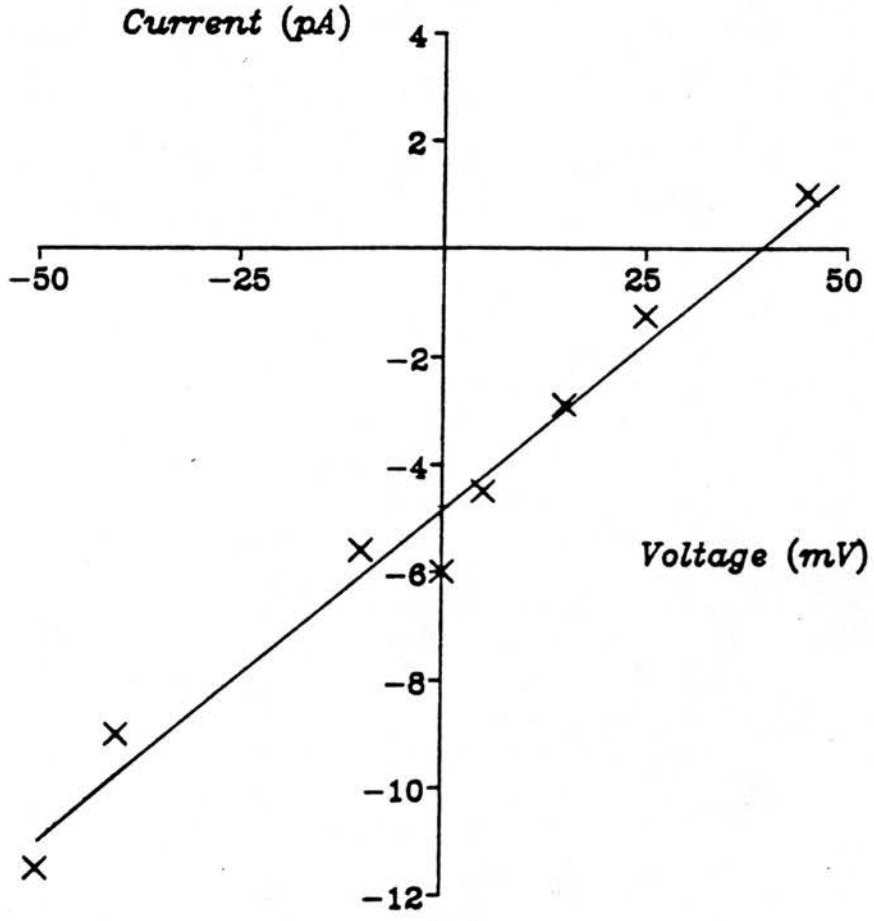
Current (pA)
4
2
−50
−25
25
50
−2
−4
−6
−8
−10
−12
Voltage (mV)

the patch (pipette) and 200 mM KCl on the intracellular surface (bath). The reversal potential was observed to be -5.7 mV. Fig. 9 shows the I/V plot obtained from an isolated inside-out patch with 50 mM KCl on the extracellular surface of the patch (pipette) and 200 mM KCl on the intracellular surface (bath). The reversal potential was +35.7 mV. Other experiments were performed with different gradients of the ions across the patch. It was found that the production of seals was considerably easier when the concentration of ions in the pipette was higher than that of the bath. This was presumed to be the result of an osmotic gradient.

To estimate the permeability ratio of the channel for potassium over chloride the derivation of the Goldman-Hodgkin-Katz (Hodgkin and Katz 1949) equation was used:-

$$E_{eq} = \frac{RT}{F} \ln \frac{P_j[C_j]_o + P_k[A_k]_i}{P_j[C_j]_i + P_k[A_k]_o} \quad \ldots(1)$$

where:

R, T, F, have their usual meanings

P_j is the permeability of the j_{th} cation

C_j is the concentration of the j_{th} cation

P_k is the permeability of the k_{th} anion

A_k is the concentration of the k_{th} anion

E_{eq} is the equilibrium potential

In KCl solutions:

$$E_{eq} = \frac{RT}{F} \ln \frac{P_k/P_{cl}[K]_o + [Cl]_i}{P_k/P_{cl}[K]_i + [Cl]_o} \quad \ldots.(2)$$

For the experiment illustrated in Fig. 8 the P_K/P_{Cl} ratio was measured as 0.009, and for that of Fig. 9 the ratio was measured as 0.09. From these results it can be seen that the channel was highly selective for anions over cations. This is in close agreement with the permeability ratios calculated by Gray et al (1984) for potassium and chloride in the chloride channel of Schwann cells.

The permeability of the channel was calculated using the equation 4 for the experiment illustrated in Fig. 3. The channel amplitude at -10 mV was used in this equation, and the channel was assumed to be exclusively permeable to chloride. The equation used was:-

$$I = \frac{F^2 PV}{RT} \frac{[Cl]_o - e^{FV/RT}[Cl]_i}{e^{FV/RT}} e^{FV/RT} \quad ..(3)$$

In symmetrical solutions this equation simplifies to :-

$$I = \frac{F^2 PV [Cl]}{RT} \quad .....(4)$$

Fig. 10: A graph of the single channel conductance of the chloride channel plotted against the concentration of NaCl. Conductances calculated by linear regression for each patch. The points plotted are the mean +/- S.E. of the conductances of at least four isolated inside-out patches bathed in symmetrical NaCl Ringer (see Table 1).

The line was fitted by non-linear regression to the equation:

$$g = G_{max} \cdot [Cl] / (K_m + [Cl])$$

where:

$$G_{max} = 422 pS \text{ and } K_m = 188 mM.$$

Patch types: isolated inside-out patches.

Solutions: NaCl solutions from 50 mM to 500 mM.

Temperature: $30^{\circ}C$.

Graph of NaCl concentration against Channel Conductance

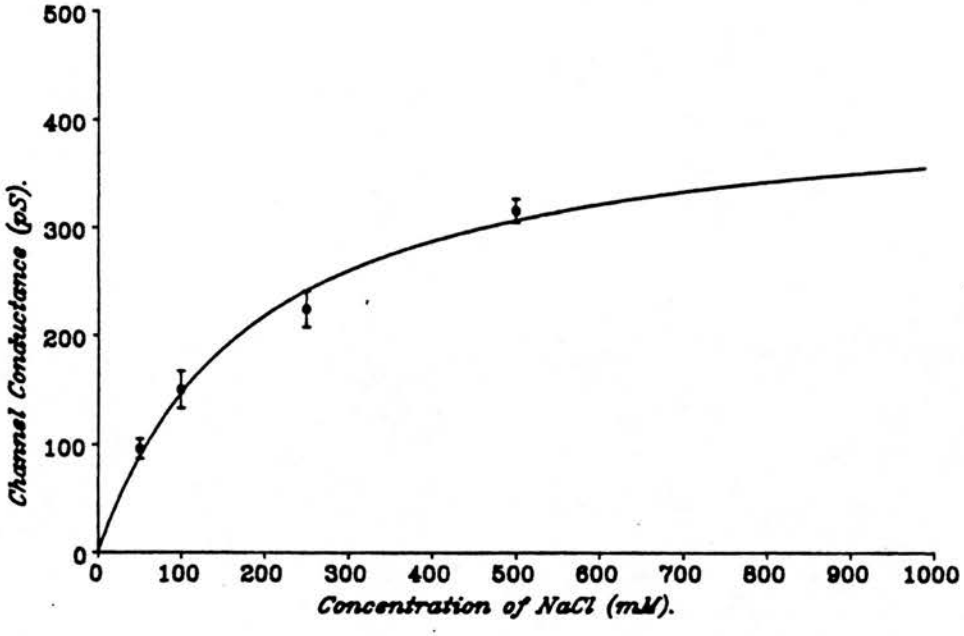

Where I is the current; V is the transpatch potential; R and F have their usual values and T was 303^{o} K.

The permeability of the channel using the above equation was calculated to be 8.79×10^{-13} cm^3s^{-1}.

Channel Saturation

If the channel obeyed the Goldman Constant field equation then increasing the ion concentration would give an increased conductance of the channel.

Fig. 10 illustrates a graph of single channel conductance against NaCl concentration obtained from a series of 16 experiments, each point representing the mean and standard error of 4 patches. The patches were all obtained from different cells, and all were isolated inside-out patches. The solutions used in these experiments had NaCl as the major salt with 1 mM calcium and 5 mM HEPES buffer. The Goldman Constant Field equation predicts a relationship between conductance and chloride concentration :-

$$g = \frac{F^2 .P.[Cl]}{RT} \quad \text{.....(5)}$$

The line drawn on the graph (Fig. 10) was fitted using non-linear regression according to a simple Michaelis-Menton

equation, using the 'Patternsearch' programme of Colquhoun (1971) adapted by R.J.Martin. The general equation was :-

$$g = G_{max} \cdot Cl / (K_m + Cl) \quad \ldots\ldots\ldots (6)$$

Where g is the conductance; G_{max} is the conductance at saturating chloride concentration; K_m is the chloride concentration producing half maximum channel conductance. The equation is based on the following simple reaction scheme :-

$$Cl_o + R = ClR = ClR = R + Cl_i \quad \ldots\ldots\ldots (7)$$

The simple saturation observed, is usually taken to indicate a single file model for ion permeation through the channel where only one ion is present inside the channel, at any one time (Hille 1983).

Chloride Channel Sub-Conductance States

The occurrence of channel openings to an amplitude below that of the full conductance state has been observed for many channels (for example Benham and Bolton 1983). Sub-conductance states were observed in the Ascaris chloride channel, only when the transpatch potential was depolarized. Fig. 11A shows an example of the current records obtained from an isolated inside-out patch held at +30 mV. The figure illustrates the types of openings that were taken to indicate the existence of sub-conductance states. In the figure the channel openings are

Fig. 11A: Channel current records from an experiment on an isolated inside-out patch showing subconductance states. On the right hand side of the figure the closed state is indicated by 'C', the main open state is shown by 'O' and the sub-conductance state is shown by 'Sc_1'.

Patch type: isolated inside-out patch.

Solutions: symmetrical solutions of Ascaris Ringer.

Temperature: 30°C.

Transpatch potential: +30 mV.

Potential +30 mV

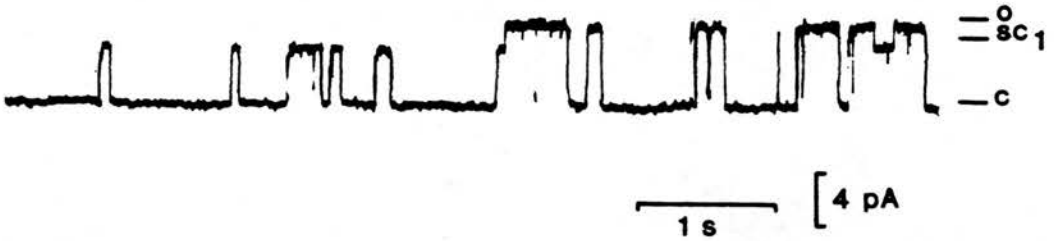

upward (outward). Initially the channel is closed and the first few openings are of a small amplitude. The channel then shows another opening to this small amplitude, which is followed by a further current step up to the full conductance state. The full conductance state was defined as the channel amplitude that had the same conductance as the single channel openings found during hyperpolarization. There follow a few closing flickers and then the current level drops indicating complete channel closure. This is followed by a complete channel opening where no discernible 'notch' or pause is seen at the previous sub-conductance current level. Further on in the current records, the channel is seen to change from the full conductance state to the sub-conductance current level and back.

Instantaneous current transitions from full to closed, and from closed to full and sub-conductance levels were taken as evidence that a single channel was capable of existing in more than one conductance state, in this case, two. Other explanations of this type of current trace would require that there were two channels carrying current in opposite directions. They would have to be linked in some way to account for the observation that the postulated smaller inward current carrying channel was not seen to open in the absence of the postulated larger outward channel currents. Alternatively two channels carrying the current in the same direction could be postulated, but again, the simultaneous closure and opening of these two postulated channels would require that they be linked. Current

Fig. 11B: A current-voltage graph drawn from the same experiment as in Fig. 11A on a cell-attached patch which showed sub-conductance states. The circles show the points obtained from the current amplitudes at the full conductance state of the channel. The triangles show the points obtained from the amplitudes of the sub-conductance states of the channel. Sub-conductance states were only seen at depolarized transpatch potentials.

Patch type: cell-attached patch.

Solutions: symmetrical solutions of Ascaris Ringer.

Temperature: 30°C.

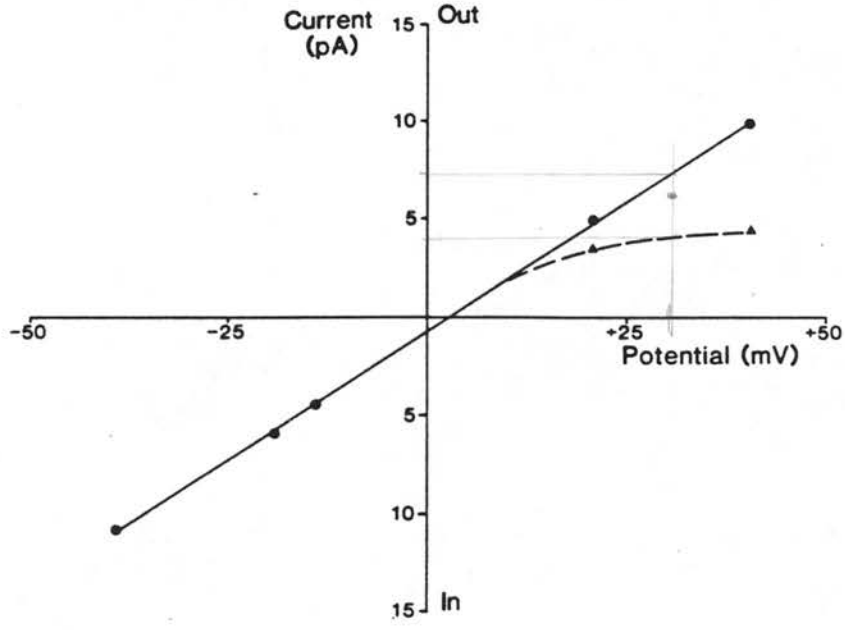
Current
(pA)
Out
15
10
5
-50
-25
+25
+50
Potential (mV)
5
10
15
In

records like those of Fig. 11A were seen in about 1 in 5 patches.

Fig. 11B shows the I/V plot drawn from the same experiment as the current records of Fig. 11A. The reduced conductance states in the depolarizing range of the holding potentials are illustrated in the figure as well as the full conductance channel currents. The phenomena of inward rectification, that is, the passage of greater current when hyperpolarized, of this channel has been described in the Ascaris chloride channel (see Fig. 4A). The I/V plot of the sub-conductance states are similar to many I/V plots of the chloride channel where only one conductance state was observed. This suggests that the apparent maximal channel amplitudes in the depolarized range, are in fact observations of channel openings to sub-conductance states in the absence of full channel amplitude openings. The channel amplitude may therefore be said to be voltage sensitive, reflecting the prevalence of sub-conductance states when the patch is depolarized.

Voltage Sensitivity

The voltage sensitivity of this channel was quantified in terms of the probability of opening and the mean open time. It was of interest to study the voltage sensitivity because of the reports of other chloride channels in skeletal muscle (Blatz and Magleby 1983) and epithelial cells (Nelson et al 1984), both of

Fig. 12: Examples of current records taken from an experiment on a cell-attached patch. The patch was held at the four different transpatch potentials of -40 mV, -20 mV, +30 mV and +60 mV indicated on the figure. The current levels with 0,1,2, and 3 channels open, are shown on the figure by C, O_1 ,O_2 ,O_3, respectively. Up to three channels are simultaneously open at the hyperpolarized potentials. One channel is open when the patch is depolarized.

Patch type: cell-attached patch.

Solution: symmetrical solutions of Ascaris Ringer.

Temperature: 30°C.

Transpatch potentials: -40 mV, -20 mV, +30 mV, +60 mV.

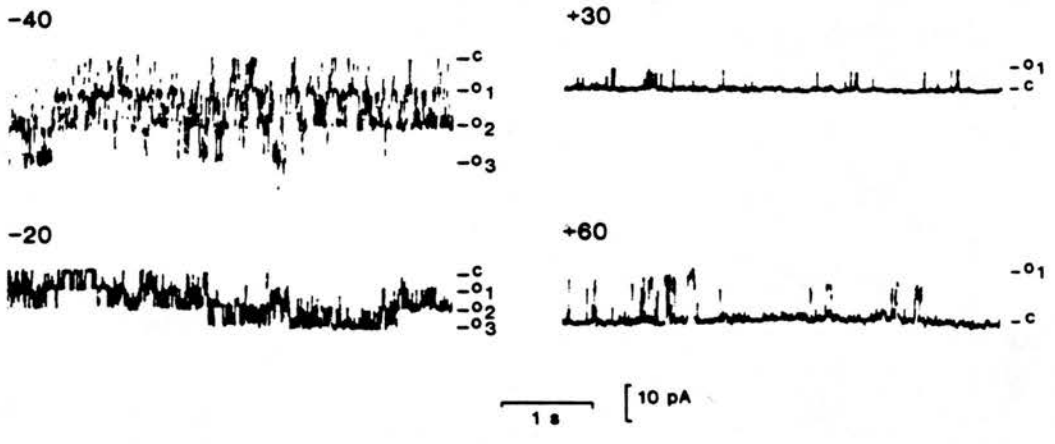
-40
-c
-o1
-o2
-o3
+30
-o1
-c
-20
-c
-o1
-o2
-o3
+60
-o1
-c
1 s
10 pA

which show inactivation with the transpatch potential held away from 0 mV. This channel has already been described as having a voltage sensitive conductance, reducing on depolarization.

Fig. 12 shows the current records obtained from a cell-attached patch and illustrates the behaviour of the channels at different applied potentials. The current records show that more than one channel was present in the patch. The opening of each of the channels is indicated on the figure. The absolute transpatch potential of a cell-attached patch was unknown because it was offset by the resting membrane potential of the cell. Measures of the resting potential after collagenase treatment (see methods) show that the error was likely to be less than 15 mV. The number of channels simultaneously open decreases from three at -40 and -20 mV to one at +30 and +60 mV. Depolarization of the patch reduced the open time and also the probability of opening.

It was of interest to attempt to quantify the effect of voltage on the open time and the probability of opening. Channel records from 11 experiments were analysed and the probability of opening and the mean open time obtained over a range of holding potentials were plotted. The distributions were then fitted using an analysis of variance BMDP programme by 3 functions: straight line, square and cubic. The residual sums of squares and the regression coefficent were used to determine the function that best fitted each distribution. In some cases the

Fig. 13A: Graphs of mean channel open time plotted against patch potential for 2 experiments. The crosses represent the mean open time obtained from computer analysis plotted against the transpatch potential. The lines on the graphs were fitted using polynomial regression.

The best fit for these two experiments was obtained using a linear relationship and the fitted lines are drawn on the graphs. Polynomials of further degrees were fitted to the data but no significant improvement in the fit was observed.

Solutions: symmetrical solutions of Ascaris Ringer.

Temperature: 30°C.

Mean Open Time
Against Voltage.
Expt. 16123*E*

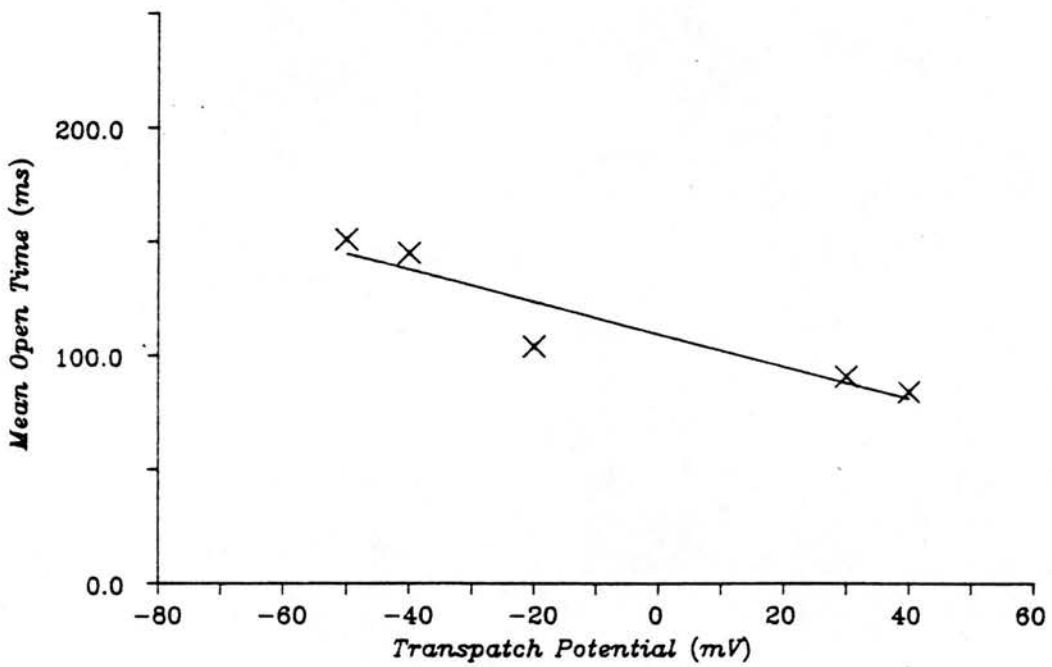

Expt. 91283*D*

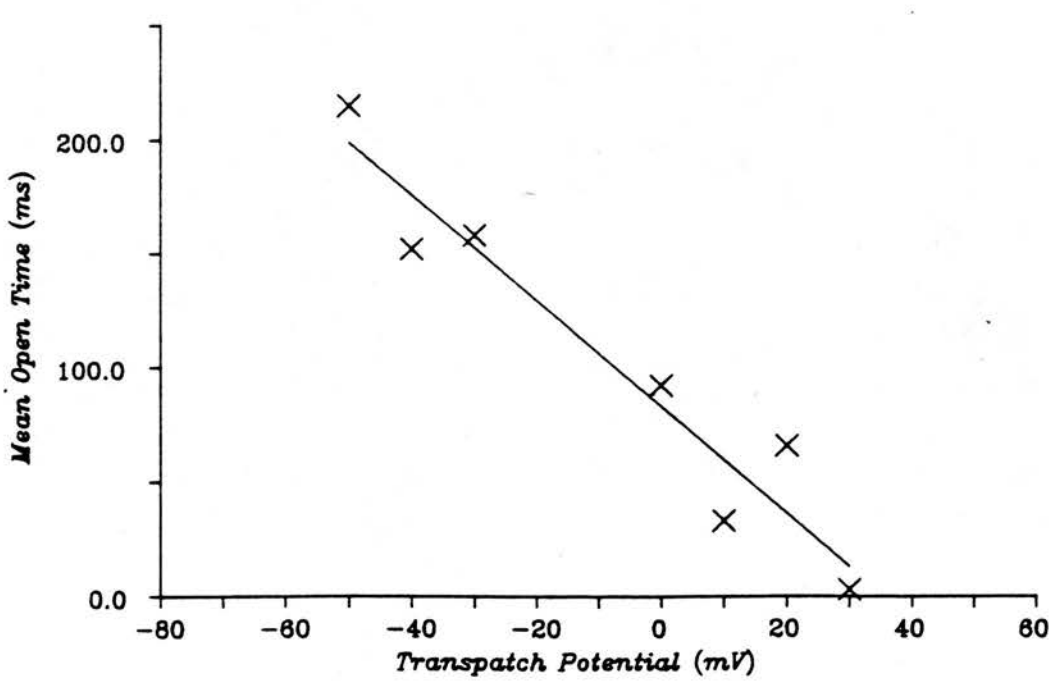

Fig. 13B: Graphs of mean channel open time plotted against patch potential for 3 experiments. The crosses represent the mean open time obtained from computer analysis plotted against the transpatch potential.

The lines on the graphs were fitted using polynomial regression.
The best fit for these three experiments was obtained using a cubic function and the fitted curves are drawn on the graphs.

Solutions: symmetrical solutions of Ascaris Ringer.
Temperature: 30°C.

Mean Open Time
Against Voltage.
Expt. 24113C

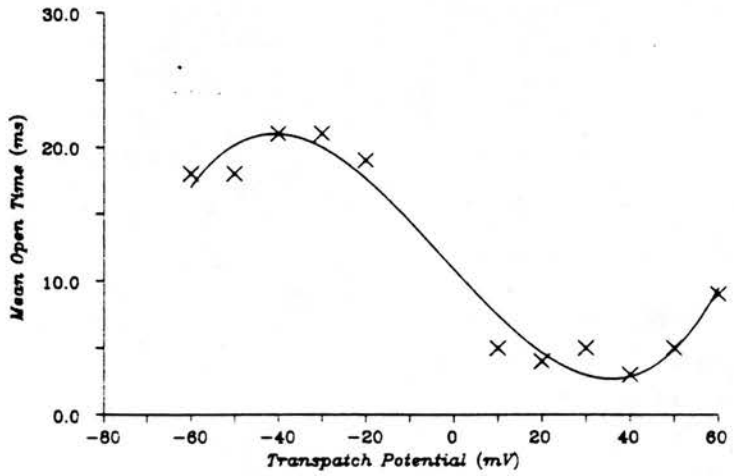

Expt. 14123B

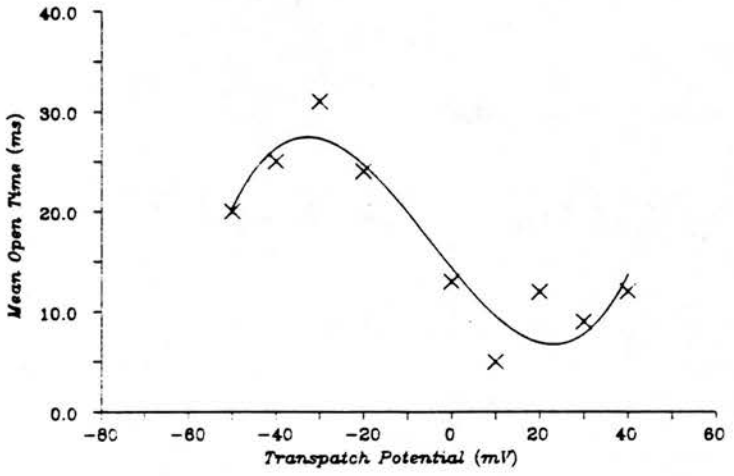

Expt. 27103A

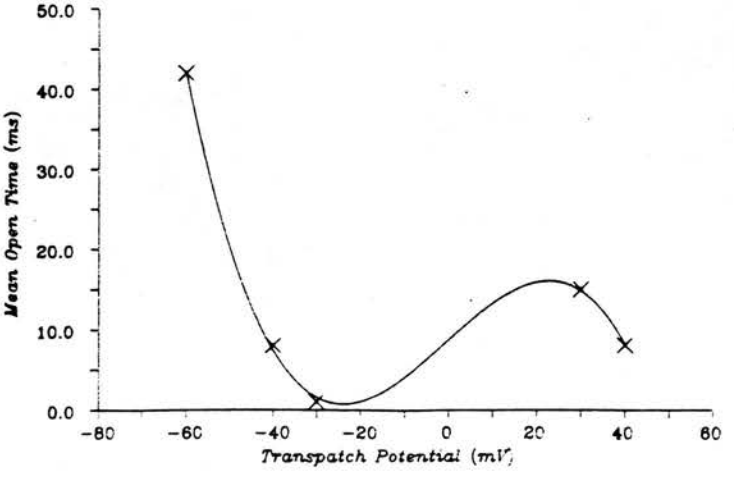

Fig. 13C: Graphs of mean channel open time plotted against patch potential for 2 experiments. The crosses represent the mean open time obtained from computer analysis plotted against the transpatch potential.

These two experiments could not be fitted adequately by polynomials up to 5 degrees.

Solutions: symmetrical solutions of Ascaris Ringer.

Temperature: 30°C.

Mean Open Time
Against Voltage.

Expt. 13123*B*

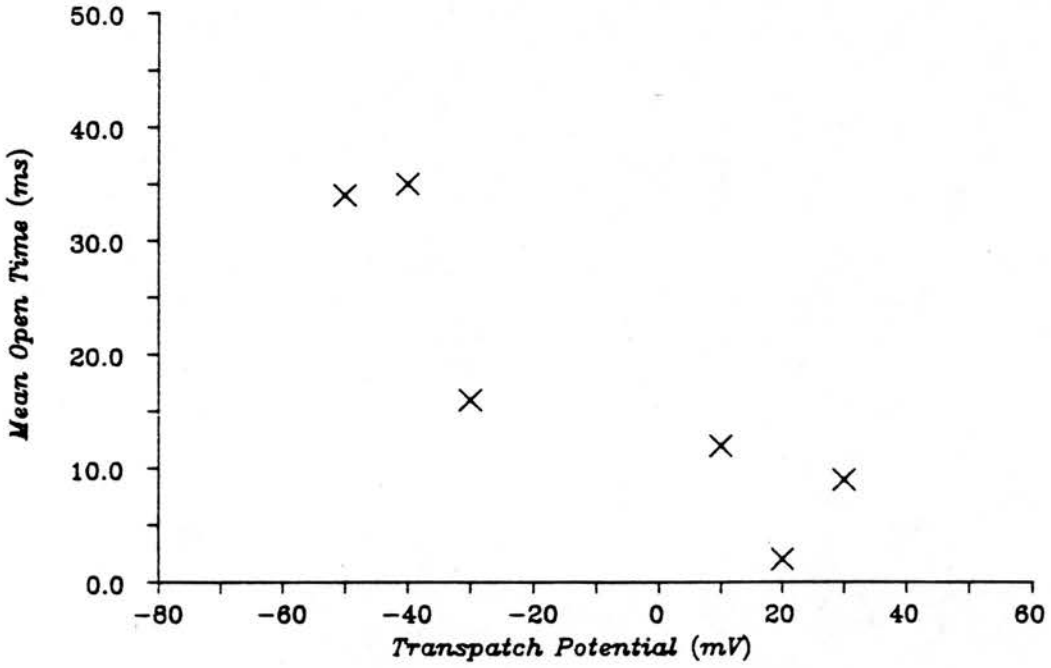

Expt. 23113*B*

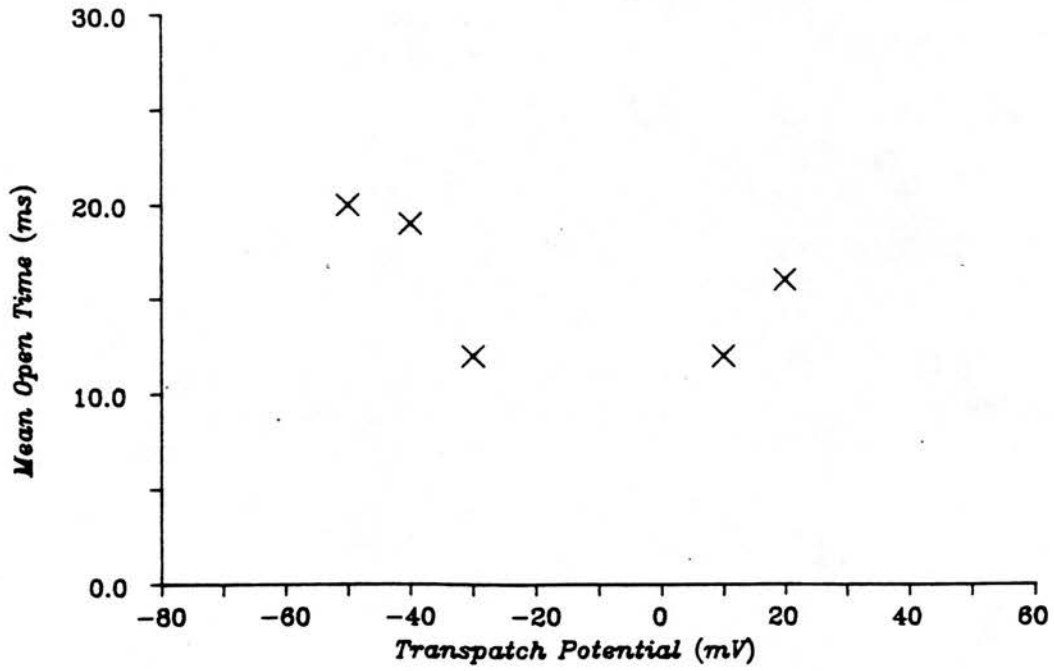

residual sums of squares and the correlation coefficent were no different for each of the fitted functions and for the purposes of these experiments the distribution was left unfitted. An assumption of this type of analysis is that the data are from a continuous function. The lack of observations at around 0 mV due to the low amplitude of the channels did not allow a test of the continuity of the distributions.

Fig. 13A, B and C show graphs of mean open time plotted against holding potential for 7 experiments. The function that best fitted the data is drawn on each graph. The 2 experiments in Fig. 13A were best fitted by a linear function, those in Fig. 13B were best fitted with a cubic function and those in Fig. 13C could not be fitted.

Fig. 13D, E and F show graphs of probability of opening against holding potential for 10 experiments. Again the function that was found to best fit the data is drawn on the graphs. Fig. 13D shows 5 experiments which were best fitted by a linear function, those experiments best fitted by a cubic function are shown in Fig. 13E and three experiments not fitted by any of the three functions are plotted in Fig. 13F.

A number of conclusions can be drawn from the plots of mean open time and probability of opening against voltage. Firstly, the graphs show the Ascaris chloride channel has a different voltage sensitivity than the high conductance, voltage sensitive anion channel channels (e.g. Blatz and Magleby 1983).

Fig. 13D: Graphs of probability of channel opening plotted against patch potential for 5 experiments. The crosses represent the probability of opening obtained from computer analysis plotted against the transpatch potential.

The lines on the graphs were fitted using polynomial regression.
The best fit for these five experiments was obtained using a linear function and the fitted lines are drawn on the graphs. An increase in the order of the polynomial did not result in a significant improvement of the fit.

Solutions: symmetrical solutions of Ascaris Ringer.
Temperature: 30°C.

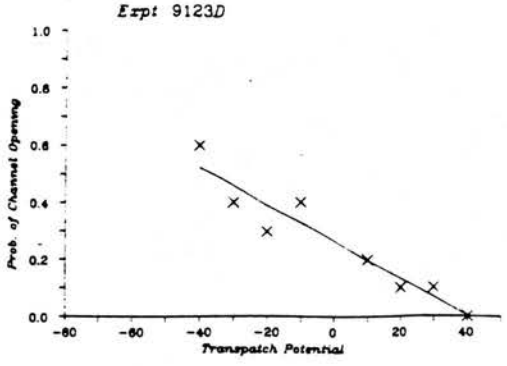
Expt 9123D
Prob. of Channel Opening
Transpatch Potential

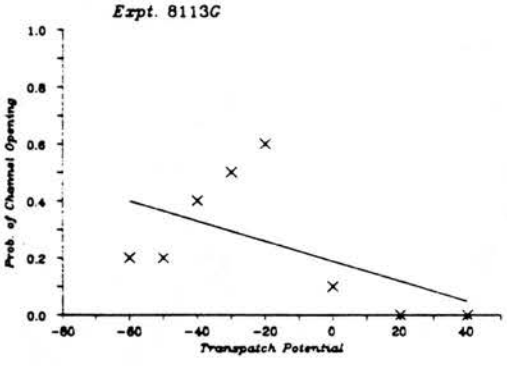
Expt. 8113C
Prob. of Channel Opening
Transpatch Potential

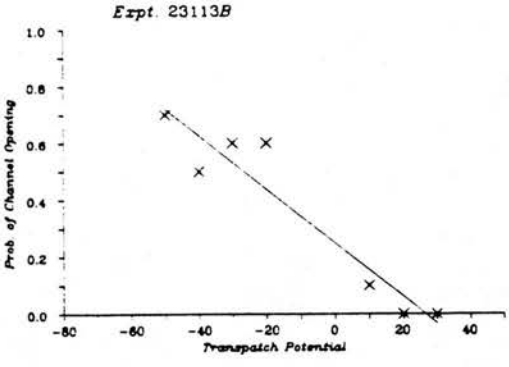
Expt. 23113B
Prob. of Channel Opening
Transpatch Potential

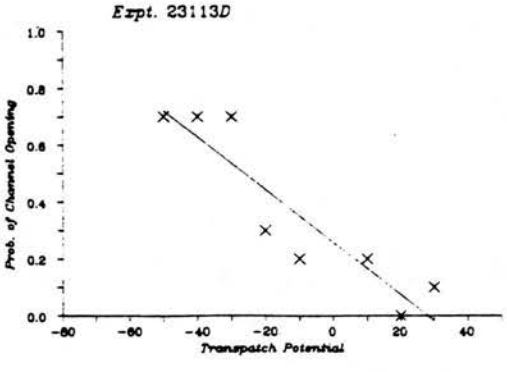
Expt. 23113D
Prob. of Channel Opening
Transpatch Potential

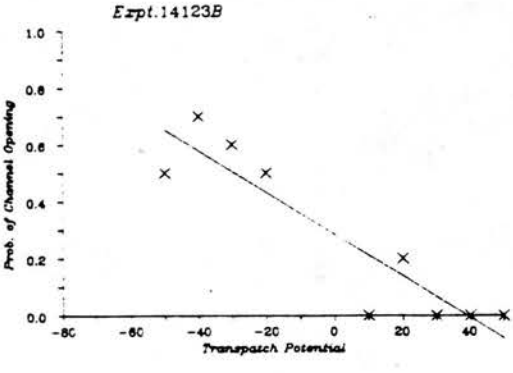
Expt.14123B
Prob. of Channel Opening
Transpatch Potential

Fig. 13E: Graphs of probability of channel opening plotted against patch potential for 2 experiments. The crosses represent the probability of opening obtained from computer analysis plotted against the transpatch potential.

The lines on the graphs were fitted using polynomial regression.
The best fit for these two experiments was obtained using a cubic function and the fitted curves are drawn on the graphs. In the upper graph the fitted curve drops below the axis at +25 mV. The actual probability of opening cannot be less than 0, therefore, the fitted line can only be taken as a mathematical approximation.

Solutions: symmetrical solutions of Ascaris Ringer.
Temperature: 30°C.

Probability of Channel Opening against Voltage
Expt. 24113C

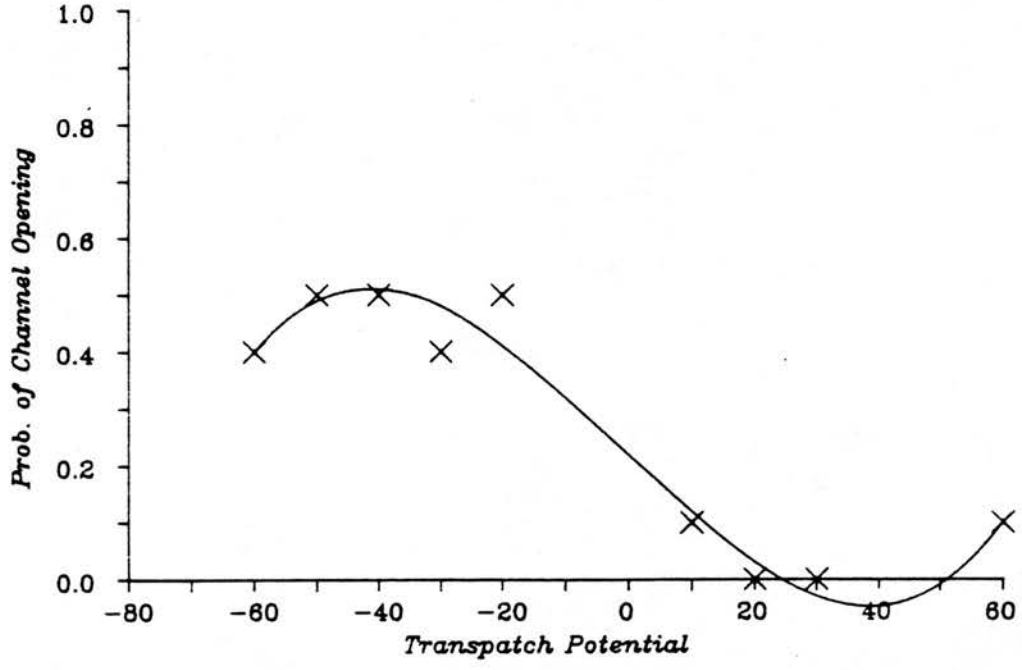

Expt. 16123E

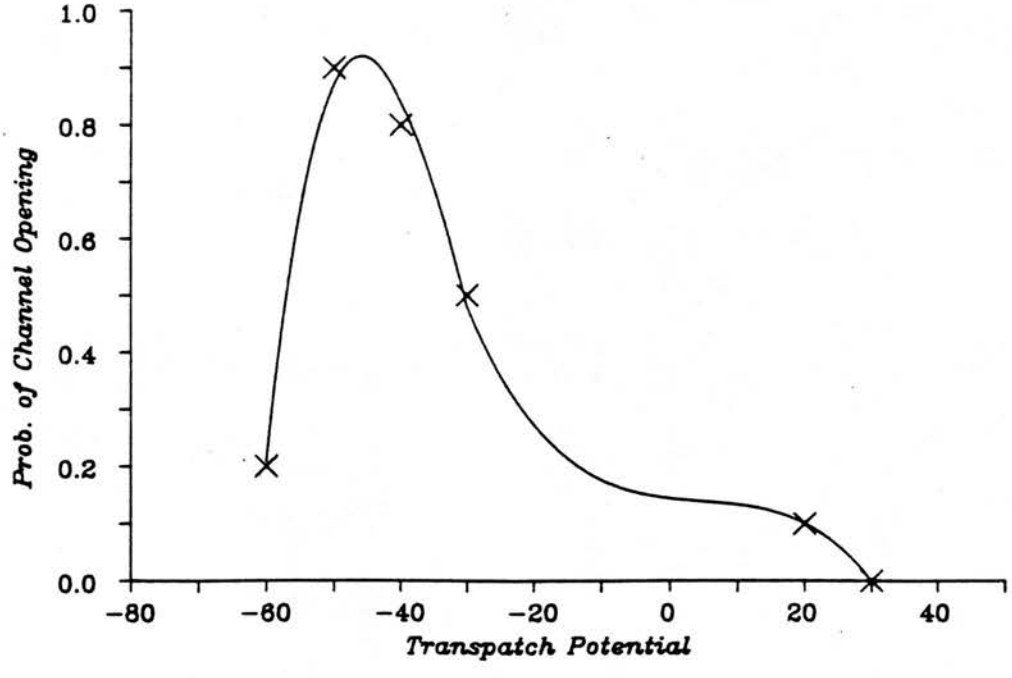

Fig. 13F: Graphs of probability of channel opening plotted against patch potential for 3 experiments. The crosses represent the probability of opening obtained from computer analysis plotted against the transpatch potential.

These three experiments could not be fitted adequately by polynomials up to 5 degrees.

Solutions: symmetrical solutions of Ascaris Ringer.

Temperature: 30°C.

Probability of Channel Opening against Voltage
Expt. 24113*E*

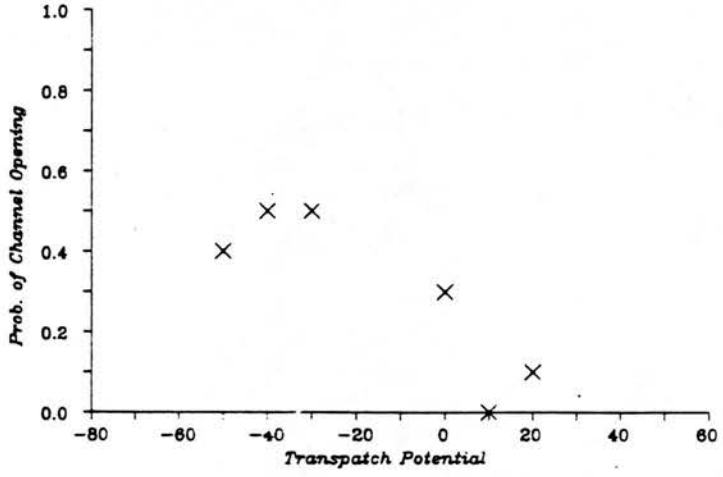

Expt. 10113*A*

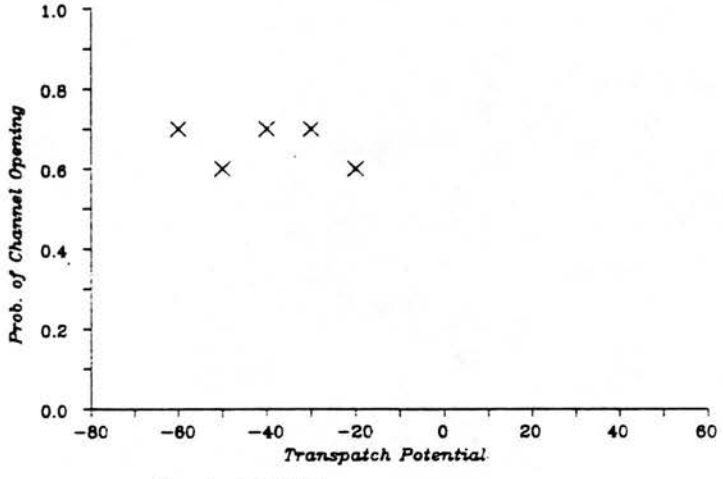

Expt. 13123*B*

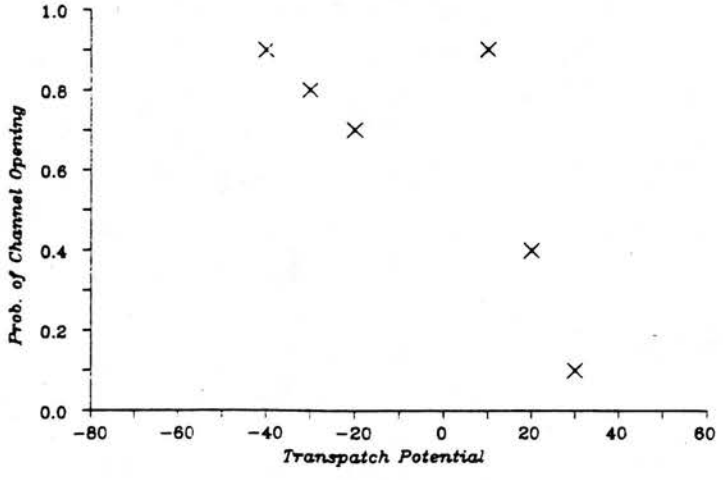

Secondly, the results show the distributions to be varied in different patches. Thirdly, the range of mean open times and probability of opening in different patches at the same holding potential demonstrate an interpatch variability. Fourthly, the distributions illustrate the difficulty in attempting to summarize the data into a coherent model. Fithly, with only two exceptions all the experiments show a reduction in the mean open time and probability of opening, when the data from depolarized potentials are compared with those at hyperpolarized potentials.

Distributions of Open and Closed Times

Results from an experiment on an isolated inside-out patch analysed by Dr.R.J.Martin show that the distributions of closed and open times can not be described by a simple single exponential. Fig. 14 shows open and closed time frequency histograms at -40 mV from an isolated-patch in symmetrical Ascaris Ringer. The records were obtained from a patch showing only a single channel opening held at -40mV. The open distribution (Fig. 14a and equation 8) at -40mV, was best described by two exponentials, which had a minor component (19% of the total openings) due to openings with a mean open time of 2.7 ms, and a major component (81% of the total openings) due to long openings with a mean open time of 61ms. The closed distribution at -40 mV (Fig. 14b and equation 5) was best described by three exponentials. There was a brief component that separated channel openings into bursts (61% of the total closings, mean closed time 1.1ms), a smaller component

Fig. 14: A: The open time histogram obtained from the analysis of an experiment on an isolated inside-out patch held at a transpatch potential of -40 mV. Only one channel was seen to open in this patch. A total of 410 channel openings were used in the production of the graph. The mean open time was 51.1 ms.

B: The closed time histogram obtained from the same record as the open time histogram. The graph was drawn from 409 closings and had a mean closed time of 13.6 ms.

Patch type: isolated inside-out patch.
Solution: symmetrical solutions of Ascaris Ringer.
Temperature: 30°C.

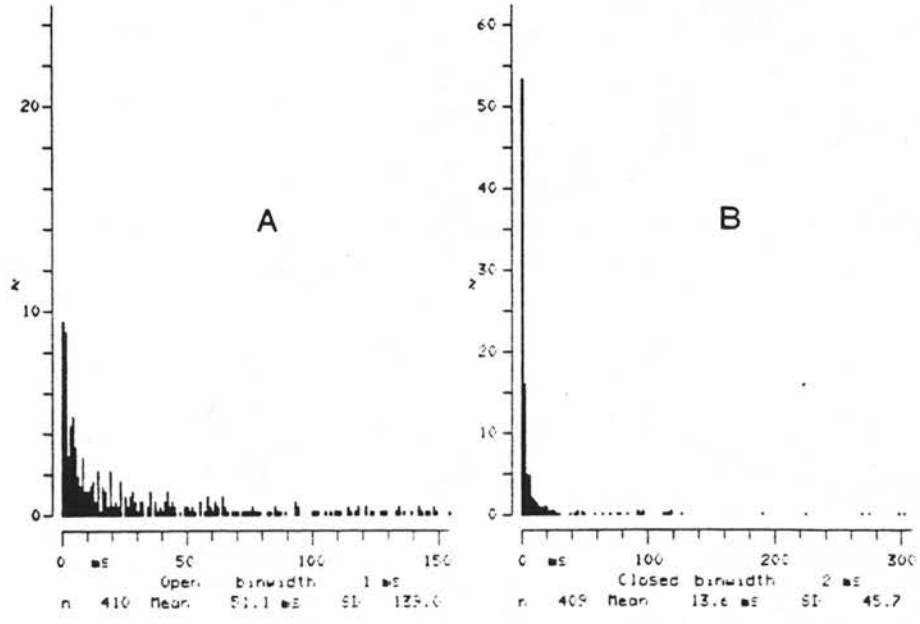
A
B
20
10
0
60
50
40
30
20
10
0
0 ms
50
100
150
0 ms
100
200
300
Open bin width 1 ms
n 410 Mean 51.1 ms SD 129.0
Closed bin width 2 ms
n 409 Mean 13.6 ms SD 45.7

separating bursts into clusters (18% of the total closings, mean closed time 10ms), and a third component separating clusters (21% of the total closings) had a mean closed time of 110 ms. These observations suggest the presence of at least two open states and three closed states at -40 mV.

$$P_{open} = 0.19/2.7\exp(-t/2.7) + 0.81/61\exp(-t/61).....(8)$$

$$P_{closed} = 0.61/1.1\exp(-t/1.1)+0.18/10\exp(-t/10)+0.21/110\exp(-t/110)..(9)$$

P is the probability density function, t is time in ms.

It is clear from these observations that the channel shows complex kinetics with the distributions of open and closed times suggesting multiple states.

Fig. 15: Graphical output of the 'Campion' programme that was used to collect and sort channel current amplitudes. The figure shows graphs obtained from a single experiment at 6 transpatch potentials. The graphs plot the frequency (expressed as a percentage of total observations) against current amplitude. For clarity the current scales on the x axis have been removed. In the first column the scales are :- 5 pA/div (top), 4 pA/div (middle), 2pA/div (bottom). In the second column the scales are:- 2 pA/div (top,middle and bottom).

The three graphs in first column were at -45 mV (top), -35 mV (middle) and -15 mV (bottom). The three graphs in the second column were at 14 mV (top), 34 mV (middle), 44 mV (bottom).

The peak where all channels are closed is shown on each graph at 'C'. The peaks with 1,2,3 channels open are indicated on the graphs by 'O_1, O_2, O_3 respectively. In this patch subconductance states were seen and are indicated by 'Sc'. The full conductance states indicated by 'Fc'.

Patch type: isolated inside-out patch.

Solutions: symmetrical solutions of Ascaris Ringer.

Temperature: 30°C.

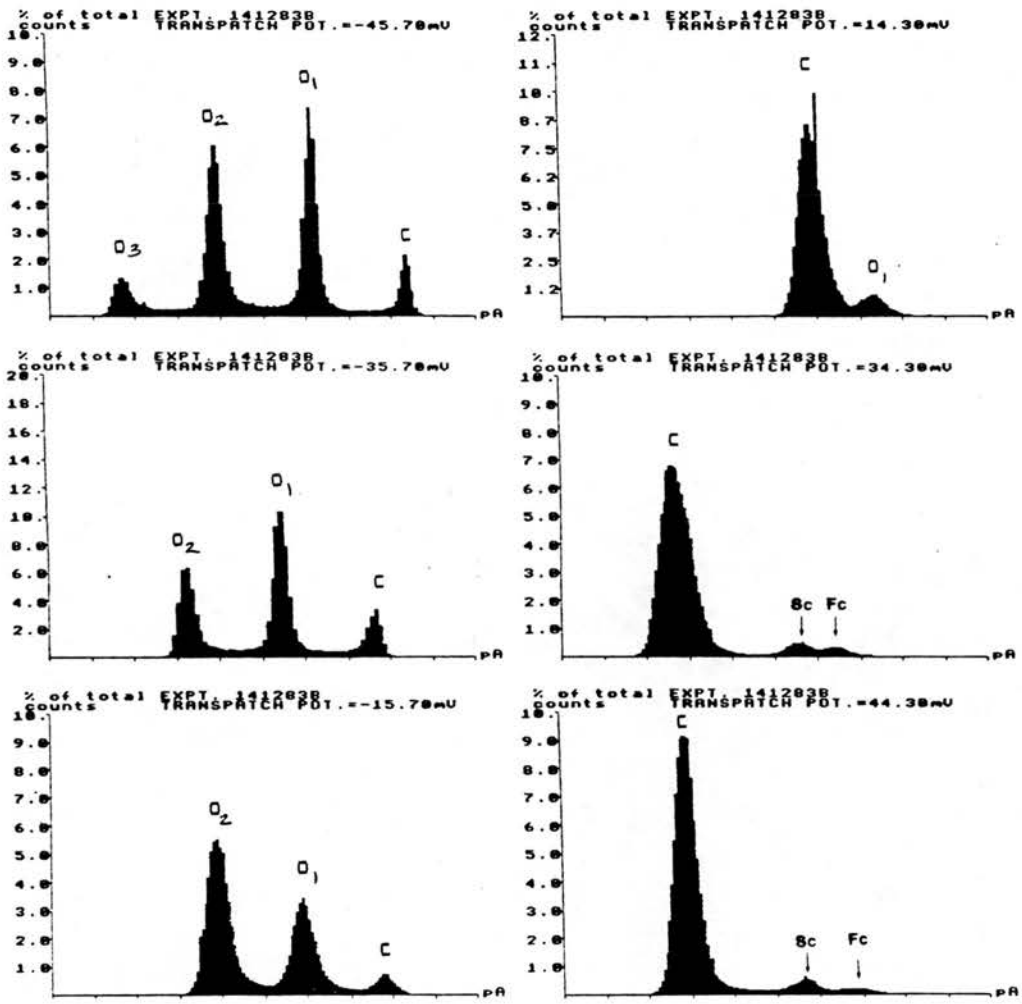
% of total counts
EXPT. 1412838
TRANSPATCH POT.=-45.70mV
O3
O2
O1
C
pA
% of total counts
EXPT. 1412838
TRANSPATCH POT.=14.30mV
C
O1
pA
% of total counts
EXPT. 1412838
TRANSPATCH POT.=-35.70mV
O2
O1
C
pA
% of total counts
EXPT. 1412838
TRANSPATCH POT.=34.30mV
C
Sc
Fc
pA
% of total counts
EXPT. 1412838
TRANSPATCH POT.=-15.70mV
O2
O1
C
pA
% of total counts
EXPT. 1412838
TRANSPATCH POT.=44.30mV
C
Sc
Fc
pA

Binomial Distribution

In a multichannel patch the opening of channels has been described by the binomial distribution (Benham and Bolton 1983). If all the channels opened independently of one another and had the same probability of opening then the proportion of time spent with 0, 1, 2....N channels open can be described by the binomial distribution. Benham and Bolton (1983) found the binomial distribution provided a reasonable fit to observations on potassium channels in the smooth muscle cells of rabbit jejunum.

Fig. 15 shows the graphical output of the programme (see Appendix III) written by Dr.R.J.Martin and adapted by myself which was used in the analysis of the mean probability of opening and in this analysis of the binomial distribution. The current signal was digitized using a Unilab interface (8 bit processor) and each record was stored in one of 256 bins depending on its amplitude. The output was displayed in the form of a frequency density histogram with frequency plotted against current amplitude. The area of the graph under each peak divided by the total area represents the proportion of time spent at that particular channel current level. The proportion of time or the probability of having 0, 1, 2, 3....N channels open may then be measured in this way. The apparent maximum number of channels in the patch was taken to be the maximum number of

Fig. 16: Graphs of the probability of 0,1,2 and 3 channels opening. The figure shows eight graphs taken from an isolated inside-out patch experiment, at the eight transpatch potentials indicated on the graph. The shaded bars show the observed probability of seeing 0,1,2,and 3, channels open. The clear bars show the probability of 0,1,2,3, channels open, calculated by the binomial distribution for the data. The graphs indicate that the binomial is not a good approximation to the data at all potentials. At depolarized potentials the fit to the binomial is better than at hyperpolarized potentials.

Patch type: isolated inside-out patch.

Solutions: symmetrical solutions of Ascaris Ringer.

Temperature: 30°C.

Graphs of observed and predicted
Probabilities of Channel Opening

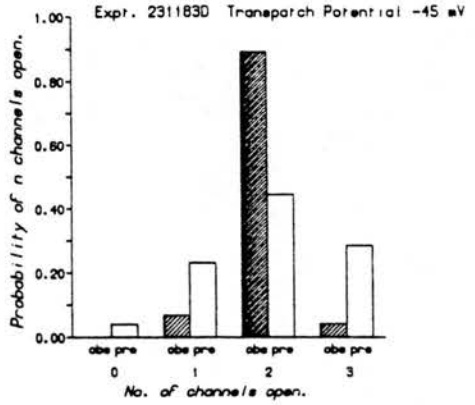

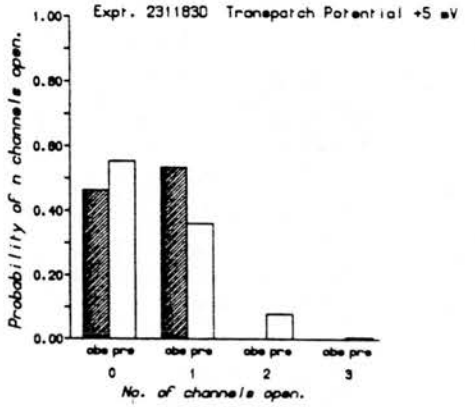

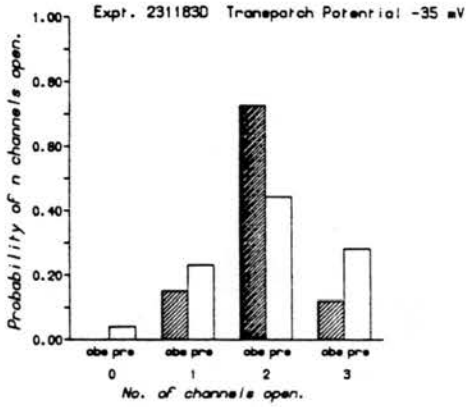

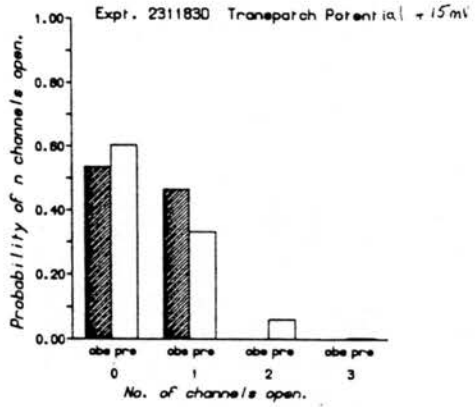

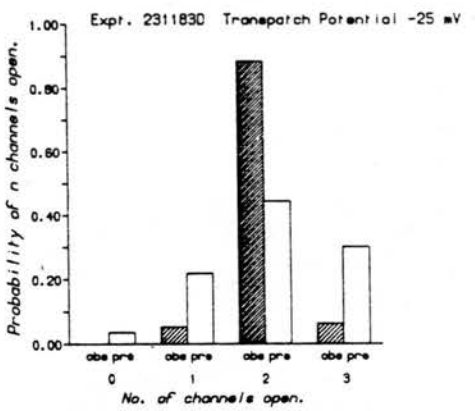

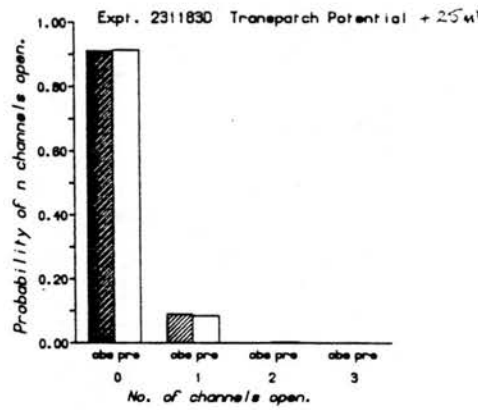

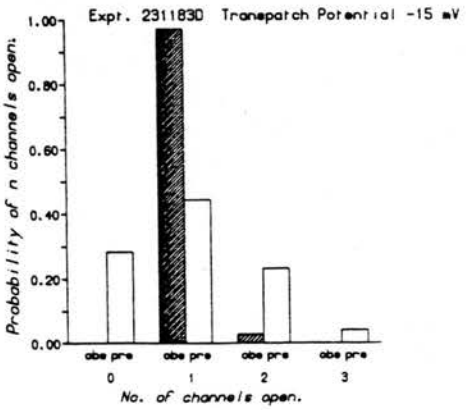

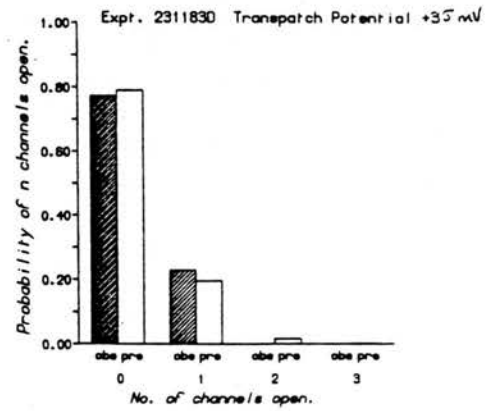

Fig. 17: Graphs of the probability of 0,1,2 and 3 channels opening. The figure shows eight graphs taken from an isolated inside-out patch experiment, at the eight transpatch potentials indicated on the graph. The shaded bars show the observed probability of seeing 0,1,2,and 3, channels open. The clear bars show the probability of 0,1,2,3, channels open, calculated by the binomial distribution for the data. The graphs indicate that the binomial is not a good approximation to the data at all potentials. At depolarized potentials the fit to the binomial is better than at hyperpolarized potentials as in the experiment of Fig. 16.

Patch type: isolated inside-out patch.
Solutions: symmetrical solutions of Ascaris Ringer.
Temperature: 30°C.

Graphs of observed and predicted
Probabilities of Channel Opening

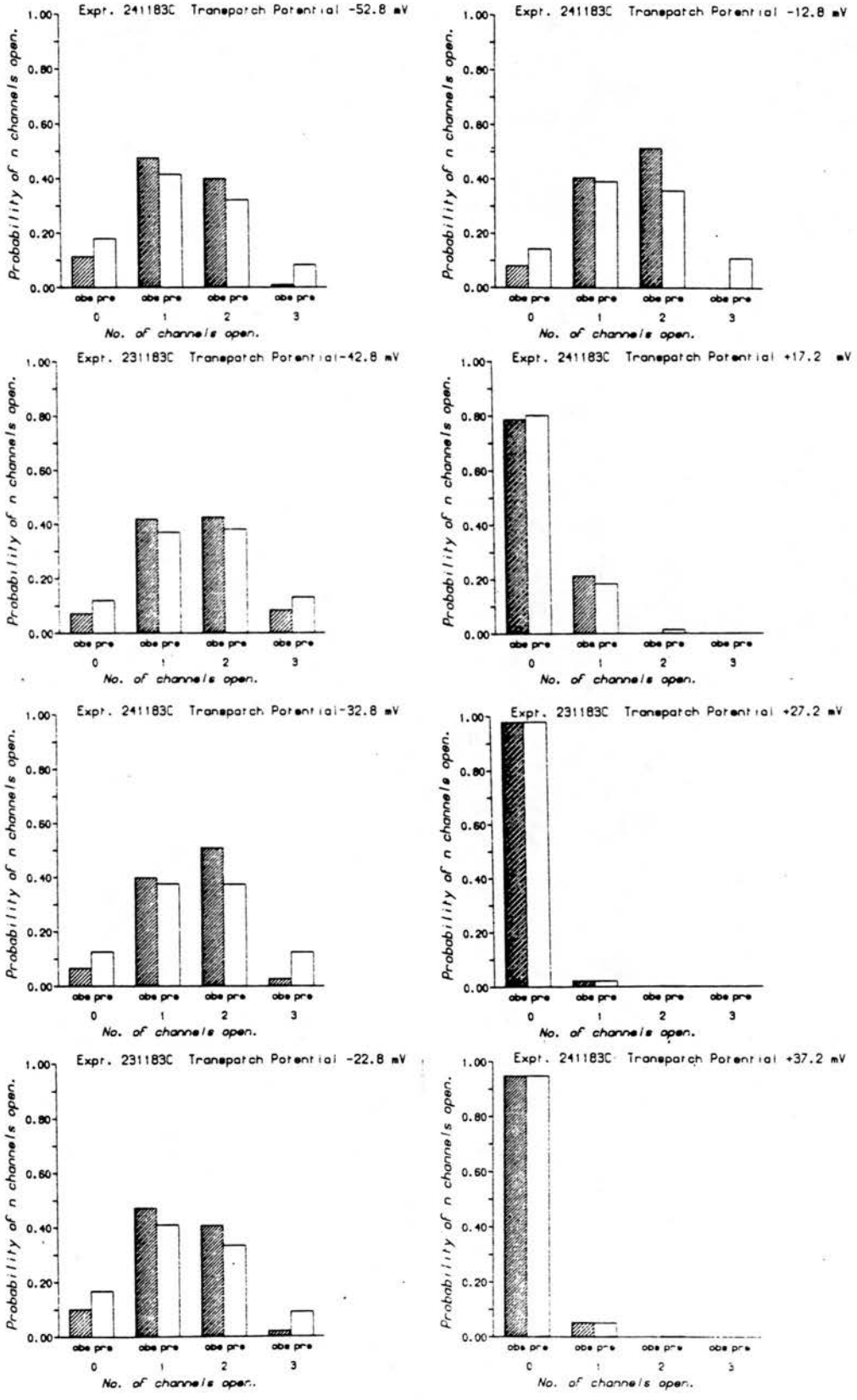

simultaneously open channels observed. More channels could be in the patch but no better estimate of the total number of channels is available. In the analysis the estimate of N (the total number of channels) was changed in an attempt to provide a better fit to the data, but in no cases did the fit improve. Using the mean probability of opening and the estimated total number of channels in the patch the predicted binomial distribution of the probability of 0, 1, 2, 3...N channels open was calculated. The equation used for the calculations was :-

$$P_r = \frac{np^r}{r(n-r)} (1 - p)^{(n-r)} \quad \ldots\ldots\ldots\ldots\ldots (10)$$

Where P_r was the calculated probability of channel opening at level r; p was the calculated mean probability of channel opening; n was the total number of channels in the patch; r was the channel current level at which the P_r was being calculated. This type of analysis was carried out for 10 experiments.

Fig. 16 and Fig. 17 show a graphical representation of the results of the observed and predicted proportion of time spent at each of the different channel levels from the current records. These experiments were taken from isolated inside-out patches with Ascaris Ringer on both sides of the patch. The histograms show the observed probabilities (shaded) and the calculated probabilities (clear) of the current being at the indicated level. At depolarized potentials the mean probability

of opening was low and the binomial distribution was a better fit. The variance of the observed distributions were less than the variance of the binomial distribution. If the estimate of the total number of channels in the patch, N, was too low then the variance of the observed distribution would be expected to be bigger than that of the binomial distribution. Fig. 16 shows an experiment where the observed and predicted distributions were markedly different. Fig. 17 shows an experiment where the observed and predicted distributions had a closer fit. The Chi-Squared test was not applicable in these analyses because it requires finite measurements of a given number of events rather than a probability or a time span. No tests for 'goodness of fit' were made.

In all 10 experiments analysed in this way the probabilities of 0, 1, 2, 3....N channels open were not well fitted by the binomial distribution. This indicated that some of the assumptions of the distribution were violated (Benham and Bolton 1983). Better fits of the channel current distributions were obtained by Dr. C.Glaseby when the individual channels in a patch were assumed to have different probabilities of opening. Another mechanism postulated to explain the distributions observed was that channel openings were dependent on each other and that when one channel opened this decreased the probability of opening of another channel. Further experimentation would be required to test these two hypotheses.

Fig. 18: Channel records showing the effect of calcium applied to the intracellular surface of an isolated inside-out patch. A broken pipette (containing 0.5mM calcium acetate) was used to apply calcium by diffusion to the intracellular side of the membrane patch for a period of 2s. The start of the application is indicated by a triangle. Immediately after the ejection of calcium a large increase in the number of channels open is seen. After 4 s the number of channels gradual decreases. This was taken to be an effect of the removal of calcium at the intracellular surface of the patch by the chelating action of EGTA.

Patch type: isolated inside-out patch.

Solutions: symmetrical solutions of calcium-free APF.

Temperature: 30°C.


1 s
20pA
US.

Calcium-dependence of Chloride Channel

The loss of channel openings after isolation of the patch suggested that there was not a simple voltage-dependent control of the channel, and that other modulating factors were involved in it functioning. Calcium-dependent potassium channels have been described (e.g. Barrett, Magleby and Palotta 1982) and it was of interest to see if this chloride channel was modulated by calcium in a similar manner. Chloride conductances with a calcium dependence have been reported in salamander retina rod inner segments Bader et al (1985); Xenopus oocytes (Barish 1983); and rat sensory neurones (Mayer 1985).

Perfusion of an isolated inside-out patch was not routinely possible without loss of channel currents and therefore another approach was used. A broken pipette with a tip diameter of approximately 500 μm was filled with calcium acetate [0.5 M] and connected at its open end to a polythene tube and a syringe. The tip of the pipette was placed close to the intracellular side of an isolated inside-out patch. Gentle pressure applied for 2 s to the syringe ejected a small amount of the calcium solution. The bathing Ringer contained a calcium-free APF [0.5 M EGTA].

Fig. 18 illustrates the effect of the application of calcium to the intracellular surface of an isolated inside-out patch on the current records. Prior to application, no channel

Fig. 19: Channel records taken from isolated patches showing the differential effect of application of $CaCl_2$ and calcium acetate to the intracellular surface of an isolated inside-out patch.

A: Current records show the effect of application of $CaCl_2$; after application (circle) there is a transient increase in the probability of opening and also an increase in the channel amplitude.

B: Current records show an increase in the probability of opening after the application of calcium acetate (circle) but no increase in the amplitude of the single channel current. This difference is explained by an increase in the chloride concentration at the intracellular surface of the membrane.

Patch type: isolated inside-out patches.
Solutions: symmetrical calcium-free APF.
Temperature: 30°C.

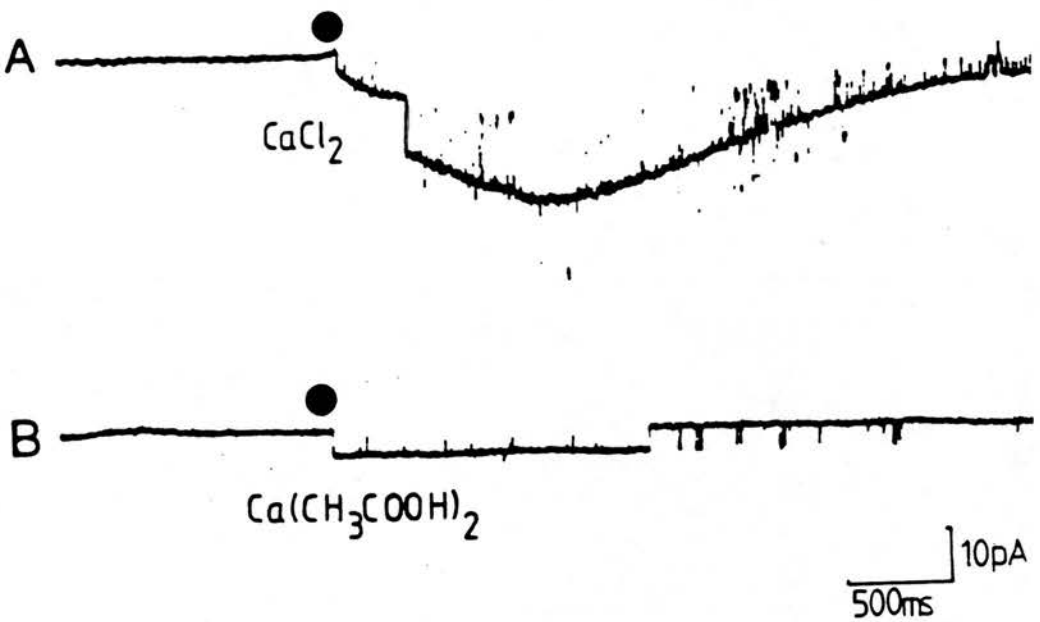
A
$CaCl_2$
B
$Ca(CH_3COOH)_2$
10pA
500ms

activity was seen. Immediately after ejection of calcium, indicated by the triangle on the figure, there was an increase in the apparent number of channels open. This was followed by a gradual decline until no channel openings were visible. The increase in channel opening was seen in 10 experiments carried out on 10 separate patches. The decline in the number of open channels, was proposed to be due to the reduction in the free calcium concentration of the bathing solution, caused by the action of the calcium chelator, EGTA. The channel activated by calcium had the same conductance as the chloride channel. The results were taken to indicate that the opening of the high conductance chloride channel was dependent on the intracellular concentration of calcium. The application of sodium acetate [500mM] to the intracellular surface of an isolated inside-out patch, had no effect on channel activity.

Fig. 19 shows an example of the current records taken from a series of experiments designed to further investigate the ion selectivity of the calcium activated channel. The same method of application was used as before, but in these experiments two separate pipettes were used to apply the calcium solutions. In one there was the calcium acetate, solution in the other there was a calcium chloride solution [0.5 M]. The upper current record shows the application of calcium chloride. The single channel currents not only increased in frequency but also increased in amplitude. This was not seen in the lower current records with the application of calcium acetate. Both the

Fig. 20: Current records from a cell-attached patch with different free calcium concentrations on the intracellular side of the patch. The preparation was made permeable to calcium using the ionophore A23187. The preparation was bathed in different free-calcium concentrations applied in random order. Each calcium concentration is indicated on the Figure, EGTA Ringer contained 0.5 mM EGTA. Up to five channels are simultaneously open in this patch. The current level indicated on the right are 'C' for all channels closed and 'O_1', 'O_2', 'O_3', 'O_4', 'O_5' for 1, 2, 3, 4, 5 channels open respectively.

Patch type: cell-attached patch.

Solutions: calcium-free APF on the intracellular side of the patch, APF with free calcium concentrations of between 0 and 1 mM on the intracellular side of the membrane.

Temperature: 20°C.

Transpatch potential: -40 mV.

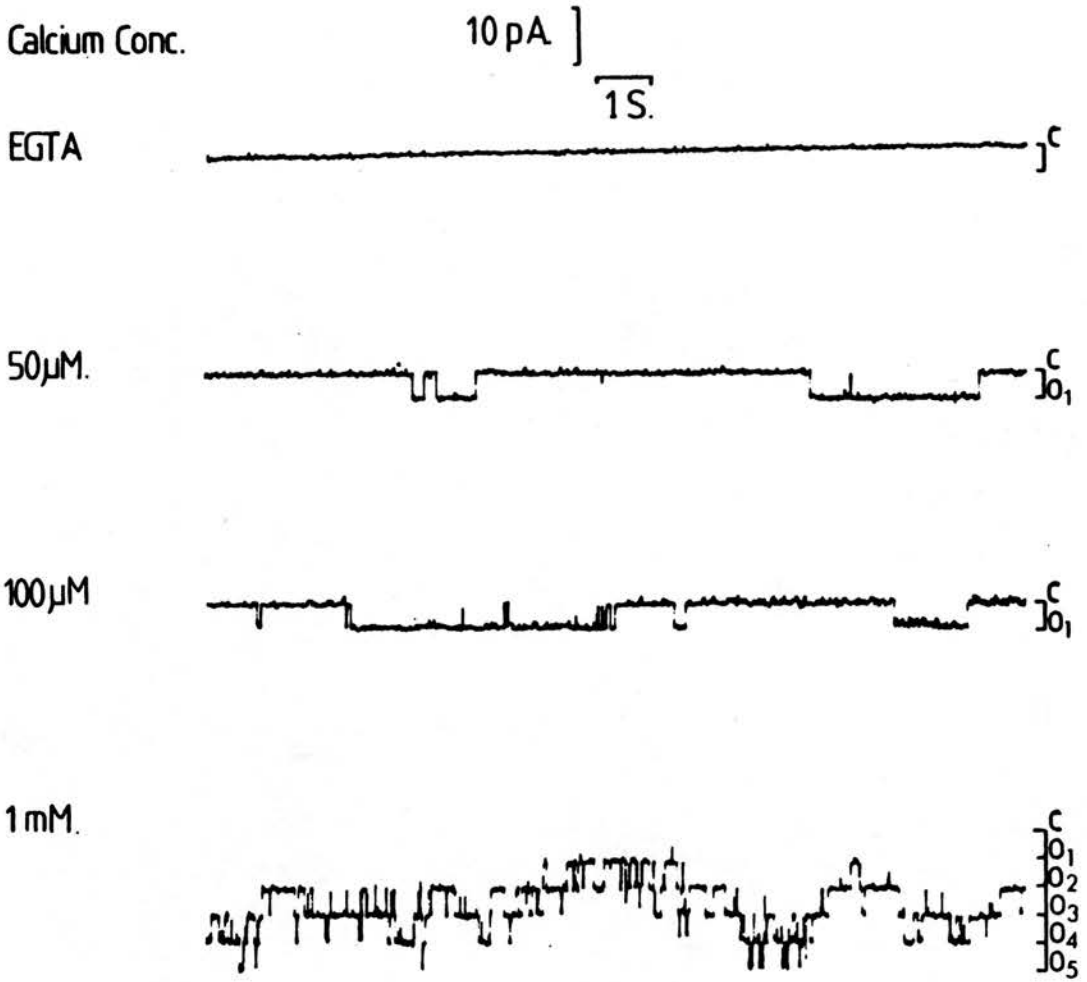
Calcium Conc.
10 pA.
1 S.
EGTA
C
50μM.
C
O1
100μM
C
O1
1 mM.
C
O1
O2
O3
O4
O5

calcium compounds increased the frequency of channel opening. The increased amplitude of the channels when calcium chloride was applied indicated the channel was permeable to chloride. These experiments indicate the high conductance chloride channel was calcium-dependent.

Isolation of patches in solutions of different calcium concentrations should enable the construction of a dose-response curve. Many experiments (N = 50) were carried out in this manner, isolating patches in Ringers containing 10^{-9} to 10^{-3} M free calcium. The main indicators of channel activation were taken to be the number of channels open in a patch, the probability of opening and the mean open time. The results from these experiments showed that the interpatch variability of the number of channels in the patch was greater than any variability due to the different calcium levels. The results indicated that channel modulation was not solely dependent on calcium and voltage and that other unknown factors were influencing channel opening. To limit the effects of interpatch variability it was necessary to attempt experiments to change the calcium at the intracellular surface of the same patch.

The next series of 17 successful experiments was carried out on both cell-attached and isolated inside-out patches. An individual patch was presented with different concentrations of calcium in a random order. Fig. 20 shows an example of the current records obtained from a cell-attached patch with

Fig. 21: A dose-response curve obtained from 13 experiments. The 'response' was crudely estimated from the maximum number of channels open simultaneously at each calcium concentration. The percentage response on the graph was measured for each calcium concentration, in each patch, as a percentage of the maximum response seen in the patch. The points represent the mean +/- S.E. and were obtained from 13 isolated inside-out patches and cell-attached patches.

Patch types: cell-attached patches and isolated inside-out patches.

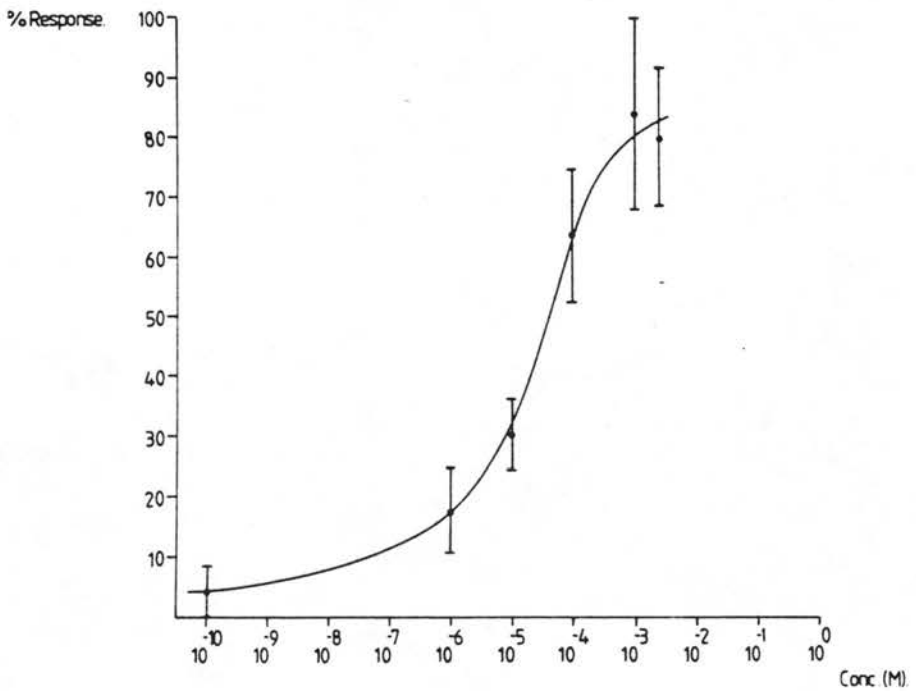
% Response
100
90
80
70
60
50
40
30
20
10
10^-10
10^-9
10^-8
10^-7
10^-6
10^-5
10^-4
10^-3
10^-2
10^-1
10^0
Conc. (M)

different concentrations of intracellular calcium. In cell-attached patch experiments the calcium ionophore, A23187 was bath applied to make the cells permeable to calcium. The experiments were also carried at 20°C in an attempt to slow any intracellular uptake mechanisms. The concentration of calcium in the cell was taken to be that of the bathing Ringer. The cells were allowed to equilibriate in each new solution for 5 to 10 mins. The absolute value of intracellular calcium was not known. In addition to cell-attached patches a number of isolated inside-out patches were obtained. Both types of patches showed essentially the same result, that is an increase in the probability of opening with increasing free calcium concentration.

Fig. 21 is a dose-response curve of free calcium concentration against response. The response was calculated by studying the current records obtained in each experiment at all the different calcium concentrations. The maximum number of simultaneously open channels was noted for each experiment. The response at each of the calcium concentrations was expressed as a fraction of the maximum number of channels observed at that concentration, against the maximum number of channels seen in the patch. The figure shows the mean and standard error of the response at each of the free calcium concentrations (N = 13). The line on the figure was drawn by eye.

The observations of the large interpatch variability in the probability of opening were taken to indicate the presence of other channel modulators. The effect of calcium suggested at least two possible modulators that should be explored. Intracellular calcium could affect the channel either directly or indirectly via intermediate pathways. In muscle, calcium is known to activate phosphorylase kinase and lead to an increase in the phosphorylation state of glycogen phosphorylase, accelerating glycogenolysis (Cohen, Burchell, Foulkes and Cohen 1978). One of the subunits of phosphokinase has been found to be identical to calmodulin, which is a protein known to be involved in other calcium-dependent enzyme processes (for reviews see Cohen 1982 and Nestler and Greengard 1983). Intracellular second messengers have been shown to affect the opening of channels. Findlay and Petersen (1985) showed that chloride channels were activated by a rise in the intracellular calcium concentration induced by the application of acetylcholine. Another example of the effect of second messengers is in the activation of a depolarizing response by cyclic AMP in Aplysia neurones (Strumwaser, Kaczmarek and Jennings 1982).

Experiments were carried out to ascertain the response of the chloride channel to the application of ATP and calmodulin (Sigma). Patches were isolated into a bathing solution of Ascaris Ringer, ATP [1 to 5 mM in Ascaris Ringer] was applied via a broken pipette to the intracellular surface of the patch, in the same manner as in the calcium experiments. No discernible

effect on either the probability of opening or the mean open time was found with the application of ATP. Patches with channels showed no inhibition with ATP application and those without channel currents showed no activation. These experiments demonstrated that the channel was not directly dependent on ATP in the manner of the potassium channels described by Noma (1983).

A second series of experiments was carried out using calmodulin applied in the same manner as the ATP to the intracellular surface of an isolated inside-out patch. In these experiments the bathing Ringer contained 1 mM ATP because the likely effect of calmodulin would be through phosphorylating the channel or some intermediary protein. None of these experiments showed any apparent effect of the application of calmodulin. This was taken to indicate the calmodulin had no direct effect on the channel protein. However, it is possible that in an intact cell, calmodulin could act on an intermediate enzyme that in turn acted on the channel. The procedure of isolation of the patch could lead to a disruption of this mechanism by removing the enzyme. Another possibility was that the calmodulin itself was inactive.

Evidence for a Cation Channel

In Ascaris Ringer a number of patches showed the activity of a small conductance channel. It was of interest to try to determine the ionic selectivity of channels other than the high

Fig. 22: Current records obtained from a cell-attached patch. There is evidence of two types of channel, opening in opposite directions. A smaller conductance channel with an amplitude of about 3 pA opens downwards, indicated by 'O_2', and a higher conductance channel with an amplitude of about 8 pA opens upwards, indicated by 'O_1'. The current level with no channels open is indicated on the right of the figure by 'O'. These current records were obtained using the List EPC7 amplifier. Currents in the downward direction are outwards.

Patch type: cell-attached patch.

Solutions: 300 mM KCl on the extracellular side of the patch and Ascaris Ringer in the pipette.

Temperature: 30°C.

Applied potential: 0 mV.


1 s
4
pA
O1
C
O2

Fig. 23: A current-voltage plot from the same experiment as the current records in Fig. 23. The current amplitudes of the larger channel are plotted by triangles. The current amplitudes of the smaller conductance channel are drawn as crosses. Although the ionic concentration of the intracellular ions was not known, the triangles were thought to be due to a chloride channel and the crosses a cation channel. The lines were calculated by linear regression. For the crosses the calculated conductance was 158 pS and the reversal potential was -24 mV. For the triangles the calculated conductance was 250 pS and the reversal potential was +32 mV.

Patch type: cell-attached patch.

Solutions: 300 mM KCl on the extracellular side of the patch and *Ascaris* Ringer in the pipette.

Temperature: 30°C.

Applied potential: 0 mV.

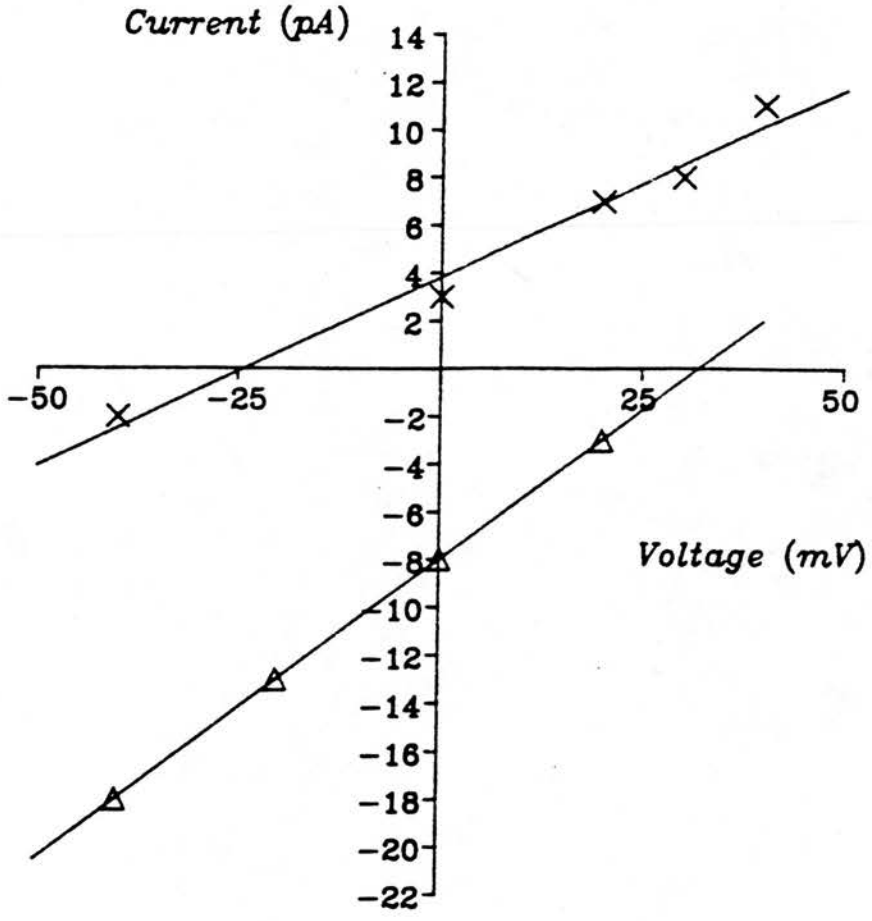
Current (pA)
14
12
10
8
6
4
2
-50
-25
25
50
-2
-4
-6
-8
-10
-12
-14
-16
-18
-20
-22
Voltage (mV)

conductance chloride channel. A number of experiments were carried out in potassium chloride solution (N = 20), with different concentrations of ions on either side of the membrane. The concentration gradient of ions on either side of the patch produced a reversal potential in opposing directions for cation and anion selective channels. This enabled positive identification of the chloride channel. The solutions contained concentrations of potassium chloride above that of Ascaris Ringer. This increased the conductance of the channels and allow easier analysis. It was found that gigohm seals were much more readily formed when the concentration of ions in the pipette was greater than in the bath.

Fig. 22 illustrates an example of the current records obtained from a cell-attached patch at 0 mV applied potential, 300 mM KCl in the pipette and Ascaris Ringer in the bath. Two types of channel opening are seen: a rapidly flickering inward (upward) channel with an amplitude of about 6 pA and a smaller outward (downward) opening channel with an amplitude of about 2 pA and longer open times. The I/V plot from the same experiment is shown in Fig. 23. There are two types of channel with different reversal potentials and different conductances(158 pS and 250 pS). The intracellular concentration of potassium chloride was not known in this experiment. Brading and Caldwell (1971) gave measurements of 99 mM and 14 mM for the intracellular concentration of potassium and chloride respectively in Ascaris muscle cells. The predicted reversal

potentials would therefore be hyperpolarized for an anion channel and depolarized for a cation channel. Other experiments performed in a similar manner, showed the separation of the reversal potentials of anion and cation channels. It was only in these conditions of elevated potassium concentrations that this cation channel was observed.

Three separate factors were thought to explain the lack of observation of cation channels in the majority of the patch-clamp experiments described in this thesis. Firstly, the potassium concentration was 3 mM in Ascaris Ringer and 27 mM in APF. Under these conditions of low potassium concentration and high chloride concentration the conductance of the potassium channel would be expected to be smaller than the chloride channel. If the potassium channel had a similar conductance/concentration curve to that of the chloride channel shown in Fig. 10 then the conductance of the potassium channel in Ascaris Ringer would be 20 pS. Secondly, in the KCl experiments of this section the cation channel was observed less frequently than the high conductance chloride channel. Thirdly the voltage clamp work reported in this thesis indicated that a potassium conductance was activated by depolarizing steps. The steady holding potentials normally used would not activate the potassium channel.

Fig. 24: A continuous current record obtained from a cell-attached patch. The voltage record (V on left of figure) is shown above each current record (I on left of figure). The volatage was stepped from a holding potential of -35 mV to +40 mV (indicated on the right of the figure). Single channel currents are visible, opening during the depolarizing steps.

Patch type: cell-attached patch.

Solutions: 50 mM KCl on the extracellular side of the patch and 200 mM KCl in the bath.

Temperature: 30°C.

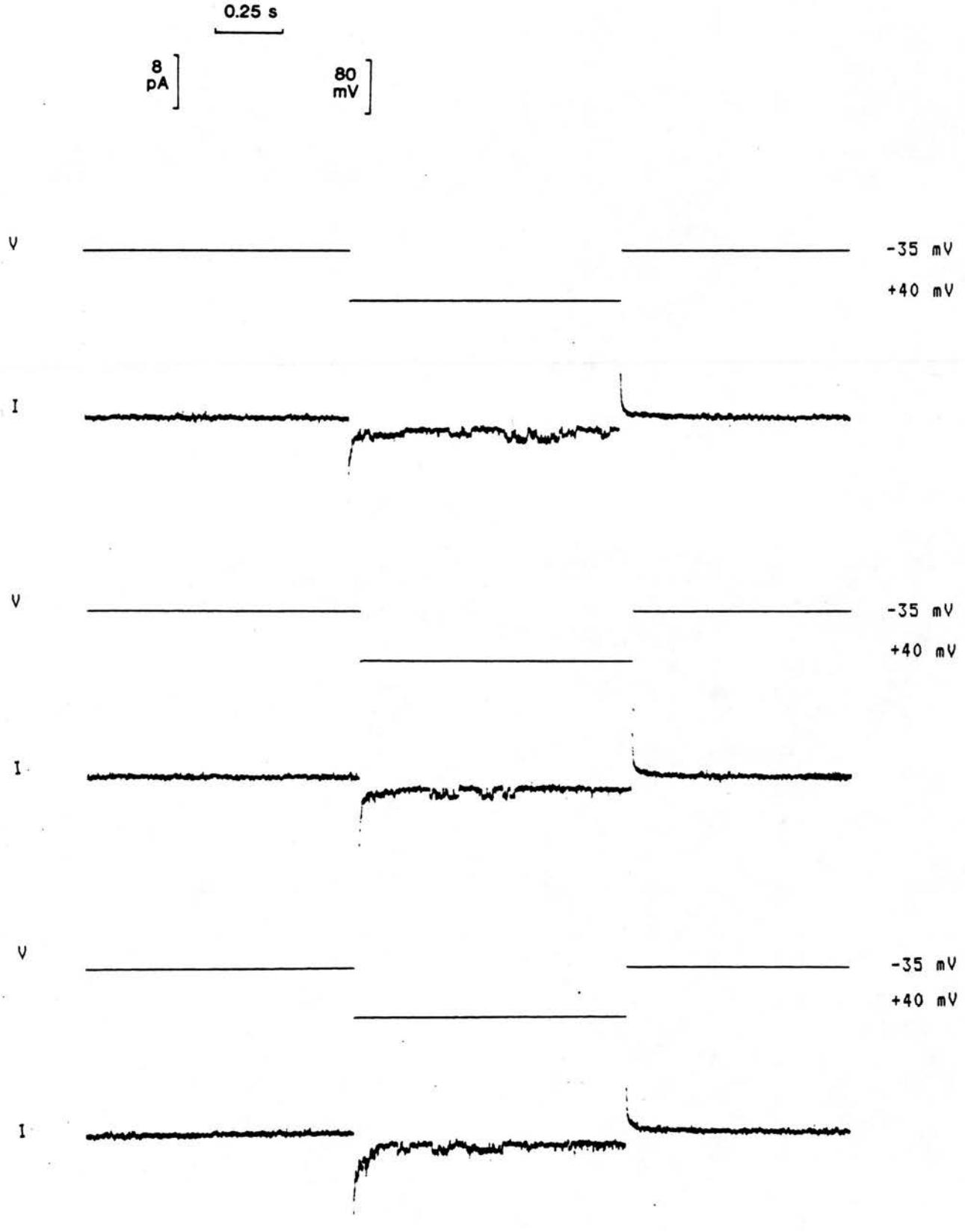
0.25 s
8
pA
80
mV
V
I
-35 mV
+40 mV
V
I
-35 mV
+40 mV
V
I
-35 mV
+40 mV

Fig. 25: The current-voltage plot from the same experiment as the current records in Fig. 24. Channel current records were only seen at depolarized step potentials and are plotted as crosses on the graph. The points obtained show a scattered distribution, This may indicate more than one channel, or a channel with subconductance states.

Patch type: cell-attached patch.

Solutions: 50 mM KCl on the extracellular side of the patch and 200 mM KCl in the bath.

Temperature: 30°C.

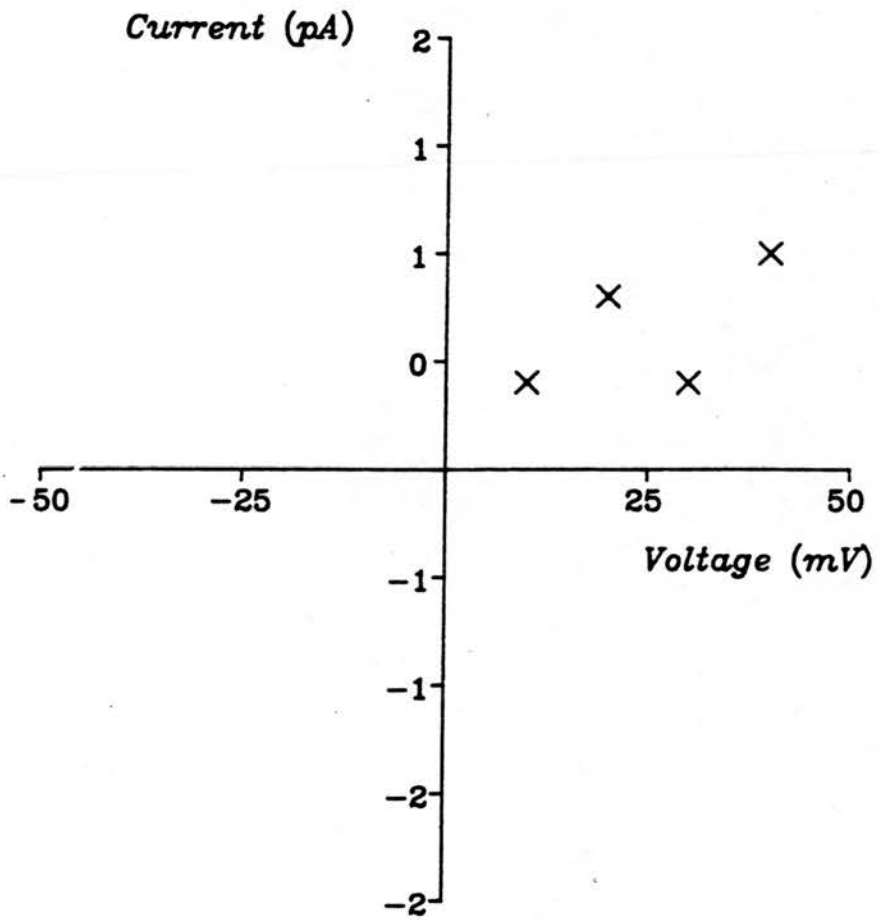
Current (pA)
2
1
1
0
-50
-25
25
50
Voltage (mV)
-1
-1
-2
-2

Fig. 24 shows the current records obtained from an isolated inside-out patch with 50 mM potassium in the pipette and 200 mM potassium in the bath. The records are a continuous trace of four consecutive depolarizing steps from -35 mV to +40 mV. The channel was activated by the depolarizing steps and was seen to open in the downward (outward direction). Fig. 25 shows the I/V plot of this channel from the same experiment as the current records in Fig. 24. The reversal potential for such a small number of observations was not calculated but is clearly at a hyperpolarized potential indicating this channel was selective for cations.

DISCUSSION

These experiments were the first to describe a chloride channel in invertebrate muscle cells. The observations on this chloride channel provide the first account of spontaneous single channel activity and extend our knowledge of the electrophysiology of *Ascaris* muscle cells. The voltage and calcium sensitivity of the chloride channel, described in these experiments, indicate a complex role in the physiology of the cell which is still to be elucidated.

Anion channels in other tissues share similar properties to the *Ascaris* chloride channel. In *Lymnea stagnalis* neurones a calcium-dependent chloride channel has been described that had a reduced probability of opening at depolarized potentials (Geletyuk and Kazachenko 1985). High conductance, voltage sensitive anion channels, and other calcium-dependent chloride channels have some similar properties with the *Ascaris* chloride channel. The apparent diversity of chloride channels in muscle has been postulated to be due in part to methodological differences, for example pH differences (review Bretag 1987). The *Ascaris* chloride channel could therefore, under different conditions, maintain similarities to some other reported chloride channels.

Description of the Ascaris Chloride Channel

The permeability of the high conductance channel in Ascaris was determined using ion substitution experiments. In preliminary experiments an ionic gradient was imposed across the patch. The solution in the pipette was the same as that in the bath but diluted by a factor of five. The measured reversal potential under these conditions was consistent with an anion channel. Experiments replacing the cations in the bathing solution with Tris, had no discernible effect on channel amplitude or channel open probability. This latter result is of interest because it illustrates a difference between the Ascaris chloride channel and the Lymnea chloride channel (Geletyuk and Kazachenko 1985). In Lymnea intracellular sodium concentration was shown to affect the voltage dependence of the open probability of chloride channel opening (Geletyuk and Kazachenko 1985). Substitution of all cations in the bathing solution, with Tris, had no affect on open probability of the Ascaris chloride channel.

In both isolated inside-out and cell-attached patches, a hyperpolarizing shift in the reversal potential was observed for the Ascaris chloride channel when the bathing solution was changed for a low chloride solution. The magnitude of the shifts in reversal potential were consistent with a channel permeable to chloride. Reversal potentials were also measured with asymmetric KCl gradients across the patch. These experiments

were used to determine the ratio of potassium to chloride permeability. In Ascaris two experiments demonstrated permeability ratios of 0.009 and 0.09 for potassium over chloride, indicating that the channel is extremely selective for chloride ions. Permeability ratios of potassium to chloride in other high conductance, voltage sensitive anion channels have been calculated. These range between 0.015 in pulmonary alveolar cells (Schneider et al 1985) and 0.14 in mitochondria (Schein et al 1976). The selectivity for anions over cations is thus greater for the Ascaris chloride channel than in these other high conductance, voltage sensitive anion channels. The conductance of the Ascaris chloride channel measured from the linear portion of the I/V relationship was 200 pS (in symmetrical 175 mM chloride). This is comparable, although smaller, than the conductances of other high conductance, voltage sensitive anion channels which are between 450 pS in the Schwann cell (Gray et al 1984) and 360 pS in the A6 cell line derived from Xenopus epithelium (Nelson et al 1984).

The Ascaris channel maintains a high anion selectivity and a high conductance, two factors which intuitively should be in conflict. That is, a highly selective channel would by necessity exclude many species of ion and therefore the channel would not be expected to have a high conductance. There is a precedent for this observation in the maxi-K potassium channel that has a 200 pS conductance and is also very selective for potassium over other cation (Latorre, Verago and Hildago 1982).

Information on the nature of ion permeation through the Ascaris chloride channel was obtained from experiments which measured channel conductance in bathing solutions of different chloride concentrations. The graph of conductance against chloride ion concentration showed a saturation function that was adequately fitted by a Michaelis-Menton type equation. Sakmann and Trube (1984) carried out similar experiments on the inward rectifier potassium channel in ventricular cells of guinea pig heart muscle. It was proposed (Sakmann and Trube 1984) that the observed saturation of conductance at high ion concentrations indicated the passage of a single file of ions through the channel.

In summary the Ascaris chloride channel has been shown to have a high conductance, a high ionic selectivity for chloride and is speculated to allow only a single file of ions to pass through the channel in its conducting state.

Voltage Sensitivity of the Channel

The probability of opening and the mean open time of the channel were observed to decrease when the patch was held depolarized. This study proved to be problematic because the interpatch variability was larger than the changes that were associated with depolarization. The relationship of potential to either the probability of opening or mean open time was not clearly defined. The results obtained are viewed as preliminary until other factors that are thought to control channel opening

are determined.

The graphs of mean open time and open probability were assumed to be continuous across the voltage range studied. The lack of data around 0 mV did not allow this assumption to be tested. The results obtained from the analysis illustrated the interpatch variability. In some distributions the best fit to the data was a straight line, in others square or cubic functions provided the best fit.

The high conductance, voltage sensitive anion channels in rat skeletal muscle (Blatz and Magleby 1983), rabbit urinary bladder epithelial tissue (Hanrahan et al 1985), Schwann cells (Gray et al 1984), mitochondria (Schein et al 1976) are maximally active at potentials around 0 mV. The decline in probability of opening as the potential is moved away from 0 mV, of these channels is unlike the voltage sensitivity of the Ascaris chloride channel.

Chloride channels in Aplysia neurones (Chesnoy-Marchais 1982), in Lymnaea stagnalis neurones (Geletyuk and Kazachenko 1985) and in crayfish muscle fibres (Ozeki, Freeman and Grundfest 1966) show similar voltage sensitivity to the Ascaris chloride channel. In Lymnea depolarization decreases the channel open probability but unlike Ascaris this effect is altered by the intracellular concentration of sodium (Geletyuk and Kazachenko 1985).

Sub-conductance Levels

When the patch was depolarized some channel records showed channel openings to full and sub-conductance states similar to those described in potassium channels by Barrett et al (1982) and Benham and Bolton (1983). The majority of current records at depolarized potentials show channel openings of a low conductance in the absence of full channel conductance openings. These current records could represent the activity of a different type of channel. There are a number of reasons why this was thought to be unlikely. Firstly, current records with openings of two types of channel when the patch was hyperpolarized were not seen. To explain the current records observed, the high conductance chloride channel would have to close at depolarized potentials and the smaller conductance channel would have to close at hyperpolarized potentials. Secondly, the observation in some patches of full and sub-conductance states indicates that the chloride channel can exist in lower conductance states. Thirdly, rectifying I/V plots were seen when all the cations of the bathing solution were replaced with Tris indicating that rectification was a property of the chloride channel.

Chloride Channel Modulators

Application of high concentrations of calcium to the

intracellular surface of an isolated inside-out patch, was found to produce an increase in the probability of opening and mean open time of a channel with the same unit conductance as the chloride channel. Application of calcium chloride and calcium acetate showed this calcium activated channel to increase its amplitude when high concentrations of chloride were present at the intracellular side of the membrane. Additionally no other high conductance channels were observed in APF or Ascaris Ringer. Taking all these points together led to the conclusion that the high conductance chloride channel was dependent on intracellular calcium.

Calcium-dependent chloride conductances have been described in Xenopus oocyte (Barish 1983) and in neurones of Lymnaea stagnalis (Geletyuk and Kazachenko 1985). Experiments to determine the nature of the calcium dependence of the Ascaris channel were complicated by the loss of channel openings when an isolated inside-out patch was perfused. The variability of the mean open time and the probability of opening of the channel added to the problems in this this study.

The high conductance, voltage sensitive anion channels in Schwann cell (Gray et al 1984) and in MDCK epithelial cells (Kolb et al 1985), both showed an increase in probability of opening when a cell-attached patch was isolated. In rat muscle, Blatz and Magleby (1983) described a large variability in the activity of the high conductance, voltage sensitive anion

channel. These reports suggest that there are other unknown factors controlling the opening of these anion channel.

In the experiments described in this thesis, a simple analysis was carried out using the maximum number of simultaneously open channels in a patch, as a measure of the activation of the channels at a given calcium concentration. This index was used so that data from as many experiments as possible could be included in the analysis. The actual value of the intracellular calcium concentration in the cell-attached patch experiments was not measured, but it was felt that the experiments could be used as a guide to the nature of the calcium effect.

Binomial Distribution

The study in Ascaris of the proportion of the time spent with 0,1,2,3..N channels open in a multichannel patch, showed that the distribution was not well fitted by the binomial distribution. Benham and Bolton (1983) in potassium channels of the smooth muscle cells of rabbit jejunum, also found that the distribution of channel openings was not fitted by the binomial distribution. Miller and White (1984) described a large conductance chloride channel in Torpedo electroplax organ. The channel was shown to exist as a dimer with two channels connected, the opening of one channel linked to that of the other (MIller and White 1984). The open probability of Torpedo

chloride channels deviated from the binomial distribution (Miller and White 1984).

In Ascaris the observed distributions of openings had a smaller variance than that predicted by the binomial distribution. In these calculations the total number of channels in a patch, N, was taken as the maximum number of simultaneously open channels observed. The observed N provided a minimum estimate of the total number of channels. However the use of larger values of N produced a greater variance and a worse fit to the data. The two assumptions of the binomial distribution are that channel openings are independent of each other and the probability of opening of each of the channels are the same. The poor fit in Ascaris chloride channels of the binomial distribution could be due to either of these assumptions being untrue. If the channels were negatively correlated, that is the opening of one channel caused the closing of another then the predicted distribution fitted the observed more closely. If the channels were assumed to have separate probabilities of opening, the predicted distribution fitted the data well. At the present stage of the analysis differentiation of the two hypotheses is not possible.

The sample times of the data used in the binomial distribution analysis were relatively short (less than 200 s), and this could be an additional factor in the poor fit of the binomial distribution. Over a given sample period two channels

in the patch could be in different open states; one with relatively short openings, the other with relatively long openings. With longer sample times these local temporal differences would be expected to average out.

Function of the Chloride Channel

The Ascaris chloride channel described has a number of characteristics that suggest at least two possible functions. Firstly, the channel is proposed to be important in the regulation of spontaneous activity. Secondly, the channel is proposed to have a function in the movement of chloride across the Ascaris body wall.

Spontaneous slow waves of depolarization and spikes associated with the slow waves have been described in Ascaris (Jarman 1959). Debell et al (1963) applied depolarizing current to the syncytial region of the arms of the muscle cells in Ascaris, and recorded a train of spikes in the soma. Direct depolarization of the soma produced only a single spike (Debell et al 1963). It was proposed that exogenous depolarizing input at the syncytial region, produced depolarization that induced spiking at a spike initiating region of the somatic muscle cell arms (Debell et al 1963). In a simple model, depolarizing waves at the syncytium would produce depolarizing slow waves and associated spikes in the muscle cell somata. This model would require an endogenous somatic hyperpolarizing current to act at

the end of a depolarizing slow wave to restore the resting membrane potential. It is proposed that the chloride channel meets the necessary requirements of this hyperpolarizing current. The voltage sensitivity of the chloride current would close the channels during the depolarizing wave. This would prevent the chloride current from short circuiting the membrane and allow for depolarizing spikes. The calcium dependence of the chloride channel, would activate the channel in response to a build up of calcium after a train of calcium spikes. In this way the depolarizing slow wave and a train of spikes would increase the intracellular calcium concentration and open the chloride channels.

The second proposed function of the chloride channel is in the movement of chloride across the membrane and in the setting of the resting potential. Hobson et al (1952a) demonstrated the presence of an active chloride pump in the body wall of Ascaris. The measured resting potential of Ascaris somatic muscle cells in different bathing solutions could not be adequately described by the Goldman-Hodgkin-Katz equation (Brading and Caldwell 1971). Brading and Caldwell (1971) proposed an active pump in the muscle cell membrane to maintain the resting potential.

Dulhunty (1978) found that in the mouse skeletal muscle the Goldman-Hodgkin-Katz equation could adequately describe the resting potential in solutions of various ionic composition, if the chloride concentration was allowed to be out of equilibrium.

Dulhunty (1978) suggested an active chloride pump was responsible for raising the intracellular chloride concentration, and maintaining a depolarized chloride equilibrium potential. Coupled with a high passive permeability to chloride, this active mechanism caused the resultant resting potential to be 15 to 40 mV more positive than predicted by the Goldman-Hodgkin-Katz equation.

Ascaris somatic muscle cells have been shown to have a high resting permeability to chloride (Caldwell and Ellory 1968, Debell et al 1964a). The single channel experiments in this thesis demonstrate a high probability of opening of the chloride channel at hyperpolarized potentials. By analogy to the experiments in mouse muscle by Dulhunty (1978), a chloride pump and a high resting permeability to chloride in Ascaris muscle cells would be predicted to have a large influence on the resting membrane potential. A chloride pump is proposed to maintain an elevated, non-equilibrium intracellular concentration of chloride, and through the high conductance chloride channel the muscle cell resting potential is held at the chloride reversal potential.

SECTION III

Potassium Currents from the Somata of Ascaris suum Muscle Cells.

INDEX

Summary

Currents in the soma of Ascaris suum muscle were studied using a two electrode voltage-clamp technique.

In APF Ringer, a depolarizing voltage-clamp step from a holding potential of -35 mV to +60 mV, elicited an outward current with a peak amplitude of 620 nA and a time to peak of 10 ms. With prolonged depolarizing steps the current decayed. The outward current was little affected by removal of chloride in the extracellular solution. In contrast an increase in the potassium concentration considerably reduced the current amplitude.

The reversal potential of the outward current was measured using a two step voltage-clamp protocol. The reversal potential showed a linear relationship, when plotted against the log of the extracellular potassium concentration [between 3 mM and 138 mM]. This was taken to indicate that the outward current was carries by potassium ions.

Tetraethylammonium APF, TEA APF, (based on APF Ringer, with elevated calcium [64 mM] and substituting sodium in APF with TEA [69 mM]) was used to observe an inward current activated by depolarizing voltage steps. The inward current showed a decrease in time to peak with more positive depolarizing steps.

The amplitude of the inward current showed an initial increase followed by a decrease with more positive depolarizing steps.

Steady-state inactivation curves were obtained from the peak amplitudes of the outward current activated by depolarizing pulses, plotted against holding potential. These experiments involved changing the holding potential and stepping to a constant depolarizing test potential. The current was 70% activated at a holding potential of -40 mV, the resting potential of the muscle cells.

A double pulse protocol showed that recovery from inactivation after the first pulse took more than 12 s. Two depolarizing pulses of the same amplitude were used with a varying interval between the pulses. Inactivation was measured as the decline in peak amplitude of the current obtained from the second pulse.

Application of 4-AP [5 mM] extracellularly, reduced the peak amplitude and increased the time to peak of the outward current. The currents obtained before and after 4-AP application were digitized and subtracted from each other. The resulting current was that blocked by 4-AP. The decay of the 4-AP blocked current was fitted by a single exponential with a time constant of 10.4 ms. The 4-AP resistant current was fitted by a single exponential with a time constant of 1.1 s.

Aims and Introduction to the Voltage-Clamp Experiments

In this study the somata of the body muscle cells of Ascaris were voltage-clamped, and the currents in response to depolarizing voltage steps observed. Jarman (1959) described depolarizing waves recorded from the somata of Ascaris muscle. In a more detailed study of the ionic basis of spontaneous electrical activity, Weisblat et al (1976) presented evidence that the spikes of Ascaris suum were carried by calcium. Debell et al (1963) showed a delayed rectification in Ascaris muscle somata under current clamp. Experiments by Martin (1982) showed that the outward current, activated by depolarizing voltage-clamp steps, was blocked by diethylcarbamazine [10^{-4} M].

Geletyuk and Kazachenko (1985) proposed that the large calcium-dependent chloride channel in Lymnea stagnalis was responsible for depolarizing the membrane after a calcium spike. Thus, it was of interest to carry out a closer investigation of the outward current in Ascaris to determine if the chloride channel described in the previous chapter of this thesis had a similar function to the chloride current described in Lymnea by Geletyuk and Kazachenko (1985).

The experiments described in Section II of this thesis demonstrated a high conductance, calcium-dependent chloride channel. This channel was shown to have a reduced open

probability and mean open time with depolarization. The voltage dependence of the Ascaris channel is the opposite of that required for repolarization after a spike. However, the chloride channel could still be activated in response to an elevated intracellular calcium concentration after a spike, as has been proposed in Lymnea by Geletyuk and Kazachenko (1985).

This study employed the voltage-clamp technique in preference to patch clamp for the following reasons:

1) the study of voltage activated currents, and the construction of activation and inactivation curves are easier than when using patch clamp,

2) previous studies using patch clamp had shown a low frequency of observation of channels other than the chloride channel,

3) currents from the whole somata can be observed.

There are a number of problems associated with the temporal and isopotential control of the area of membrane under voltage-clamp. These problems have been described by Cole (1968) in Aplysia neurones. Voltage-clamp of molluscan somata (up to 500 μM diameter) have employed a number of methods to reduce the errors produced as a result of inadequate isopotential control. Connor and Stevens (1971a, 1971b) tied off the somata of Archidoris and Anisidoris neurones thus physically isolating the soma from the axon. A similar technique using enzymatic isolation of the soma from the axon in Helix pomatia neurones

was used by Kostyuk, Krishtal and Doroshenko (1975a,b). Neher (1971) used a pipette with a large tip diameter to isolate a small area of membrane in the somata of Helix pomatia neurones and study the currents of this 'patch' in isolation.

The result of inadequate temporal and isopotential control has been described by Taylor, Moore and Cole (1960) as a notching or dipping of current waveforms seen under voltage-clamp. In the experiments on Ascaris described in this thesis no notching was seen. To confirm isopotential control a third microelectrode was placed at various locations in the Ascaris somata, and the potential measured. This methodology has been used by Connor and Stevens (1971a) in Archidoris neurones, and by Alving (1969) and Geduldig and Gruener (1970) in the somata of Aplysia giant neurones. In the experiments of this thesis on Ascaris, the voltage at the third electrode was seen to follow that of the command voltage indicating adequate isopotential control of the soma. Unfortunately voltage control of the spindle region could not be determined because access to the muscle spindle is not possible in Ascaris without damage to the cell body.

Preliminary voltage-clamp experiments were carried out in Ascaris Ringer to determine the gross form of the currents activated by depolarization. An outward current was observed and graphs of current amplitude and time to peak were plotted

against the step potential. An inward calcium current was also observed. The outward current was studied using ion substitution experiments and found to be a potassium current. The outward current was seen to decay over the time of the pulse (approx. 200 ms).

The decay of the outward current in Ascaris could result either from an accumulation of potassium in the extracellular spaces, or a time-dependent inactivation of the potassium channels. In frog skeletal muscle, Frankenhauser and Hodgkin (1957) measured the reversal potential of the outward current, at the beginning and end of a long depolarizing voltage-clamp pulse. Small shifts in the reversal potential, were taken to indicate some potassium accumulation in the extracellular spaces (Frankenhauser and Hodgkin 1957). Aldrich, Getting and Thompson (1979) found no difference in the reversal potential of the outward potassium currents in neurones of the molluscs Archidoris and Anisidoris, when measured 5 ms and 50 ms after a depolarizing pulse. In Helix pomatia neurones Kostyuk et al (1975a) measured the reversal potential of the outward current at intervals after the onset of a depolarizing pulse. No more than a 5 mV shift in the reversal potential of the potassium current was seen, indicating that the current decay was due to inactivation of the potassium channels. Experiments on Ascaris were carried out to determine if potassium accumulation in the extracellular spaces accounted for potassium current decay.

Outward potassium currents develop rapidly after the onset of a depolarizing voltage-clamp pulse. With a maintained depolarizing step, the currents rise to a peak and then decay. The decay has been approximated to a single exponential with time constants of between 400 ms in frog skeletal muscle (Adrian, Chandler and Hodgkin 1970), and 3.7 s in the isolated neural somata of the marine gastropods Archidoris and Anisidoris (Connor and Stevens 1971b).

The activation and inactivation of the outward potassium current in Ascaris was studied using a range of holding and step potentials. Previous studies of outward potassium currents have shown that the total current may be subdivided into component parts, on the basis of activation and inactivation characteristics (e.g. Thompson 1977). Three separate types of outward potassium current have been distinguished. These are:

1) A fast transient, I_a current (Connor and Stevens 1971b),

2) A slow delayed outward current, I_k current (Neher 1971),

3) A calcium-dependent current, I_c current (Thompson 1977).

Thompson (1977) described an outward potassium current activated by depolarized voltage-clamp steps in neurones of Tritonia diomedia. This current was produced by a combination of

I_a, I_k and I_c currents. In other cell types that possess outward potassium conductances, one or any combination of the three main types of current may be present.

The two currents, I_a and I_k have been distinguished by the rates of activation and inactivation, and by the steady-state inactivation. The rate of activation and inactivation of the currents can be measured from current records. Decay of the I_a current and decay of the I_k current have been fitted by single exponentials (Connor and Stevens 1971b). Voltage steps from a range of holding potentials to a fixed step potential have been used to estimate the steady-state inactivation curves of the I_a and I_k currents (Aldrich et al 1979). The peak outward current amplitude, obtained by voltage-clamp steps from each of the holding potentials, was then plotted against the holding potential.

The I_a or I_k currents can be studied in isolation by the use of pharmacological agents to specifically block one of the currents (Thompson 1977). Kostyuk et al (1975a) studied the I_k and I_a components of the outward potassium current in Helix pomatia, separately, using voltage-clamp steps from different holding potentials. At a holding potential of -90 mV both currents were fully activated. However at a holding potential of -40 mV, the I_a current was almost completely inactivated, allowing observation of the I_k current (Kostyuk et al 1975a). In the neural somata of Archidoris and Anisidoris

the I_k current was studied by the application of depolarizing steps from a holding potential of -40 mV, (Connor and Stevens 1971b). The I_a current was inactivated at a holding potential of -40 mV and was studied by the application of depolarizing steps from a holding potential of -100 mV (Connor and Stevens 1971b). In the neural somata of Tritonia diomedia Thompson (1977) separated the I_a and I_k currents by using a holding potential of -40 mV to study the I_k and a holding potential of -90 mV to study the I_a current. Experiments in Ascaris, described in this thesis, show an inactivation of the outward current at more depolarized holding potentials. However at a holding potential of -40 mV the fast I_a type current was still significantly activated.

The time to peak and rates of decay of outward potassium currents, have been used to differentiate between components of the outward current. The I_a currents of isolated neural somata of Helix pomatia had a time to peak of 10 ms (Kostyuk et al 1975a), and a decay, approximated by a single exponential, with time constants of between 10 ms and 50 ms in Helix (Kostyuk et al 1975a) and between 220 ms and 600 ms in Archidoris and Anisidoris neural somata (Connor and Stevens 1971b, Aldrich et al 1979). The I_k current had a time to peak of 30 ms to 60 ms in Helix pomatia (Kostyuk et al 1975a), and time constants of decay of between 1 s to 2 s in Helix pomatia (Kostyuk et al 1975a) and 3.7 s to 10 s in the neural somata of Archidoris and Anisidoris (Aldrich et al 1979, Connor and Stevens 1971b). The rates of decay of the I_a and I_k currents were

voltage-dependent and decrease with more positive depolarizing steps (Kostyuk et al 1975a). Experiments were carried out in Ascaris to determine the time to peak of the outward current and to attempt to fit the decay with exponentials.

Aldrich et al (1979) used a two pulse regime, with two depolarizing pulses of equal amplitude, to study the recovery of the outward current from inactivation, in Archidoris and Anisidoris neural somata. The interval between the two pulses was varied. The peak amplitude of the current activated by the second, test pulse, was compaired to the peak amplitude of the outward current activated by the first conditioning pulse. The peak amplitude of the second current was calculated as a percentage of the peak amplitude of the first current, this percentage value was then plotted against the interpulse interval. At interpulse intervals of between 0 and 1 s, the peak amplitude of the second current successively decreased. At interpulse intervals of between 1 s and 100 s the peak amplitude of the second current successively recovered to 100% of the peak amplitude of the first current. In the neural somata of Helix pomatia, Kostyuk et al (1975a) and Heyer and Lux (1976) measured the time course of recovery from inactivation using a two step voltage regime similar to that of Aldrich et al (1979). Kostyuk et al (1975a) showed that full recovery took 25 s. Experiments similar to those of Aldrich et al (1979) showed that the outward current in Ascaris decreased in amplitude when an initial depolarizing pulse was followed by a second, test pulse

(interval of less than 12 s). The results section of this thesis describes these results in detail.

Thompson (1977) bath applied 4-aminopyridine (4-AP) and found it blocked the I_a current (K_d 1.5 x 10^{-3}). Experiments in Ascaris were carried out to determine the effect of 4-AP [5 mM] on the outward current. The results were analysed in a similar way to that described by Thompson (1977).

METHODS

Experimental Arrangement

The experimental chamber consisted of a central bath with a liquid capacity of 1.8 ml. The bath was surrounded by a water jacket through which water was circulated to maintain the preparation at a constant temperature. The central chamber was bolted onto a large metal base plate which was supported on a foam pad to reduce the effects of vibration. Micromanipulators (Leitz and Narashige), bolted to the base plate, were used to position the current and voltage electrodes. Illumination was provided by a fibre optic 'light pipe', this enabled the bulb to be placed some distance from the recording area. The tip of the 'light pipe' was positioned close to the area of the preparation from which recordings were being made. The worm was viewed from above through a Bausch and Lomb Zoom microscope.

The Dissection

Worms were prepared as before for the patch clamp experiments. An anterior section of the worm, 2 cm long was cut along a lateral line and the worm pinned cuticle side down onto a layer of Sylgard in a bath. In these experiments no enzyme treatment was used.

Perfusion System

Continuous perfusion of the preparation was provided by a Shuco perfusion pump, and was carried out by means of a small diameter polythene tube inlet into one end of the bath and a drain at the other. The connecting tube between the pump and the bath was contained in a water jacket. A local perfusion system was also used to enhance the rapidity of the effects when changing the Ringers. This system consisted of a broken pipette positioned using a Narashige micromanipulator 500 uM away from the cell being recorded from. The pipette was connected to the perfusion pump via a connecting tube contained in the same water jacket as that of the bath perfusion system. The flow rate for the total perfusion system was set at 8 ml/min and was found to clear the bath filled with blue dye in 4.5 minutes. The interval allowed after changing the Ringer before recording was 7 to 15 minutes.

Temperature Control

Throughout these experiments the temperature was maintained at 37 ^{o}C with a Grant FH15 circulating water pump. Hot water was circulated through the water jacket that surrounded the central chamber and around the jacket that surrounded the perfusion inlet tubes. This heated the Ringer contained in jars at room temperature to 37 ^{o}C before bathing the preparation. Adequacy of the temperature maintenance was continually monitored using a digital

TABLE 2: Solutions used in the voltage-clamp experiments. Ringers were adjusted to pH 7.6 with maleic acid. APF solutions were adjusted to pH 7.6 with NaOH.

Table of Solutions used in Voltage-Clamp experiments.

All the concentrations are expressed in mM.

	NaCl	NaAc	KCl	KAc	CaCl	MgCl	CaAc	MgAc	Glu	Tris	HEPES	EGTA	La	TEACl
APF	23	110	24	-	6	5	-	-	11	-	5	-		-
Ca-free APF	23	110	24	-	-	5	-	-	11	-	5	0.5	-	-
Cl-free APF	-	133	-	24	-	-	6	5	11	-	5	-	-	-
High-K APF	-	-	157	-	6	5	-	-	11	-	5	-	-	-
TEA APF	-	-	-	24	-	-	64	5	11	-	5	-	-	69
Ascaris Ringer	135	-	3	-	3	15.7	-	-	3	5	-	-	-	-
Ca-free Ringer	135	-	3	-	-	15.7	-	-	3	5	-	0.5	-	-
lanthanum Ringer	135	-	3	-	-	15.7	-	-	3	5	-	0.5	1	-
K Ringers	135 to 0	-	3 to 135	-	-	15.7	-	-	3	5	-	0.5	1	-
low Cl Ringer	-	135	-	3	-	15.7	-	-	3	5	-	0.5	1	-

All solutions were adjusted to pH 7.6 with maleic acid for Tris buffered Ringers, or NaOH with HEPES buffered APF solutions.

thermometer and found to be 37 °C +/- 0.2 °C.

Electrodes

Electrodes were pulled on a glass microelectrode puller (David Kopf) using filamented glass tubing (Clarke Electromedical Instruments GC 150f- 15). The current electrodes were pulled to a resistance of 4 MΩ and the voltage electrodes to 11 MΩ. They were filled with potassium acetate [3 M] by initial inversion in the solution and then back filling with potassium acetate. In experiments on the reversal potential of the currents the electrodes were filled with a magnesium sulphate solution [3 M] to prevent the possibility of loading the cells with potassium.

Solutions

Table 2 shows the composition of the solutions used in these experiments. Initially APF was used but in the later experiments, that form the bulk of those presented here, solutions based on Ascaris Ringer were used. Calcium-free Ringer was based on Ascaris Ringer solutions, it had no added calcium and included EGTA [0.5 mM] to further reduce the calcium concentration. TEA Ringer was based on APF, it had a calcium concentration of 64 mM, and 69 mM of sodium was substituted with sodium. Lanthanum Ringer solutions contained EGTA [0.5 mM], and lanthanum [1.0 mM] which has been shown to block calcium currents (Thompson 1977). Permeability experiments

were carried out using ion substitution methods. Potassium was replaced with sodium, and chloride was replaced with acetate. All solutions were adjusted to pH 7.6 with sodium hydroxide or maleic acid.

Calcium free and lanthanum Ringers were used to try to block calcium or calcium-dependent currents. There was no control of any sodium inward current.

Recording System

A Dagan 8500 voltage clamp was used and all output was displayed on a Gould digital storage oscilloscope (OS400) with an IEEE 488 interface. The amplifier was calibrated using an RC network in place of the electrodes and the cell. Data was stored on a Racal Store Four DS tape recorder with a bandwidth of up to 2.5 KHz. The signal was played back and hard copies were produced either on a chart recorder (lectromed) or on a Gould Series 6000 XY Plotter. All pulse regimes were controlled by a Digitimer (D100) and stimulus input was provided by Digitimer isolated stimulators (DS2). The voltage input of the Dagan used a voltage divider and this was calibrated at the start of each experiment. Amplifier gain was adjusted for each cell and was in the range 2500 to 5000 depending on the stability of the recording. Controls on the amplifier for capacity compensation and phase, were adjusted for each cell, to give the optimal recording as judged by the fidelity of the voltage pulses and

the current response. Leak subtraction, where used, was performed by the summation of the two current responses to equal voltage steps of the opposite polarity. The current response to hyperpolarizing steps was assumed to be linear and therefore to represent the leak current.

Analysis

The peak amplitude and time to peak of the current responses were measured from graphs of current plotted against time. A BBC microcomputer was used to record the current decay. Sampling rates were adjusted between 1 KHz and 0.05 KHz, depending on the length of the sample. The digitized decay was then analysed using a Biomedical Computer Programs (BMDP) non-linear regression programme, 'P3R', on the Edinburgh Regional Computing Centre, (ERCC) mainframe computer. The programme used for sampling was a Unilab 'Grapher' programme modified by myself to allow for a trigger on a separate channel. The various programmes required to edit and transform the data were written by me. Some of the procedures required a subtraction of currents for which I wrote a short Basic programme. The presentation of the results in a graphical form was done using written programmes for the Easygraph package produced by Mr.N.Stroud of Edinburgh Regional Computing Centre (ERCC).

Fig. 26: Two families of currents obtained from the same cell under voltage clamp. The currents are shown above the imposed voltage steps. The top two sets of records were obtained with the cell bathed in APF. The lower two sets of records were obtained from the same cell bathed in 'calcium-free' APF. The cell was stepped from a holding potential (H_p) of -35 mV, in increments of 10 mV, to a series of step potentials (S_p).

Records A: H_p=-35mV, S_p= -25mV, -15mV, -5mV, 5mV, 15mV, 25mV, 35mV,45mV.

Records B: H_p=-35mV, S_p= -45mV, -55mV, -65mV, -75mV, -85mV, -95mV, -105mV,-115mV.

Records C: H_p=-35mV, S_p= -25mV, -15mV, -5mV, 5mV, 15mV, 25mV, 35mV,45mV.

Records D: H_p=-35mV, S_p= -45mV, -55mV, -65mV, -75mV, -85mV, -95mV, -105mV, -115mV.

Note that the voltage records in the hyperpolarizing direction saturated the amplifier on the tape recorder and are therefore attenuated on this Figure.

Bathing Solutions: upper records, APF.
lower records, calcium-free APF

Temperature: 37°C.

Holding Potential: -35mV.

Step Potentials: from -115mV to +45mV.

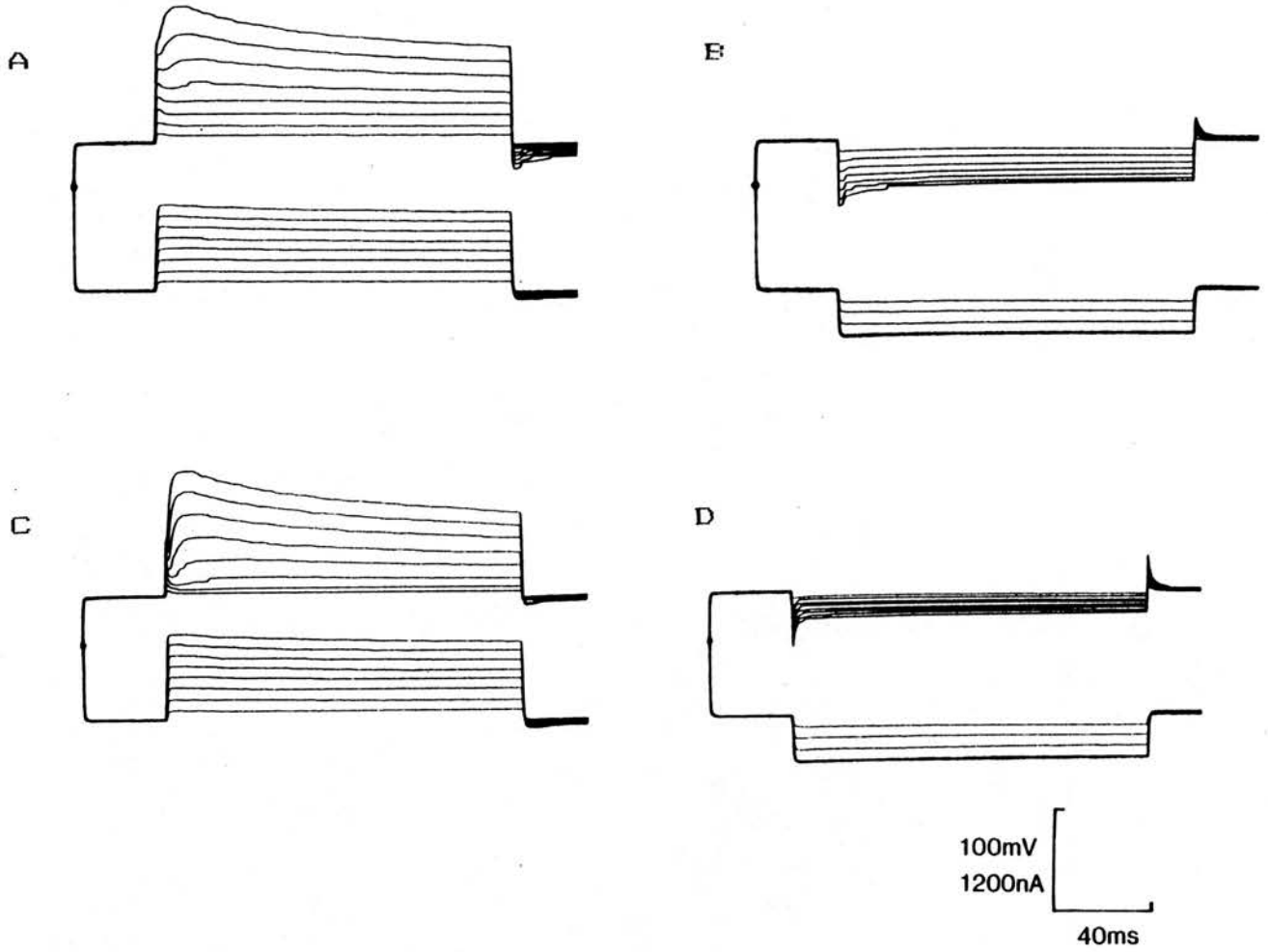
A
B
C
D
100mV
1200nA
40ms

RESULTS

This chapter describes the results from 49 successful voltage-clamp experiments performed on the somata of *Ascaris* body muscle cells.

Fig. 26 (A and B) show a typical family of currents obtained from a cell bathed in Artificial Perienteric Fluid (APF), at 37°C. The cell was voltage clamped at a holding potential of -35 mV and stepped to depolarized (Fig. 26 A) and hyperpolarized (Fig. 26 B) potentials for 200 ms. The currents have not been corrected for leakage currents. Beneath the two current records are the command voltage pulses from the holding potential of -35 mV to potentials between -115 mV and +45 mV in steps of 10 mV. Note that the larger hyperpolarizing voltage steps (Fig. 26 B and D) saturated the amplifier of the voltage channel on the tape recorder and were not reproduced on Fig. 26. The currents were reproduced faithfully.

With hyperpolarized voltage pulses (Fig. 26 B), the current amplitude decayed to a steady level at the onset of the pulse and after returning to the holding potential. The decay or relaxation was thought to indicate either the activation or inactivation of channels. With depolarized voltage pulses (Fig. 26 A) outward currents were observed, these rose to a peak and then decayed. As the depolarization steps were made more

positive the outward current peak became pronounced and a small inward current developed just after the onset of the pulse. After returning to the holding potential the currents showed relaxations.

Fig. 26 (C and D) show a family of currents obtained from the same cell as the upper current, 7 minutes after the preparation was bathed in a calcium-free APF [0.5 mM EGTA], at 37 ^{o}C. The cell was voltage-clamped at a holding potential of -35 mV and stepped to depolarized (Fig. 26 C) and hyperpolarized (Fig. 26 D) potentials for 200 ms. Beneath the two current records are the command voltage pulses from the holding potential of -35 mV to potentials between -115 mV and +45 mV in increments of 10 mV.

With hyperpolarized potential steps (Fig. 26 D) the current relaxations at the onset of the pulse and after returning to the holding potential, were reduced compared to those in APF. The amplitude of the steady state currents were also reduced indicating an increase in the input resistance. With depolarized potential steps (Fig. 26 C) the peak outward current was similar to the currents obtained in APF, indicating no significant calcium-dependent outward current. At the onset of the depolarizing pulse the rate of rise of the outward current was faster than that seen in APF.

Fig. 27: Current-voltage graph drawn from the same experiment as that in Fig. 26, with the cell bathed in APF. The current was measured 20 ms after the start of the step potential, at each step potential. The currents obtained were then plotted against the step potential. The graph is approximately linear with voltage steps in the hyperpolarizing direction and shows a developing outward current with depolarizing voltage steps.

Bathing Solutions: APF.

Temperature: 37°C.

Holding Potential: -35mV.

Step Potentials: from -95mV to +45mV.

I/V Plot from Voltage Clamped Cell.

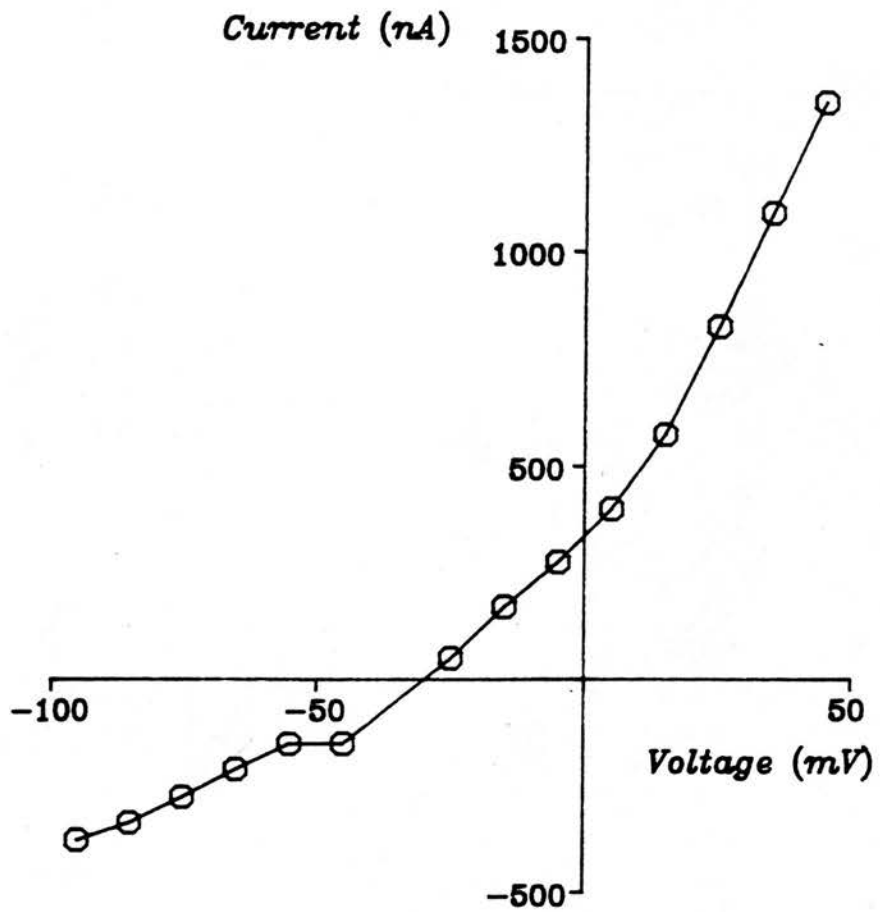

Fig. 28: Two sets of leak subtracted current records obtained from the same experiment as in Fig. 26. In the upper set of records the bathing solution was APF. The lower set of current records were obtained from the same cell in a bathing solution of calcium-free Ringer. In both sets of records the currents were obtained by stepping from a holding potential, (H_p) of -35 mV, in increments of 10 mV, to a series of hyperpolarized and depolarized step potentials (S_p). Potential steps were imposed on the cell in pairs of equal amplitude but in opposite directions. First a hyperpolarizing step was applied. This was followed by a step of the same amplitude, but in the depolarizing direction. The currents obtained from each hyperpolarized step potential were then subtracted, point for point, from the currents obtained by the paired, depolarizing step potential.

Bathing Solutions:	upper records, APF.
	lower records, calcium-free APF.
Temperature:	37^{o}C.
Holding Potential:	-35mV.
Step Potentials:	from -115mV to +45mV.

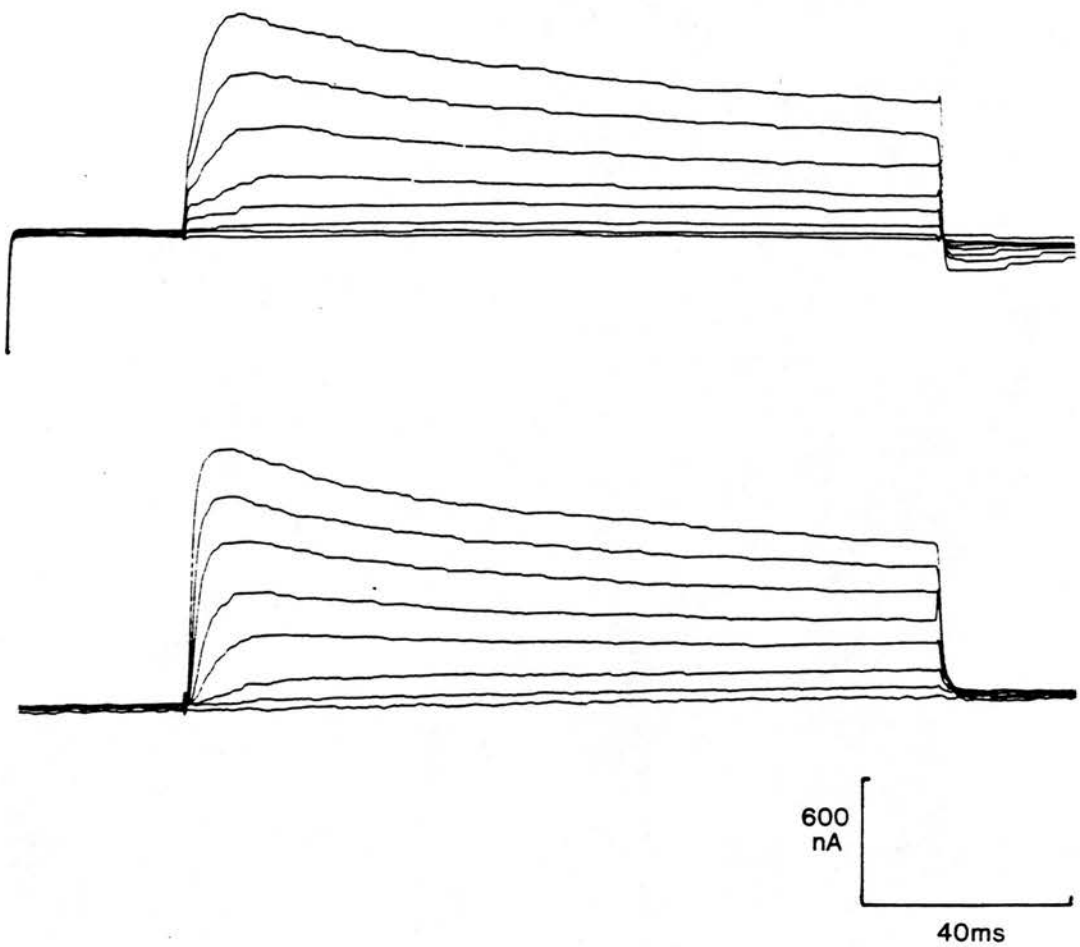
600
nA
40ms

These results were taken to indicate that either calcium or a calcium-dependent permeability were present in the muscle cell soma membrane. The removal of calcium from the bathing solution would therefore prevent inward current from passing through calcium channels or lead to the inactivation of calcium-dependent channels. The increased rate of rise of the delayed outward current was thought to be the result of the removal of an inward current carried by calcium.

Fig. 27 shows a graph of current against step potential, taken from the same experiment as illustrated in Fig. 26 with the cell bathed in calcium-free APF. The cell was maintained at a holding potential of -35 mV, and stepped to the depolarized and hyperpolarized potentials indicated on the graph. The current amplitude was measured 20 ms after the start of the pulse. At hyperpolarized potentials the current was less than 500 nA and increased with more negative hyperpolarizations in a linear manner. At depolarized potentials the outward current increased, as the depolarized step was made more positive up to 1400 nA at +45 mV. The currents obtained during hyperpolarizing steps in calcium-free Ringers were used as a measure of the leak current.

Fig. 28 shows two sets of leak corrected currents obtained from the same experiment as in Fig. 26. The leak subtraction procedure was outlined in the methods. The currents obtained from positive and negative voltage steps of equal magnitude were

Fig. 29: Graph of peak leak subtracted current and time to peak plotted against step potential for an experiment on a cell bathed in calcium-free APF. The step potentials on the graph are the potential to which the steps were made. The circles show the points obtained from the peak current amplitude at each step potential. The squares show the points obtained from the time taken for the current to peak at each step potential. The time to peak of the outward current is seen to decrease with increasing depolarizing steps. The peak amplitude of the outward current is seen to increase with increasingly depolarized steps.

Bathing Solutions: calcium-free APF.

Temperature: 37°C.

Holding Potential: -35mV.

Step Potentials: from -130mV to +60mV.

Graph of Peak Outward Current and Time to Peak against Step Potential.

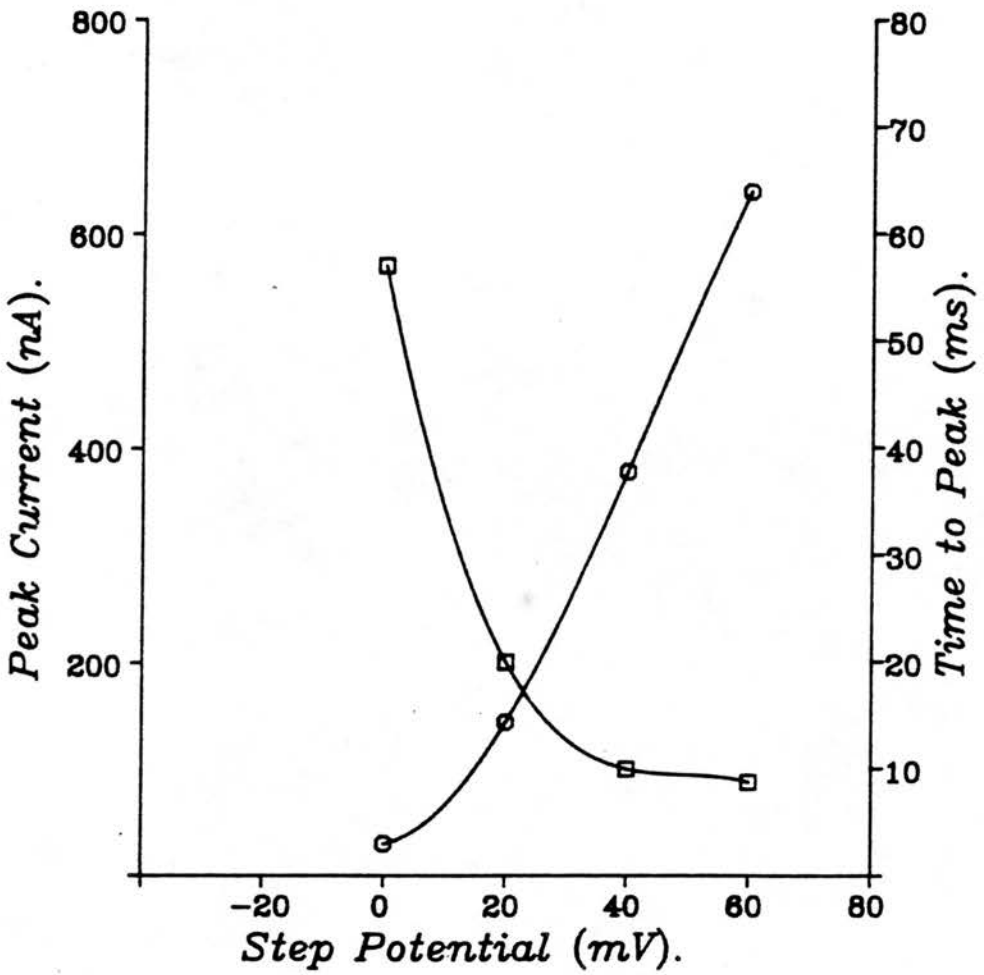

Peak Amplitude– circles
Time to Peak– squares.

subtracted point for point. This method allowed observation of the current activated by depolarization and removed the voltage independent leakage current. The upper current records of Fig. 28 were obtained when the cell was bathed in APF. The outward currents in the lower current records were obtained 7 minutes after changing the bathing solution to a calcium-free APF. A faster rate of rise and larger peak amplitude were observed in the calcium-free APF. The results were interpreted as indicating the loss of a calcium inward current in calcium-free APF.

Time to Peak and Peak amplitude Plots

Fig. 29 shows a graph of the time to peak and the peak amplitude of the leak corrected outward current plotted against potential. The holding potential was -35 mV and depolarizing steps to the potentials indicated on the graph were applied. The points were taken from a typical voltage-clamp experiment performed in calcium-free APF. The currents were outward at step potentials to 0 mV. With more positive step potentials the amplitude of the outward current increased. The current did not reach a maximum with a step potential to +60 mV. The time to peak showed a reduction from 58 ms at a step potential to 0 mV, to 10 ms at a step potential to +60 mV.

Fig. 30: Leak subtracted current records obtained from a cell bathed in TEA APF. The cell was stepped from a H_p=-35mV to S_p=-25mV, -15mV, -5mV, +5mV, +15mV, +25mV; paired hyperpolarizing pulses were used for the leak subtraction proceedure. An inward current was activated when stepping to -5mV. With increased depolarizing steps the inward (downward) current showed a decreasing latency of onset and a decreasing amplitude. A small outward current is also seen following the inward current.

Bathing Solutions: TEA APF.

Temperature: 37°C.

Holding Potential: -35mV.

Step Potentials: from -95mV to +25mV.

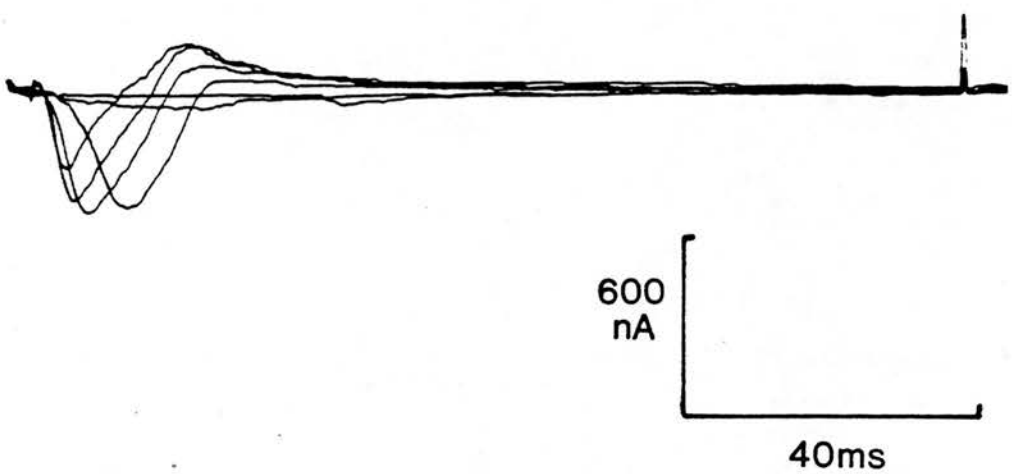
600
nA
40ms

Inward Current

Jarman and Ellory (1969) demonstrated that the spikes of Ascaris somatic muscle were calcium-dependent. The maximum spike amplitude was observed to be dependent on the extracellular calcium concentration (Weisblat et al 1976). Harrow and Gration (personal communication) showed the calcium channel blocker lanthanum blocked the transient inward current surge produced by a depolarizing voltage-clamp step. It was of interest to further investigate the inward current using voltage clamp.

Fig. 30 shows an example of the leak subtracted current Records obtained from an experiment where the cells were bathed in TEA APF, in which the monovalent cations of APF were replaced with tetraethylammonium (TEA) and the calcium concentration increased to 64 mM. Other experiments in this series (N=5) showed similar but not as dramatic results. Cells bathed in TEA APF showed a decrease in the input conductance. The recordings were not very stable and the cells deteriorated rapidly. The holding potential was -35 mV, and steps to potentials between -25 mV and +25 mV were imposed. A step to -25 mV did not activate any currents. With a step to -5 mV a transient inward current of 350 nA was observed, followed by an outward current. The time to peak of the inward current decreased with more positive step potentials. The amplitude of the transient inward current initially increased and then decreased with more positive depolarizing steps. In TEA APF the major permeant

Fig. 31: A consecutive series of leak subtracted current records obtained from a voltage-clamp experiment on the same cell bathed in different solutions. In each solution the cell was stepped from a H_p=-35mV to S_p=-25mV, -15mV, -5mV, +5mV, +15mV, +25mV, +35mV, +45mV, +55mV; paired hyperpolarizing pulses were used for the leak subtraction proceedure. The bathing solution used in each record were:

Record A: APF bathing solution

Record B: calcium-free bathing solution

Record C: return to APF bathing solution

Record D: chloride-free APF bathing solution

Record E: return to APF bathing solution

Record F: high-potassium APF bathing solution

Record G: return to APF bathing solution

Temperature: 37^{o}C.

Holding Potential: -35mV.

Step Potentials: from -95mV to +25mV.

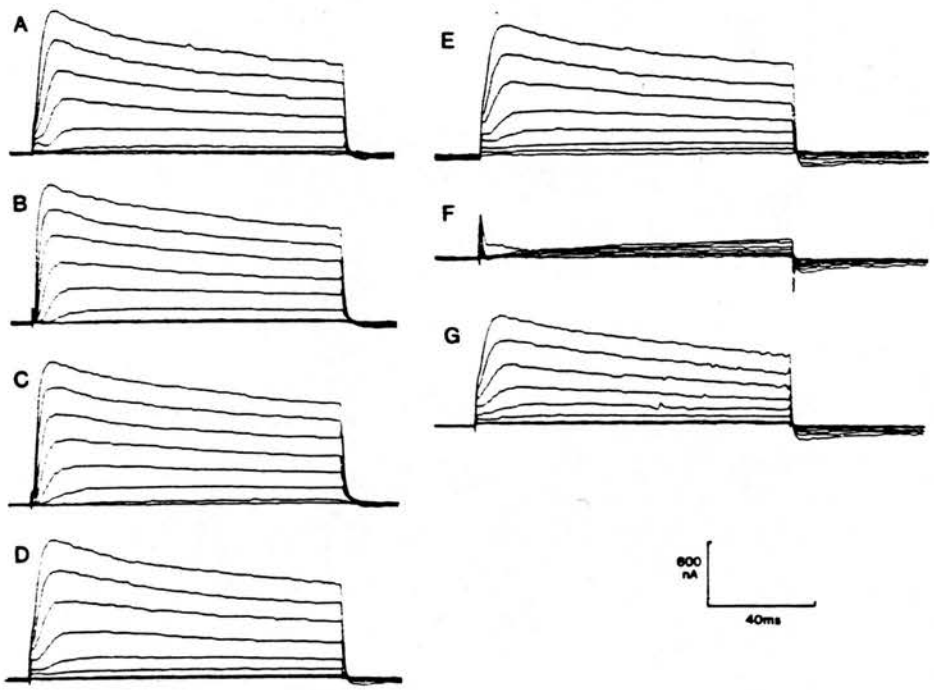
A
B
C
D
E
F
G
600
nA
40ms

cation was calcium, the inward current was therefore proposed to be carried by calcium ions.

Permeability of the Outward Current

(a) Preliminary Experiments

The next series of experiments were performed in order to determine the ion species carrying the outward current. The preparation was bathed in APF and solutions based on APF modified by ion substitution. Fig. 31 shows the leak corrected currents obtained for depolarizing steps in chloride deficient (Cl substituted 1:1 with acetate) and high potassium Ringers (Na substituted 1:1 with K). The leak subtracted currents in Fig. 31 were obtained from the same cell. The holding potential was -35 mV, depolarizing steps were applied, in 10 mV increments, up to a membrane potential of +45 mV. Fig. 31(A) shows the control currents obtained in APF. The rapid rise and slow decay of the outward current are seen. Fig. 31(B) are the currents obtained in calcium-free APF and Fig 31(C) are the currents after returning to APF.

Fig. 31(D) shows the currents obtained from the same cell with the same depolarizing pulses, after bathing for 30 minutes in chloride free APF. Fig. 31(E) shows the currents obtained

from the same cell under the same voltage pulses, after returning the bathing solution to APF for 12 minutes. The currents showed little discernible change when bathed in a chloride free APF, indicating that the outward conductance was not significantly chloride dependent.

Fig. 31(F) illustrates the currents 15 minutes after increasing the potassium concentration of the bathing Ringer to 138 mM. The currents in Fig. 31(G) were observed after returning to APF. There was a reversible reduction in the amplitude of the outward current in high potassium solution. The current remaining in the high potassium Ringer rose very slowly after the onset of the pulse and did not show inactivation.

The experiments illustrated in Fig. 31 present evidence that the outward current was potassium dependent. Other experiments (N=5) showed similar effects: in some the reduction of the chloride concentration led to a reduction of the outward current, in some the increase in potassium concentration did not have such a dramatic effect. These results taken together indicate that chloride can carry part of the outward current when the cell was bathed in APF. However the experiments indicated that potassium was the predominant ion carrying the outward current.

Fig. 32: A graph of the tail current amplitude plotted against length of prepulse. In this experiment the cell was stepped from a H_p=-35mV to a S_p=+55mV. The duration of the S_p was varied between 0 and 2.2 s. At the end of the Step the potential was returned to the Holding potential, and the maximum amplitude of the decaying tail current was measured. The current amplitude for each of the step durations was then plotted against that step duration.

Solutions:	lanthanum Ringer
Temperature:	37°C.
Holding Potential:	-35mV.
Step Potentials:	to +55mV.

Graph of Amplitude of Current Tails Measured at −35mV after a Prepulse of +90mV.

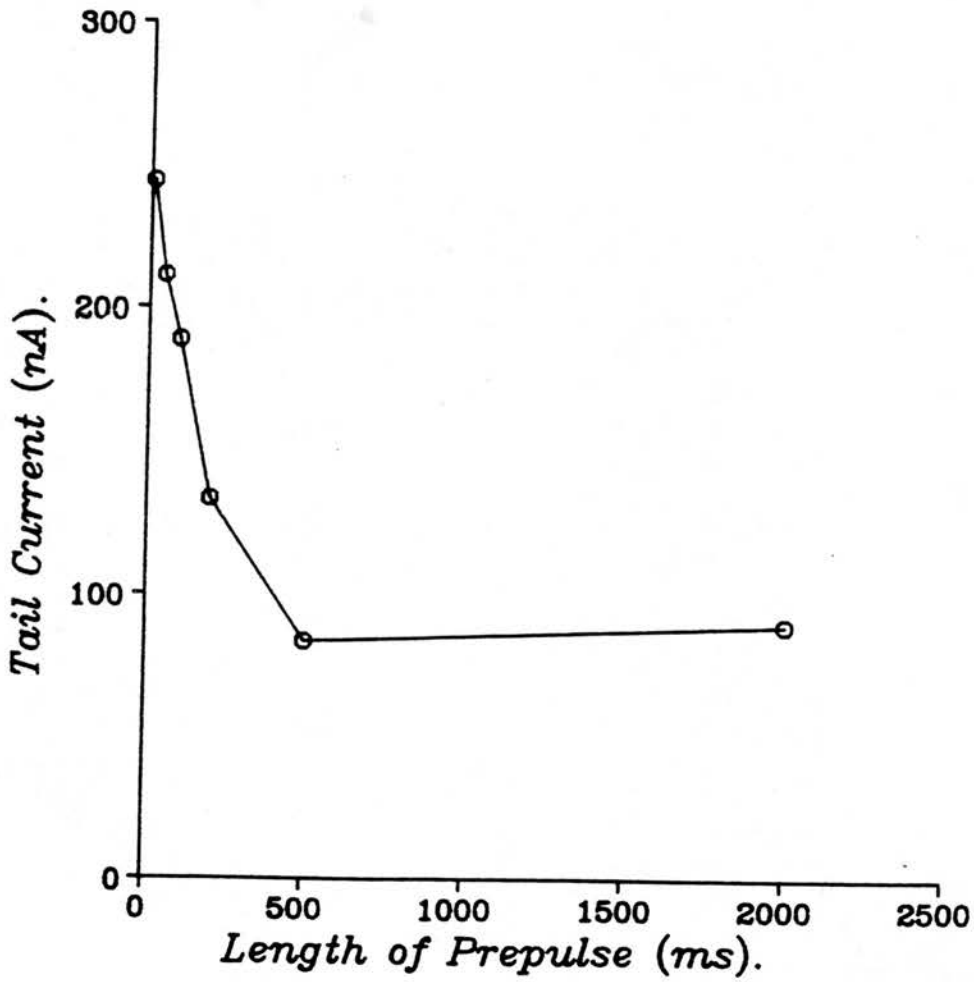

(b) Measurement of Reversal Potential with Different Extracellular Potassium Concentrations

In the following experiments the cells were bathed in a lanthanum Ringer based on *Ascaris* Ringer (see Table 2). Lanthanum has been used both by Meech and Standen (1975) and Thomas (1984) to block the early inward current, and the demonstration by Harrow and Gration (personal communication) of its effect in reducing the inward current in *Ascaris*, led to its use in these experiments. The effect of a sodium conductance in the *Ascaris* membrane was not controlled for. The removal of sodium from the bathing Ringer had no discernible effect on the outward current.

The reversal potential of the outward current was determined in Ringers of different potassium concentration. These experiments used a two pulse protocol. A depolarizing prepulse of 10 to 20 ms was applied to activate the outward current. The voltage was then stepped to one of a range of potentials and the currents recorded at these test pulses. The tail currents observed at the onset of the test pulses declined in amplitude to a steady-state value. The decline was due to inactivation of the outward current. The amplitude and direction of the tail currents were dependent on the reversal potential of the ions carrying the outward current.

Fig. 32 shows the results of an experiment to confirm that

the tail currents were linked to the outward current. In this experiment, the holding potential was -35 mV, depolarizing steps of various lengths to a potential of +55 mV were applied. Tail currents were observed when the voltage was stepped back to the holding potential. The tail currents were composed of both an initial capacitive surge and a following current relaxation. The peak amplitude of the tail current relaxations were measured.

Fig. 32 is a graph of the amplitude of tail currents plotted against length of the depolarizing step. The tail current amplitude was measured by subtracting the steady state amplitude of the current (I_{ss}) from the peak amplitude of the current (I_p). Tail current amplitude decreased as the length of the prepulse was increased, and the time course of the decay closely followed the decay of the outward current. This result has been taken as confirmation that the tail currents are linked to the outward current (Stanfield 1970, Adrian et al 1970), and a similar conclusion is drawn in Ascaris.

Fig. 32 shows that a residual current of 80 nA was present 500 ms after the depolarizing pulse. There are a number of possible explanations. The outward current may not have decayed fully, another ion channel activated by depolarization could be contributing to the tail current, the current remaining could be either a capacitive artifact or a product of the settling of unclamped regions of the cell.

Fig. 33: A consecutive series of leak subtracted current records, obtained from a voltage-clamp experiment on the same cell bathed in lanthanum Ringers of different potassium concentrations. A two step protocol was used, the potential was stepped from a H_p=-35mV to a first S_p1=+55mV, after 10 ms a second S_p2 was applied to one of a range of potentials: -125mV, -115mV, -105mV, -95mV, -85mV, -75mV, -65mV, -55mV, -45mV, -25mV, -15mV, -5mV, 5mV, 15mV, 25mV, 35mV, 45mV, 55mV. The command voltage steps are shown at the bottom left. The cell was bathed for 10 minutes in each solution before recording the currents. The bathing solutions were presented in a random order. The tail currents at the onset of S_p2 are clearly seen. The bathing solutions used in each record were:

Record A: potassium-free lanthanum Ringer.

Record B: 3 mM potassium lanthanum Ringer.

Record C: 30 mM potassium lanthanum Ringer.

Record D: 138 mM potassium lanthanum Ringer.

Bathing Solutions:	0-138 mM potassium lanthanum Ringer.
Temperature:	37°C.
Holding Potential:	-35mV.
Step Potentials:	S_p1=+55mV S_p2 between -125mV and 55mV.

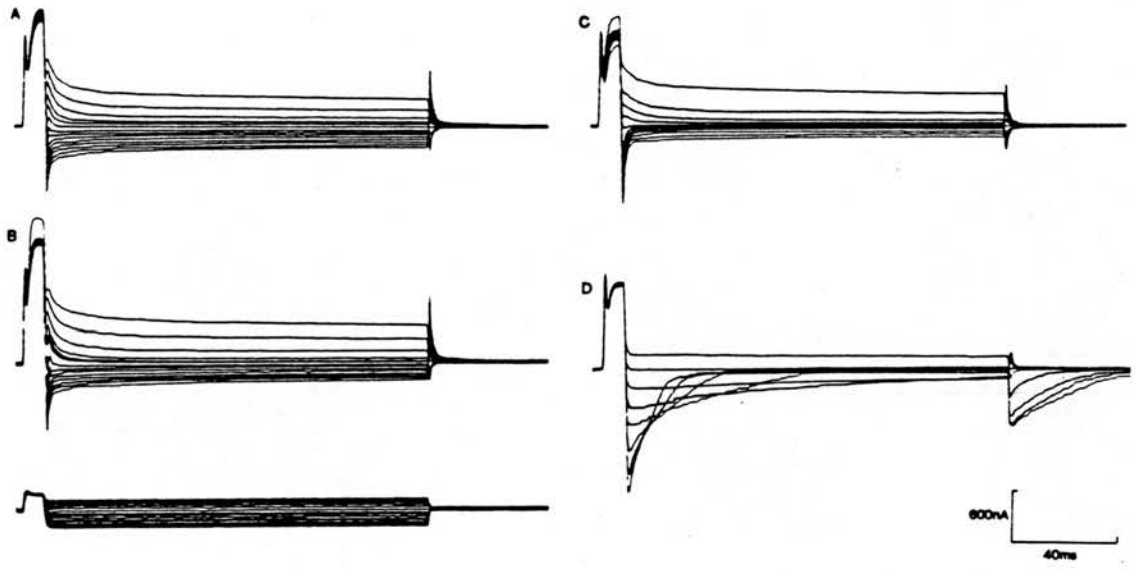
A
B
C
D
600nA
40ms

Fig. 34: Graph of outward current reversal potential, obtained from an experiment conducted in the same manner as that in Fig. 33, plotted against the Log potassium concentration of the bathing Ringer. The points were obtained by estimating the 10 mV range over which the current tails reversed in direction. The bars on either side of the points show the potential range over which the current was estimated to have reversed. The graph shows linearity down to 10 mM extracellular potassium, but at lower potassium concentrations the curve was non-linear.

Bathing Solutions:	0-138 mM potassium lanthanum Ringer.
Temperature:	$37^{o}C$.
Holding Potential:	-35mV.
Step Potentials:	S_p1=+55mV S_p2 between -125mV and 55mV.

Graph of Extracellular Log K Concentration against Reversal Potential.

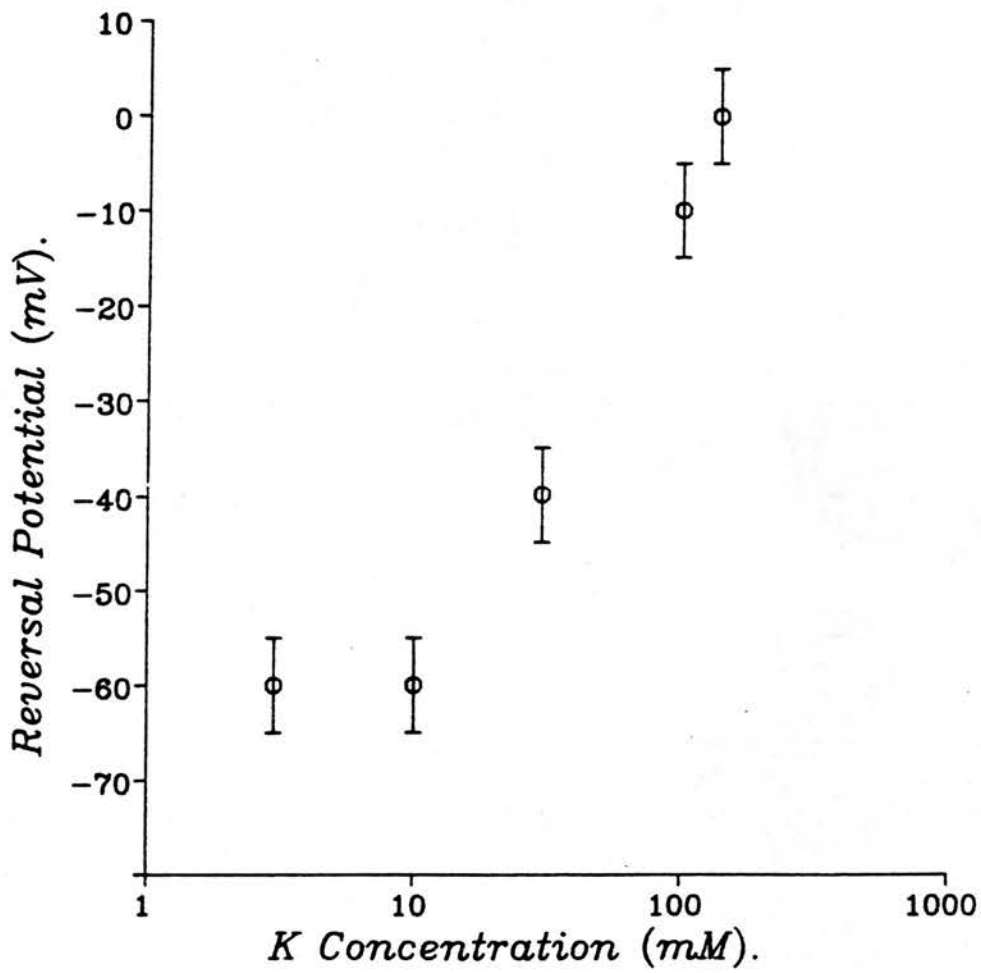

The aim of the next series of experiments was to determine the reversal potential of the outward current. Fig. 33 shows the currents obtained from an experiment on a voltage-clamped cell bathed in four different concentrations of potassium. The holding potential was -35 mV, a 10 ms depolarizing prepulse to +55 mV was followed by a test pulse to a range of voltages between -125 mV and +55 mV. The prepulse activated the outward current and the amplitude and direction of the tail currents at each of the different test pulses were observed. The potassium concentration of the bathing Ringer was changed by 1:1 substitution with sodium. Fig. 33(A) shows the currents obtained in a bathing solution of 0 mM potassium. Fig. 33(B), (C), (D), show the currents obtained in 3 mM, 30 mM, and 138 mM potassium respectively. The imposed voltage steps are shown in the bottom left of Fig. 33.

A total of 8 cells were used in this type of experiment. The micropipettes used were filled with magnesium sulphate [3 M] to prevent loading the cells with potassium. Where the effect of potassium substitution could not be shown to be reversible, the cell was assumed to be damaged and the results rejected. The apparent reversal potential was seen to move in the depolarizing direction, as the extracellular potassium concentration was increased.

Fig. 34 is a graph of the reversal potential of the outward current plotted against log potassium concentration for a

different experiment than the current records of Fig. 33. The graph was approximately linear for potassium concentrations above 3 mM as predicted by the Nernst Equation for a potassium selective conductance. The reversal potential in 0 mM potassium was less than that predicted by the Nernst Equation. Two explanations were proposed for the observed difference. Firstly, the potassium concentration at the extracellular surface of the membrane was greater than that in the bath. Secondly, the channels could be permeable to another ion which alters the reversal potential measurement. This other ion species could either be passing through separate channels, or possibly the potassium channel carrying the outward current has a small permeability to another ion. Assuming that the other ion was sodium, a permeability ratio of P_{Na}/P_K equal to 0.04 gave an adequate fit to the data.

To test the comparative effect of potassium and chloride on the outward current, a short series of experiments were carried out (N=12). The reversal potential was determined by measuring the tail current amplitude as in the experiments above. In lanthanum Ringer (K=3 mM, Cl=170 mM) the mean reversal potential was found to be -47 mV (N=12). The bathing solution was then changed for either a high potassium or low chloride Ringer and the reversal potential of the outward current was again measured. In a high potassium lanthanum Ringer (K=138 mM, Cl=170 mM) the mean reversal potential was 0 mV (N=10). In a low chloride lanthanum Ringer (K=3 mM, Cl=31 mM) the mean reversal

Fig. 35: Leak subtracted current records obtained from a single cell. The cell was stepped to a S_p=50mV from a series of holding potentials, H_p=-70mV, -60mV, -50mV, -40mV, -30mV, -20mV, shown on the right of the figure. As the H_p was made more depolarized the peak amplitude of the outward current was observed to decline. This indicates that a component of the outward current was dependent on the holding potential.

Bathing Solutions: lanthanum Ringer.

Temperature: 37°C.

Holding Potential: between -70mV and -20mV.

Step Potentials: S_p=+55mV.

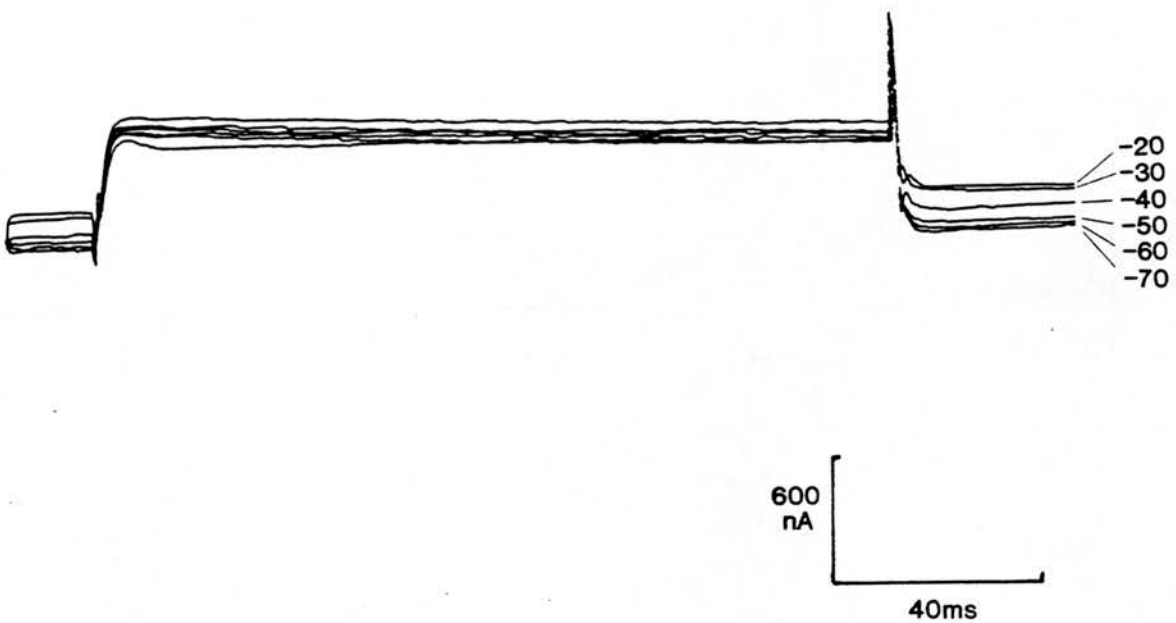
-20
-30
-40
-50
-60
-70
600
nA
40ms

potential was -42 mV (N=8). These results show that a reductionin chloride concentration depolarized the reversal potential by 5 mV, compaired to a 47 mV depolarization produced by an increase in potassium concentration. The conclusion of these experiments was that chloride had a minimal effect on the outward current.

Dependence of Outward Current on Holding Potential

The I_a currents of Helix pomatia have been shown to inactivate at holding potentials of -40 mV (Kostyuk et al 1975a). This inactivation has been called steady-state inactivation and has been observed in many cells for example Anisidoris and Archidoris neurones (Connor and Stevens 1971b). It was therefore of interest to see if the outward currents of Ascaris suum had similar steady-state inactivation characteristics.

Fig. 35 shows a typical example of the leak subtracted currents obtained from a series of experiments (N = 12) designed to study the steady-state inactivation. The cell was held at various holding potentials ranging from -70 to -20 mV, and depolarizing steps to a constant potential of +50 mV were applied. The outward current was observed for each of the steps and the time to peak and peak amplitude were measured. The amplitude of the currents increased as the holding potential was made more hyperpolarized.

Fig. 36: A graph of the peak outward current amplitude plotted against the holding potential. In experiments similar to that shown in Fig. 36 the peak outward current observed at each different holding potential was expressed as a fraction of the peak current obtained at a holding potential of -70mV. This normalized the currents which were then plotted at each of the holding potentials. The circles show the points obtained from 6 experiments (mean +/- S.E.) in lanthanum Ringer. The squares are the points obtained from 6 experiments (mean +/- S.E.) in lanthanum Ringer containing 4-AP [5 mM].

Bathing Solutions: lanthanum Ringer.

Temperature: 37°C.

Holding Potential: between -70mV and -20mV.

Step Potentials: S_p=+55mV.

Graph of Peak Normalised Outward Current against Holding Potential.

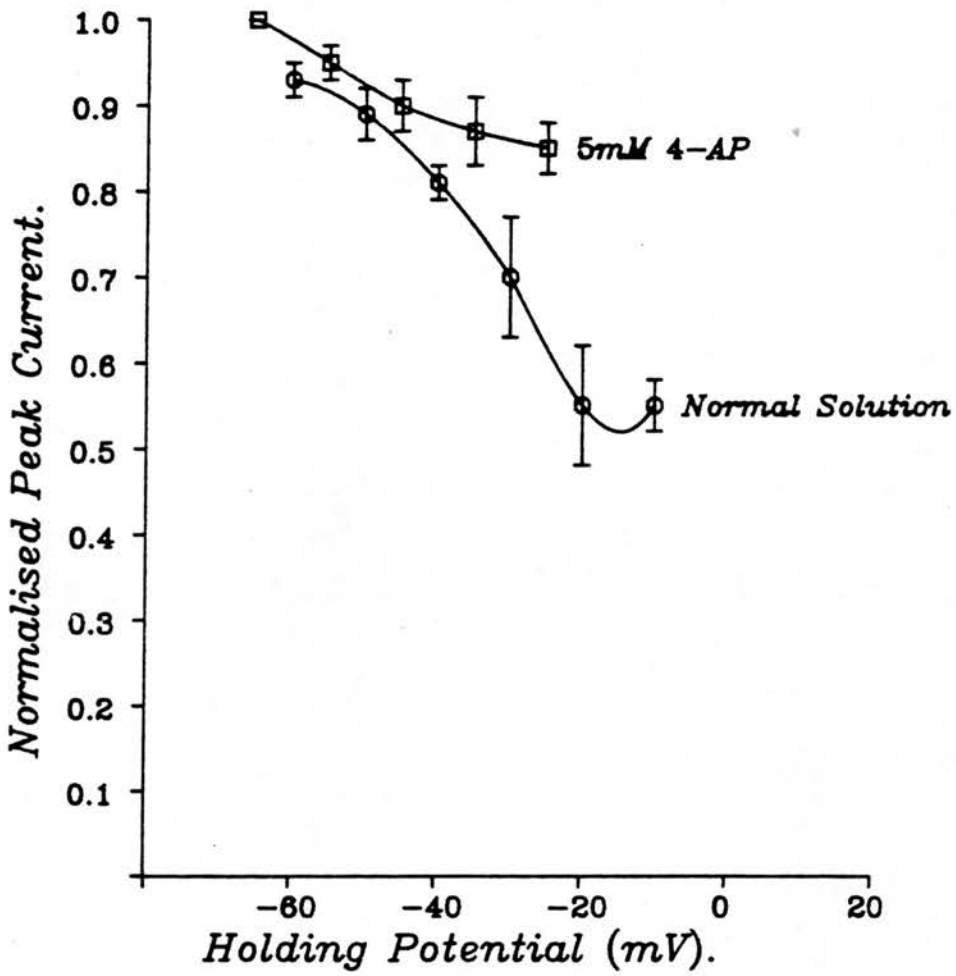

Current Normalised for Maximum Current in Each Cell. Points are Mean +/−SEM.

Fig. 37: Current (top) and voltage (bottom) records from an experiment to determine the time taken for the outward current to recover after activation. The cell was stepped from a H_p=-35mV to a first conditioning pulse, C_p=+55mV, this was followed by a test pulse, T_p=+55mV at successively increasing intervals after C_p. The peak amplitude of the current activated by the test pulse was initially much reduced but recovered as the interpulse interval increased.

Bathing Solutions: lanthanum Ringer.

Temperature: 37°C.

Holding Potential: -35mV.

Step Potentials: C_p=+55mV, T_p=+55mV.

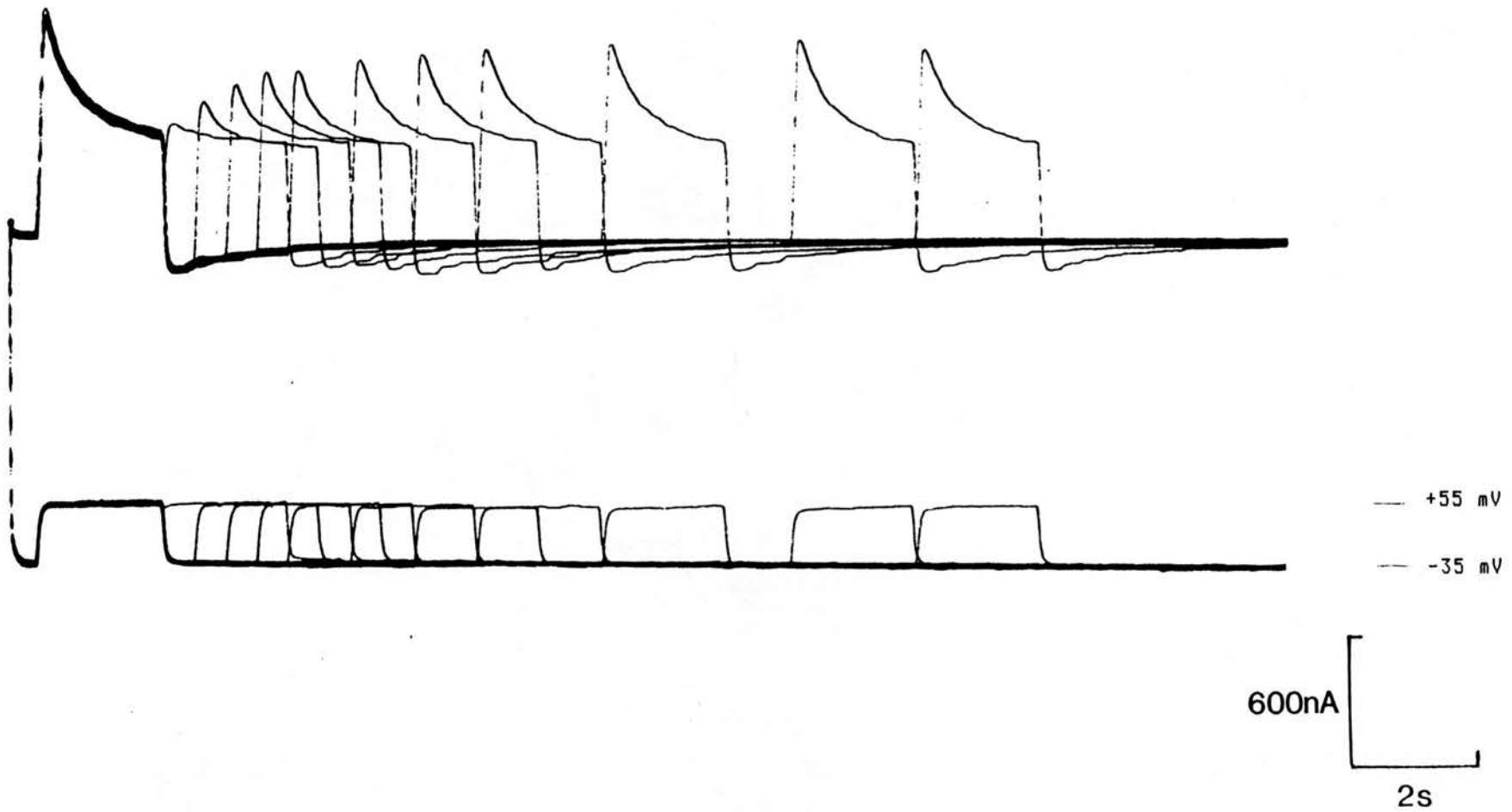
+55 mV
-35 mV
600nA
2s

The most hyperpolarized holding potential used in these experiments was -70 mV. The peak of the current obtained from each holding potential was plotted as a fraction of the peak current obtained from a holding potantial of -70 mV in the same cell, in order to normalize the results. Fig. 36 is a graph of the normalized peak currents plotted against the holding potential. The circles represent the mean of 6 experiments all carried out in lanthanum Ringer. At holding potentials around the resting potential of the muscle cells (-35 to -40 mV), the graph illustrates that the outward current was 70% maximally activated. The squares on the graph are the mean normalized currents obtained in a 4-AP Ringer, these results will be discussed later.

Recovery of the outward current after Activation

Fig. 37 illustrates a typical example of the current records of 12 experiments carried out to investigate the recovery of the delayed outward current after activation. The holding potential was -35 mV, two depolarizing steps 2 s long to a potential of +55 mV were applied. The second, test pulse, was imposed at various intervals after the first, conditioning pulse. The current records from each two-pulse series in the same cell were superimposed to produce the illustration in Fig. 37. A time span of a minute between each series of two pulse applications was adequate to allow complete recovery, as judged by the constant amplitude of the first outward current in each two-pulse series. The peak current amplitudes showed a gradual

Fig. 38: A graph of the peak outward current of the test pulse against interpulse interval obtained from 6 experiments conducted in the same manner as Fig. 38. The peak outward currents produced by the test pulse, T_p, were expressed as a proportion of the peak current amplitude produced by the conditioning pulse, C_p. The points represent the mean +/- S.E. and show a gradual recovery of the current with increasing interpulse intervals. The line on the graph was drawn by eye.

Graph of the Time Course of Recovery of Outward Current.

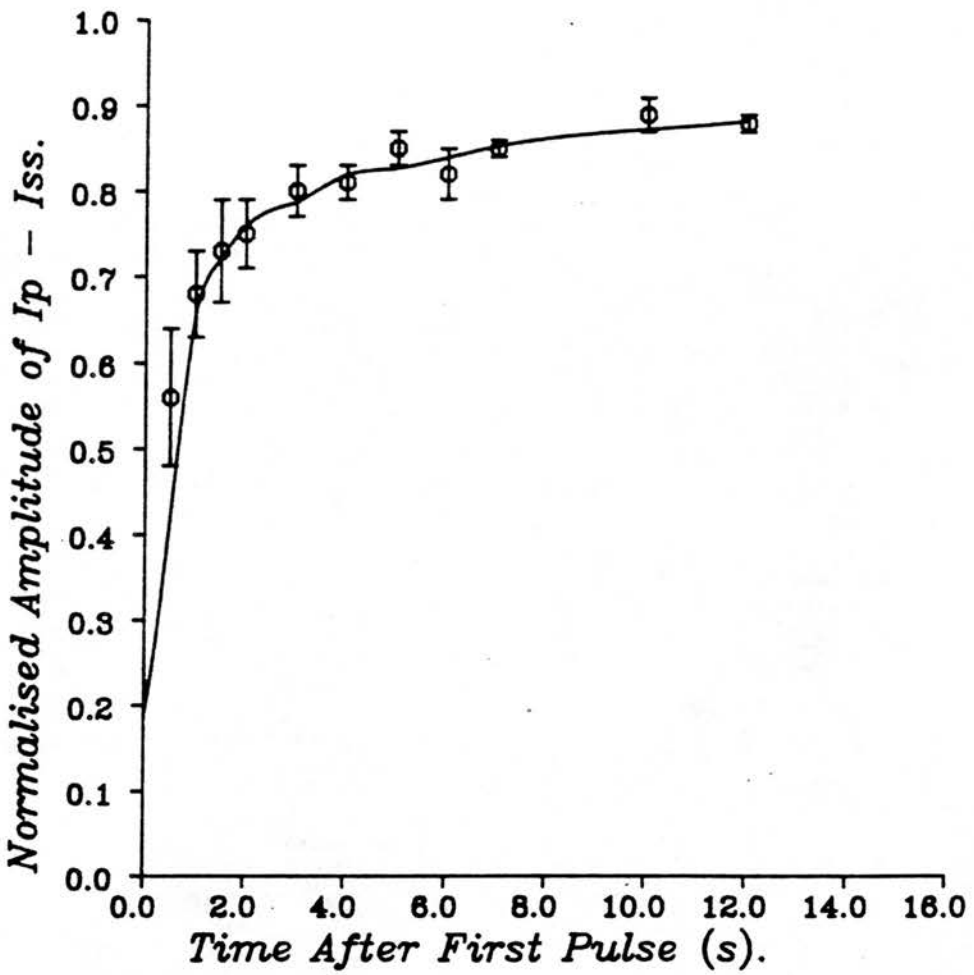

Points show mean +/−sem.

recovery as the interpulse interval was lengthened. At the maximum interpulse interval of 12 s full recovery to the amplitude of the first pulse was not seen.

The recovery from decay of the outward current in neurones of Helix pomatia (Heyer and Lux 1976, Kostyuk et al 1975a) and Anisidoris and Archidoris neurones (Aldrich et al 1979) showed continued inactivation up to 3 s after the initial prepulse, followed by a gradual recovery. This was measured by an initial decrease in the amplitude of the current at the second pulse between 1 to 3 s, followed by a recovery of the outward current amplitude.

Fig. 38 shows a graph of the mean of the normalized current amplitude against the interpulse interval, for 6 experiments conducted in the same way as the experiment illustrated in Fig. 37. The amplitude of the outward current was measured as the peak current amplitude minus the steady-state current amplitude, $(I_p - I_{ss})$. In these experiments the steady-state current was taken as the current amplitude at the end of the 2 s pulses. The currents were normalized by plotting the current amplitude at the second pulse, as a fraction of the first, conditioning pulse, current amplitude. The outward current recovered to 50% of its original value within 2 s and reached 90% of its initial value in 12 s. Full recovery of the current was not seen at the maximum interpulse interval used. The line on the graph was drawn by eye.

The Effect of Drugs on the Outward Current.

Outward potassium currents of mollusca have been shown to be blocked by 4-AP and TEA (review Adams, Smith and Thompson 1980). These drugs have differential effects on the components of the outward potassium current. Externally applied 4-AP [ED_{50} = 2 mM] blocks an I_a current elicited by steps to -30 mV from a holding potential of -90 mV in Tritonia diomedia (Thompson 1977). Bath applied TEA [1 mM] blocked the slow, I_k component of the outward potassium current in Helix pomatia (Kostyuk et al 1975b). It was of interest to study the effects of TEA and 4-AP on Ascaris somatic muscle.

Application of TEA [64 mM] in the external Ringer effectively blocked most of the outward current (see Fig. 31). However, at this concentration the recordings were unstable and the cells deteriorated rapidly. It was decided to bath apply 4-AP at a single concentration of 5 mM. Thompson (1977) blocked 80% of the I_a current in Tritonia diomedia with extracellularly applied 4-AP [5 mM]. The results of 4-AP application from eight cells, from different worms are presented here. Washing the preparation for 30 minutes in fresh Ringer did not reverse the effect of 4-AP.

Effect of 4-AP on the Outward Current

An example of the leak subtracted currents obtained from a

Fig. 39: Two sets of leak subtracted currents from the same cell, the upper set was from the cell bathed in lathanum Ringer and the lower set was from the cell bathed in 4-AP lanthanum Ringer. The holding potential was -35 mV and the cell was stepped to S_p=-25mV, -15mV, -5mV, +5mV, +15mV, +25mV, +35mV, +45mV, +55mV; paired hyperpolarizing pulses were used for the leak subtraction proceedure. The currents in 4-AP lanthanum Ringer show the loss of a fast component to the outward current.

Bathing Solutions:	upper, lanthanum Ringer.
	lower, 4-AP lanthanum Ringer.
Temperature:	37^{o}C.
Holding Potential:	-35mV.
Step Potentials:	between -125mV and +55mV.

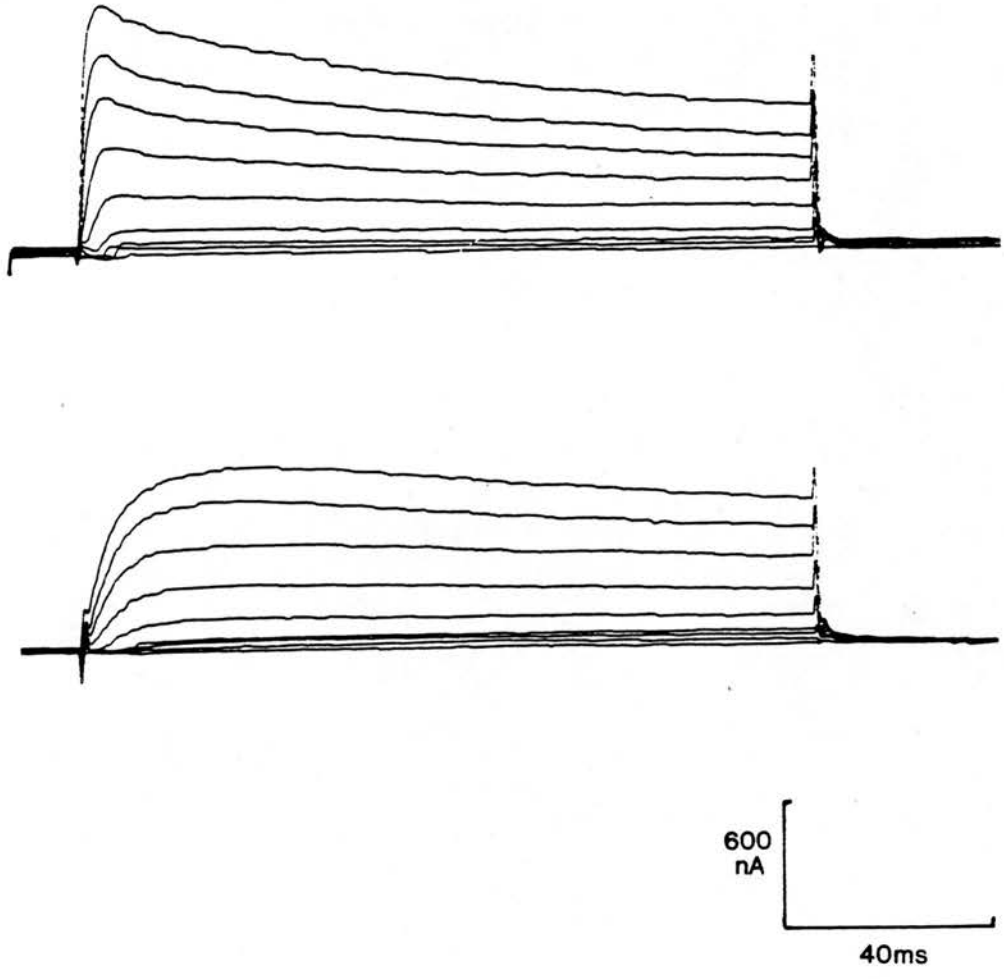
600
nA
40ms

Fig. 40: Graph of peak leak subtracted current and time to peak plotted against step potential for an experiment on a cell bathed in lathanum Ringer and then in 4-AP lanthanum Ringer. The step potentials on the graph are the potentials to which the steps were made.

lanthanum Ringer: the circles represent the peak amplitude of the outward current, and the squares represent the time to peak at each of the step potentials.

4-AP lanthanum Ringer: the triangles represent the peak amplitude of the outward current, and the diamonds represent the time to peak at each of the step potentials.

Bathing Solutions:	lanthanum Ringer and 4-AP lanthanum Ringer.
Temperature:	$37^{\circ}C$.
Holding Potential:	-35mV.
Step Potentials:	from -125mV to +55mV

Graph of Peak Outward Current and Time to Peak against Step Potential Before and after 4AP.

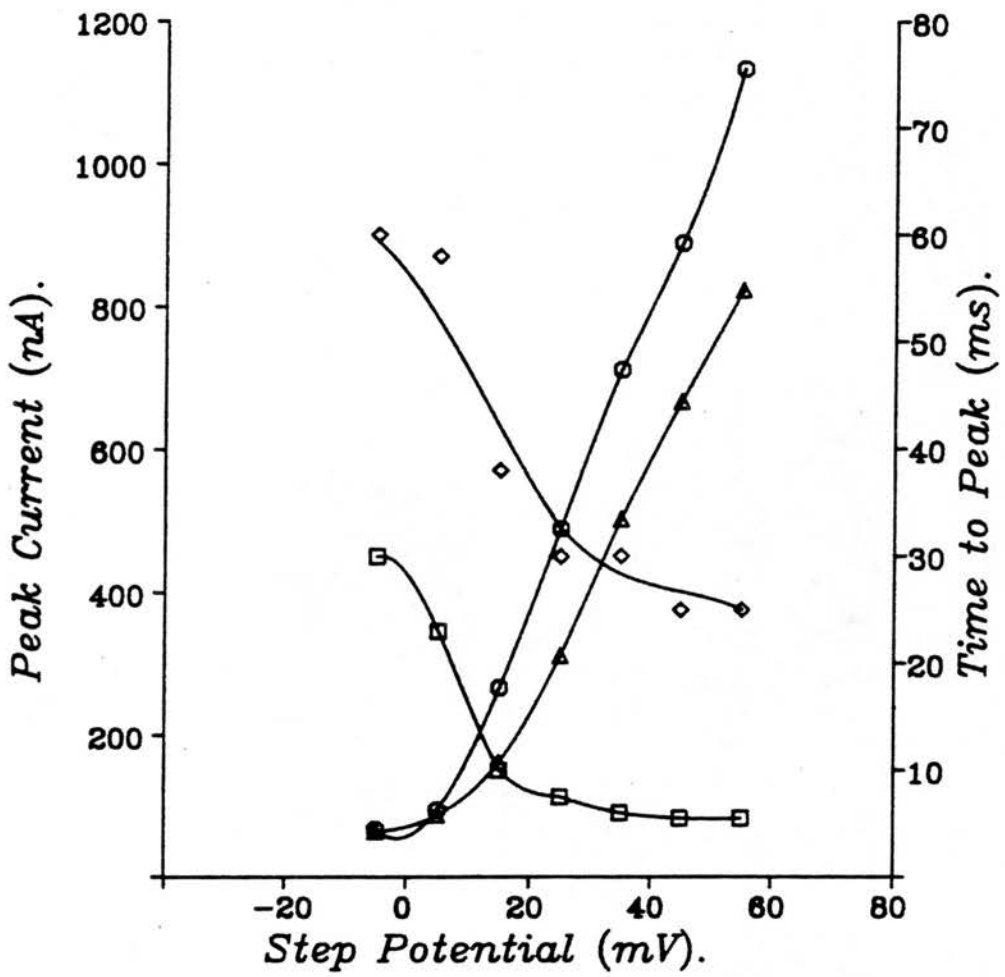

Peak Amplitude– circles
Time to Peak– squares.
Peak Amplitude after 4AP– Triangles.
Time to Peak after 4AP– Diamonds.

cell bathed in lanthanum Ringer is illustrated in Fig. 39(top). The holding potential was -35 mV, depolarizing steps to between -25 mV and +55 mV were applied. Currents from the same cell bathed in 4-AP [5 mM] lanthanum Ringer, with the same voltage-clamp steps are shown in Fig. 39 (bottom). The currents obtained after the addition of 4-AP showed an increase in the time to peak and a decrease in the peak amplitude. The decay of the current in 4-AP lanthanum Ringer was approximated by a single exponential. In all 8 experiments where 4-AP was applied similar effects on the outward current were seen.

Fig. 40 is a graph from the same experiments as Fig. 39 showing the time to peak and peak amplitude of the outward current plotted against potential before and after bath application of 4-AP. The holding potential was -35 mV, depolarizing steps to potentials between -5 mV and +55 mV were imposed. The peak current amplitude increased with more positive depolarized steps. Stepping to +55 mV, the current in lanthanum Ringer was 1150 nA and had not reached a maximum. After 4-AP treatment the peak current amplitudes were less than in lanthanum Ringer. At +55 mV the current was 70% of its original value. The time to peak decreased with more positive depolarized steps for both the control lanthanum Ringer solution and 4-AP solutions. At each potential the time to peak in the 4-AP Ringer was longer than in lanthanum Ringer, for example it was 5 times longer at +55 mV.

These results indicated that 4-AP affected the rise time

and initial amplitude of the outward current. Thompson (1977) showed a similar effect of 4-AP in Tritonia diomedia neurones and concluded that 4-AP preferentially blocked the fast transient, I_a component, of the outward current. Further analysis of the Ascaris outward current was carried out to investigate the effect of 4-AP more closely.

Effect of Holding Potential on the 4-AP Resistant Currents

If 4-AP blocked the fast transient I_a current in a similar manner to that reported by Thompson (1977) then the remaining current could have properties similar to the I_k. The most important difference between the I_a and I_k currents apart from time course and amplitude, were the steady-state inactivation curves (Connor and Stevens 1971b). The I_k current showed little inactivation at holding potentials of -40 mV, while in contrast the I_a was almost completely inactivated at these holding potentials (Kostyuk et al 1975a).

Fig. 36 (circles) shows the dependence of the total outward current on the holding potential. This current would include both I_a and I_k components. On the same graph are plotted the normalized peak currents after 4-AP application (squares). The peak current at each holding potential was divided by the peak current obtained at -65 mV to normalize the results. The points were the mean of 4 experiments. Both the plots show a decrease in the peak current with more depolarized holding potentials. In

Fig. 41: A graph of the digitized current records from a single cell bathed in lanthanum Ringer and 4-AP lanthanum Ringer. The cell was stepped from a holding potential of -35mV to S_p=+55mV. Three currents are shown on the graph. The upper current was obtained in lanthanum Ringer and shows a rapid rise to a peak followed by a decay. The middle current was obtained from the same cell bathed in 4-AP lanthanum Ringer and shows gentle rise to a peak followed by a decay. The lower, smaller current was obtained by point for point subtraction of the upper two records, the resulting current represents the component of the outward current removed by application of 4-AP. This 4-AP resistant current shows a rapid rise followed by a rapid decay that could be approximated by a single exponential.

Bathing Solutions:	lanthanum Ringer and 4-AP lanthanum Ringer.
Temperature:	37°C.
Holding Potential:	-35mV.
Step Potentials:	+55mV.

Graph of the Decay of the Outward Current with Time.

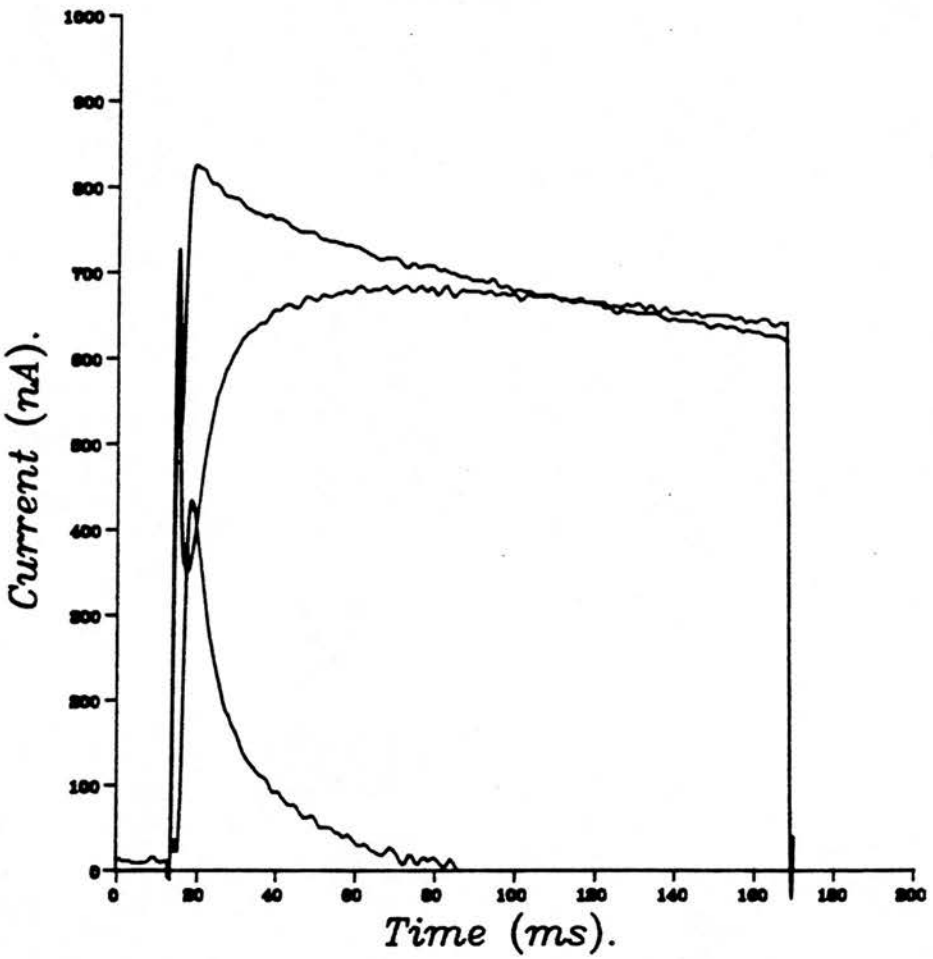

lanthanum Ringer this effect was more pronounced. The gross current that includes the current blocked by 4-AP is shown to have a greater dependence on holding potential than the slow component left after 4-AP application.

Current Decay Before and After 4-AP Application.

Neher (1971) and Neher and Lux (1972) have used estimates of the rate constants and time constants of current activation and inactivation, to produce a mathematical description of the outward current. These models were fitted to the observed outward currents before and after the application of TEA, and have enabled the outward current to be described in terms of two components (Neher 1971). In this study on Ascaris the currents before and after 4-AP application were subtracted from each other to allow measurement of the current blocked by 4-AP. This method gave a direct measure of the currents. The currents before and after 4-AP application were digitized using a modified Unilab programme (Grapher), and subtracted point for point using a programme written for the purpose.

Fig. 41 illustrates an example from a series of experiments of the currents before and after 4-AP and the current obtained by subtraction of these two currents. In both currents the holding potential was -35 mV and depolarizing steps to a potential of +55 mV were applied. The time after the start of the trigger is indicated on the graph. The upper current trace

was obtained with the cell bathed in lanthanum Ringer, and showed a rapid rise followed by a complex decay. The middle current record was obtained after bathing in 4-AP Ringer. The characteristic of this current was a slow rise time and exponential decay. Point for point subtraction of the two currents gave the lower current record. The lower current record was that component of the current blocked by 4-AP. The subtracted current had a rapid rise time and an exponential decay. This method of analysis was carried out for all 8 experiments.

The Decay of the Outward Current.

The outward current decay before and after 4-AP application was digitized and edited for use with a BMDP curve fitting programme to test the hypothesis that the currents decayed with a single exponential. A similar process was applied to the currents obtained by the subtraction procedure. A less than 20 nA difference between the two currents was disregarded because this was less than the errors involved in the digitization procedure. The currents observed in lanthanum Ringer were not well described by a single exponential. The decay of the 4-AP resistant current was adequately described by a single exponential, and the subtracted current was also adequately described by a single exponential.

The criteria used to estimate the number of exponentials

Fig. 42: A graph of the digitized current records obtained from a different cell, under the same protocol as that in Fig. 41. The cell was bathed in lanthanum Ringer and then 4-AP Ringer and steps from H_p=-35mV to S_p=+55mV were applied. Only every third point obtained from digitizing the currents is shown for reasons of clarity.

lanthanum Ringer: the crosses represent the points obtained.

4-AP lanthanum Ringer: the triangles represent the points obtained, and the line drawn through these points was a single exponential with a time constant of 1.1 s, fitted to the current.

Subtracted Current: the diamonds represent the points obtained after subtraction of the above two currents. The curve drawn through these points was a single exponential with a time constant of 10.4 ms, fitted to the current.

Bathing Solutions:	lanthanum Ringer and 4-AP lanthanum Ringer.
Temperature:	37°C.
Holding Potential:	-35mV.
Step Potentials:	+55mV.

Graph of the Decay of the Outward Current with Time.

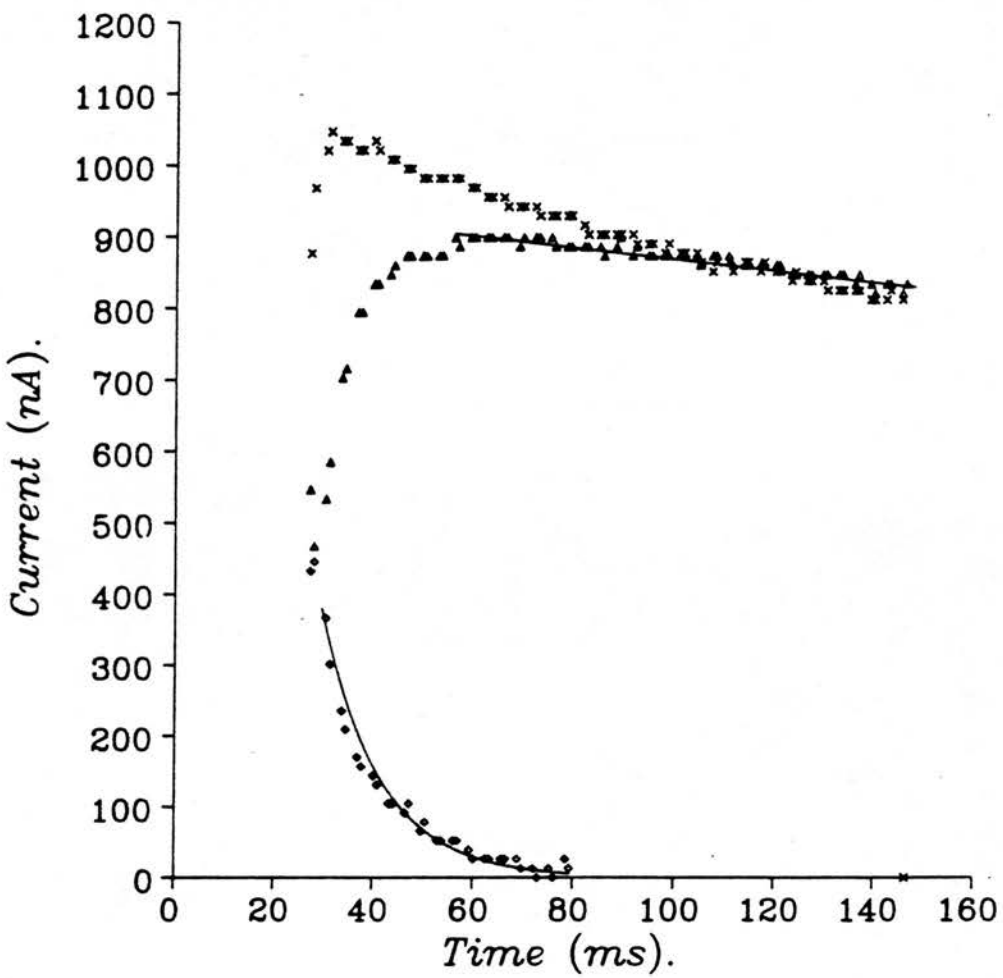

that produced the best fit to the data using the curve fitting procedure were as follows. Firstly, the residual sums of squares of the fitted curve was small and the addition of another exponential component did not significantly reduce the sums of squares. In this context small residual sums of squares were taken as less than $5x10^{-3}$ and a significant reduction was greater than $1x10^{-3}$. Secondly, the number of iterations required was small, a large number of iterations was taken as an indicator that either the fit was difficult or that the parameter estimations were widely out. Thirdly, the analysis was rejected if the fitted parameters gave rise to a positive slope, the hypothesis being that the current decayed. Finally, the analysis was accepted if the graphical display of fitted and observed curves were seen by eye to be in good agreement.

Fig. 42 shows the results of such an analysis on one of the eight 4-AP experiments. The graph shows the points obtained after digitizing the full current (crosses), the current after 4-AP (triangles), the subtracted current (diamonds). For clarity, only every third point was plotted although the full number of points were used in the analysis. The lines drawn were those fitted for the decay of the 4-AP resistant current and the decay of the subtracted current. Both of these decays could be adequately described by a single exponential with time constants of 1.1 s for the 4-AP resistant current and 10.4 ms for the subtracted current.

The observation that the subtracted current decay may be adequately described by a single exponential (in 6 of the 8 experiments), suggests that 4-AP was acting to block a fast transient current that was separate from the remaining delayed current. The qualitative similarities between these currents and the I_a and I_k currents described in Archidoris (Connor and Stevens 1971b) and Helix pomatia (Neher and Lux 1972) indicate an equivalent description of the outward current in Ascaris suum. The observation that the delayed outward current that remained after 4-AP application, showed less steady-state inactivation at more depolarized holding potentials than the current obtained in lanthanum Ringer, provides further evidence that the Ascaris currents have similar properties to those described in molluscan somata.

Discussion

Potassium Conductance

The voltage-clamp experiments described in chapter III of this thesis, are the first to attempt to isolate and characterize a voltage activated current using voltage-clamp in Ascaris. The outward potassium current described in Ascaris suum is similar to that described in molluscan somata (eg. Thompson 1977). The activation and inactivation characteristics of the Ascaris suum potassium current were described using a range of holding and step potentials.

Exogenous neural control, of the spontaneous depolarizing slow waves and the spikes associated with the resting potential (Jarman 1959), has been suggested from experiments where depolarizing current injected into the syncytial region, elicited a train of spikes recorded in the somata of Ascaris muscle cells (Debell et al 1963). In this model the cell resting potential would be maintained endogenously. Spikes would be produced in a spike initiation region near to the syncytium, and both spikes and depolarizing slow waves would spread to the rest of the cell either electrotonically or actively. The experiments presented in this chapter show the soma is capable of producing a spike and therefore active spread of spikes and slow waves is possible. The outward potassium current described in

Ascaris, inactivates after activation and takes over 12 s to fully recover. This behaviour is consistent with a mechanism to maintain a wave of depolarization. An interspike interval of less than 12 s would lead to inactivation of the outward potassium current, and in the absence of other mechanisms would tend to depolarize the membrane.

It is proposed that the outward potassium current is involved in restoring the resting potential after a calcium spike. The experiments undertaken indicate the outward current can be sub-divided into two components. The following discussion will compare the results obtained in Ascaris with other potassium currents.

Calcium Current

The use of a TEA APF in Ascaris led to a rapid loss in membrane resistance, as measured by the current response to voltage steps. However, it was of interest to note the inward currents observed when the potential was stepped depolarized to -5 mV and more positive from a holding potential of -35 mV. Voltage steps of increased depolarization reduced the amplitude of the inward current and also reduced the time to peak.

An inward calcium current has been described in Lymnea stagnalis nerve cell bodies (Byerly and Hagiwara 1982). The inward current was activated by depolarizing voltage clamp steps

(Byerly and Hagiwara 1982). With increasingly depolarized steps the amplitude of the inward current at first increased in amplitude, and then decreased. The reduction in amplitude of the inward current as the depolarizing step was made more positive, was proposed to be due to step potential approaching the calcium reversal potential, thus reducing the driving force (Byerly and Hagiwara 1982).

The voltage-clamp experiments described in this thesis, and those of Gration and Harrow (personal communication) in Ascaris, provide the first direct evidence of an inward calcium current, and confirm the single electrode experiments of Weisblat et al (1976).

Description of the Outward Current

From a holding potential of -35 mV depolarizing voltage-clamp steps to 0 mV activated the outward current. The peak of the outward current showed a steady increase with more positive depolarization and did not reach a maximum at the most depolarized pulse of +50 mV. The current rose rapidly, 10 ms, after the onset of the pulse. The time to peak decreased with depolarizing pulses of increasing magnitude. After reaching a peak the current decayed and was not well described by a single exponential. This decay was shown to be due to a reduction in the conductance and was not the result of an increase in the extracellular potassium concentration.

The permeability of the outward current was determined using ion substitution experiments and a two pulse protocol. The imposed voltage was stepped from a holding potential of -35 mV to a potential of +55 mV. This activated the outward current. A second step to a range of potentials was then made. The outward current amplitude during the second step was plotted against the step potential, and used to measure the reversal potential of the outward current. This type of protocol was used in preparations bathed in a range of different potassium concentrations, and demonstrated that the outward current was largely permeable to potassium. At low potassium concentrations (> 3 uM) the observed reversal potential was less than that calculated by the Nernst equation. Using the Goldman constant field equation this deviation could be accounted for by allowing for a 3 % permeability to sodium in the outward current. These results indicate that the outward current was largely permeable to potassium.

Current Kinetics

Two equal depolarizing pulses were used to measure the inactivation of the outward current. The peak amplitude of the second current was compared to the first at different interpulse intervals. The current amplitude of the second pulse was reduced compaired to the current amplitude at the first pulse, indicating an inactivation of the outward current. Full recovery from inactivation was not seen at interpulse intervals of 12 s.

Aldrich et al (1979) in Archidoris and Anisodoris showed that the amplitude of the outward current of the second pulse decreased at intervals less than 1 s, and then increased reaching full amplitude with a time constant of 28 s at an interval of 100 s. Kostyuk et al (1975a) and Heyer and Lux (1976) measured the time course of recovery in the neural somata of Helix pomatia, full recovery took 25 s.

Steady-state inactivation of the outward potassium current in Ascaris was studied using a range of holding potentials. In Helix pomatia (Kostyuk et al 1975a), in Archidoris somata (Connor and Stevens 1971b) and in Tritonia diomedia Thompson (1977), two components of the outward current were observed to have different potential ranges of steady-state inactivation. The I_k current was not significantly inactivated at holding potentials between -90 and -40 mV. In contrast the I_a component was almost fully inactivated at a holding potential of -40 mV (Kostyuk et al 1975a, Connor and Stevens 1971b, Thompson 1977). In Ascaris somatic muscle cells, holding at depolarized potentials reduced amplitude of the outward current. It was shown that at -40 mV the current was about 70 % activated and this possibly indicates the presence of an I_a like current although the time to peak did not show any differences with different holding potentials. The same experiments performed on 4-AP treated cells, which has been described as blocking the I_a component of the outward current (Thompson 1977), showed

that the voltage dependence of the remaining outward current was much less than that of the full current as would be expected for an I_k type current. The results obtained in Ascaris indicate that although the outward potassium currents are similar to those found in other cells, there are some differences that could point to functional differences in Ascaris.

Effect of 4-AP on the Outward Current

An irreversible reduction in peak amplitude and an increase in the time to peak were observed in experiments in Ascaris with bath applied 4-AP [5mM]. Thompson (1977) described a similar effect in neurones of Tritonia diomedia, point for point subtraction of the full and the 4-AP resistant current revealed a fast transient current with a decay that was described by a single exponential. In Ascaris these experiments allowed the separation of two components of the outward current and computer analysis was used to describe the rates of decay of the fast transient, and slow components of the outward current. The fast transient current decay was approximated by a single exponential with a time constant of 10.4 ms. The slow current decay was also adequately fitted by a single exponential with a time constant of 1.1 s. The results are similar to those of Kostyuk et al (1975a). In the somata of Helix pomatia Kostyuk et al (1975a) describe rates of decay of 10 ms - 50 ms and 1 s - 2 s for the fast and slow outward current components

respectively. At 3 ^{o}C, in the somata of Archidoris and Anisidoris, the decays of the two components were slower (Connor and Stevens 1971b, Aldrich et al 1979). The fast component decayed with a time constant of between 220 ms and 600 ms, the slow component decayed with a time constant of between 3.7 s and 10 s

Connor and Stevens (1971c) proposed that in response to a depolarizing stimulus, a spike would be followed by repolarization due to the action of the slow delayed outward current. The subsequent hyperpolarization would remove the inactivation from the I_a conductance which would activate as the cell was depolarized again and act in opposition to the imposed depolarization. The time course of the inactivation of the I_a conductance would effectively determine the interspike interval. Once the I_a current was inactivated the cell would be able to depolarize and spike again. In Ascaris a similar mechanism could operate to determine the interspike interval.

In summary the outward potassium current in Ascaris has been shown to be activated by depolarizing steps, and on the basis of steady-state inactivation and the application of 4-AP has been sub-divided into two components. The Ascaris outward current is proposed to act to repolarize the membrane after a spike. The time taken to recover from inactivation is taken as

evidence that the potassium current could contribute towards maintaining the length of the slow depolarizing waves.

SECTION IV

Epilogue

Discussion

The two sets of experiments in this thesis describe in detail two types of conductance in the somata of Ascaris suum muscle cells. The patch-clamp experiments demonstrated a high-conductance chloride channel that was proposed to give rise to the resting chloride conductance observed by Del Castillo et al (1964a). It was thought that the calcium-dependence of the chloride channel could act to repolarize the cell after a calcium spike. Voltage-clamp experiments were carried out to test this hypothosis and are described in Section III of this thesis. The results from the voltage-clamp experiments demonstrated an outward current that was carried by potassium, not chloride. Analysis of the potassium outward current employed lanthanum Ringers to block an inward calcium current. The use of lanthanum Ringers would prevent the observation of any current, dependent on the influx of calcium. It is possible that the use of Ringers with normal calcium concentrations would have led to the observation of a chloride component to the outward current.

The discussions at the end of Sections II and III of this thesis have looked at each experimental series and discussed the results with respect to relevant data in the literature. The following account is an attempt to present the proposed functions of the chloride channel and potassium conductance in a single summary.

The high conductance chloride channel in Ascaris somatic muscle cells is discussed with reference to the following four possible functions:.

(1) The Resting Chloride Conductance

Del Castillo et al (1964a) and Caldwell and Ellory (1968) have demonstrated a high resting chloride conductance. The chloride channel described in this thesis was observed to have an inward rectification and is proposed to undelie the high resting chloride permeability. The open probability and mean open time of the channel decreased when the patch was depolarized. Sub-conductance states of the channel were only observed when the patch was depolarized. The effective current passed by the chloride channels in the cell would therefore be maximal at hyperpolarized, resting potentials. A chloride pump has been proposed to be present in the body wall of Ascaris (Hobson et al 1952a). It was proposed in the discussion of the chloride channel that the combination of a chloride pump and a high resting chloride conductance would effectively 'set' the resting membrane potential.

(2) Maintenance of the Resting Potential.

The observed voltage sensitivity and sub-conductance states act in an opposite manner to that required for a mechanism of positive feedback in the maintenance of resting potential. If another conductance were available in the cell to

hyperpolarize the membrane potential, then the chloride channel would be expected to open and subsequently govern the magnitude of the resting potential. It is proposed that in a simple model the potassium currents described in the voltage-clamp experiments of this thesis would act to repolarize the membrane and move the membrane potential to a range at which the chloride conductance would activate.

(3) The Repolarization of the Muscle Cell Membrane.

The patch-clamp study showed the chloride channel to be dependent on the intracellular calcium concentration. It was proposed that a rise in intracellular calcium concentration during a spike would result in the activation of the chloride channel. The voltage-clamp experiments demonstrated the major outward current that could repolarize the membrane was carried by potassium not chloride. In the light of the voltage clamp experiments it is now thought unlikely that the chloride channel has a direct repolarization function after each individual spike. However, the spontaneous activity seen in Ascaris (Jarman 1959) is composed of depolarizing slow waves, with superimposed trains of spikes superimposed during the depolarizations. Each spike in a train, would let in more calcium, and after a number of spikes the intracellular concentration of calcium could reach a level to activate the chloride channel. In this hypothosis the chloride channel would act to regulate the interwave interval by hyperpolarizing the cell after a train of spikes.

An interaction between the intracellular calcium concentration and any other modulators of channel activity would act to determine the time interval between slow waves.

(4) To Allow Activity of Other Smaller Conductances.

Chloride has been shown to be the predominant conductance at the resting potential (Del Castillo et al 1964a). The chloride channel described in this thesis, had a high conductance and was the predominant channel observed in the patches. It can therefore be considered to 'short circuit' the membrane. Smaller currents in the membrane would have little effect on the membrane potential if a large chloride conductance remained. It is therefore proposed that the voltage sensitivity of the chloride channel acts to enable smaller currents such as the calcium current to have a greater effect on the membrane potential.

The outward potassium currents observed in voltage-clamp experiments are proposed to have two major functions:

(1) The Regulation of Interspike Interval.

The fast component of the outward potassium current is proposed to determine the interval between spikes. Connor and Stevens (1971c) postulated a similar function for the fast, I_a current in Archidoris. The inactivation of the fast current at

depolarized potentials would regulate the effect of the inward current at the beginning of a spike. With a fast potassium current, fully recovered, depolarization of the cell by the inward current would initially be opposed by the action of the fast potassium current. However, this fast potassium current would inactivate at depolarized potentials and would therefore decrease in amplitude and allow a spike to develop. The interaction between the strengths of the inward, and fast outward currents would determine the time taken to spike. The repolarization of the cell after a spike by the slow potassium current removes the inactivation of the fast potassium current. In this way the slow potassium current has an indirect regulatory effect on the interspike interval.

(2) The Regulation of Interwave Interval.

The interval between slow waves has been proposed to be affected by the chloride channel, see above. It is also proposed that the slow outward potassium current observed in voltage-clamp experiments determines, to some extent the interwave interval. The time dependent recovery from inactivation of the slow potassium current would reduce the repolarization effect of the current during a train of spikes. It is proposed that the inactivation of the slow potassium current would stop a repolarization of the cell. An inactivation of the calcium current would then result in a cessation of spiking. Through the repolarizing action of the slow potassium

current the cell would hyperpolarize and remove the inactivation from the calcium current. The cell would then be ready to depolarize and spike, possibly in response to an exogenous signal. The interwave interval would therefore be at least partially regulated by the inactivation kinetics of the slow potassium current.

In conclusion the experiments in this thesis describe two major conductances in Ascaris somatic muscle cells. The proposed functions of these conductances are speculative, and further experimentation is required to determine the nature of the many interacting components in the spontaneous activity of the muscle cells.

SECTION V

REFERENCES

Adams,D.J., Smith,S.J. and Thompson,S.H. (1980). Ionic currents in molluscan soma. Annual Review of Neuroscience 3, pp141-147.

Adrian,R.H. , Chandler,W.K. and Hodgkin,A.L. (1970). Slow changes in potassium permeability in skeletal muscle. Journal of Physiology 208 pp645-668.

Aldrich,R.W., Getting,P.A. and Thompson,S.H. (1979). Inactivation of delayed outward current in molluscan somata. Journal of Physiology 291 pp507-530.

Alving,B.O. (1969). Differences between pacemaker and nonpacemaker neurones of Aplysia on voltage clamping. Journal of General Physiology 54 pp512-531.

Barrett,J.N., Magleby,K.L. and Pallotta,B.S. (1982). Properties of single calcium-activated potassium channels in cultured rat muscle. Journal of Physiology 331 pp211-230.

Bader,C.R., Bertran,D. and Schwartz,E.A. (1982). Voltage activated and calcium activated currents studied in solitary rod inner segments from the salamander retina. Journal of Physiology 331 pp253-284.

Barish,M.E. (1983). A transient calcium dependent chloride current in the immature Xenopus oocyte. Journal of Physiology 342 pp309-325.

Benham,C.D. and Bolton,T.B. (1983). Patch-clamp studies of slow potential-sensitive potassium channels in longitudinal smooth muscle of rabbit jejunum. Journal of Physiology 340 pp469- 486.

Berridge,M.J., Lindley,B.D. and Prince,W.T. (1975). Membrane permeability changes during stimulation of isolated salivary glands of Calliphora by 5-HT. Journal of Physiology 244 pp549-567.

Blatz,A.L. and Magleby,K.L. (1983). Single voltage dependent chloride selective channels of large conductance in cultured rat muscle. Biophysical Journal 43 pp237-241.

Brading,A.F. and Caldwell,P.C. (1971). The resting membrane potential of the somatic muscle cells of Ascaris lumbricoides. Journal of Physiology 217 pp605-624.

Bretag,A.H. (1987). Review: Muscle Chloride Channels. Physiological Reviews 67 No.2 pp618-724.

Buchli,E. (1874). Beitrage zur kenntniss des nervensystems der

nematoden. Archives Microanatomy Anatomy 10 pp74-100.

Byerly,L and Hagiwara,S (1982). Calcium currents in internally perfused nerve cell bodies of Lymnea stagnalis. Journal of Physiology 322 pp503-523.

Caldwell,P.C. (1974). Possible mechanisms for the linkage of membrane potentials to metabolism by electrogenic transport processes with special reference to Ascaris muscle. Bioenergetics 4 pp201-209.

Caldwell,P.C. and Ellory,J.C. (1968). Ion movements in the somatic muscle cells of Ascaris lumbricoides. Journal of Physiology 197 75-76P.

Cappe De Ballon.P. (1911). Etude sur les fibres musculaires d' Ascaris 1. FIBRES PARIETALES. Cellule 27 pp165-211.

Chesnoy-Marchais,D. (1983). Characterization of a chloride conductance activated by hyperpolarization in Aplysia neurones. Journal of Physiology 342 pp277-308.

Cohen,P., Burchell,A., Foulkes,J.G., Cohen,P.T. (1978). Identification of the calcium-dependent modulator protein on the 4th. sub-unit of rabbit skeletal muscle phosphorylase kinase. FEBS Letters 92 No.2. pp287-293.

Cohen,P. (1982). Review article: The role of protein phosphorylation in neural and hormonal control of cellular activity. Nature 296 pp613-620.

Cole,K.S. (1968). Membranes, ions and impulses. Berkeley, University of California Press.

Colquhoun,D. (1971). Lectures on biophysics. Clarendeon Press Oxford.

Connor,J.A. and Stevens,C.F. (1971a). Inward and delayed outward currents in isolated neural somata under voltage clamp. Journal of Physiology 213 pp1-19.

Connor,J.A. and Stevens,C.F. (1971b). Voltage clamp studies of a transient outward membrane current in gastropod neural somata. Journal of Physiology 213 pp20-30.

Connor,J.A. and Stevens,C.F. (1971c). Prediction of repetitive firing behaviour from voltage clamp data on an isolated neurone soma. Journal of Physiology 213 pp31-53.

De Bell,J.T. (1965). A long look at neuromuscular junctions in Nematodes. The Quarterly Review of Biology 40 (3) pp233-251.

De Bell,J.T., Del Castillo,J., Sanchez,V. (1963).

Electrophysiology of somatic muscle cells of Ascaris lumbricoides Journal of cellular and Comparative Physiology 62 pp159-177.

Del Castillo,J., De Mello,W.C. and Morales,T. (1963). The physiological role of acetylcholine in the neuromuscular system of Ascaris lumbricoides. Archives of International Physiology 71 pp741-757.

Del Castillo,J., De Mello,W.C. and Morales,T. (1964a). Influence of some ions on the membrane potential of Ascaris muscle. Journal of General Physiology 48 pp129-140.

Del Castillo,J., DeMello,W.C. and Morales,T. (1964b). Inhibitory action of GABA on Ascaris muscle. Experientia 20 pp141-145.

Del Castillo,J., DeMello,W.C. and Morales,T. (1964c). The mechanism of the paralysing action of piperazine in the somatic musculature of Ascaris lumbricoides. British Journal of Pharmacology 22 pp463-477.

Del Castillo,J., De Mello,W.C. and Morales,T. (1967). The initiation of action potentials in the somatic musculature of Ascaris lumbricoides. Journal of Experimental Biology 46 pp263-279.

Dulhunty,A.F. (1978). The dependence of membrane potential on extracellular chloride concentration in mammalian skeletal muscle fibres. Journal of Physiology 276 pp67-82.

Findlay,I. and Petersen,O.H. (1985). Acetylcholine stimulates a calcium dependent chloride conductance in mouse lacrimal acinar cells. Pflugers Archives 403 pp328-330.

Frankenhauser,B and Hodgkin,A.L. (1957). The action of calcium on the electrical properties of squid axons. Journal of Physiology 137 pp218-243.

Geduldig,D and Gruener,R. (1970). Voltage clamp of the Aplysia giant neurones: early sodium and calcium currents. Journal of Physiology 211 pp217-244

Geletyuk,V.I and Kazachenko,V.N. (1985). Single chloride channels in molluscan neurones: multiplicity of the conductance states. Journal of Membrane Biology 86 pp9-15.

Gray,P.T.A., Bevan,S. and Ritchie,J.M. (1984). High conductance anion selective channels in rat cultured Schwann cells. Proceedings of the Royal Society. London. B. 221 p395-409.

Hamill,O.P., Marty,A., Neher,E., Sakmann,B. and Sigworth,F.J. (1981). Improved patch-clamp techniques for high-resolution current recording from cells and cell-free membrane

patches. Pflugers Archives 391 pp85-100.

Hanrahan,J.W., Alles,W.P. and Lewis,S.A. (1985). Single anion-selective channels in basolateral membrane of a mammalian tight epithelium. Proceedings of the National Academy of Science USA 82 pp7791-7795.

Harpur,R.P. and Popkin,J.S. (1973). Intestinal fluid transport: studies with the gut of Ascaris lumbricoides. Canadian Journal of Physiology and Pharmacology 51 pp79-90.

Heyer,C.B. and Lux,H.D. (1976). Control of the delayed outward potassium currents in bursting pacemaker neurones of the snail, Helix pomatia. Journal of Physiology 262 pp349-382.

Hille,B. (1984). Ionic channels of excitable membranes. Sinaeur.

Hobson,A.D., Stephenson,W. and Beadle,L.C. (1952a). Studies on the physiology of Ascaris lumbricoides 1. The relation of the total osmotic pressure, conductivity and chloride content of the body fluid to that of the external environment. Journal of Experimental Biology 29 pp1-21.

Hobson,A.D., Stephenson,W. and Eden,A. (1952b). Studies on the physiology of Ascaris lumbricoides 2. The inorganic composition of the body fluid in relation to that of the enviroment. Journal of Experimental Biology 29 pp22-29.

Hodgkin,A.L. and Katz,B. (1949). The effect of sodium ions on the electrical activity of the giant axon of the squid. Journal of physiology 103 pp37-77.

Jarman,M. (1959). Electrical activity in the muscle cells of Ascaris lumbricoides . Nature (Lond.) 184 pp1244.

Jarman,M. and Ellory,J.C. (1969). Effect of TTX on Ascaris somatic muscle. Experientia 25 p507.

Kolb,H.A., Brown,C.D.A. and Murer,H. (1985). Identification of a voltage dependent anion channel in the apical membrane of a chloride secretory epithelium (MDCK). Pflugers Archives 403 pp262-265.

Kostyuk,P.G., Krishtal,O.A. and Doroshenko,P.A. (1975a). Outward currents in isolated snail neurones:- 1. Inactivation kinetics. Comparative Biochemistry and Physiology 51C pp259- 263.

Kostyuk,P.G., Krishtal,O.A. and Doroshenko,P.A. (1975b). Outward currents in isolated snail neurones:- 2. Effect of TEA. Comparative Biochemistry and Physiology 51C pp265-268.

Krouse,M.E., Schneider,G.T. and Gage,P.W. (1986). A large anion selective channel has seven conductance levels. Nature 319 pp58-60.

Latorre,R., Coronado,R. and Vergara,C. (1984). Review: Potassium channels gated by voltage and ions. Annual Review of Physiology 46 pp485-95.

Latorre,R., Veraga,C. and Hildago,C. (1982). Reconstitution in planar lipid bilayers of a calcium-dependent potassium channel from transverse tubule membranes isolated from rabbit skeletal muscle. Proceedings from the National Academy of Science (USA). 79 pp808-809.

Lee,D.L., (1965). The Physiology of Nematodes. Oliver and Boyd, Edinburgh.

MacDonald,J.F., Owen,D.G. and Barker,J.L. (1985). Voltage sensitive, spontaneously occurring chloride channels in cultured spinal neurones. Abstracts, Society for Neuroscience 11 (2) p785.

Martin,R.J. (1982). Electrophysiological effects of piperazine and diethylcarbamazine on Ascaris suum somatic muscle. British Journal of Pharmacology 77 pp255-265.

Martin,R.J. (1985). GABA and piperazine activated single channel currents from Ascaris suum body muscle. British Journal of Pharmacology 84 pp445-461.

Martin,R.J. and Thorn,P. (1984). A high conductance anion channel in the somatic muscle cells of Ascaris suum.

Journal of Physiology 354 46P.

Marty,A., Tan,Y.,P. and Trautman,A. (1984). Three types of calcium- dependent channel in rat lacrimal glands. Journal of Physiology 357 pp293-325.

Mayer,M.L. (1985). A calcium-activated chloride current generates the after depolarization of rat sensory neurones in culture. Journal of Physiology 364 pp217-239.

Meech,R.W. and Standen,N.B. (1975). Potassium-activation in Helix aspera neurones under voltage clamp: a component mediated by calcium influx. Journal of Physiology 249 pp211-240.

Miledi,R. (1982). A calcium-dependent transient outward current in Xenopus laevis oocytes. Proceedings of the Royal Society, B. 215 pp491-497.

Miledi,R and Parker,I. (1984). Chloride current induced by injection of calcium in to Xenopus oocytes. Journal of Physiology 357 pp173-183.

Miller,C. and White,M.M (1984). Dimeric structure of single chloride channels from Torpedo electroplax. Proceedings of the National Academy of Science 81 pp2772-2775.

Nelson,D.J, Tang,J.M and Palmer,L.G. (1984). Single channel recordings of apical membrane chloride conductance in A6 epithelial cells. Journal of Membrane Biology 80 pp81-89.

Neher,E. (1971). Two fast transient current components during voltage clamp on snail neurones. The Journal of General Physiology 58 pp36-53.

Neher,E. and Lux,H.D. (1972). Differential action of TEA on two potassium current components of a molluscan neurone. Pflugers Archives 336 pp87-100.

Nestler,E.J. and Greengard,P. (1983). Review article: Protein posphorylation in the brain. Nature 305 pp583-588.

Noma,A. (1983). ATP-regulated potassium channels in cardiac muscle. Nature 305 pp147-148.

Owen,D.G., Segal,M. and Barker,J.L. (1984). A calcium-dependent chloride conductance in cultured mouse spinal neurones. Nature 311 pp567-570.

Ozeki,M., Freeman,A.R. and Grunfest,H. (1966). The membrane components of crustacean neuromuscular system. II Analysis of interactions among the electrogenic components. Jouranl of General Biology 49 pp1335-1349.

Robinson,R.A., and Stokes,R.H. (1972). Electrolyte solutions. Butterworths, London.

Rohde,E. (1885). Beitrage zur kenntuiss der anatomie der nematoden. Zool. Beitr. Bresl. 1 pp11-32.

Rosenbluth,J. (1963). Fine structure of body muscle cells and neuromuscular junctions in Ascaris lumbricoides. Journal of Cellular Biology 19 82A.

Rosenbluth,J. (1965). Ultrastructure of somatic muscle cells in Ascaris lumbricoides 2. intermuscular junctions, neuromuscular junctions and glycogen stores. Journal of Cellular Biology 26 pp579-591.

Sakmann,B. and Neher,E. (1984). Patch-clamp techniques for studying ionic channels in excitable tissues. Annual Review of Physiology 46 pp455-472.

Sakmann,B. and Trube,G. (1984). Conductance properties of single inwardly rectifying potassium channels in ventricular cells from guinea pig heart. Journal of Physiology 347 pp641-657.

Schein,S.J., Colombini,M., and Finkelstein,A. (1976). Reconstitution in planar lipid bilayers of a voltage

dependent anion selective channel obtained from Paramecium mitochondria. Journal of Membrane Biology 30 p99-120.

Schneider,G.T., Cook,D.I., Gage,P.W. and Young,J.A. (1985). Voltage sensitive high conductance chloride channels in the luminal membrane of cultured pulmonary alveolar (type 2) cells. Pflugers Archives 404 pp354-357.

Stanfield,P.R. (1970). The effect of TEA ion on the delayed currents of frog skeletal muscle. Journal of Physiology 209 pp209-

Stretton,A.O.W. (1976). Anatomy and development of the somatic musculature of the nematode of Ascaris. Journal of Experimental Biology 64 pp773-788.

Stretton,A.O.W., Fishpool,R.M., Southgate,E., Dommoyer,J.E., Walrond,J.P., Moses,J.E.R., and Kass,I.S. (1978). Structure and physiological activity of the motorneurones of the nematode Ascaris. Proceedings National Academy of Science U.S.A. 75 pp3493-3497.

Strumwaser,F., Kaczmarek,L.K. and Jennings,K.R. (1982). Intracellular modulation of membrane channels by cyclic-AMP mediated protein phosphorylation in peptidergic neurones of Aplysia Federation Proceedings 41 pp2933-2939.

Taylor,R.E., Moore,J.W. and Cole,K.S. (1960). Analysis of certain errors in squid axon voltage clamp experiments. Biophysics Journal 1 pp161-202.

Thomas,M.V. (1984). Voltage-clamp analysis of a calcium-mediated potassium conductance in cockroach (Periplaneta americana) central neurones. Journal of Physiology 350 pp159-178.

Thompson,S.H. (1977). Three pharmacologically distinct potassium channels in molluscan neurones. Journal of Physiology 265 p465- 488.

Thorn,P. and Martin,R.J. (1987) A high conductance calcium-dependent chloride channel in Ascaris suum muscle. Quarterly Journal of Experimental Physiology 72 pp31-49.

Toscano Rico,J. (1926). Sur la sensilitie de l' Ascaris a l'action de quelques drogues. Comp. Rend. Soc. Biol. Paris, 94 pp921- 923.

Weisblat,D.A. ,Byerly,L. and Russell,R.L. (1976). Ionic mechanisms of electrical activity in somatic muscle of the nematode Ascaris lumbricoides. Journal of Comparative Physiology A. 111 (2) pp93-113.

Welsh,.M.J. (1986). An apical membrane chloride channel in human tracheal epithelium. Science 232 pp1648-1650.

Yellen,G. (1982). Single calcium-activated nonselective cation channels in neuroblastoma. Nature 296 pp357-359.

Appendix I

Probear Basic Programme

Computer programme used to analyse the probabilities of channel openings in terms of the binomial distribution. The programme was called Probear and was written in BBC Basic for use with the BBC microcomputer. The observed probabilities of 1,2,3....N channels open and the maximum number of channel observed to be simultaneously open were keyed into the computer in response to prompting questions. The output of the programme displayed the variance and the probabilities of opening of the observed and predicted distributions.

```
)LOAD"PROBEAR"
).
   10REM PROG. TO CALC. BINOMIAL DISTRIBUTION
   20 REM USES PROMPTS TO TAKE IN THE AREA UNDER THE GRAPH MEASUREMENTS FROM THE
   30 REM CAMPION PROG.
   40MODE0
   50 DIM prob(10,10),pprob(10,10),nexc(10),rexc(10),rnexc(10),area(10),tp(10),meanprob(10),mean(10)
,VARIANCE(10),VARIANCEp(10)
   60VDU 19,131,4,0,0,0
   70COLOUR2:COLOUR131:CLS
   80VDU28,7,20,37,13
   90PRINT"This program requires"
  100PRINT"an input of the max."
  110PRINT"number of channels"
  120PRINT"and the observed"
  130PRINT"probability of being"
  140PRINT"at a given level"
  150 FOR I=1 TO 2000:NEXTI
  160PROCbegin:PROCcalc:PROCprintprob:IFY$="Y"GOTO160:ELSE PROCfile
  170 CLS:INPUTTAB(0,10)"Next set of data...Y/N";new$
  180 IF new$="Y" GOTO 160 ELSE END
  190 DEFPROCbegin
  200totalarea=0:prop=0:A$=" ":y=0:xI=0:meanprob=0:f=0:g=0
  210CLS:VDU28,7,20,37,13:INPUT"Same expt and                    no. of channels.....Y/N";REP$:CLS:IF
REP$="Y" GOTO240:ELSE GOTO220
  220FI=0:INPUT"Experiment";EPT$
  230CLS:INPUT"Maximum no. of channels",MI
  240FI=FI+1:INPUT"Transpatch potential = ";tp(FI)
  250FOR II=0 TO MI
  260BI=&01020004:NUM$=STR$(II):@I=20509:CLS:PRINT;"Observed I area of ";PRINT;NUM$;" channels being
 open";
  270INPUT area(II)
  280CLS:NEXTII
  290totalarea=0:FORII=0 TO MI
  300 totalarea=totalarea+area(II)
  310 NEXTII
  320 prop=100/totalarea
  330 FORII=0 TO MI
  340 prob(II,FI)=(prop*area(II))/100
  350 NEXTII
  360 ENDPROC
  370DEFPROCprintprob
  380 @I=&20509
  390 VDU26:KI=-3
  400PRINTTAB(0,0)"Expt. = ";EPT$;" Transpatch pot. = ";tp(FI)
  410 PRINTTAB(0,1)"Mean prob. of opening = ";meanprob(FI)
  420PRINT:FOR II=0 TO MI
  430 KI=KI+4
  440PRINTTAB(0,II+KI+2);"Observed probability of ";LEFT$(STR$(II),1);" channels"
  450PRINTTAB(0,II+KI+3);"being open = ";prob(II,FI)
  460PRINTTAB(0,II+KI+4);"Predicted probability of ";LEFT$(STR$(II),1);" channels"
  470PRINTTAB(0,II+KI+5);"being open = ";pprob(II,FI)
  480PRINT:NEXTII:VDU3:IF A$="P" GOTO500 ELSE INPUTTAB(22,31)"Press P to print";A$
  490IF A$="P" THEN CLS:VDU2:PRINT"All observed probs are corrected to 100I":GOTO390:ELSE GOTO500
  500CLS:INPUTTAB(0,20)"New data....Y                          RETURN for File";Y$
  510 ENDPROC
  520 DEFPROCcalc
  530 meanprob(FI)=0:FOR II=1 TO MI
  540 mean(FI)=mean(FI)+(prob(II,FI)*II)
  550 NEXTII
  560 meanprob(FI)=mean(FI)/MI
  570 FOR II=0 TO MI
  580 VARIANCE(FI)=VARIANCE(FI)+(((mean(FI)-II)^2)*prob(II,FI))
  590 NEXT II
  600 xI=MI:PROCexc:nexc=y
  610 FOR rI=0 TO MI
  620 xI=rI:PROCexc:rexc(rI)=y
  630 xI=MI-rI:PROCexc:rnexc(rI)=y
  640 f=meanprob(FI)^rI:g=(1-meanprob(FI))^(MI-rI)
  650 pprob(rI,FI)=(nexc/(rexc(rI)*rnexc(rI)))*f*g
  660 NEXTrI
  670 FOR II=0 TO MI
  680 VARIANCEp(FI)=VARIANCEp(FI)+(((mean(FI)-II)^2)*pprob(II,FI))
  690 NEXT II
  700 ENDPROC
  710 DEFPROCexc
  720 y=1
  730 IF xI=0 THEN y=1:ENDPROC:ELSE GOTO740
  740 FOR JI=xI TO 1 STEP -1
  750 y=y*(JI)
  760 NEXTJI
  770 ENDPROC
  780 DEFPROCfile
  790 AI$=STRING$(50," "):N=1:K=1:AI$=""+JI=0:CLS
  800 INPUTTAB(3,10)"Filename";B$
  810 IF LEN(B$)>7 CLS:PRINTTAB(3,9)"Name too long":GOTO800:ELSE GOTO820
  820 I=OPENOUT(B$
  830 AI$=" Experiment "+EPT$
  840 FOR KI=1 TO LEN(AI$)
  850 BPUT#I,ASC(MID$(AI$,KI,1)):NEXTKI:BPUT#I,13
  860 @I=&01020005
  870 AI$=" Max. no. of channels seen = "+STR$(MI)
  880  FOR KI= 1 TO LEN(AI$)
  890 BPUT#I,ASC(MID$(AI$,KI,1)):NEXTKI:BPUT#I,13:BPUT#I,13
  900FOR II=1 TO FI:@I=&01020205
  910FOR HI=1 TO 40:BPUT#I,&2:NEXT HI:BPUT#I,13:AI$="Transpatch potential = "+STR$(tp(II))
  920 BPUT#I,13
  930 FOR KI= 1 TO LEN(AI$)
```

```
 940 BPUT#I,ASC(MID$(AZ$,K%,1)):NEXTK%:BPUT#I,13
 950 G%=&01020405:AZ$="Observed mean of distribution = "+STR$(mean(I%))
 960 FOR K%= 1 TO LEN(AZ$)
 970 BPUT#I,ASC(MID$(AZ$,K%,1)):NEXTK%:BPUT#I,13
 980AZ$="Observed variance = "+STR$(VARIANCE(I%))
 990 FOR K%= 1 TO LEN(AZ$)
1000 BPUT#I,ASC(MID$(AZ$,K%,1)):NEXTK%:BPUT#I,13
1010AZ$="Predicted variance = "+STR$(VARIANCEp(I%))
1020 FOR K%= 1 TO LEN(AZ$)
1030 BPUT#I,ASC(MID$(AZ$,K%,1)):NEXTK%:BPUT#I,13
1040 G%=&01020405:AZ$="Mean prob. of opening from data = "+STR$(meanprob(I%))
1050 FOR K%= 1 TO LEN(AZ$)
1060 BPUT#I,ASC(MID$(AZ$,K%,1)):NEXTK%:BPUT#I,13:BPUT#I,13
1070 FOR G%= 0 TO N%
1080 G%=&01020005:no$=STR$(G%):G%=&01020509
1090 AZ$="Obs. prob. of opening of "+no$+" channels = "+STR$(prob(G%,I%))
1100 FOR K%= 1 TO LEN(AZ$)
1110 BPUT#I,ASC(MID$(AZ$,K%,1)):NEXTK%:BPUT#I,13
1120 AZ$="Pred. prob. of opening of "+no$+" channels = "+STR$(pprob(G%,I%))
1130 FOR K%= 1 TO LEN(AZ$)
1140 BPUT#I,ASC(MID$(AZ$,K%,1)):NEXTK%:BPUT#I,13:BPUT#I,13
1150 NEXT G%:BPUT#I,13
1160 NEXT I%
1170 CLOSE#I
1180 ENDPROC
```

Appendix II

Campion Computer Programme

Computer programme, Campion, used to collect and display the channel amplitudes. This programme was written in BBC Basic for use with a BBC microcomputer and a Unilab interface. The data collection part of the programme was written in Assembler language to increase the speed of sampling. The current signal was played into the interface and the current amplitudes were digitized by the programme. The collected amplitudes were then used to produce a frequency/amplitude histogram. The histogram showed peaks at current amplitudes representing 0,1,2,3....N channels open (see FIG.15). The programme then calculated the proportion of time (probability) spent at each of the current levels.

```
%.)
  10 REM PROGRAM CAMPION THIS PROGRAM HAS A NUMBER OF FACILITIES.
  20 REM IT COLLECTS CHANNEL DATA INTO INPUT 0. IT THEN OFFERS A MENU OF COMMANDS
  30 REM IT CAN PLOT HISTOGRAMS OF FREQUENCY AGAINST AMPLITUDE
  40 REM IT CAN DETERMINE AREAS UNDER THE GRAPH AND LIST THEM ON THE PRINTER
  50 REM IT CAN ALSO STORE AN ASCII FILE ON DISK OF THE RAW BINED DATA
  60MODE4
  70VDU 3:VDU 23;8202;0;0;0;
  80VDU 19,128,4,0,0,0:COLOUR 1
  90VDU 23,1,0;0;0;
 100CLS:PRINTTAB(12,10)"HISTOG"
 110PRINTTAB(3,13)"R. J. Martin & P. Thora...1985 "
 120PRINTTAB(3,15)"Press space-bar to continue "
 130REPEAT:UNTIL GET=32
 140CNTRLC1=5:?&FCC3=255:?&FCC2=0:?&FCC1=CNTRLC1
 150 AGAIN1=0:REPRINT=0
 160 DIM PEAK(50):DIM HEIGHT1(256):DIM BIN1%(10):DIM BINN1(10):DIM area%(10)
 170DIM HIGH 255:DIM MEDIUM 255:DIM LOW 255:DIM LOC1 340
 180DIM START 100
 190PROCaanu
 200 DEFPROCaanu
 210 CLS:IF REPRINT<>0 GOTO 220 ELSE PROCTH:*FX4,1
 220REPRINT=0
 230 PROCcon:*FX15,1
 240K$=GET$:IFK$="B"VDU26:CLS:PROCbins:PROCaanu
 250IFK$="D"repeat=0:VDU26:PROCsetup:PROCcollect:PROCdisplay:PROCprint:PROCaanu
 260IFK$="G"VDU26:noraL=0:FILE=0:PROCplotdata:VDU 23,1,0;0;0;0;:PROCplot:PROCGraphrepeat
 270IFK$="N"VDU26:FILE=0:noraL=1:aagL=1:PROCplotdata:VDU 23,1,0;0;0;0;:PROCplotnora:PROCGraphrepeat
 280IFK$="A"VDU26:PROCarea:PROCaanu
 290IFK$="C"VDU26:PROCAMP:PROCaanu
 300IFK$="F"VDU26:FILE=1:PROCplotdata:PROCfile:PROCaanu
 310GOTO260
 320DEFPROCTH
 330VDU28,12,21,19,14:ENDPROC
 340DEFPROCcon
 350PRINT"Data in Graph   NoragrphArea    Ch.aap. Bins    File "
 360ENDPROC
 370DEFPROCGraphrepeat
 380VDU21:INPUT""print$
 390IF print$="P" THEN VDU6:PROCSDUMP:CALL SDUMP
 400VDU6
 410VDU28,32,7,39,0:REPRINT=1:PROCaanu
 420ENDPROC
 430DEFPROCsetup
 440 AGAIN1=0:aapL=0:IF repeat()0 THEN CLS:GOTO360:ELSE GOTO 450
 450AGAIN1=0:aapL=0:CLS:PRINTTAB(5,10)"PLEASE PLACE INPUT SIGNAL IN ""B""":PRINTTAB(5,12)"THIS PROG
RAMME HAS AN INPUT RANGE":PRINTTAB(5,14)"OF 0 TO 1 V AND ASSUMES":PRINTTAB(5,16)"A 10mV PER pA CONVE
RSION"
 460OSBYTE=&FFF4
 470OSRDCH=&FFE0
 480FOR I%=0 TO 255
 490?(HIGH+I%)=0:?(MEDIUM+I%)=0:?(LOW+I%)=0
 500NEXTI%
 510FOR I%=0 TO 2 STEP 2:P%=START
 520[OPT I%
 530.LOOP1
 540LDA &FCC0:TAX
 550INC LOW,X:BNE LOOP1
 560TXA &70
 570LDA &69:LDX &0:JSR OSBYTE:CPY &0:BEQ FINISH
 580LDX &70
 590INC MEDIUM,X:BNE LOOP1
 600INC HIGH,X:LDA HIGH,X:CMP &255:BNE LOOP1
 610.FINISH
 620RTS:]
 630NEXTI%
 640ENDPROC
 650DEF PROCcollect
 660:PRINTTAB(1,28)"Press space_bar to start sampling "
 670REPEAT UNTIL GET=32
 680CLS:PRINTTAB(5,10)"Sampling now! "
 690PRINTTAB(5,15)"Type Q to Quit!"
 700time1=TIME
 710*FX15,1
 720*FX11,0
 730*FX2,0
 740CALL START
 750time1=TIME-time1
 760CLS
 770ENDPROC
 780DEF PROCdisplay
 790SIZE1=0
 800FOR I%=0 TO 255
 810HI=HIGH+I%:MI=MEDIUM+I%:LI=LOW+I%
 820HEIGHT1(I%)=65536*?(HI)+256*?(MI)+?(LI)
 830SIZE1=SIZE1+HEIGHT1(I%)
 840IF HEIGHT1(I%)=0 THEN GOTO 860
 850PRINTHEIGHT1(I%);"  Bin no. = ";I%
 860NEXTI%
 870PRINT
 880PRINT" Time taken for sample = ";time1/100" seconds "
 890PRINT
 900PRINT"  Sample size = ";SIZE1
 910PRINT
 920PRINT" Sample rate = ";(SIZE1/time1)/10;" per msec "
 930ENDPROC
 940DEF PROCprint
 950INPUT"  Print output Y/N ";RESPONSE$
 960IF RESPONSE$="Y" THEN VDU2 ELSE ENDPROC
 970FOR I%=0 TO 255
 980IF HEIGHT1(I%)=0 THEN GOTO 1000
 990PRINTHEIGHT1(I%);"  Bin no. = ";I%
1000NEXTI%:VDU3
1010ENDPROC
1020REM PLOT DATA
1030DEF PROCplotdata
1040IF AGAIN1<>0 THEN GOTO 1090
1050A1=&01020204:CLS:INPUTTAB(1,10)" EXPERIMENT NO. ",IP$
1060INPUTTAB(1,11)" Pipette potential ",pp
1070INPUTTAB(1,12)" Patch potential ",tp
1080MV$=STR$(pp-(tp)):PRINTTAB(1,14)" Transpatch potential = ";MV$:INPUTTAB(28,14)" Y/N",Y$:A1=10:I
F Y$="Y" GOTO 1090:ELSE CLS:GOTO1060
1090IF FILE<>0 ENDPROC:IF AGAIN1<>0 GOTO 1120:ELSE GOTO1100
1100CLS:PRINTTAB(0,9)" IF SIG. AMP.=1 MAXIMUM AMPLITUDE= 100pA IF SIG. AMP.=3 MAXIMUM AMPLITUDE= 30
pA  IF SIG. AMP.=10 MAXIMUM AMPLITUDE= 10pA"
```

```
1110INPUTTAB(1,14)" SIGNAL AMPLIFICATION"¦aapI :PRINTTAB(2,14)
1120IF aaraI(>0 GOTO1130:ELSE CLS:INPUTTAB(1,10)"  Maximum bin size "¦MBSIZI:GOTO1140
1130CLS:INPUTTAB(1,10)"  Magnification factor"¦aagI:SCALEY=(900/SIZEI):GOTO1150
1140SCALEY=900/MBSIZI
1150CLS:INPUTTAB(1,10)"  Lowest current amplitude"¦LBINI
1160CLS:INPUTTAB(1,10)"   Highest current amplitude"¦HBINI:CLS
1170RANGEI=HBINI-LBINI
1180SCALEI=1100/((RANGEI/0.4)*aapI)
1190ABAINI=ABAINI+1
1200ENDPROC
1210DEF PROCplot
12200I=&01020309
1230N=0:NI=1:kI=45:LPAI=0:HPAI=0:SCAL=0:nI=0:IL=0:YL=0
12406=RANGEI/10
1250VDU24,1¦10¦1280¦1000¦
1260VDU5
1270MOVE 99,49:DRAW 1199,49:MOVE 99,49
1280FORII=99TO1199 STEP 110
1290Q=LBINI:Y$=STR$(Q+(Q*N))
1300MOVE II,49:DRAW II,39:MOVE II-kI,30:PRINT LEFT$(Y$,3):N=N+1:kI=60:NEXTII:MOVE 1210,70:PRINT"pA"
:MOVE 99,49
1310N=1:0I=&01020003:FORII=139 TO 949 STEP 90:DRAW 99,II:DRAW 91,II:MOVE 0,(II+9):PRINT LEFT$(STR$(
((MBSIZI/10)*N)/10000),3):N=N+1:MOVE 99,II+1:NEXTII:0I=10:MOVE 100,50
1320LPAI=(LBINI/0.4)*aapI:HPAI=(HBINI/0.4)*aapI
13300I=&20009:FOR II=LPAI TO HPAI-1:SCAL=(II-LPAI)*SCALEI
1340YL=((50+HEIGHTI(II)*SCALEY))
1350FOR nI=0 TO SCALEI-1
1360IL=(100+SCAL+nI)
1370IF YL)949 DRAW IL,1000:GOTO1400:ELSE GOTO 1380
1380IF HEIGHTI(II)=0 GOTO1400:ELSE GOTO 1390
1390DRAW IL,YL
1400MOVE (IL+1),50:NEXT nI:NEXTII
1410VDU4:VDU26:0I=10:PRINTTAB(0,0)"Bin size"
1420PRINTTAB(0,1)"/10000"
1430PRINTTAB(12,0)"EXPT. "¦IP$
1440PRINTTAB(12,1)"TRANSPATCH POT."¦MV$
1450ENDPROC
1460REM
1470DEF PROCSDUMP
1480REM
1490REM VDU codes used
1500REM
1510PRNTRONLY=1
1520PRNTRON=2
1530PRNTROFF=3
1540CR=13
1550NOPAGE=15
1560CAN=24
1570ESC=27
1580REM
1590REM Zero page addresses
1600REM
1610DBASE=&7B
1620DWORK=DBASE+2
1630DLLNTH=DWORK+9
1640DBYTS=DLLNTH+2
1650DCPL=DBYTS+1
1660DMASK=DCPL+1
1670DNSTY=DMASK+1
1680DLINES=DNSTY+1
1690DBITS=DLINES+1
1700TEMP1=DBITS+1
1710TEMP2=TEMP1+1
1720REM
1730REM Miscellaneous addresses
1740REM
1750OSWRCH=&FFEE
1760OSBYTE=&FFF4
1770REM
1780REM Assembler code
1790REM
1800FOR pass=0 TO 2 STEP 2
1810PI=LOCI
1820[OPT pass
1830.SDUMP
1840\
1850\ Initialisation
1860\
1870LDA #NOPAGE:JSR OSWRCH  \Turn page mode off
1880LDA #PRNTRON:JSR OSWRCH \Turn printer on
1890LDA #CAN:JSR PRIN       \Delete printer buffer
1900LDA #ESC:JSR PRIN       \
1910LDA #ASC("3"):JSR PRIN  \ Set line spacing to 0 dots
1920LDA #24:JSR PRIN        \
1930LDA #&84                \Get the bottom address
1940JSR OSBYTE              \of the display in the current mode
1950STX DBASE:STY DBASE+1   \and store it in DBASE
1960\
1970\ Store default mode parameters
1980\
1990LDA #64:STA DLLNTH      \Bytes per line
2000LDA #1:STA DLLNTH+1
2010STA DMASK               \Dot bit map mask byte
2020STA DDOTS               \Horizontal dots per pixel
2030LDA #80:STA DCPL        \Characters per line
2040LDA #ASC("K"):STA DNSTY \Density character for printer
2050LDA #8:STA DBITS        \Pixels per byte
2060LDA #32:STA DLINES      \Lines on screen
2070\
2080\ Despatch on the mode
2090\
2100LDA #&87
2110JSR OSBYTE              \Get the mode
2120TYA
2130BEQ MD0
2140CMP #1:BEQ MD1
2150CMP #2:BEQ MD2
2160CMP #3:BEQ MD3
2170CMP #4:BEQ MD4
2180CMP #5:BEQ MD5
2190CMP #6:BEQ MD6
2200JMP DUMPEXIT            \Exit if bad mode
2210\
```

```
2220\ Set up the non-default parameters
2230\
2240.ND6:LDA &40:STA DCPL:LDA &25:STA DLINES:JSR LS6:JMP LSTART
2250.ND5:LDA &17:STA DMASK:LDA &2:STA DDOTS
2260LDA &40:STA DCPL:LDA &4:STA DBITS:JMP LSTART
2270.ND4:LDA &40:STA DCPL:JMP LSTART
2280.ND3:LDA &120:STA DLLNTH:LDA &2:STA DLLNTH+1
2290LDA &ASC("L"):STA DMSTY:LDA &25:STA DLINES:JSR LS6:JMP LSTART
2300.ND2:LDA &85:STA DMASK:LDA &2:STA DDOTS:STA DBITS:JMP LSTART
2310.ND1:LDA &17:STA DMASK:LDA &4:STA DBITS:JMP LSTART
2320.ND0:LDA &120:STA DLLNTH:LDA &2:STA DLLNTH+1
2330LDA &ASC("L"):STA DMSTY
2340\
2350\ Start of screen line
2360\
2370.LSTART
2380LDA DCPL:STA TEMP1
2390LDA &ESC:JSR PRIN       \Enter bit image mode
2400LDA DMSTY:JSR PRIN      \with double or single density
2410LDA DLLNTH:JSR PRIN     \and set the number of bytes
2420LDA DLLNTH+1:JSR PRIN   \of bit-mode data expected
2430\
2440\ Build up DBITS graphics bytes for the printer into workspace
2450\ from eight bytes of display memory
2460\
2470.DCHAR
2480LDY &0              \(DBASE),Y points into display memory
2490.L1:LDX DBITS       \DWORK,X points into workspace
2500LDA DMASK:STA TEMP2 \Copy mask byte
2510.L2:ASL DWORK,X     \This is a no-op first time round
2520LDA (DBASE),Y       \Get the display byte
2530AND TEMP2           \Mask off all but this pixel
2540BEQ L3              \Is it bright or dim?
2550INC DWORK,X         \Set wire if bright
2560.L3:ASL TEMP2       \Shift mask along for next pixel
2570DEX:BNE L2          \Continue for as of pixels in this display byte
2580INY:CPY &8:BNE L1   \Do all 8 display bytes
2590\
2600\ Printout DBITS dot image bytes DDOTS times
2610\
2620LDX &0
2630.L3:LDA DDOTS:STA TEMP2
2640.DDTS
2650DEC TEMP2
2660LDA DWORK+1,X       \Get the graphics byte
2670JSR PRIN            \and send it out
2680LDA TEMP2
2690BNE DDTS            \Do DDOTS copies of each byte
2700INX:CPX DBITS
2710BNE L5              \Do all DBITS bytes in workspace
2720\
2730\ Finished that character position
2740\
2750CLC
2760LDA DBASE:ADC &8:STA DBASE      \Bump up base pointer to
2770LDA DBASE+1:ADC &0:STA DBASE+1  \point to next 8 display bytes
2780DEC TEMP1:LDA TEMP1:BNE DCHAR   \Test for end of line
2790\
2800\ End of line
2810\
2820LDA &CR:JSR PRIN
2830DEC DLINES:BNE LSTART       \Test for end of screen
2840\
2850\ Exit from screen dump
2860\
2870.DUMPEXIT
2880JSR LS6
2890LDA &PRNTROFF:JSR OSWRCH
2900RTS
2910\
2920\ Set line spacing to 1/6"
2930\
2940.LS6
2950LDA &ESC:JSR PRIN:LDA &ASC("2"):JSR PRIN
2960RTS
2970\
2980\ Send character in A to printer only
2990\
3000.PRIN
3010PHA:LDA &PRNTRONLY:JSR OSWRCH:PLA:JSR OSWRCH
3020RTS
30301
3040NEXT pass
3050ENDPROC
3060DEF PROCarea:CONS=" ":tareaI=0:aI=1:@I=&20209
3070IF AGAINI()0 GOTO3080:ELSE CLS:INPUTTAB(3,10)"Signal amp"¡ampI
3080tareaI=0:areaI(aI)=0
3090CLS:INPUTTAB(0,10)"Low amp limit"¡BINLI(aI):CLS
3100INPUTTAB(0,10)"High amp limit"¡BINHI(aI):CLS
3110LPAI=(BINLI(aI)/0.4)*ampI:HPAI=(BINHI(aI)/0.4)*ampI
3120FOR II=LPAI TO HPAI:areaI(aI)=areaI(aI)+HEIGHTI(II):NEXTII
3130FOR II=0 TO 250:tareaI=tareaI+HEIGHTI(II):NEXTII
3140PRINTTAB(0,10)"Area between amp "¡BINLI(aI)¡" & "¡BINHI(aI) " ="¡(areaI(aI)/tareaI)*100"":aI=a
I+1:PRINTTAB(0,12)¡LPAI:PRINTTAB(1,13)¡HPAI
3150INPUTTAB(0,15)"Again....Y/N"¡DE$
31601F DE$="Y" GOTO 3080
3170CLS:INPUTTAB(0,10)"PRINT AREA Y/N"¡AE$
31801F AE$="N"GOTO3220
3190CLS:VDU2:IF ampI=1 GOTO3200:PRINTTAB(0,8)"Signal amplified by "¡ampI" times"
3200aI=aI-1:@I=&20209:FORII=1TOaI:PRINT:PRINTTAB(0,10+II)"Area between amp "¡BINLI(II)¡" & "¡BINHI
(II) " = "¡(areaI(II)/tareaI)*100""¡NEXTII
3210PRINT:PRINTTAB(0,20)"Length of sample = "¡timeI/100" seconds":PRINT:PRINTTAB(0,21) "Sample rate
    = "¡(SIZEX/timeI)/10¡" per msec":PRINT
3220VDU3:INPUTTAB(2,30)"PRESS C TO CONTINUE "CONS:ENDPROC
3230DEFPROCAMP
3240IF AGAINI()0 GOTO 3250 ELSE CLS:INPUTTAB(3,10)"Signal Amplification"¡ampI
3250@I=&20209:CONS=" ":PENI=1:TTALPEAK=0:CHMP=0:CHMPL=0:HB1=0:HB2=0:HB3=0
3260FOR II=5 TO 242
3270HB1=(HEIGHTI(II-5)+HEIGHTI(II-4)+HEIGHTI(II-3)+HEIGHTI(II-2)+HEIGHTI(II-1))
3280HB2=(HEIGHTI(II)+HEIGHTI(II+1)+HEIGHTI(II+2)+HEIGHTI(II+3)+HEIGHTI(II+4))
3290HB3=(HEIGHTI(II+5)+HEIGHTI(II+6)+HEIGHTI(II+7)+HEIGHTI(II+8)+HEIGHTI(II+8))
3300IF HB2<2000 GOTO3320:ELSE GOTO3310
```

```
3310IF MB1<MB2 AND MB2>MB3 THEN PEAK(PENI)=II*5:PENI=PENI+1:II=II+12 ELSE GOTO3320
3320NEXTII
3330FORII=PENI-1 TO 2 STEP-1
3340TTALPEAK=TTALPEAK+(PEAK(II)-PEAK(II-1))
3350NEXTII
3360IF PENI=0 ENDPROC
3370CHMP=TTALPEAK/(PENI-2)
3380CHMPL=(CHMP*0.4)/aspI:CLS
3390FOR II=1 TO PENI-1:PRINTTAB(3,10+II*2)"Channel peaks at:  "¦PEAK(II)*0.4/aspI:NEXTII
3400PRINTTAB(3,25)"No. of channels = "¦PENI-2
3410PRINTTAB(3,27)"Average channel amplitude = "¦CHMPL" pA":VDU3
3420IF CON$="P" ENDPROC:ELSE GOTO3430
3430INPUTTAB(2,30)"PRESS P TO PRINT"¦CON$
3440IF CON$="P" CLS:VDU2:GOTO3390:ELSE ENDPROC
3450DEF PROCplotnorm
3460GI=&01020309
3470N$="":N=0:MI=1:kI=45:LPAI=0:HPAI=0:SCAL=0:nI=0:IL=0:YL=0
3480G=RANGEI/10
3490VDU24,1;10;1280;1000;
3500VDU5
3510MOVE 99,49:DRAW 1199,49:MOVE 99,49:FORII=99TO1199 STEP 110:MOVE II,49:DRAW II,39:MOVE II-kI,30:
G=LBINI:Y$=STR$(G+(G*N)):PRINT LEFT$(Y$,3):N=N+1:kI=&0:NEXT II:MOVE 1210,70:PRINT"pA":MOVE 99,49
3520N=10:GI=&01020103:FORII=139 TO 949 STEP 90:DRAW 99,II:DRAW 91,II:MOVE 0,(II+9):N$=STR$(N/aspI):
PRINT LEFT$(N$,3)
3530MOVE 99,II+1:N=N+10:NEXTII:MOVE 100,50:GI=10
3540LPAI=(LBINI/0.4)*aspI:HPAI=(HBINI/0.4)*aspI
3550SI=&20009:FOR II=LPAI TO HPAI-1:SCAL=(II-LPAI)*SCALEI
3560YL=(50+((HEIGHTI(II)*SCALEY)*aspI))
3570FOR nI=0 TO SCALEI-1
3580IL=(100+SCAL+nI)
3590IF HEIGHTI(II)=0 GOTO3610:ELSE GOTO3600
3600DRAW IL,YL
3610MOVE (IL+1),50:NEXT nI:NEXTII
3620VDU4:VDU26:GI=10
3630PRINTTAB(0,0)" I of total"
3640PRINTTAB(0,1)" counts"
3650PRINTTAB(12,0)"EXPT. "¦IP$
3660PRINTTAB(12,1)"TRANSPATCH POT.="¦HV$¦"mV"
3670ENDPROC
3680 DEFPROCfile
3690 N=1:K=1:AZ$="":JI=0:CLS
3700 INPUTTAB(3,10)"Filename"¦B$
3710 IF LEN(B$)>7 CLS:PRINTTAB(3,9)"Name too long":GOTO3700:ELSE GOTO3720
3720 I=OPENOUTB$
3730 AZ$=" Experiment "+IP$
3740 FOR KI=1 TO LEN(AZ$)
3750 BPUTEI,ASC(MID$(AZ$,KI,1)):NEXTKI:BPUTEI,13
3760 AZ$=" Transpatch potential = "+HV$
3770 FOR KI= 1 TO LEN(AZ$)
3780 BPUTEI,ASC(MID$(AZ$,KI,1)):NEXTKI:BPUTEI,13:BPUTEI,13
3790 AZ$="      Bins     Nos."
3800 FOR K=1 TO LEN(AZ$)
3810 BPUTEI,ASC(MID$(AZ$,K,1)):NEXTK:BPUTEI,13:BPUTEI,13
3820 FORII=0 TO 250
3830 FORN=1 TO 2
3840 GI=&01020104
3850 IF N=1 GOTO3860:ELSE GOTO3870
3860 AZ$=STR$(II):GOTO3880
3870 AZ$=STR$(HEIGHTI(II))
3880 IF 1=LEN(AZ$):FOR JI=1TO8:BPUTEI,32:NEXT JI:GOTO3970
3890 IF 2=LEN(AZ$):FOR JI=1TO7:BPUTEI,32:NEXT JI:GOTO3970
3900 IF 3=LEN(AZ$):FOR JI=1TO6:BPUTEI,32:NEXT JI:GOTO3970
3910 IF 4=LEN(AZ$):FOR JI=1TO5:BPUTEI,32:NEXT JI:GOTO3970
3920IF 5=LEN(AZ$):FOR JI=1TO4:BPUTEI,32:NEXT JI:GOTO3970
3930IF 6=LEN(AZ$):FOR JI=1TO3:BPUTEI,32:NEXT JI:GOTO3970
3940IF 7=LEN(AZ$):FOR JI=1TO2:BPUTEI,32:NEXT JI:GOTO3970
3950IF 8=LEN(AZ$):BPUTEI,32:GOTO3970
3960 IF 9=LEN(AZ$)
3970 FOR K=1 TO LEN(AZ$)
3980 BPUTEI,ASC(MID$(AZ$,K,1)):NEXTK:NEXTN
3990 BPUTEI,13:NEXTII:CLOSEEI
4000 ENDPROC
4010 DEF PROCbins
4020 FOR II=1 TO 250
4030 IF HEIGHTI(II)=0 THEN GOTO4050
4040 PRINTHEIGHTI(II);"   Bin no. = "¦II
4050NEXTII
4060 VDU3:INPUT"PRINT   Y/N"¦PETE$
4070 IF PETE$="P" VDU2:GOTO4020:ELSE GOTO4080
4080 ENDPROC
```

Appendix III

Reprints published from the experiments presented in Section II of this thesis.

Martin, R.J. and Thorn, P. (1984) A high conductance anion channel in somatic muscle cells of *Ascaris suum*. Journal of Physiology *354* 46P.

Thorn, P. and Martin, R.J. (1987) A high conductance calcium-dependent chloride channel in *Ascaris suum* muscle. Quarterly Journal of Experimental Physiology *72* pp31-49.

[*From the Proceedings of the Physiological Society*, 12–13 *April* 1984
Journal of Physiology, **354**, 46*P*]

A high conductance anion channel in somatic muscle cells of *Ascaris suum*

BY R. J. MARTIN and P. THORN. *Department of Veterinary Pharmacology, Royal (Dick) School of Veterinary Studies, University of Edinburgh EH9 1QH*

Ascaris muscle cells have been shown to have a high permeability to Cl^- (Del Castillo, De Mello & Morales, 1964). We used the patch-clamp technique with giga-seal recordings (Hamill, Marty, Neher, Sakmann & Sigworth, 1981) to observe unitary currents in collagenase-treated preparations. We recorded from the membrane in the

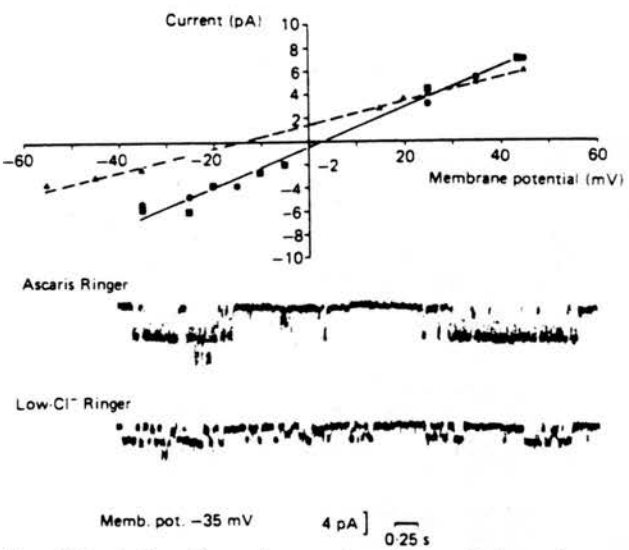

Fig. 1 shows the I/V relationship and examples of inward channel currents (opening downwards) with up to two channels present in an inside-out patch with different Cl^- concentrations on the intracellular side of the patch and 140 mM-Tris Cl^- in the pipette. Membrane potentials were corrected for a measured pipette potential of +4·7 mV. Control *Ascaris* Ringer: □ and continuous line ((mM) 135 NaCl, 3 KCl, 15·7 $MgCl_2$, 3 $CaCl_2$, 5 Tris, 3 glucose, pH 7·6). Low-Cl^- *Ascaris* Ringer: △ and dotted line (substitution of 85 mM-NaCl with 85 mM-Na acetate). Return to *Ascaris* Ringer: ●. Lines calculated by linear regression. 30 °C.

cell body region of somatic muscle cells. A spontaneous high conductance (130–230 pS) channel was seen in most of the cell-attached and isolated inside-out patches. The channel conductance and reversal potential were unaffected by substitution of the cations with Tris. Lowering the Cl^- concentration on the intracellular side of the patch had a reversible effect on the I/V relationship and reversal potential (Fig. 1). These experiments are consistent with this channel being permeable to Cl^-.

P.T. holds a S.E.R.C.–C.A.S.E. studentship with Pfizer Central Research.

REFERENCES

DEL CASTILLO, J., DE MELLO, W. C. & MORALES, T. (1964). *J. gen. Physiol.* **48**, 129–140.
HAMILL, O. P., MARTY, A., NEHER, E., SAKMANN, B. & SIGWORTH, F. J. (1981). *Pflügers Arch.* **391**, 85–100.

Quarterly Journal of Experimental Physiology

Quarterly Journal of Experimental Physiology (1987) **72**, 31–49
Printed in Great Britain

A HIGH-CONDUCTANCE CALCIUM-DEPENDENT CHLORIDE CHANNEL IN *ASCARIS SUUM* MUSCLE

P. THORN AND R. J. MARTIN

Department of Preclinical Veterinary Sciences, R.(D.)S.V.S., Summerhall, University of Edinburgh EH9 1QH

(RECEIVED FOR PUBLICATION 3 JUNE 1986)

SUMMARY

The properties of a high-conductance Ca-dependent Cl channel in the body muscle membrane of the nematode parasite *Ascaris suum* were examined with the patch-clamp technique. In *Ascaris* Ringer solution the current–voltage relationships of the channel appeared linear during hyperpolarization with a slope conductance of 200 pS (in symmetrical 175 mM-Cl): during depolarization the slope conductance reduced. Cation and anion replacement experiments showed this channel to be permeable to Cl ions. In artificial perienteric fluid (in symmetrical 78 mM-Cl) the channel conductance was found to be 114 pS. Subconductance states were seen when the patch was depolarized. The channel conductance showed saturation with increasing Cl concentrations. The channel was voltage sensitive: the probability of the channel being open and the mean open time of the channel reduced when the patch was depolarized. Mean channel open times between 2·4 and 215 ms were observed. Frequency histograms of the distributions of open and closed times were fitted with two and three exponentials respectively; this suggests complex channel kinetics with multiple open and closed states. Ca applied to the intracellular surface of the patch increased in a dose-dependent manner the number and probability of the channels being open. These channels were seen in about 20% of all patches and occasionally up to 15 channels were seen in a single patch. The distributions of the probabilities of seeing N channels open in multichannel patch records were not always well fitted by the binomial distribution: it is suggested that adjacent channels could have different probabilities of being open. The possible functions of this channel are discussed.

INTRODUCTION

Ascaris suum is a worm-like nematode parasite found in the small intestine of pigs. The *Ascaris* body cavity contains a perienteric fluid (Fig. 1*A*) which has a Cl concentration of 52 mM (Hobson, Stephenson & Eden, 1952). Hobson, Stephenson & Beadle (1952) have shown that the Cl concentration of the perienteric fluid is maintained at a lower concentration than that of the environment. They demonstrated that Cl is transported across the body wall to the outside and that the active site of this transport is a feature of the muscle or hypodermis. One possible pathway for the movement of Cl is through the bag regions of the muscle cells.

Electrophysiological studies on the bags have shown a high membrane permeability to Cl compared with K (Del Castillo, De Mellow & Morales, 1964; Brading & Caldwell, 1971). Subsequent studies have indicated an influence of Ca on its membrane permeability (Weisblat, Byerly & Russel, 1976). During patch-clamp studies on the extrasynaptic γ-aminobutyric acid (GABA) receptor (Martin, 1985) a large-conductance ion channel was frequently observed which was abolished by perfusing the preparation with a low-Ca Ringer solution. This paper describes the results of a patch-clamp study which has characterized the channel as Ca dependent, voltage sensitive and permeable to Cl. A preliminary account of some of this work has already been published (Martin & Thorn, 1984).

METHODS

Details of the preparation and methods have been described previously (Martin, 1980, 1985). They are outlined below.

The preparation

Specimens of *Ascaris suum* obtained from the local slaughter-house were maintained in Locke solution (replaced daily) at 32 °C in a water-bath. The *Ascaris* were about 20 cm in length and used within 4 d. A 2 cm flap preparation, made from a section taken 5 cm from the head was pinned into the experimental chamber. The temperature (25–30 °C) of the preparation and chamber was maintained by a water-jacket and monitored by a thermocouple device. The preparation was continuously perfused only during experiments involving the application of different experimental solutions.

Enzyme treatment

Clean muscle membranes were prepared with collagenase (1 mg in 1 ml) applied to the preparation for a period of 0·5–1·5 h. It was then washed liberally to remove the debris before recording. The enzyme treatment lowers the resting potential and causes an increase in intracellular Cl to near extracellular levels (Martin, 1985).

Ringer solutions

Several different types of bathing Ringer solution were used (Table 1). *Ascaris* Ringer solution was used for most experiments since it readily permitted giga-seal formation and its high Cl concentration facilitated the examination of Cl currents by increasing their amplitudes. An artificial perienteric fluid (APF) with HEPES buffer was also used because its ionic concentrations (particularly the lower Cl) approximates to normal extracellular ionic concentrations in the whole parasite (Hobson *et al.* 1952) and allowed a check on the properties of the anion channel. The NaCl solutions used in the determination of the Cl concentration–channel conductance relationship contained 5 mM-HEPES and 1 mM-$CaCl_2$, adjusted to pH 7·6 with NaOH.

Patch-electrode solution

Except where stated the patch electrode was filled with the same (but filtered) solution as the bathing Ringer solution. During studies on the channel permeability it was filled with either *Ascaris* Ringer solution, one-fifth *Ascaris* Ringer solution, or Tris Ringer solution (Table 1). These allowed an examination of the effect of anion and cation replacement.

Fabrication of patch electrodes

The patch pipettes were made from glass microhaematocrit tubing (Hawksley Cat. No. 1604, external diameter 1·4 mm) and pulled on a vertical micro-electrode puller (SRI Cat. No. 2001); the tip diameters were approximately 0·5 μm and filled electrodes had resistances of 2–4 MΩ.

Recording

A cell-attached patch was formed when a patch electrode was pushed gently against the bag membrane (see Fig. 1*A* and *B*) and suction applied to the pipette. The seal resistance, in favourable preparations, then gradually increased to greater than 1 GΩ. Isolated inside-out patches were easily formed by gently lifting the patch of the bag membrane. In some patches, immediately after isolation, the channel currents were very small in amplitude (conductance < 20 pS) and opened with slow rise times; in these cases exposure to air (Hamill, Marty, Neher, Sakmann & Sigworth, 1981) produced channel openings of full conductance and rapid rise times.

Two types of high-gain current–voltage (I–V) converters were used to monitor the currents. Initially a laboratory-made amplifier based on a Teledyne Philbrick op-amp with a 1 GΩ feed-back resistor and 3 dB cut off of 1 kHz was used. Subsequently a List EP-7 was used and the signals actively filtered using a Kemo VBF/4 at 1 kHz (3 dB). Both systems gave similar results.

The signal was recorded on a Racal Thermionic Store Four FM tape recorder (slowest frequency response used 1250 Hz, 1 dB) and monitored on an oscilloscope (Tektronix 5103N) and a chart recorder (Lectromed type MX 216).

Table 1. *Solutions: electrolyte concentrations (mM)*

	NaCl	NaAc	KCl	$CaCl_2$	$MgCl_2$	Glucose	Tris	HEPES
Ascaris Ringer solution	135	—	3·0	3·0	15·7	3·0	5·0	—
Tris Ringer solution	—	—	—	3·0	15·2	3·0	140	—
One-fifth *Ascaris* Ringer solution	27	—	0·6	0·5	3·14	0·6	1·0	—
Low-Cl *Ascaris* Ringer solution	50	85	3·0	3·0	15·7	3·0	5·0	—
APF	23	110	24	6·0	5·0	11	—	5·0
Low-Ca APF	23	110	24	—	11	11	—	5·0
NaCl Ringer solutions	50–500	—	—	1	—	—	—	5·0

The Ringer solutions containing 5 mM-Tris were corrected to pH 7·6 with Maleic acid; Tris Ringer solution containing 140 mM-Tris was corrected to pH 7·6 with HCl; the Ringer solution containing HEPES were corrected to pH 7·6 with NaOH. Low-Ca APF contained a total Ca of 3·7 μM as measured by flame photometry; this gave an estimated free-Ca of 1·5 μM. A zero-Ca APF Ringer solution was prepared by adding 0·5 mM-EGTA to the low-Ca APF

Junction potentials

In order to minimize the effect of junction potentials an agar-bridge bath electrode was used. The electrode for the pipette was prepared using an Ag wire fused with AgCl. Zero current potentials were routinely measured for each pipette before forming a seal; these initial electrode potentials were offset.

Data analysis

Single-channel current amplitudes were measured by hand from chart recordings at different patch potentials. Often the I–V relationships showed non-linearity on depolarization; therefore slope conductances were estimated by regressions of the linear portion of the I–V relationship mostly obtained during hyperpolarization of the patch.

Records showing only a single-channel opening were analysed with the aid of a Cromemco microcomputer programmed to sample and digitize every 200 μs. Channel openings were registered when the current level was greater than 75% of the full channel amplitude. Closings were registered when the current level fell below 25% of the full amplitude. Channel records containing subconductance levels were excluded. Effective mean open and closed times are quoted without correction for unresolved short intervals. The channel records were checked for stationarity using Q-sums and the K–S statistic (Glasbey & Martin, 1986). The distributions of the open and closed times greater than 0·5 or 1 ms were fitted by the sum of a number (1, 2, 3 and 4 of exponentials) using a maximum-likelihood procedure (Martin, 1985). It was taken that a reduction of 3 log units following the addition of each extra exponential component indicated a significant improvement in fit.

Multichannel records were analysed using a BBC microcomputer and Unilab interface sampling at 100 kHz to give probability density histograms of current amplitude. This allowed estimates of the proportion of the time spent with 0, 1, 2...n channels open to be made.

Drugs

Collagenase (C-1030 Sigma) and the Ca ionophore A23187 (Calbiochem) were used. The A23187 was applied in a concentration of 10 μg ml^{-1} in the perfusing Ringer solution. It was made up from a stock 0·5 mg ml^{-1} solution in methanol.

RESULTS

The following experiments were carried out on the muscle cells from more than 200 preparations. Most experiments were completed within 4 h following enzyme treatment; this was because the membrane gradually became too fragile and easily broke after giga-seal formation. More than 200 successful giga-seal recordings were made during this study.

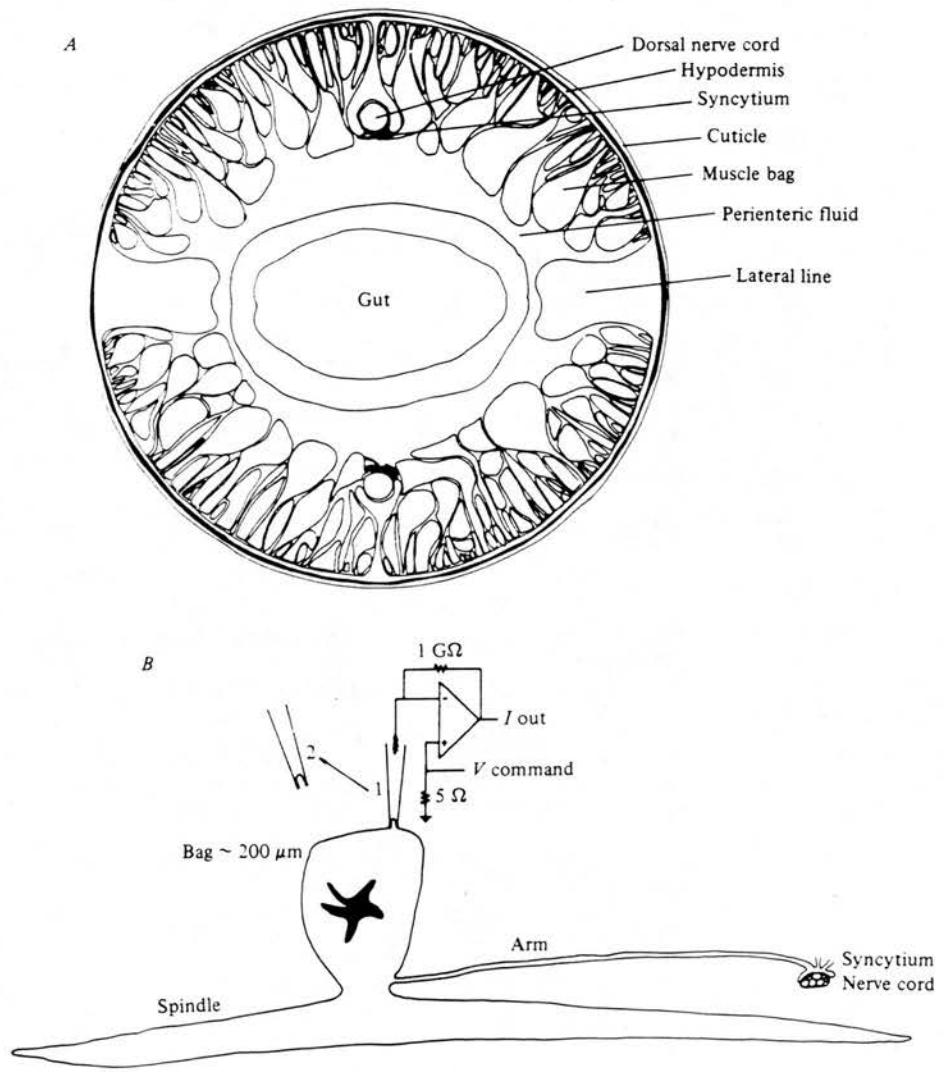

Fig. 1. *A*, diagram of a cross-section through the anterior region of *Ascaris suum*. The nerve cords are held in an extension of the hypodermis which form a cup-like structure. All the muscle cell bodies (bags) project into the body cavity which is filled with perienteric fluid. In the centre is the gut. *B*, diagram of a single muscle cell and recording technique. The cell is divided into three main regions: the cell body or bag region overlies the contractile muscle spindle: an arm extends from the bag to a nerve cord. The muscle is electrically coupled to adjacent muscle cells and also receives chemical synaptic contact with the nerve cords at the syncytium. The bag membrane was the main recording site in these experiments. We used both cell-attached patches (1) and isolated inside-out patches (2).

Initial observations on channel behaviour

Many cell-attached or isolated inside-out recordings using *Ascaris* Ringer solution resulted in current records like those seen in Fig. 2*A*. These show the activity of a large-conductance channel with a reversal potential near 0 mV. On average one in five

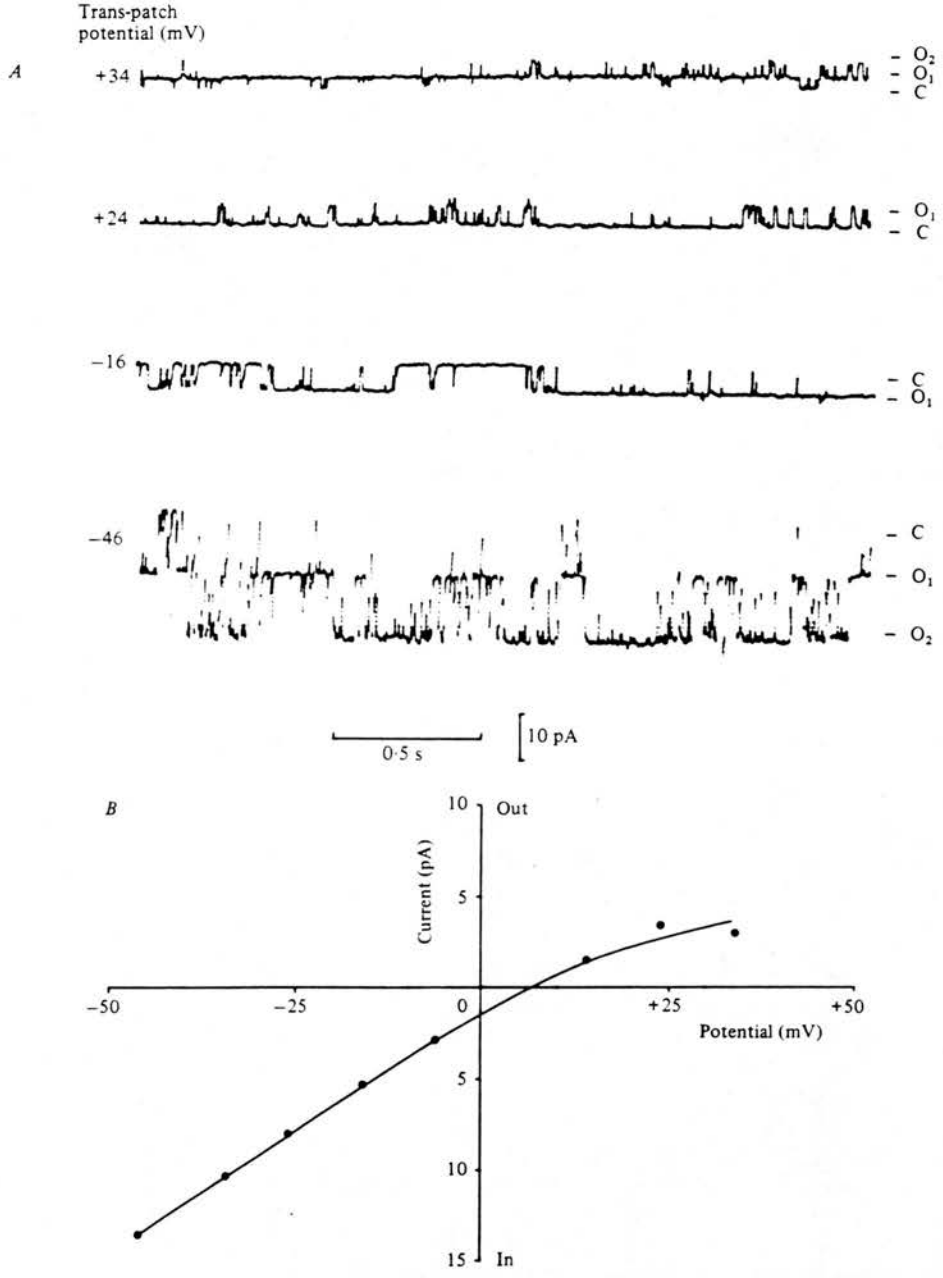

Fig. 2. *A*, current records obtained at different trans-patch potentials for the high-conductance channel. The records were obtained from an isolated inside-out patch held at the four different potentials indicated. The patch was bathed on both sides of the membrane with *Ascaris* Ringer solution, 30 °C. The currents are inward for the two negative or hyperpolarized holding potentials and outward for the two positive or depolarized holding potentials. Up to two channels are seen. The current levels with no channels open are indicated by C. The current levels with one channel opening are indicated by O_1, two channels open are indicated by O_2. *B*, a plot of the single-channel current amplitude against the trans-patch potential from the same experiment. The relationship is linear during hyperpolarization although there are deviations at depolarized potentials. The linear portion of the line gives a conductance of 220 pS.

patches showed the presence of this channel: however, this average varied dramatically from preparation to preparation. In some preparations patches from different cells all showed channel openings while in other preparations no patches showed channel activity: the reason for this is not known.

With trans-patch potentials held between +50 and −50 mV, smaller-conductance channels were only rarely observed and were excluded in the analysis. The effect of isolating the patch on channel opening also varied with preparations: in some preparations there was an immediate increase in channel opening with up to fifteen channels being observed in the patch; some cell-attached patches, which had a great deal of channel activity, showed little increase in activity on isolation. This variation in behaviour was subsequently explained by variations in intracellular Ca and the Ca-dependent nature of the large-conductance channel. Perfusion of the intracellular side of the isolated patches, often within a period of minutes, lead to a reduction in the number of active channels in the patch. This loss was due to the mechanical disturbance by the perfusion rather than any change in the ionic constituents of the perfusing Ringer solution: this problem of the loss of activity made the effects of changing Ca and Cl concentrations difficult to study.

Channel conductance

Fig. 2*A* and *B* shows typical current records and the channel *I–V* relationship. In this experiment the patch was an isolated inside-out patch with *Ascaris* Ringer solution on both sides of the membrane. The *I–V* relationship was linear during hyperpolarization but on depolarization the slope conductance often reduced considerably. This rectification was seen in over half the channel records and is not predicted on the basis of the constant field equation for a channel bathed in symmetrical solutions. In twenty experiments at 30 °C this channel had a slope conductance during hyperpolarization of 200 ± 7 pS (mean ± S.E.M.) when measured using isolated patches and symmetrical *Ascaris* Ringer solution.

Channel permeability

Initially in order to look at the channel permeability, patch recordings were made using one-fifth *Ascaris* Ringer solution in the patch electrode: with *Ascaris* Ringer solution in the bath, shifts in the channel reversal potential would indicate whether the channel was permeable to anions or cations. In all these experiments the reversal potential moved up to a maximum of 40 mV in the depolarizing direction; this is predicted by the Nernst equation for an anion channel. Further studies were conducted where the cations were placed in the patch electrode with the large impermeant ion Tris: these experiments showed no effect on conductance or the reversal potential of the channel *I–V* plot, again indicating an anion channel. Fig. 3 shows the effect of cation replacement on the *I–V* relationship using an isolated patch. The filled circles show the points obtained with Tris Cl in the patch pipette and *Ascaris* Ringer solution in the bathing solution.

In seven such experiments the mean slope conductance was 204 ± 16 pS (mean ± S.E.M.) and the reversal potential was always near 0 mV. Also shown in Fig. 3 is the lack of effect on the channel currents of replacing cations on both sides of the membrane with Tris.

The effect of anion replacement was also examined using cell-attached and isolated patches. The bag membrane of *Ascaris* is permeable to Cl; after collagenase treatment the intracellular Cl concentration approaches that of the bathing Ringer solution (Martin, 1985). It was therefore possible to reduce the intracellular Cl concentration after cell-attached patches had been formed by reducing the Cl in the bathing Ringer solution. In all such experiments bathing the preparation in low-Cl *Ascaris* Ringer solution reduced the

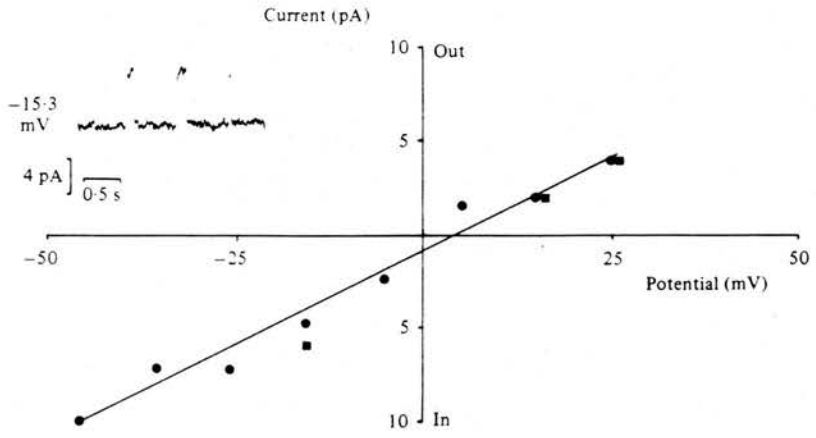

Fig. 3. A plot of single-channel current amplitude against the trans-patch potential of an isolated patch with Tris Cl in the pipette. The points (●) were obtained with Tris Cl on the extracellular side of membrane patch and *Ascaris* Ringer solution on the intracellular side. The points (■) were obtained from the same experiment with Tris on both the intracellular side and the extracellular side of the membrane patch. In the top left-hand corner is an example of the current records obtained at −15 mV with Tris Cl on both sides of the patch.

slope of the conductance and shifted the reversal potential in the hyperpolarizing direction. Similar experiments with isolated patches were more difficult to do since changing the bathing Ringer solution on the intracellular side of the patch was often associated with loss of channel activity; however, Fig. 4 shows one such successful experiment. It can be seen from the *I–V* plot that when the patch is bathed with symmetrical 175 mM-Cl there is a slope conductance of 200 pS, and a 0 mV reversal potential. When the Cl on the intracellular side of the patch was reduced to 90 mM there was a reduction in the slope conductance to 100 pS and an 18 mV hyperpolarizing shift in the reversal potential. An 18 mV shift was predicted by the Nernst equation for a Cl channel.

It was concluded from these observations that this large-conductance channel has a high permeability to Cl with no discernible permeability to cations. The conductance of this channel was therefore tested in APF Ringer solution which approximates more closely to the normal extracellular milieu and has a lower Cl concentration. The channel conductance in this medium was found to be 114 ± 5 pS (mean $\pm$, S.E.M., $n = 5$).

Channel conductance–Cl-concentration relationship

It is clear from the preceding section that the channel conductance varies with Cl concentration. The constant field equation predicts a linear relationship between channel conductance and Cl concentration with equal concentrations on both sides of the membrane (eqn. (1)).

$$g = F^2/RT.P.\mathrm{Cl}, \tag{1}$$

where g is the channel conductance, Cl is the concentration on both sides of the patch and P is the channel permeability. R, T and F have their usual meaning.

Fig. 5 illustrates the effects of Cl concentration on channel conductance: isolated inside-out patches bathed in symmetrical NaCl Ringer solution (Table 1) at 30 °C were used, conductances were measured as before. The relationship showed saturation at high Cl concentrations; such saturation has been reported previously e.g. Sakmann & Trube

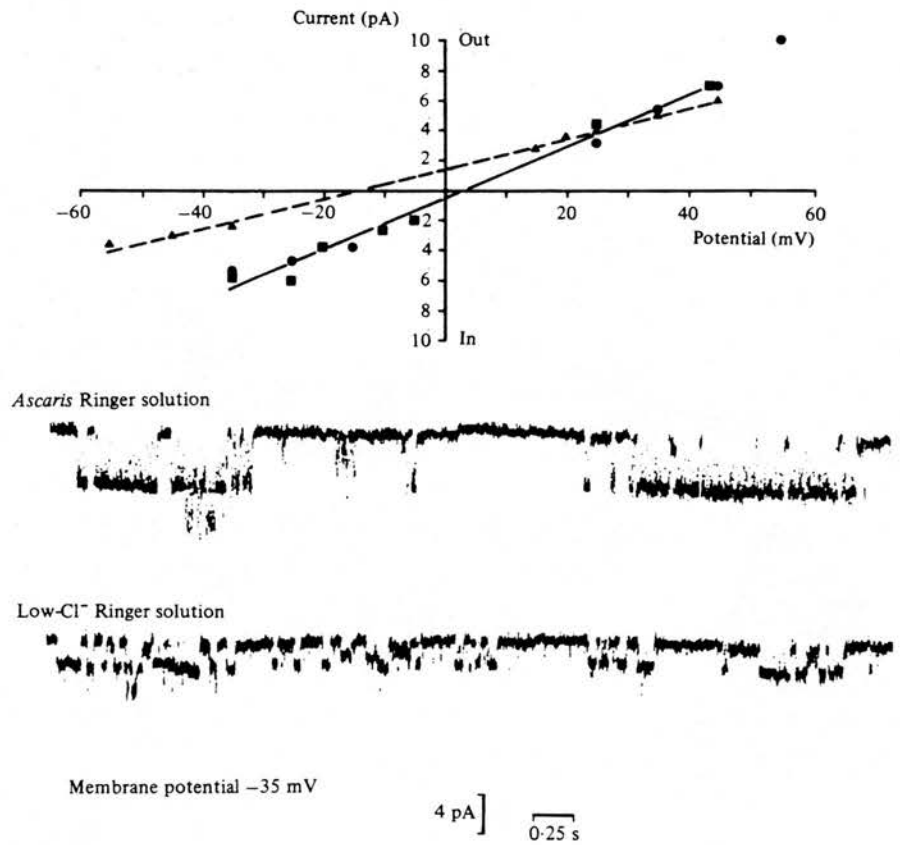

Fig. 4. The *I–V* relationship and representative examples of inward currents (openings downwards) with up to two channels present in an inside-out patch with different Cl concentrations on the intracellular side of the patch and Tris Cl in the pipette. Control *Ascaris* Ringer solution: ■ and continuous line. Low-Cl *Ascaris* Ringer solution: ▲ and dashed line. Return to *Ascaris* Ringer solution: ●, lines calculated by linear regression. 30 °C.

(1984). The line drawn in Fig. 5 has been fitted to the points using non-linear regression and the Michaelis–Menten equation:

$$g = G_{\max} \cdot \mathrm{Cl}/(K_m + \mathrm{Cl}), \tag{2}$$

where g is the conductance, $G_{\max}$ is the conductance at saturating Cl and K_m is the Cl concentration producing half saturation. $G_{\max}$ was 422 pS and K_m was 188 mM; non-linear regression was used. The equation is based on the following reaction scheme (eqn. (3)), where R stands for a binding site of the channel, $\mathrm{Cl_o}$ and $\mathrm{Cl_i}$ are extracellular and intracellular Cl concentrations respectively,

$$\mathrm{Cl_o} + R \leftrightharpoons \mathrm{Cl}R \cdots \mathrm{Cl}R \leftrightharpoons R + \mathrm{Cl_i}.$$

Subconductance states

Fig. 6*A* is an example of channel currents showing a subconductance state 75% of the main state; it was from an isolated patch with symmetrical *Ascaris* Ringer solution and a trans-patch potential of +30 mV. This interpretation was made on the grounds that the

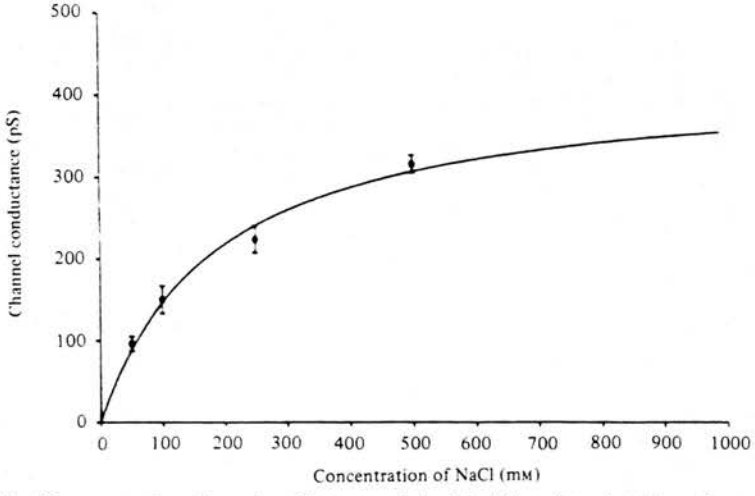

Fig. 5. The Cl concentration–channel conductance relationship. The points plotted are the mean ± S.E.M. of the conductances from observations on the I–V relationship of at least four isolated patches bathed in symmetrical NaCl Ringer solution (Table 1) and at 30 °C. The line was fitted to the equation $g = G_{max} \cdot Cl/(K_m + Cl)$ by non-linear regression where $G_{max} = 422$ pS and $K_m = 188$ mM.

records show 'instantaneous' steps to the subconductance level and to the full conductance level from the closed level, as well as 'instantaneous' steps between the subconductance and full conductance levels. During depolarization several subconductance levels were seen. No systematic study of the levels of subconductance and their relationship with membrane potential was made. No subconductance states were observed during hyperpolarization. Similar observations were obtained using APF Ringer solution and cell-attached patches.

Fig. 6*B* shows the I–V plot for a cell-attached patch recording made with *Ascaris* Ringer solution; the continuous line shows the relationship with the full main-state conductance of the channel and the dashed line shows the relationship of the most frequently observed subconductance state.

Voltage sensitivity

Fig. 7*A*, *B* and *C* illustrates the voltage-sensitive behaviour of this channel at different patch potentials. This experiment was on a cell-attached patch where the cell resting potential is unknown. The quoted potentials will therefore be offset by the resting potential. Previous work suggests that the resting potential in these conditions was below −15 mV (Martin, 1985). This cell-attached patch recording using *Ascaris* Ringer solution shows a feature of all recordings, that is, a decrease in channel opening as the patch is depolarized; the number of channels opening simultaneously declines on depolarization from three to one. Fig. 7*B* shows the relationship between the probability of the channel being open and the applied patch potential. Here it was assumed that the probability of opening was the same for each channel in the patch. Fig. 7*C* shows the relationship between mean open time and the patch potential in the same patch as before. In ten similar experiments it was found that the probability of opening measured at patch potentials between −55 and +70 mV decreased, on average, 6% for every 10 mV depolarization. The mean channel open time, which varied between 2·4 and 215 ms, decreased on average by 6 ms for every 10 mV (mean of six observations).

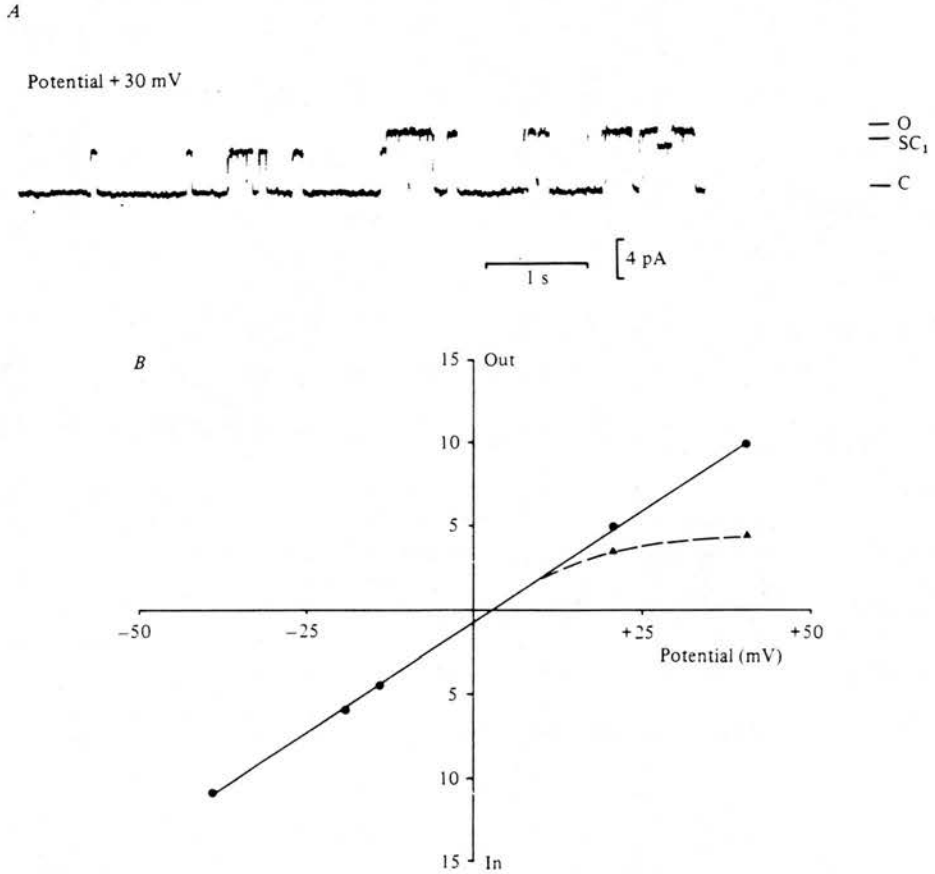

FIG. 6. *A*, channel current records showing subconductance states: isolated inside-out patch; patch potential +30 mV; symmetrical *Ascaris* Ringer solution; main open state, O; closed state, C; subconductance state, SC_1. *B*, a plot of single-channel current amplitudes against trans-patch potential for a cell-attached patch. This graph shows the full conductance of the channel (●) and also the subconductance state of the channel (▲). Subconductance states were only seen at depolarized trans-patch potentials. *Ascaris* Ringer solution was used for the pipette and bathing Ringer solution.

The mean open time for multichannel patches was calculated by the summation of the times spent above each channel level, divided by the total number of observed openings. Similar observation were made using APF Ringer solution.

Distribution of open and closed times suggest complex channel kinetics

Fig. 8 shows open and closed time frequency histograms at −40 and −10 mV from an isolated patch in symmetrical *Ascaris* Ringer solution. The records were obtained from a patch showing only a single-channel opening; at −40 mV the channel was in its main-state conductance. The open distribution (Fig. 8*A* and eqn. (4)) at −40 mV was best described by two exponentials which had a minor component (19% of the total openings) due to openings with a mean open time of 2·7 ms and a major component (81% of the total openings) due to long openings with a mean open time of 61 ms. The closed distribution

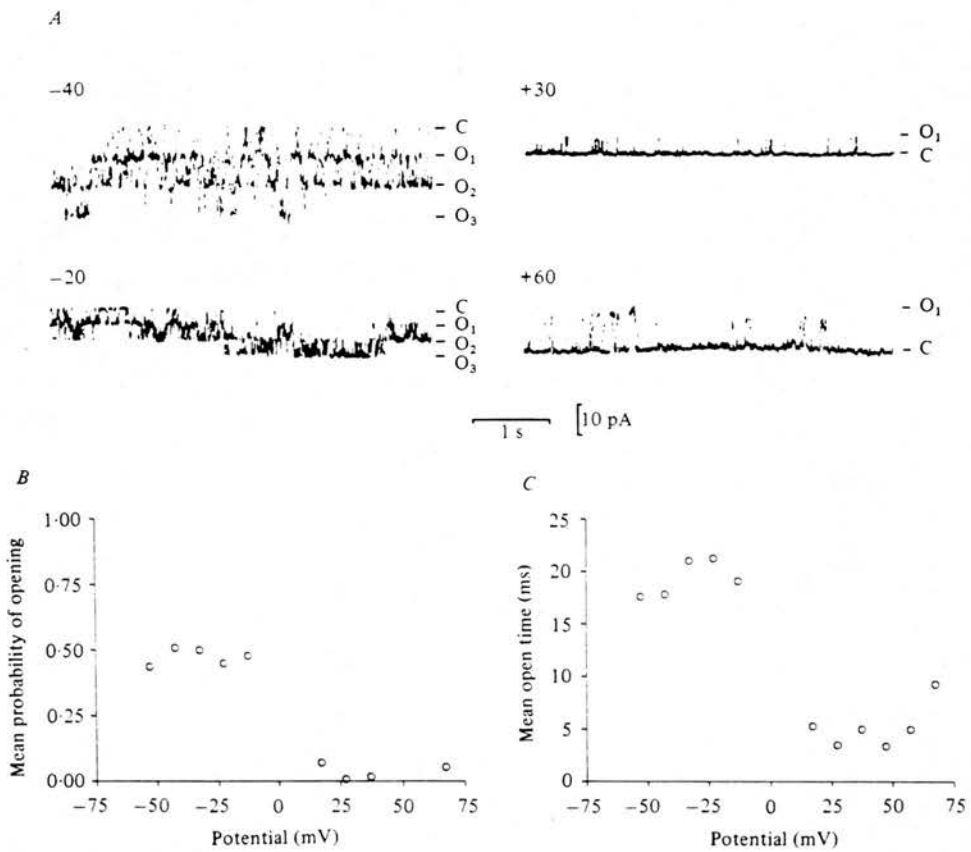

Fig. 7. *A*, examples of current records taken from the same cell-attached patch held at different applied potentials. The current levels indicating zero, one, two and three channels open are shown by C, O_1, O_2 and O_3 respectively. There seem to be up to three channels opening at the hyperpolarized potentials. This is reduced to only one channel open at any given time when the patch is depolarized. The voltage sensitivity is due to marked reduction in the probability of opening and the mean open time. *B*, a graph of the probability of the channel opening against the patch potential derived from the same cell-attached-patch experiment as the channel records in *A*. The dramatic reduction in the probability of the channel opening seen as the patches depolarized was typical of the activity of this high-conductance anion channel. *C*, a graph of the mean open time of the channel against the patch potential derived from the same cell-attached-patch experiment as in *A*. The reduction in the mean open time when the patch was depolarized again was typical of the activity of this high-conductance anion channel.

at −40 mV (Fig. 8 *B* and eqn. (5)) was best described by three exponentials: there was a brief type separating openings into bursts (61 % of the total closings, mean closed time 1·1 ms); there was a smaller component separating bursts into clusters (18 % of the total closings, mean closed time 10 ms); the third component separating clusters (21 % of the total closings) had a mean closed time of 110 ms. These observations suggest the presence of at least two open states and three closed states at −40 mV.

$$P_{\text{open}-40} = 0{\cdot}19/2{\cdot}7 \exp(-t/2{\cdot}7) + 0{\cdot}81/61 \exp(-t/61) \text{ and} \quad (4)$$

$$P_{\text{closed}-40} = 0{\cdot}61/1{\cdot}1 \exp(-t/1{\cdot}1) + 0{\cdot}18/10 \exp(-t/10) + 0{\cdot}21/110 \exp(-t/110). \quad (5)$$

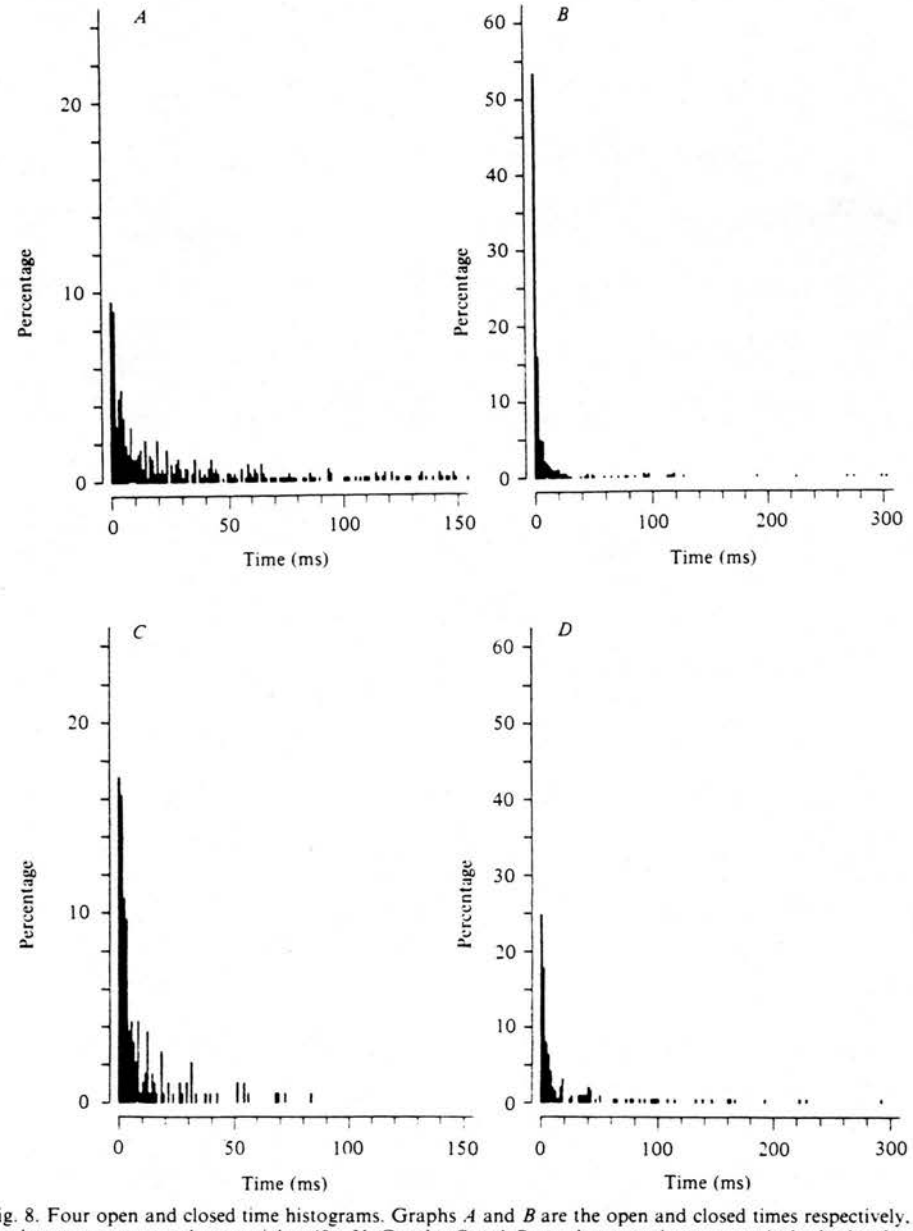

Fig. 8. Four open and closed time histograms. Graphs *A* and *B* are the open and closed times respectively, both taken at a trans-patch potential −40 mV. Graphs *C* and *D* are the open times respectively, both taken at a trans-patch potential of −10 mV. An isolated patch with symmetrical *Ascaris* Ringer solution was used. Only single-channel openings were seen. The probability density functions of the open and closed times are described in the text. Bin widths: open times, 1 ms; closed times, 2 ms. $n = 409$ in *A* and *B*; 185 in *C* and *D*. Mean times: 51 ms (*A*); 14 ms (*B*); 11 ms (*C*); 79 ms (*D*).

where $P_{\text{open}-40}$ and $P_{\text{closed}-40}$ are the probability density functions of open and closed states at -40 mV and t is the time in milliseconds.

Two components in the open time distributions and three components in the closed time distributions were distinguished at potentials between -40 and -10 mV; however, the proportion of time the channel was open decreased on depolarization. Eqns. (6) and (7) describe the distribution of the open and closed times at -10 mV.

$$P_{\text{open}-10} = 0{\cdot}58/1{\cdot}9 \exp(-t/1{\cdot}9) + 0{\cdot}62/16 \exp(-t/16) \text{ and} \quad (6)$$

$$P_{\text{closed}-10} = 0{\cdot}66/3{\cdot}5 \exp(-t/3{\cdot}5) + 0{\cdot}25/44 \exp(-t/44) + 0{\cdot}19/242 \exp(-t/242), \quad (7)$$

where $P_{\text{open}-10}$ and $P_{\text{closed}-10}$ are the probability density functions of open and closed states at -10 mV.

At depolarized potentials the number of components recognized in the open time distribution varied between one and two; the number of components in the closed distribution varied between two and three: this variation was in part due to reduced resolution because of the very brief open times and the appearance of subconductance states. It is clear from these observations that the channel shows complex kinetics with the distributions of open and closed times suggesting multiple states.

Effect of intracellular Ca

Fig. 9 shows the typical effect of Ca application to the intracellular side of an isolated patch. In this experiment the bath was perfused with symmetrical zero-Ca APF Ringer solution. It can be seen that when Ca was applied briefly (2 s) using diffusion from a second micropipette placed nearby and containing 0·5 M calcium acetate, there is a dramatic increase in the number of channels open. The channels then closed down as the Ca concentration declined.

Fig. 10 *A* and *B* shows similar experiments on two separate isolated patches in symmetrical zero-Ca APF which were designed to compare the effects of intracellular application of $CaCl_2$ and calcium acetate. It can be seen that calcium acetate only stimulates channel openings but that $CaCl_2$ increases the amplitude of channel current as well. This latter effect can be explained by an increase in Cl on the intracellular side of the patch producing an increase in channel conductance. The *I–V* plot of the Ca-activated channel in APF and *Ascaris* Ringer solution showed that it had the same high conductance as the channel previously described. These results taken together indicate the presence of a Ca-dependent Cl channel in the membrane.

Dose-dependent effect of Ca

Fig. 11 shows examples of current records using a cell-attached patch from a preparation previously treated with the Ca ionophore A23187. Different intracellular free-Ca concentrations were achieved by perfusing the preparations with different Ca concentrations in the bath (applied randomly). It can be seen that the number of channels opening and the probability of being open increases with the free-Ca concentration. The dose producing 50% of the maximum response (ED_{50}) in this preparation was 200 μM. Similar results were obtained from three other preparations. Although this approach illustrates the Ca-dependent nature of the channel, uncertainties about the concentration of Ca inside the cell prevent an accurate estimation of the ED_{50}. In an attempt to overcome the equilibration problem associated with cell-attached patches isolated patches were used, but this was more difficult since channel activity was frequently lost as a result of the mechanical disturbance associated with perfusion.

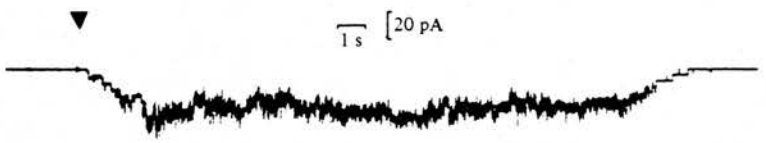

Fig. 9. Channel records showing the effect of Ca applied to the intracellular surface of an isolated patch. A broken pipette (containing 0·5 mM calcium acetate) was used to apply Ca by diffusion to the intracellular side of the membrane patch for a period of about 2 s. The start of the application indicated by (▼). The trans-patch potential was maintained throughout the experiment at −35 mV: the bathing Ringer solution was Ca-free APF; the patch pipette contained the same Ringer solution.

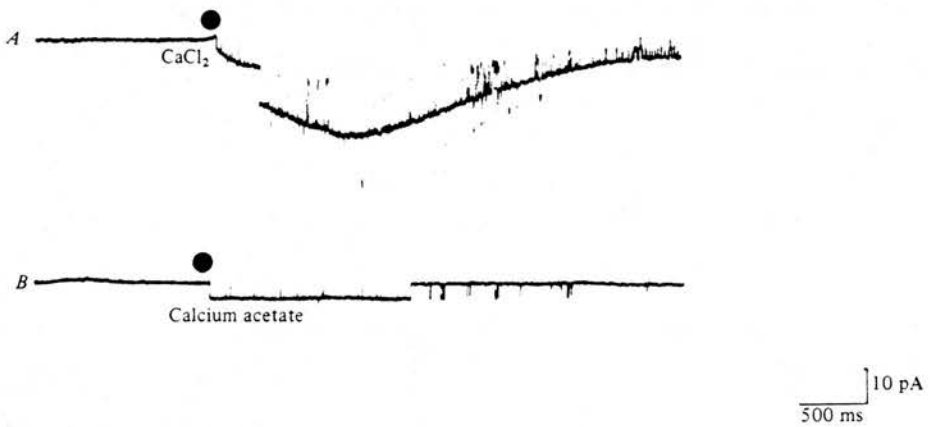

Fig. 10. Current records taken from isolated patches showing the differential effect of application of $CaCl_2$ and calcium acetate to the intracellular surface of an isolated patch. Patch potentials −40 mV. *A*. current records showing the effect of application of $CaCl_2$: after application (●) there is a transient increase in the probability of opening and also an increase in the channel amplitude. *B*. current records showing an increase in the probability of opening after the application of calcium acetate (●) but no increase in the amplitude of the single-channel current. This difference is explained by an increase in the Cl concentration at the intracellular surface of the membrane.

Binomial distribution

Fig. 12 shows the observed times (bars) 0, 1, 2 and 3 channels were open in a multichannel isolated-patch recording (using *Ascaris* Ringer solution) at four different patch potentials. If the channels were operating independently with the same probability of opening, the time spent with 0, 1, 2...n channels open would be described by the binomial distribution (eqn. (10)).

$$P_r = \frac{n}{r\,(n-r)}\,P^r(1-P)^{n-r}, \tag{10}$$

where n is the number of channels in the patch, r is the number of channels open and P is the probability that any given channel is open. P was estimated from the total proportion of open time spent at each channel level divided by n. Fig. 12 also shows the prediction of the binomial distribution. It can be seen that when the patch was hyperpolarized two channels were open more frequently than predicted; less time was spent with one and three channels open than predicted. At more depolarized patch potentials the deviations from the binomial distribution were less. The probability of each channel opening was found to

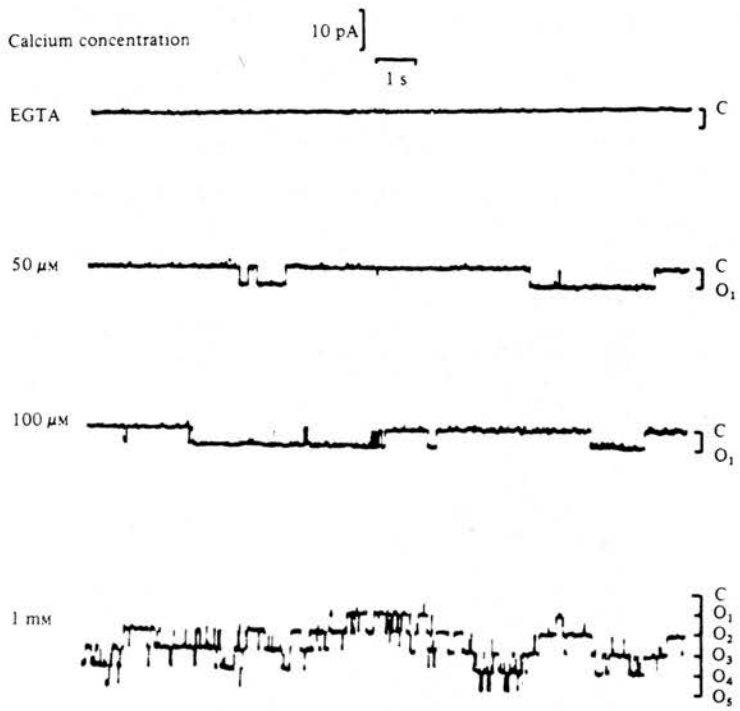

Fig. 11. Current records from a cell-attached patch all held at a trans-patch potential of −40 mV. The preparation was made permeable to Ca using the ionophore A23187. The preparation was bathed in different free-Ca concentrations applied in random order, by constant perfusion for at least 300 s. Up to five channels are open in this patch. The current level indicates the different number of channels open C, O_1, O_2, O_3, O_4 and O_5. EGTA contains zero-Ca.

decrease considerably on depolarization. Similar results were obtained from twelve experiments analysed in the same way. There is more than one explanation for these observations centred on the fact that the assumptions of the binomial distribution are not adequate during hyperpolarization but that they become an adequate approximation during depolarization. They are discussed later.

DISCUSSION

Voltage sensitivity

The Ca-dependent Cl channels of the *Ascaris* preparation increased their probability of being open as the membrane potential was hyperpolarized. This particular pattern of behaviour is similar to the Cl conductance of *Aplysia* neurones reported by Chesnoy-Marchais (1983) and the Cl channel of the mollusc, *Lymnaea stagnalis*, studied by Geletyuk & Kazachenko (1985). The voltage dependence of the molluscan Cl channel was shown to be dependent on the extracellular K ion concentration, this contrasts with apparently normal channel behaviour of the *Ascaris* Cl channel in the absence of K and Na ions. The Ca-dependent Cl conductance found in *Xenopus* oocytes was activated by depolarization (Miledi, 1982). High-conductance voltage-sensitive anion channels have been found in

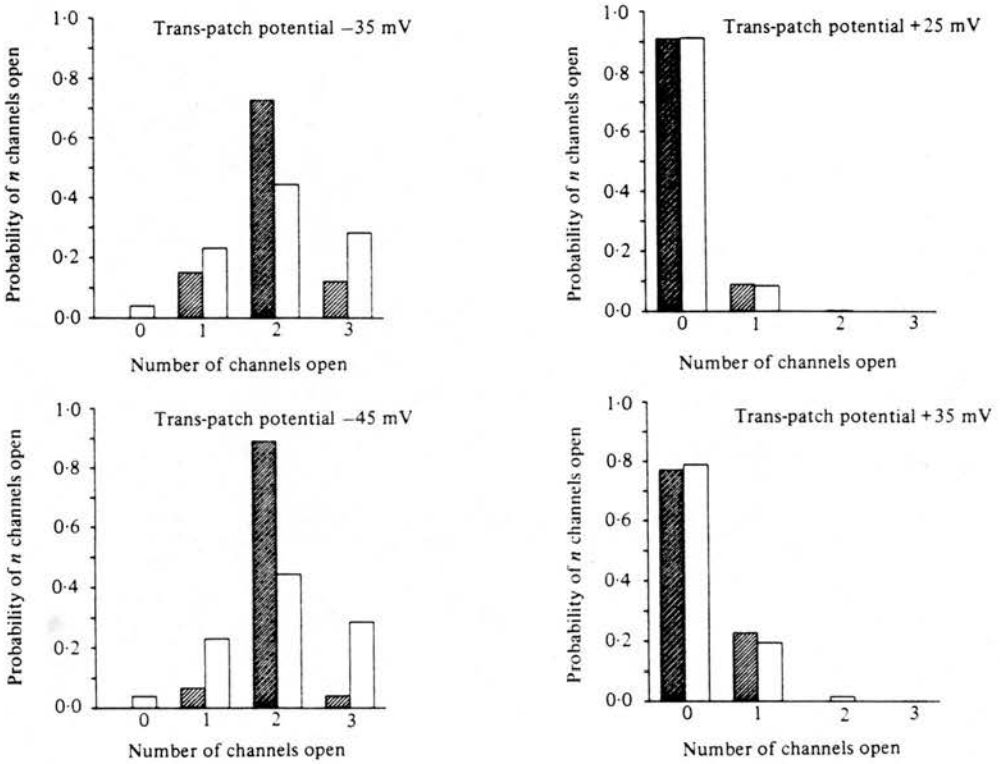

Fig. 12. Plots of the probability of zero, one, two and three channels opening. There are four graphs taken from the same isolated-patch experiment, each at the indicated trans-patch potential. The open bars show the probability of zero, one, two and three channels open predicted by the binomial distribution calculated from the observed mean probability of opening. The shaded bars show the observed probability of seeing zero, one, two and three channels open. The values are not in close agreement over all potentials.

many other preparations. These include: rat muscle (Blatz & Magleby, 1983), rabbit bladder epithelial tissue (Hanrahan, Alles & Lewis, 1985) and Schwann cells (Gray, Bevan & Ritchie 1984). All are characterized as having a voltage 'window'. In the Schwann cell the Cl channel is active only within a limited range of potentials, i.e. between -10 and -40 mV. Outside this range the channel probability of being open decreases. In epithelial tissue a high-conductance Cl channel is described as being spontaneously active between ± 20 mV. In rat muscle the channel is active at around a trans-patch potential of 0 mV rapidly and reversibly closing at potentials away from 0 mV. These observations taken together indicate the wide and varying voltage sensitivity for Cl channels.

Other modulating factors

Isolated patches from the *Ascaris* preparation often lost their activity during mild mechanical disturbance of the patch such as perfusion, even in the presence of Ca. Gray *et al.* (1984) have described a Cl channel in the Schwann cell and Kolb, Brown & Murer (1985) describe a Cl channel in MDCK secretory epithelial cells; both types of channels show an increase in the probability of opening when the patch is isolated. This behaviour on isolation is opposite to that which is observed for this *Ascaris* channel. The suggested

modulating factor or factors in *Ascaris* may be responsible for some variations seen in the Ca sensitivity of individual preparations. However, this is not the only explanation; for example the Ca sensitivity of channels may change during development (Blair & Dionne, 1985).

Subconductance

Reduced current steps at depolarized potentials were a property of the Cl-channel I–V relationships. The non-linearity was thought to be due to the reduced probability of the channel being open in the main state and the occurrence of subconductance levels at depolarized potentials. We also considered the possibility that the non-linearity represented the activity of other channels which were observed only when the high-conductance Cl channel was turned off during depolarization. We have not observed in this preparation smaller-conductance channels in the absence of the large Cl channel which are voltage sensitive and also close down on depolarization. We therefore believe that the non-linearity seen in the I–V plots is due only to the appearance of subconductance states during depolarization. We have not seen subconductance during hyperpolarization.

Binomial distribution and channel opening

In this study of the Ca-dependent Cl channel of *Ascaris* we found that the behaviour of multichannel records could not be well described by the binomial distribution. This observation contrasts with some other reports from multichannel records e.g. Barratt, Magleby & Pallotta (1983); where the distributions of the time spent with different numbers of channels open in the patch were well described by the binomial distributions. However, other studies on channel activity described by Miller (1982), have shown distributions different to that predicted by the binomial. In the *Torpedo* electroplax preparation, Miller (1982) suggested that two channels are coupled together and that their openings are linked.

One explanation for our observations on multichannel records not fitting with the binomial could be due to the relatively short (200 s) sample times we have used compared with the slow channel kinetics: since there are likely to be at least two open main states it could have been that the sample favoured the long opening state of one channel but the brief opening state of another. Thus it would appear that two channels observed have a different probability of being open. Another possible explanation for the behaviour of the channels is a connexion between the channels opening such that when one channel opens this makes the opening of another adjacent channel less likely. In fact our observations are consistent with both types of behaviour. However, we believe that the simpler explanation is that the channels do indeed have differing probabilities of opening. This difference in the probability of opening may decline on depolarization so that the binomial distribution better describes the number of channels open.

Function of the Ca-dependent Cl channel

The resting membrane potential of the *Ascaris* has been the subject of a number of studies (e.g. Del Castillo *et al.* 1964; Brading & Caldwell, 1971). One of the conclusions of their work was the fact that membrane potential is not greatly influenced by K but that Cl has a marked effect. Cl has also been shown to have a greater permeability than Na or K (Caldwell & Ellory, 1968). The large conductance of the Ca-activated Cl channels described in this paper, the frequency with which they were observed and the fact that they can be fully activated at -35 mV suggests that they can contribute to the resting Cl permeability of the membrane. This is particularly likely if the intracellular Ca concentration is high.

The movement of Cl ions against an ionic gradient observed by Hobson *et al.* (1952) indicates the presence of a Cl pump. This may be situated either in the hypodermis or the somatic muscle. If the pump were situated in the somatic muscle cells the membrane potential would be critically dependent on the activity of this pump given the high permeability of the membrane to Cl (Cauldwell & Ellory, 1968). In mammalian skeletal muscle for example the combination of high permeability to Cl and a Cl pump have been used to account for the resting potential which may not be adequately described by the passive distribution of ions (Dulhunty, 1978).

The bag membrane of *Ascaris* normally shows regular depolarizing and spike potentials involving the influx of Ca (Jarman, 1959; Weisblat *et al.* 1976). A rise in the intracellular Ca concentration associated with the spike could lead to the activation of Ca-dependent Cl channels. Other Ca-activated Cl conductances have been reported in mouse spinal neurones (Owen, Segal & Barker, 1983), *Xenopus* oocyte (Miledi, 1982) and molluscan neurones (Geletyuk & Kazachenko, 1985); all have been suggested to produce a repolarization after an action potential. A Ca-activated Cl conductance in rat dorsal root ganglia cells observed by Mayer (1985) has been proposed to give rise to depolarizing long-lasting after-potentials. In the *Ascaris* Cl channel the voltage sensitivity is not compatible with a function of repolarization after a Ca spike.

Ca-dependent Cl channels have also been described in glandular secretory tissue where their existence is important for salt secretion e.g. Marty, Tan & Trautmann (1984) and Findlay & Petersen (1985). In the lacrimal-gland preparation (Marty *et al.* 1984) the unit conductance of the Ca-dependent Cl channel is 1–2 pS which is two orders of magnitude smaller than channels reported here. None the less, it is possible that this channel found in *Ascaris* is also involved in movement of Cl across the body wall.

We would like to thank the technical staff of the department, and also the staff at the abattoir for supply of *Ascaris* throughout this project. P. Thorn is a S.E.R.C. C.A.S.E. student with Pfizer Central Research; we are pleased to acknowledge the advice of Dr R. A. F. Gration.

REFERENCES

BARRETT, J. N., MAGLEBY, K. L. & PALLOTTA, B. S. (1982). Properties of single calcium-activated potassium channels in cultured rat muscle. *Journal of Physiology* **331**, 211–230.

BLAIR, L. C. S. & DIONNE, V. E. (1985). Developmental acquisition of Ca sensitivity by K channels in spinal neurons. *Nature* **315**, 329–330.

BLATZ, A. L. & MAGLEBY, K. L. (1983). Single voltage-dependent chloride selective channels of large conductance in cultured rat muscle. *Biophysics Journal* **43**, 237–241.

BRADING, A. F. & CALDWELL, P. C. (1971). The resting membrane potential of somatic muscle cells of *Ascaris lumbricoides*. *Journal of Physiology* **217**, 605–624.

CALDWELL, P. C. & ELLORY, J. C. (1968). Ion movements in somatic muscle cells of *Ascaris lumbricoides*. *Journal of Physiology* **197**, 75–76*P*.

CHESNOY-MARCHAIS, D. (1983). Characterization of a chloride conductance activated by hyperpolarization in *Aplysia* neurones. *Journal of Physiology* **342**, 277–308.

DEL CASTILLO, J., DE MELLOW, W. C. & MORALES, T. (1964). Influence of some ions on the membrane potential of *Ascaris* muscle. *Journal of General Physiology* **48**, 129–140.

DULHUNTY, A. F. (1978). The dependence of membrane potential on extracellular chloride concentration in mammalian skeletal muscle fibres. *Journal of Physiology* **276**, 67–82.

FINDLAY, I. & PETERSEN, O. H. (1985). Acetylcholine stimulates a Ca^{2+} dependent Cl^- conductance in mouse lacrimal acinar cells. *Pflügers Archives* **403**, 328–330.

GELETYUK, V. I. & KAZACHENKO, V. N. (1985). Single Cl^- channels in molluscan neurones: multiplicity of conductance states. *Journal of Membrane Biology* **86**, 9–15.

GLASBEY, C. A. & MARTIN, R. J. (1986). Exploratory and confirmatory plots of single channel records. *Journal of Neuroscience Methods* **16**, 239–249.

GRAY, P. T. A., BEVAN, S. & RITCHIE, J. M. (1984). High conductance anion-selective channels in rat cultivated Schwann cells. *Proceedings of the Royal Society* B **221**, 395–409.

HAMILL, O. P., MARTY, E., NEHER, B., SAKMANN, B. & SIGWORTH, F. J. (1981). Improved patch-clamp techniques for high-resolution current recording from the cells and cell-free membrane patches. *Pflügers Archiv* **391**, 85–100.

HANRAHAN, J. W., ALLES, W. P. & LEWIS, S. A. (1985). Single anion-selective channels in basolateral membrane of a mammalian tight epithelium. *Proceedings of the National Academy of Sciences of the U.S.A.* **82**, 7791–7795.

HOBSON, A. D., STEPHENSON, W. & BEADLE, L. C. (1952). Studies on the physiology of *Ascaris lumbricoides*. 1. The relation of the total osmotic pressure, conductivity and chloride content of the body fluid to that of the external environment. *Journal of Experimental Biology* **29**, 1–21.

HOBSON, A. D., STEPHENSON, W. & EDEN, A. (1952). Studies on the physiology of *Ascaris lumbricoides*. 2. The inorganic composition of the body fluid in relation to that of the external environment. *Journal of Experimental Biology* **29**, 22-29.

JARMAN, M. (1959). Electrical activity in the muscle cells *Ascaris* muscle. *Nature* **184**, 1244.

KOLB, H. A., BROWN, C. D. A. & MURER, H. (1985). Indentification of a voltage-dependent anion channel in the apical membrane of a Cl^--secretory epithelium (MDCK). *Pflügers Archiv* **403**, 262–265.

MARTIN, R. J. (1980). The effect of γ-aminobutyric acid on the input conductance and membrane potential of *Ascaris* muscle. *British Journal of Pharmacology* **71**, 99–106.

MARTIN, R. J. (1985). γ-aminobutyric acid- and piperazine-activated single-channel currents from *Ascaris suum* body muscle. *British Journal of Pharmacology* **84**, 445–461.

MARTIN, R. J. & THORN, P. (1984). A high conductance anion channel in somatic muscle cells of *Ascaris suum*. *Journal of Physiology* **354**, 46*P*.

MARTY, A., TAN, Y. P. & TRAUTMANN, A. (1984). Three types of calcium-dependent channel in rat lacrimal glands. *Journal of Physiology* **357**, 293-325.

MAYER, M. L. (1985). A calcium-activated chloride current generates the after-depolarization of rat sensory neurones in culture. *Journal of Physiology* **364**, 217–239.

MILEDI, R. (1982). A calcium-dependent transient outward current in *Xenopus laevis* oocytes. *proceedings of the Royal Society* B **215**, 491-497.

MILLER, C. (1982). Open-state substructure of single chloride channels from *Torpedo* electroplax. *Philosophical Transactions of the Royal Society B* **299**, 401–411.

OWEN, D. G., SEGAL, M. & BARKER, J. L. (1983). A Ca-dependent Cl conductance in cultured mouse spinal neurones. *Nature* **311**, 567–570.

SAKMANN, B. & TRUBE, G. (1984). Conductance properties of single inwardly rectifying potassium channels in ventricular cells from guinea-pig heart. *Journal of Physiology* **347**, 641–657.

WEISBLAT, D. A., BYERLY, L., & RUSSEL, R. L. (1976). Ionic mechanisms of electrical activity in somatic muscle of the nematode *Ascaris lumbricoides*. *Journal of Comparative Physiology* **111**, 93–113.